

AD-A209 744

SPECIAL PUBLICATIONS BRL-SP-77

BRL

THE FOURTH ANNUAL CONFERENCE
ON HAN-BASED LIQUID PROPELLANTS
VOLUME I



MAY 1989

CB 11

APPROVED FOR PUBLIC RELEASE; DISTRIBUTION UNLIMITED.

U.S. ARMY LABORATORY COMMAND

BALLISTIC RESEARCH LABORATORY
ABERDEEN PROVING GROUND, MARYLAND

DESTRUCTION NOTICE

Destroy this report when it is no longer needed. DO NOT return it to the originator.

Additional copies of this report may be obtained from the National Technical Information Service, U.S. Department of Commerce, Springfield, VA 22161.

The findings of this report are not to be construed as an official Department of the Army position, unless so designated by other authorized documents.

The use of trade names or manufacturers' names in this report does not constitute indorsement of any commercial product.

UNCLASSIFIED
SECURITY CLASSIFICATION OF THIS PAGE

Form Approved
OMB No. 0704-0188

REPORT DOCUMENTATION PAGE															
1a. REPORT SECURITY CLASSIFICATION Unclassified		1b. RESTRICTIVE MARKINGS													
2a. SECURITY CLASSIFICATION AUTHORITY		3. DISTRIBUTION/AVAILABILITY OF REPORT Approved for Public Release; Distribution Unlimited.													
2b. DECLASSIFICATION/DOWNGRADING SCHEDULE															
4. PERFORMING ORGANIZATION REPORT NUMBER(S) BRL-SP-77, VOLUME I		5. MONITORING ORGANIZATION REPORT NUMBER(S)													
6a. NAME OF PERFORMING ORGANIZATION US Army Ballistic Rsch Lab	6b. OFFICE SYMBOL <i>(If applicable)</i> SLCBR-IB	7a. NAME OF MONITORING ORGANIZATION													
6c. ADDRESS (City, State, and ZIP Code) Aberdeen Proving Ground, MD 21005-5066		7b. ADDRESS (City, State, and ZIP Code)													
8a. NAME OF FUNDING/SPONSORING ORGANIZATION	8b. OFFICE SYMBOL <i>(If applicable)</i>	9. PROCUREMENT INSTRUMENT IDENTIFICATION NUMBER													
8c. ADDRESS (City, State, and ZIP Code)		10. SOURCE OF FUNDING NUMBERS <table border="1"><tr><td>PROGRAM ELEMENT NO.</td><td>PROJECT NO.</td><td>TASK NO.</td><td>WORK UNIT ACCESSION NO.</td></tr></table>		PROGRAM ELEMENT NO.	PROJECT NO.	TASK NO.	WORK UNIT ACCESSION NO.								
PROGRAM ELEMENT NO.	PROJECT NO.	TASK NO.	WORK UNIT ACCESSION NO.												
11. TITLE <i>(Include Security Classification)</i> THE FOURTH ANNUAL CONFERENCE ON HAN-BASED LIQUID PROPELLANTS (VOLUME I)															
12. PERSONAL AUTHOR(S) <i>(editor) Josephine Q. Wojciechowski</i>															
13a. TYPE OF REPORT SP	13b. TIME COVERED FROM _____ TO _____	14. DATE OF REPORT (Year, Month, Day)	15. PAGE COUNT												
16. SUPPLEMENTARY NOTATION															
17. COSATI CODES <table border="1"><tr><th>FIELD</th><th>GROUP</th><th>SUB-GROUP</th></tr><tr><td> </td><td> </td><td> </td></tr><tr><td> </td><td> </td><td> </td></tr><tr><td> </td><td> </td><td> </td></tr></table>		FIELD	GROUP	SUB-GROUP										18. SUBJECT TERMS <i>(Continue on reverse if necessary and identify by block number)</i> Liquid Propellant HAN Compatibility Physical Properties Hydroxylammonium Nitrate TEAN Production Triethanolammonium Nitrate Combustion Stability	
FIELD	GROUP	SUB-GROUP													
19. ABSTRACT <i>(Continue on reverse if necessary and identify by block number)</i>															
This report contains the abstracts and viewgraphs of the papers presented at the BRL's Fourth Annual Conference on HAN-Based Liquid Propellants.															
20. DISTRIBUTION/AVAILABILITY OF ABSTRACT <input type="checkbox"/> UNCLASSIFIED/UNLIMITED <input checked="" type="checkbox"/> SAME AS RPT <input type="checkbox"/> DTIC USERS		21. ABSTRACT SECURITY CLASSIFICATION Unclassified													
22a. NAME OF RESPONSIBLE INDIVIDUAL Josephine Q. Wojciechowski		22b. TELEPHONE <i>(Include Area Code)</i> (301) 278-6160	22c. OFFICE SYMBOL SLCBR-IB-B												

TABLE OF CONTENTS

CONT'D from pg. 1

INTRODUCTION	1
LIQUID PROPELLANT FAIL-SAFE CRITERIA PROGRAM; Stanley Griff and Gerald Doyle	3
AN OVERVIEW OF THE THERMAL REACTIVITY OF SUBSTITUTED AMMONIUM NITRATES; V.R. Pai Verneker, S.C. Deevi and C.K. Law	24
IMPACT SENSITIVITY OF HAN-BASED LIQUID MONOPROPELLANTS; I. Stobie, B.D. Bensinger and J.D. Knapton	40
QUANTITATIVE ANALYSIS OF HAN-BASED LIQUID PROPELLANTS. Dr. H.J. de Greiff	53
AN OVERVIEW OF THE U.K. APPROACH TO THE CHARACTERIZATION AND CLASSIFICATION OF HAN-BASED LIQUID PROPELLANT LP101. S. Westlake	64
POSSIBLE TEST METHODS TO STUDY THE THERMAL STABILITY OF HYDROXYLAMMONIUM NITRATE BASED LIQUID GUN PROPELLANTS; P.F. Bunyan and S. Westlake	74
HYDRODYNAMIC THEORY OF LIQUID PROPELLANT DYNAMICS; J.W. Haus and F. Chung-Yau	102
IONIC ASPECTS OF THE DECOMPOSITION OF HAN SOLUTION. W.S. Koski	115
REACTION KINETICS OF HAN, TEAN AND WATER MIXTURES USING A PERSONAL COMPUTER; A.K. Macpherson and A.J. Bracuti	116
ELECTRICAL IGNITION OF HAN-BASED LIQUID PROPELLANTS; G. Klingenberg, H.J. Frieske and H. Rockstroh	117
THE BURNING RATE OF HAN-BASED LIQUID PROPELLANTS: THE EFFECTS OF HAN CONCENTRATION ON BURNING RATES; S. Vosen	131
STUDY OF THERMAL DIFFUSIVE-REACTIVE INSTABILITY IN LIQUID PROPELLANTS: THE EFFECTS OF SURFACE TENSION AND GRAVITY. R.C. Armstrong and S.B. Margolis	154
THE RESPONSE OF AN LP TO HEATING AT HIGH PRESSURE. R.A. Beyer	155

Preceding Page Blank



Justification	
By _____	
Distribution/ _____	
Availability Codes _____	
Dist	Avail and/or Special
A-1	

TABLE OF CONTENTS (Cont.)

EQUATION OF STATE AND THERMODYNAMIC PROPERTIES OF THE HAN-TEAN-WATER SYSTEM. J. Frankel, W. Scholz and J.F. Cox	179
PHYSICAL PROPERTIES OF LIQUID PROPELLANTS: MEASUREMENTS OF SHEAR VISCOSITY, VOLUME VISCOSITY AND DENSITY; J. Schroeder, C.S. Choi and Y.T. Lee	195
THE SOLUBILITY OF GASES UNDER PRESSURE IN LIQUID PROPELLANTS: S. Murad and P. Ravi	222
COMPATIBILITY OF ELASTOMERIC MATERIALS WITH HAN-BASED LIQUID PROPELLANT 1846. G. Rodriguez, H.O. Feuer and A.R. Teets	245
THE INFLUENCE OF METAL IONS ON THE STABILITY OF LIQUID GUN PROPELLANTS CONTAINING HAN. Dr. R. Hansen	273
SELECTION CRITERIA FOR METALS AND PLASTICS AS CONSTRUCTION MATERIALS FOR LONG TERM PRESSURE-TESTING APPARATUS ON LIQUID PROPELLANTS (LPS). Dr. E. Backof	284
COMPATIBILITY STUDY WITH 60% HAN SOLUTION. O. Briles and L.S. Joesten	309

INTRODUCTION

The US Army is currently investigating the use of liquid propellants (LPs) in large and medium caliber guns. These LPs are characterized by the use of hydroxylammonium nitrate (HAN) as their oxidizer. On 30 August - 1 September 1988, the Fourth Annual LP Conference on HAN-Based Liquid Propellant Structure and Properties was held at the BRL with Dr. Walter F. Morrison as General Chairman. The papers presented at this highly successful conference were given by people from academia, industry, and other government agencies.

This report is a compilation of the abstracts and viewgraphs of these papers where available. The final program is included in appendix A and a list of attendees in appendix B.

LIQUID PROPELLANT FAIL-SAFE CRITERIA PROGRAM

The use of Liquid Propellant (LP) as a replacement for solid propellants in some applications requires complete and extensive characterization of these new propellant systems in order to establish fail-safe criteria. The fail-safe criteria program is designed to provide information to relate propellant composition and condition with performance. Prolonged aging effects on LP will be determined in order to recommend storage containers for long-term storage of LP. Analytical methodology is currently being established to monitor the LP during storage as well as during production to provide necessary and reasonable specifications for LP.

The phase of the program which is now in progress has dealt with (1) reviewing, recommending and developing applicable analytical methods for monitoring the LP before, during and after storage; (2) determining physical properties required for this study; (3) initiating and monitoring pressure-time studies as a function of temperature, composition, impurities and ullage; (4) utilization of the pressure-time studies to determine degradation products, rates of pressure build-up and rates of formation of degradation products; (5) establishing which components or degradation products are the best indicators of propellant utility or instability; (6) determining which impurities or degradation products or combinations are most detrimental to the propellant stability and (7) establishing long-term storage container design based on pressure-time study data.

Preceding Page Blank

LIQUID PROPELLANT FAIL-SAFE CRITERIA PROGRAM

STANLEY GRIFF

GERALD DOYLE

**GEO-CENTERS, INC.
LAKE HOPATCONG, N.J.**

**WILLIAM SEALS
ARDEC, PICATINNY ARSENAL
DOVER, N.J.**

AUGUST 1988

OBJECTIVES

- 1. DEVELOP ANALYTICAL METHODOLOGY FOR MONITORING THE LP.**
- 2. DETERMINATION OF PRESSURE BUILD-UP FOR STORAGE CONTAINER DESIGN.**
- 3. SELECTION OF VARIABLES TO SUBJECT THE LP TO DURING STORAGE.**
- 4. COORDINATION OF BALLISTICS AND RELATED TESTING.**

GOALS

- 1. LIFETIME AND SAFETY FACTORS FOR LP UNDER STORAGE CONDITIONS.**
- 2. EFFECT OF CONTAMINANTS AND OTHER VARIABLES.**
- 3. ESTABLISH SPECIFICATIONS FOR LP.**
- 4. ESTABLISH RATES, KINETICS AND DECOMPOSITION MECHANISMS.**
- 5. FLAGS FOR ESTABLISHING CONDITION OF LP.**
- 6. ANALYTICAL METHODOLOGY FOR MONITORING LP DURING STORAGE.**
- 7. APPLICABILITY OF ANALYTICAL METHODOLOGY FOR QC OF LP DURING PRODUCTION.**
- 8. EFFECT OF LP COMPOSITION ON BALLISTICS.**

LIQUID GUN PROPELLANT COMPOSITION

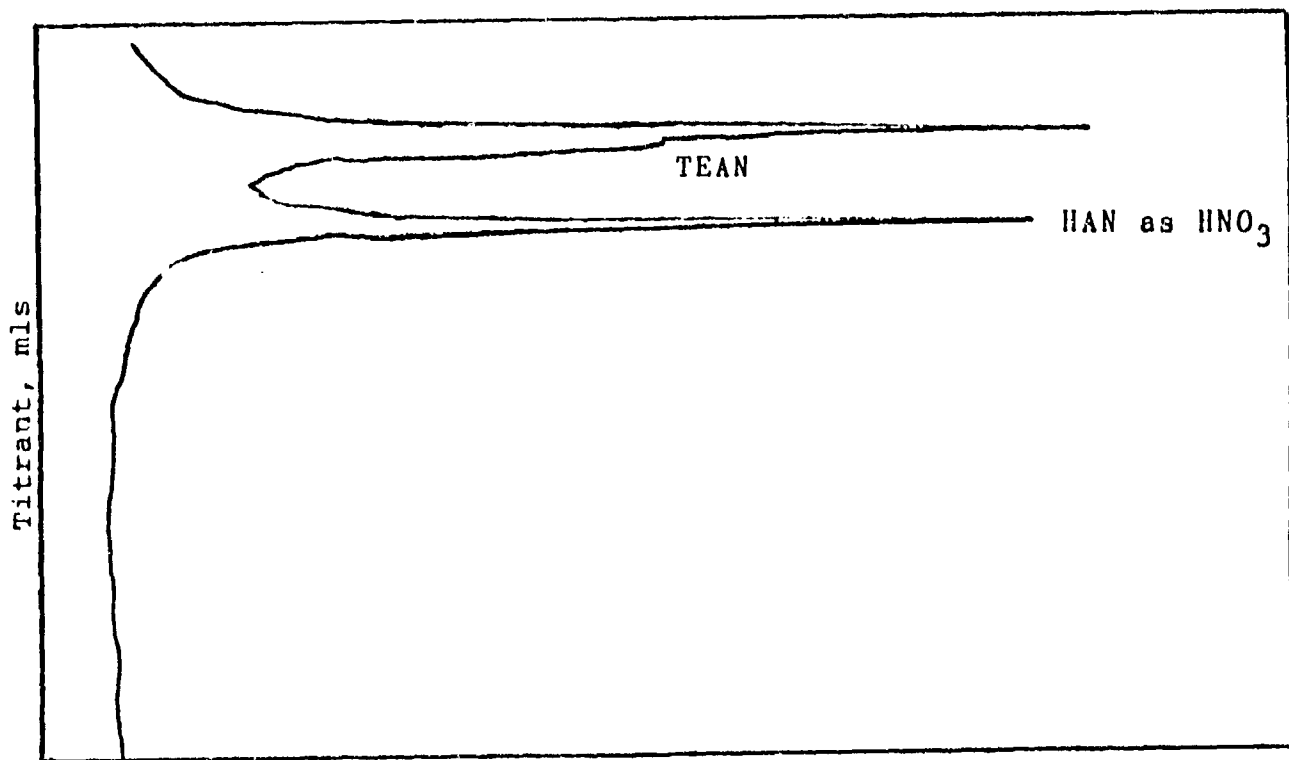
THE LIQUID PROPELLANT (LP) FORMULATIONS SELECTED FOR EVALUATION ON THE FAIL-SAFE CRITERIA PROGRAM WERE LP 1845 AND LP 1846. TYPICAL COMPOSITIONS OF THESE LP'S ARE LISTED BELOW:

	<u>LP1845</u>	<u>LP1846</u>
HYDROXYLAMMONIUM NITRATE (HAN)	63	61
TRIETHANOLAMMONIUM NITRATE (TEAN)	20	19
WATER	17	20

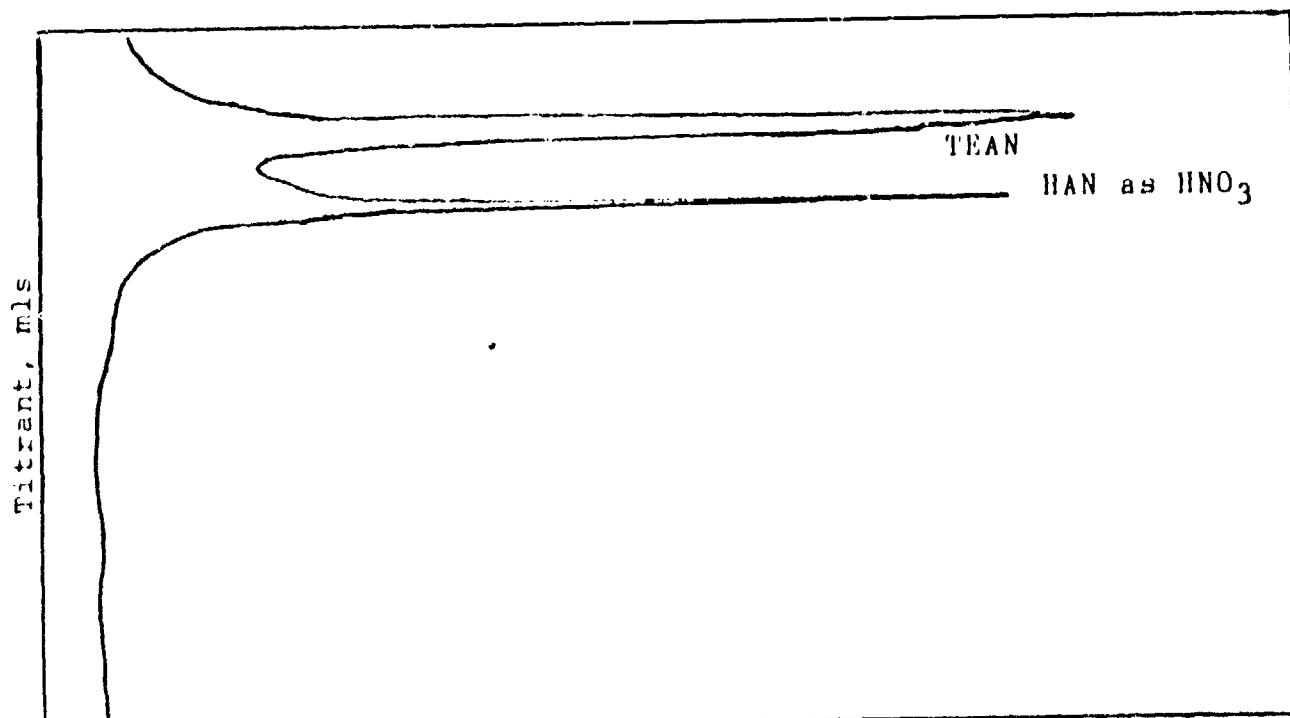
ANALYTICAL MONITORING TECHNIQUES

<u>Component</u>	<u>Recommended</u>
HAN	IC-sensitive to small variations
TEAN	IC-sensitive to small variations
H ₂ O	Titration
Nitric acid	Titration
Metals	IC-all TM+2 in one run; TM+3 method being coordinated with Waters
AN, EAN, DEAN	IC
Gas Phase degradation products	GC-Two column method
Liquid Phase degradation products	LC-method being coordinated with Waters

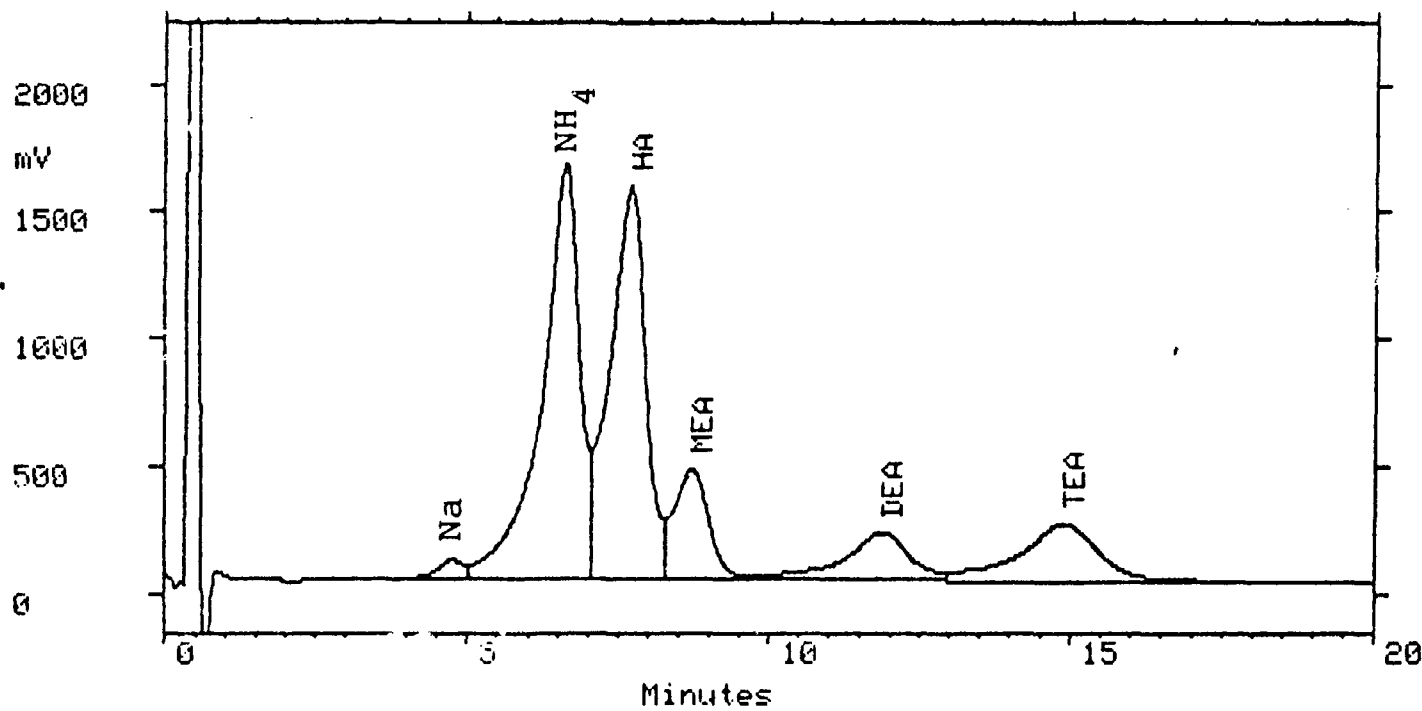
LP with ~ 2% Ammonium Nitrate



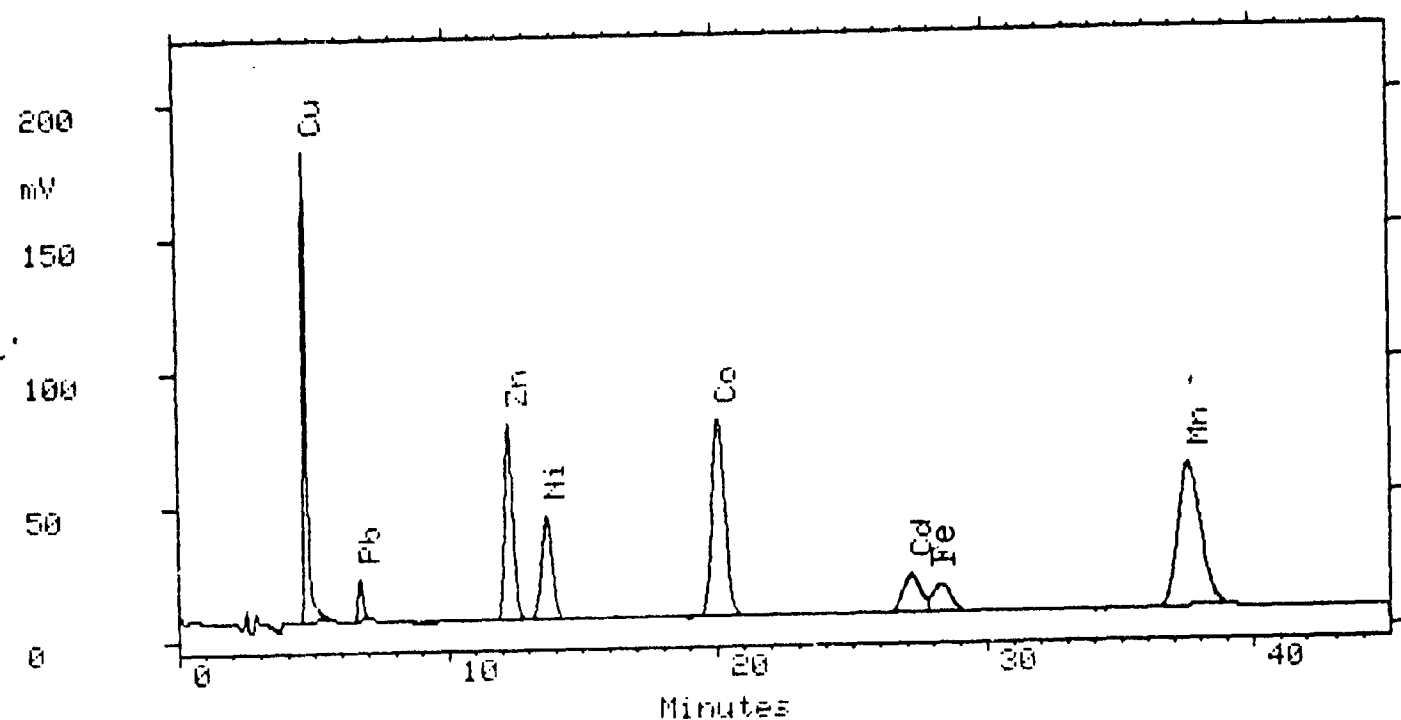
LP with Trace Ammonium Nitrate



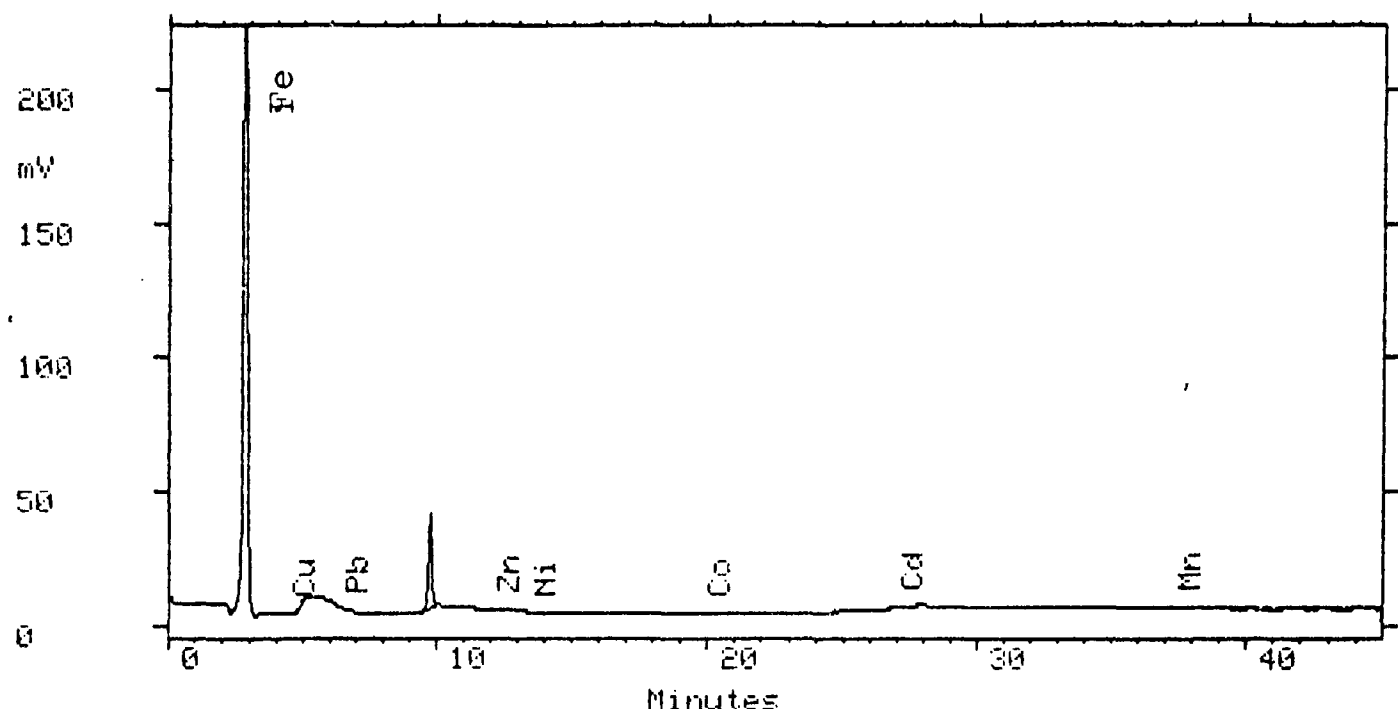
TITRATION CURVES - FIRST DERIVATIVE



**ION CHROMATOGRAM - STANDARDS
(SAMPLES 1/5000 DILUTION)**



ION CHROMATOGRAM - METAL STANDARDS
TM+2 0.5 TO 1.0 PPM

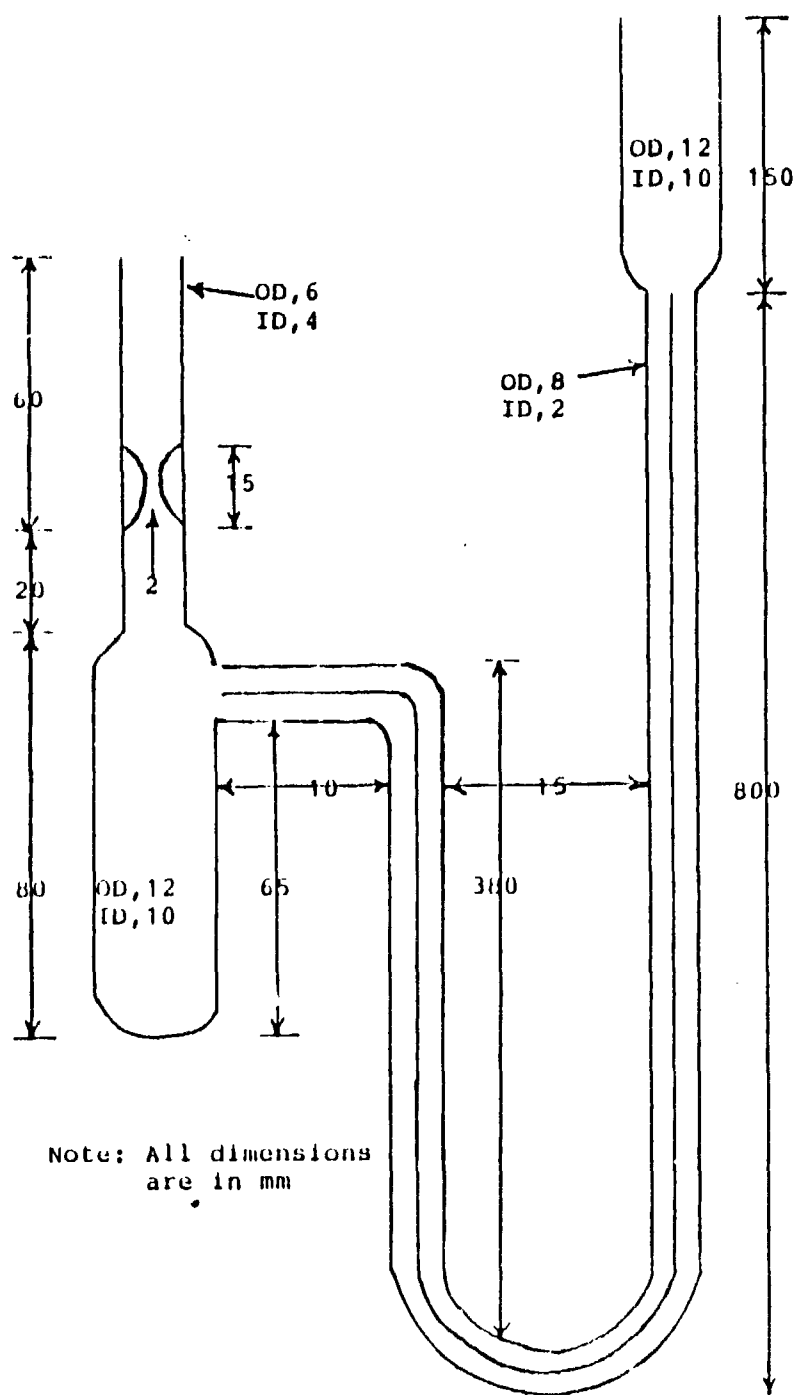


**ION CHROMATOGRAM - LP 1846 FOR TM
1/10 DILUTION**

METALS ANALYSIS OF LP 1846 (LP-2 & LP-3) BY ICP

<u>Metal</u>	<u>LP-2, ppm</u>	<u>LP-3, ppm</u>
Iron	<0.09	2.06
Chromium	0.74	0.40
Copper	<0.18	<0.17
Nickel	0.88	0.34
Cobalt	<0.09	<0.09
Lead	<0.87	<0.87
Tin	3.06	3.03

Iron by polarography: 0.31(Fe⁺³)



PRESSURE - TIME STUDY APPARATUS

**COMPOSITIONAL ANALYSIS OF LP 1846
BEFORE AND AFTER EXPOSURE AND RATE
OF DECOMPOSITION AS A FUNCTION OF
TEMPERATURE AND NITRIC ACID AT
65% ULLAGE**

<u>LP1846</u>	<u>Temp. °C</u>	<u>%HAN</u>	<u>%HNO₃</u>	<u>Days</u>	<u>Rate</u>
LP-2**		59.3	0.44		
0.44%HNO ₃	25	59.7	0.48	136	0.1
0.44%HNO ₃	50	58.4	0.74	116	2.0
0.44%HNO ₃	65	57.7	1.18	48	8.5

Note: All rates are final rates in mmHg/day.

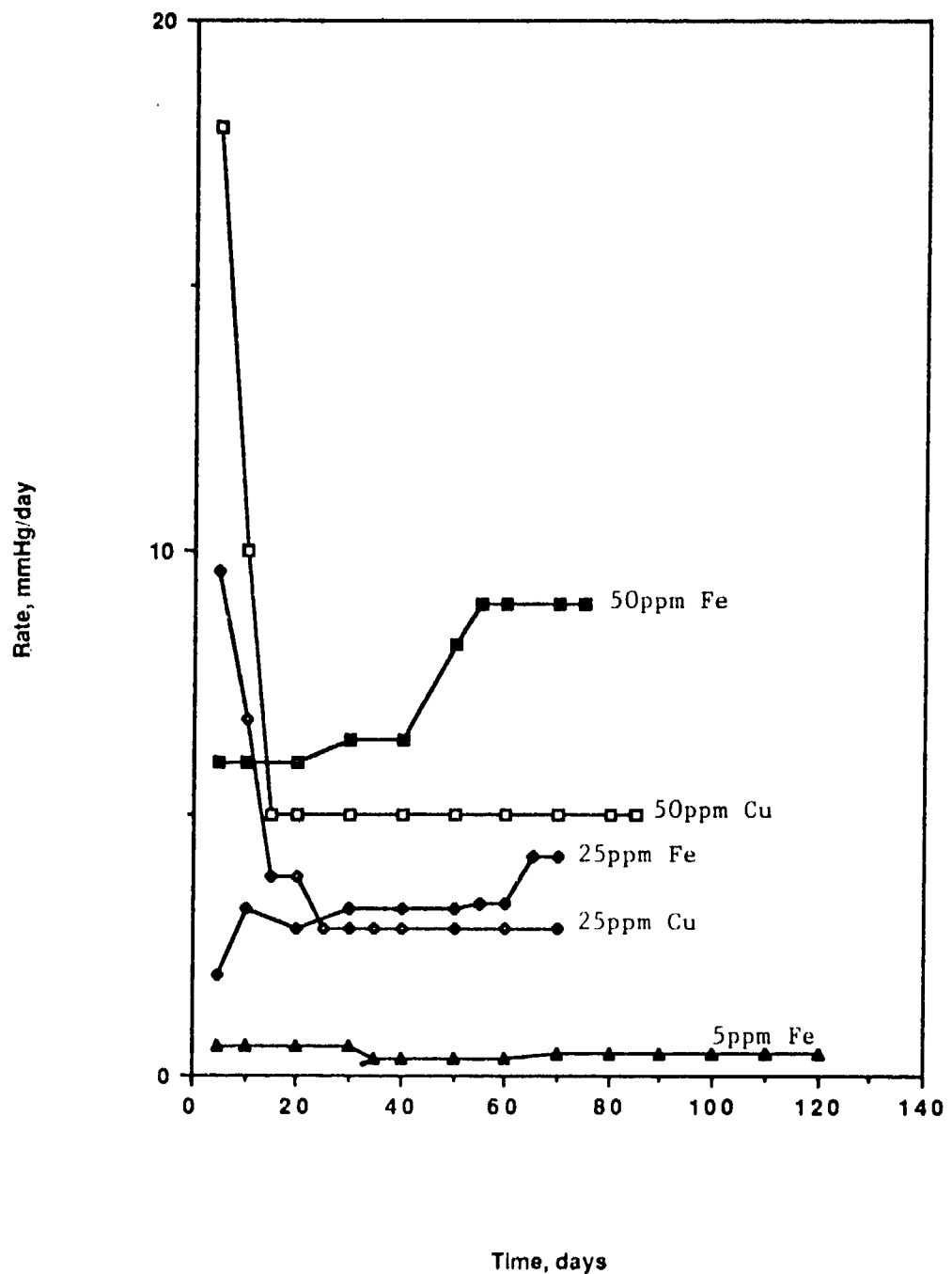
**-Initial composition (LP-2: Lot # ABY87FS2C013).

**COMPOSITIONAL ANALYSIS OF LP 1846
BEFORE AND AFTER EXPOSURE AND RATE
OF DECOMPOSITION AS A FUNCTION OF
TEMPERATURE AND IRON AT
65% ULLAGE**

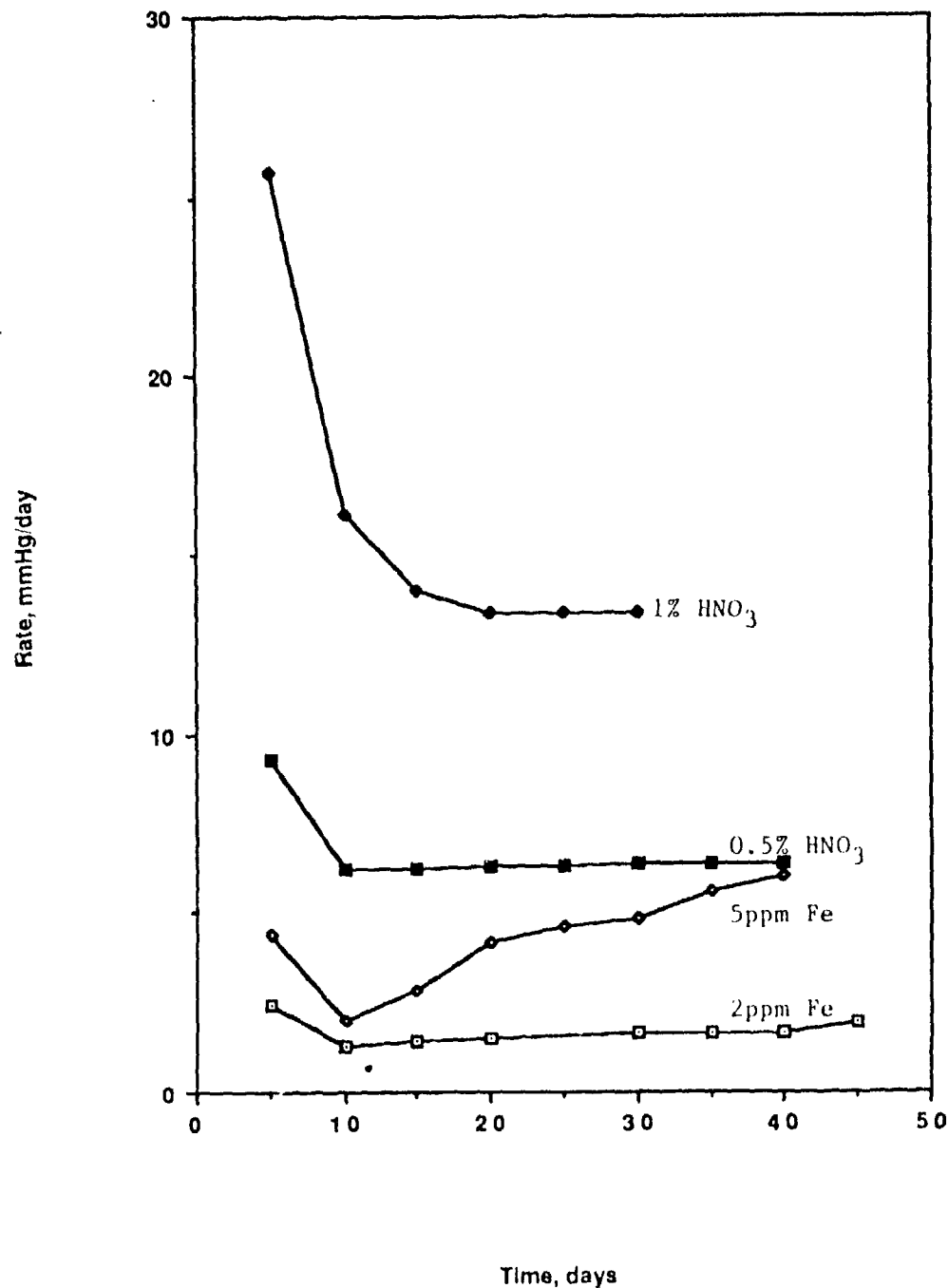
<u>LP1846</u>	<u>Temp.,°C</u>	<u>%HAN</u>	<u>%HNO₃</u>	<u>Days</u>	<u>Rate</u>
LP-3**		59.4	0.03		
2.1ppmFe	25	60.0	0.12	120	0
7.25ppmFe	25	59.9	0.14	120	0
2.1ppmFe	50	59.8	0.23	120	0
7.0ppmFe	50	59.5	0.28	120	0.42
49.9ppmFe	50	58.4	0.80	70	9.0

Note: All rates are final rates in mmHg/day.

**-Initial composition (LP-3: Lot # 1846-01).



RATE AT 50°C FOR LP 1846 IRON VS COPPER



RATE AT 65°C FOR LP 1846 IRON VS NITRIC ACID

**PRESSURE BUILD-UP IN STORAGE
CONTAINERS HOLDING LIQUID PROPELLANT
CONTAMINATED WITH NITRIC ACID**

<u>LP1846 Type</u>	<u>Temp.C</u>	<u>Pressure, psig/yr</u>
0.44% HNO ₃	25	0.71
0.44% HNO ₃	50	14.1
0.44% HNO ₃	65	60.0
0.54% HNO ₃	65	45.1*
0.98% HNO ₃	65	94.6

* - Denotes current rates from pressure-time studies
that are still in progress.

**PRESSURE BUILD-UP IN STORAGE
CONTAINERS HOLDING LIQUID PROPELLANT
CONTAMINATED WITH IRON**

<u>LP1846 Type</u>	<u>Temp.C</u>	<u>Pressure, psig/yr</u>
2ppm Fe	25	0
2ppm Fe	50	0
2ppm Fe	65	21.2*
7ppm Fe	25	0
7ppm Fe	50	3.0
7ppm Fe	65	56.5*
25ppm Fe	50	29.6*
50ppm Fe	25	0.1*
50ppm Fe	50	63.5

* - Denotes current rates from pressure-time studies
that are still in progress.

**PRESSURE BUILD-UP IN STORAGE
CONTAINERS HOLDING LIQUID PROPELLANT
CONTAMINATED WITH COPPER**

<u>LP1846 Type</u>	<u>Temp.C</u>	<u>Pressure, psig/yr</u>
25ppm Cu	50	19.8*
50ppm Cu	25	0.1*
50ppm Cu	50	35.3

* - Denotes current rates from pressure-time studies
that are still in progress.

PROGRAM STATUS

- 1. Analytical methods have been selected for monitoring the LP during storage.**
- 2. Preliminary pressure-time screening studies of LP1846 are nearing completion.**
 - a. Preliminary data has provided patterns of decomposition and effects of various contaminants.**
 - b. Data reduction is in progress to establish pressure build-up during long-term storage.**

FUTURE PLANS

- 1. Samples of LP 1845 and LP 1846 from current production lots will be tested.**
 - a. Pressure-time screening studies will be conducted.**
 - i. Clarification of current pressure-time studies.**
 - ii. Effect of other variables and contaminants.**
 - iii. Effect of inhibitors.**
 - b. Initiation of long-term storage studies.**
 - i. Correlation of data from pressure-time studies with data from long-term storage studies.**
 - (a) Establish liquid propellant specifications.**
 - (b) Establish kinetics.**
 - (c) Establish decomposition mechanism.**
 - ii. Comparison of ballistics from exposed and unexposed samples.**
 - III. Determination of propellant lifetime and other safety considerations.**

4th ANNUAL CONFERENCE ON HAN-BASED LIQUID PROPELLANT
STRUCTURE AND PROPERTIES
US ARMY BALLISTIC RESEARCH LABORATORY
ABERDEEN PROVING GROUND, MD
30 AUG - 1 SEP 88

Title of Paper An Overview of the Thermal Reactivity of Substituted
Ammonium Nitrates

Presentation Time Request 30 (min)

Type of Paper: Progress; Summary; State-of-art; Other
Speaker's Name Dr. V. R. Pai Verneker Phone Number (301) 247-0700

Affiliation/address Martin Marietta Laboratories, 1450 South Rollings Rd.
Baltimore, MD 21227

Co-author(s) name(s) S. C. Deevi and C.K. Law, Univ. Of California, Davis, CA 95616

ABSTRACT (Use reverse side if necessary)

The importance of alkyl and aryl substituted ammonium nitrates as energetic materials stems from the fact that both the fuel and oxidizer groups are present within the molecule. An indepth study has been carried out (a) to evaluate the relative thermal stability with increase of substitution on the central nitrogen atom, (b) to examine the thermal stability of the substituted ammonium nitrate due to the configurational stability of the cation, (c) to investigate the role of basicity of the central nitrogen atom on the thermal stability of the ammonium nitrate and (d) to establish a unified mechanism of thermal decomposition process for the substituted ammonium nitrates. Our results based on a variety of thermoanalytical techniques coupled with mass spectrometry revealed that the thermal stability decreases with increase of methyl substitution in the case of mono-, di, and tri-methyl ammonium nitrates. Tetramethyl ammonium nitrate exhibited high thermal stability as compared to the mono-, di- and tri-methyl ammonium nitrates due to the configurational stability of the compact tetramethyl ammonium ion. The overall decomposition process in the case of mono-, di- and tri-methyl ammonium nitrates involves dissociation of the nitrate via proton transfer. Proton transfer process has been shown to occur as in the case of hydroxyl ammonium perchlorate. We present an overview of the thermal behavior of substituted ammonium nitrates and present a unified picture of the decomposition of ammonium nitrates.

MARTIN MARIETTA LABORATORIES

1450 SOUTH ROLLINGS ROAD
BALTIMORE, MARYLAND 21227 3888
TELEPHONE: (301) 247-4700
FAX: (301) 236-9076 E-MAIL: X012474949

THERMAL REACTIVITY OF SUBSTITUTED AMMONIUM NITRATES

BY

V. R. PAI VERNEKER

MARTIN MARIETTA LABORATORIES
BALTIMORE, MARYLAND

AND

S. C. DEEVI AND C. K. LAW
UNIVERSITY OF CALIFORNIA
DAVIS, CALIFORNIA

PRESENTATION WILL DEAL WITH THE THERMAL DECOMPOSITION OF:

1. $\text{NH}_4 \text{ NO}_3$
2. $(\text{CH}_3)_4 \text{ NNO}$
3. $\text{CH}_3 \text{ NH}_3 \text{ NO}_3$, $(\text{CH}_3)_2 \text{ NH}_2 \text{ NO}_3$, $(\text{CH}_3)_3 \text{ NHNO}_3$
4. Ring substituted Aryl ammonium nitrates



WHY STUDY THERMAL DECOMPOSITION...

WHEN THE REAL

INTEREST IS IN COMBUSTION?

SOLID PROPELLANTS:

AGING - ACCELERATED AGING

ROLE OF CONDENSED PHASE

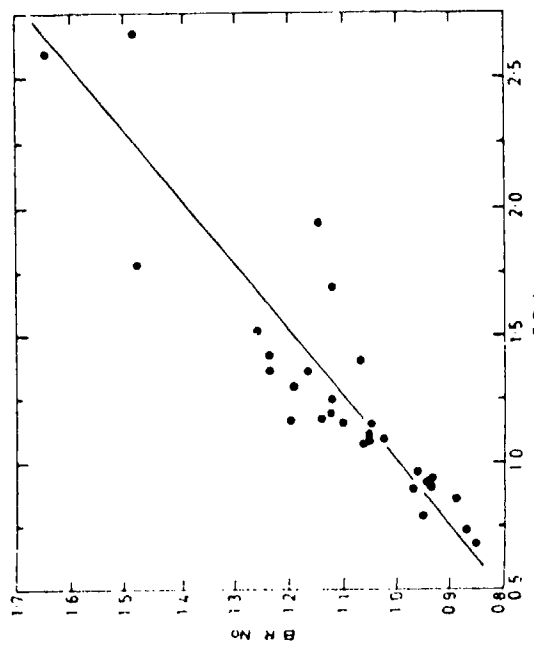


Figure 1 Dependence of B.R. No. on T.D. No. of composite solid propellants

Fuel 56,347,1977

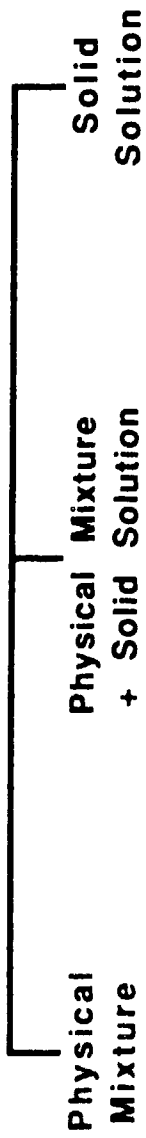
Slope = 1/3

HAN BASED LIQUID PROPELLANTS
(AQUEOUS SOLUTION OF TWO SUBSTITUTED AMMONIUM NITRATES)

- : AGING - NOT RELEVANT
- CONDENSED PHASE - ?

IF WATER LEAVES THE SYSTEM FIRST (LASER HEATING)

THE RESIDUE



ARE SOLID SOLUTIONS POSSIBLE?

ARE THERMAL PROPERTIES ALTERED?

RELATED SYSTEMS AP + KP

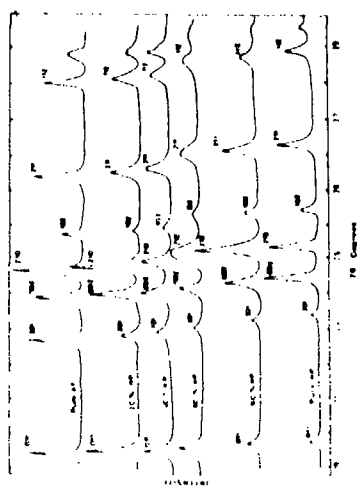


FIG. 5. X-Ray diffractograms of crystallized AP,
KP, and co-crystallized AP-KP mixtures.

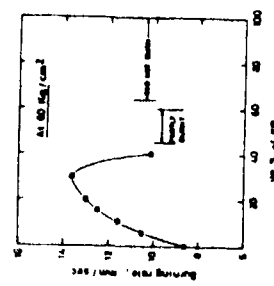
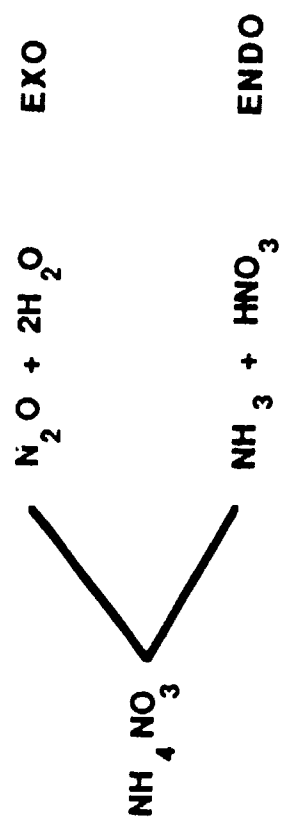


FIG. 8. Variation of burning rate with KP content.

SOLID STATE CHEMISTRY 39, 154, 1981

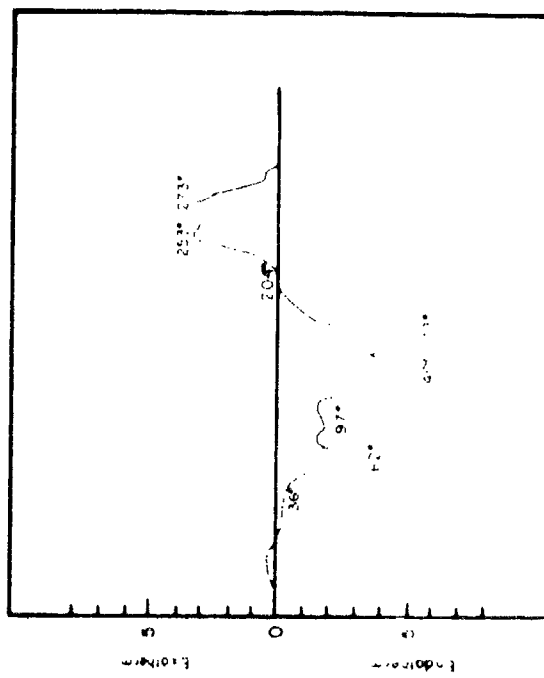
NH_4NO_3 (MELT)



(NO_2 , NO ALSO AT HIGH TEMPERATURE)

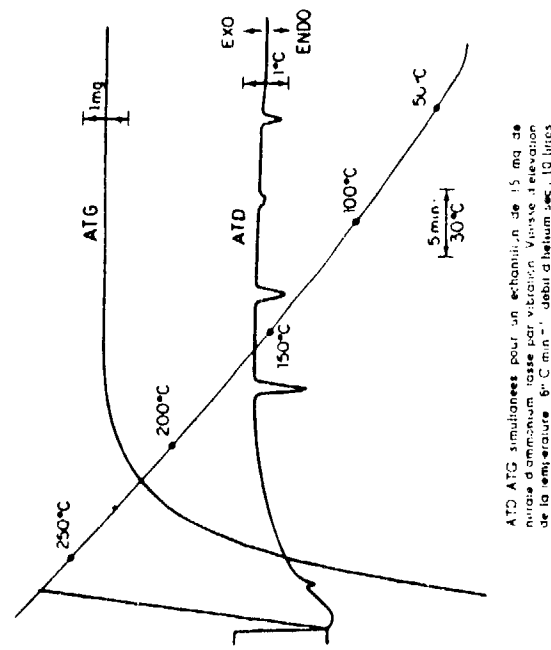
DTA RESULTS

<u>Source</u>	<u>Observations</u>
Robertson 1948	Broad exo resolved 253° C, 273° C
Keenan 1955	Broad exo 280° C
Gordon, Campbell 1955	Endo 308° C
Krien 1965	Endo + exo 250° C
PaiVerneker, Maycock 1969	Broad endo superposed exo 250° C (He atmosphere)
PaiVerneker, Jain, Rao 1978	Exo (1 atmosphere air) 285° C
Kolaczkowski, Biskupski 1981	Endo (Vac 0.5 mm) 209° C Exo 200° C



32

Fig. 4 Differential thermal analysis of NH_4NO_3 .



ATG ATG simultanées pour un échantillon de 15 mg de nitrate d'ammonium, tassé par vibration. Vitesse d'élévation de la température: 6°C min^{-1} ; débit d'hélium: $10 \text{ litres heure}^{-1}$.

Fig. 4
Chem Soc. Ind. London
67, 221, 1948

Fig. 5
Explosives 22, 5, 1969

SPECULATION:



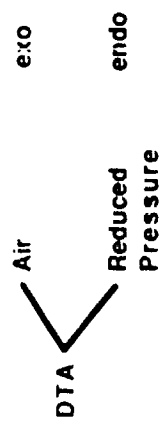
FAST SCAN FTIR RESULTS:



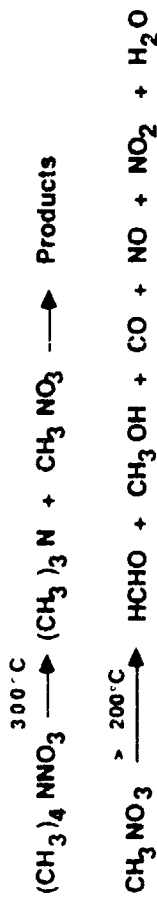
Figure 9. The concentration-time profile of the gas products from NH₄NO₃, heated at 145 K s⁻¹ ($T_f \approx 905$ K, $P = 1.5$ psi of Ar).

Fig. 6
Phys. chem 89, 4328, 1985

$(\text{CH}_3)_4 \text{NNO}_3$ (SOLID)



Analogy



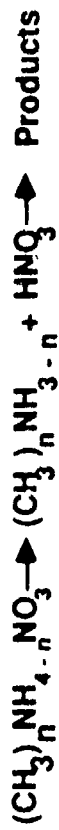
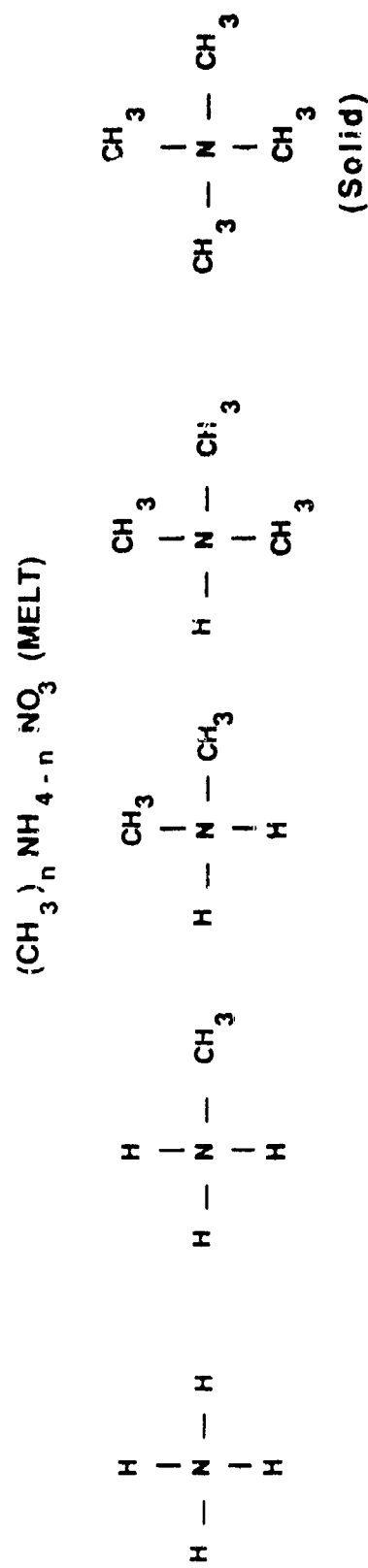
Products (mass spec.)

m/e	Probable assignments	loss current $\times 10^{14}$
1	H_3^+	0.78
12	C_2^+	0.31
14	N_2^+	0.83
15	CH_3^+	2.44
16	$\text{O}^+; \text{CH}_2^+$	0.4
17	OH^+	0.22
18	H_2O^+	1.20
20	C_2H_2^+	0.34
26	$\text{CO}_2^+; \text{N}_3^+$	1.12
28	CH_3O^+	2.0
30	$\text{NO}^+; \text{HCHO}^+; \text{C}_2\text{H}_3^+$	12.9
31	$\text{O}_2^+; \text{CH}_3\text{OH}^+$	3.0
32	$\text{O}_2^+; \text{CH}_3\text{OH}^+$	2.22
42		0.16
43		1.23
44	$\text{CO}_2^+; \text{N}_2\text{O}^+$	5.0
45	$\text{NO}_2^+; \text{HCOOH}^+$	0.10
52	$\text{H}_2\text{C}=\text{N}^+(\text{CH}_3)_2$	0.95
56	$(\text{CH}_3)_2\text{N}^+$	0.10
59		2.40
		0.9

PROC INDIAN ACAD. SCI 187, 31, 1978
ACTIVATION ENERGY
(ISOTHERMAL KINETICS)

TOTAL WT. LOSS 82 KCAL/MOLE
PRODUCTION OF $(\text{CH}_3)_3 \text{N}$ 88 KCAL/MOLE

$\text{H}_3\text{C-N}$ BOND DISSOCIATION ENERGY 80 KCAL/MOLE.



Expected Products

Compound	<u>if H⁺ transfer</u>	<u>if CH₃⁺ transfer</u>
CH_3NH_3^+ NO ₃	CH_3NH_2	NH_3
$(\text{CH}_3)_2\text{NH}_2\text{NO}_3$	$(\text{CH}_3)_2\text{NH}$	CH_3NH_2
$(\text{CH}_3)_3\text{NHNHNO}_3$	$(\text{CH}_3)_3\text{N}$	$(\text{CH}_3)_2\text{NH}$

	Reaction conditions	$(\text{CH}_3)_2\text{NH}_2\text{NO}_2$ Temp. 197°C	$(\text{CH}_3)_2\text{NH}_2\text{NO}_2$ Temp. 160°C
2	H_2^+	0.22	0.44
3	C^+	0.10	0.23
4	N^+	0.49	0.93
5	CH_3^+	0.39	0.53
6	$\text{CH}_3^+ \text{CH}_2^+$	0.16	0.33
7	OH^+	0.47	0.20
8	$\text{NH}_2^+ \text{NH}_3^+$	0.46	0.60
9	H_2O^+	0.22	2.0
10	CO_3^{2-}	0.08	0.97
11	NO_2^-	0.08	0.14
12	$\text{H}^+ \text{CO}_2^+$	0.12	0.10
13	$\text{H}_2^+ \text{NO}_2^+$	0.43	17.2
14	NO_2^+	1.36	0.4
15	CH_3NO_2^+	0.20	4.15
16	O_2^-	0.2	6.04
17	O_3^-	0.36	0.20
18	O_2^-	0.07	0.12
19	O_2^-	0.19	0.10
20	O_2^-	0.12	0.10
21	$\text{CH}_3^+ \text{NO}_2^+$	0.70	4.0
22	$\text{CH}_3\text{NO}_2^+ + (\text{CH}_3)_2\text{NH}_2^+$	0.03	0.12
23	NO_2^-	0.60	2.0
24	O_2^-	0.09	0.16
25	O_2^-	0.26	0.03
26	CH_3NO_2^+	0.2	0.03

Propellants & Explosives

PRIMARY PROCESS IS PROTON TRANSFER

ABSENCE OF $(CH_3)_3N$ MEANS THE SECONDARY PROCESS IS FASTER.

DTA SHOULD CONFIRM.

DTA RESULTS

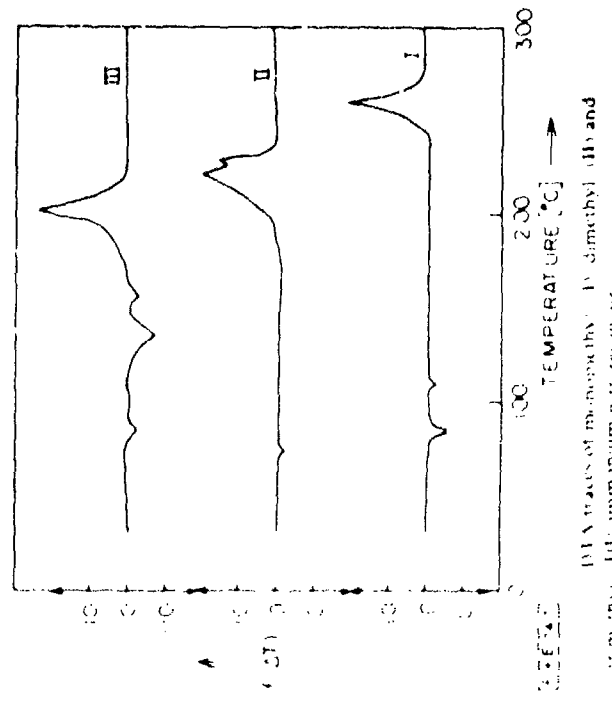


Fig. 7

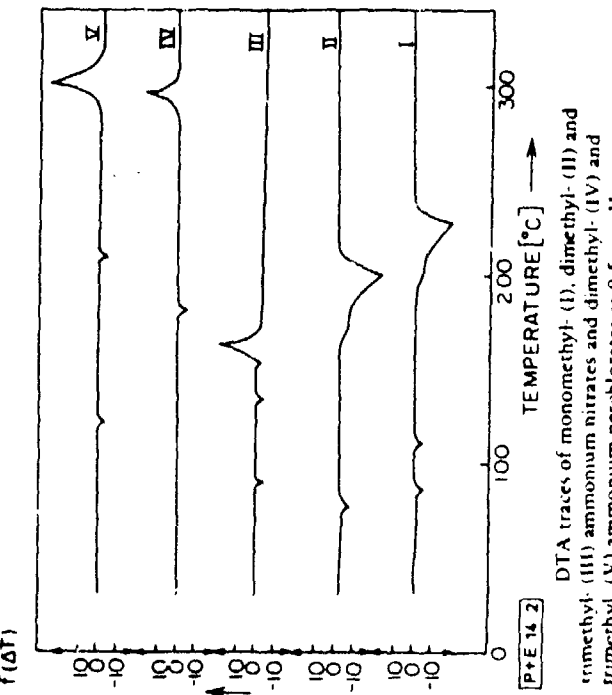
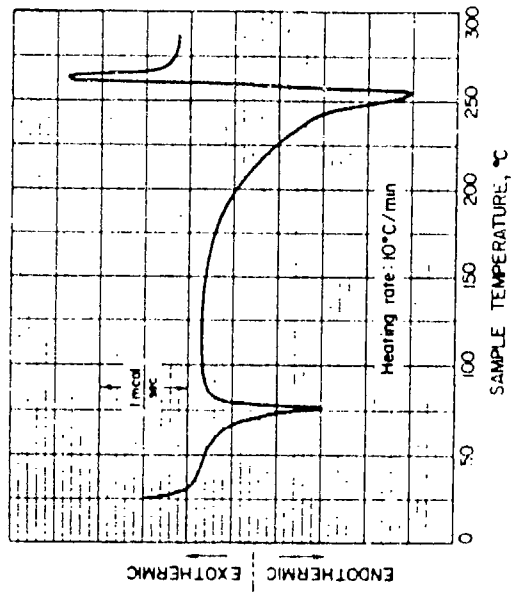


Fig. 8

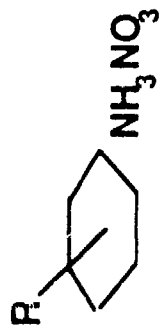
- o Even under reduced pressure, exo is observed for $(\text{CH}_3)_3\text{NHNQ}_3$.
- o Both endo and exo temperatures decrease as methyl substitution on N atom increases.
- o Is there a relationship between structure and stability?
- o In mono substituted arylammonium nitrates, an aryl ring bonded to the basic N atom provides a way to alter basicity.

Different substituents on the aryl ring should change basicity.



MMA-N crystals, dry, sample was prepared in the oven to avoid moisture pickup.
Differential Scanning Calorimeter thermogram for dry MMA-N crystals.

HARZARDOUS MATERIALS
3, 301, 1980



	σ	DTA exo temp	A.E. (isothermal)
$R = NO_2$	13.01	+0.78	15.2kcal/h
$R = CO_2H$	11.62	+0.40	
$R = Cl$	10.01	+0.23	
$R = H$	9.4	0	166°C
$R = CH_3$	8.9	-0.17	185°C
$R = NH_2$	7.9	-0.66	190°C
			202°C
			209°C
			245°C
			26.8kcal/h

4th ANNUAL CONFERENCE ON HAN-BASED LIQUID PROPELLANT
STRUCTURE AND PROPERTIES
US ARMY BALLISTIC RESEARCH LABORATORY
ABERDEEN PROVING GROUND, MD
30 AUG - 1 SEP 88

Title of Paper IMPACT SENSITIVITY OF HAN-BASED LIQUID MONOPROPELLANTS

Presentation Time Request 20 (min)

Type of Paper: Progress; Summary; State-of-art; Other

Speaker's Name Irv Stobie Phone Number (301) 278-6154

Affiliation/address Ballistic Research Laboratory SLCBR-IB-B,

Aberdeen Proving Ground, Md. 21005

Co-author(s) name(s) Bruce D. Bensinger John D. Knapton

ABSTRACT (Use reverse side if necessary)

IMPACT SENSITIVITY OF LIQUID MONOPROPELLANTS

I.C. Stobie, B.D. Bensinger, J.D. Knapton

Ballistic Research Laboratory
Aberdeen Proving Ground, MD. 21005-5066

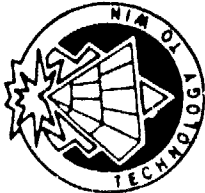
A Technoproduts drop weight tester was used to evaluate impact sensitivity of four liquid monopropellants; OTTO II, NOS 365, LP 1843, LP 1844, LP 1845, and LP 1846. The monopropellants were evaluated for impact sensitivity at ambient temperature and at temperatures in excess of 50 degrees C with energies at and below 100 kg-cm. Four additional propellants, (LGP 1561, LGP 1654, LGP 1798, and LGP 2099) were evaluated with increased diaphragm thickness to study the drop weight sensitivity of the propellants at higher energy values using a technique developed by Princeton Combustion Research Laboratory (PCRL). The propellants were all relatively insensitive to impact at ambient temperatures and the hydroxyl ammonium nitrate based propellants sensitivity increased slightly at temperatures up to 50 degrees. The impact sensitivity of OTTO II increased dramatically as a function of increased temperature. The present tests agreed with the PCRL method using NOS-365 and LP 1845 at higher energy levels. The effect of water content of the LGP propellants was not measurable using the PCRL method.

Reproduced From
Best Available Copy

IMPACT SENSITIVITY OF HAN-BASED LIQUID MONOPROPELLANTS

**Irvin C. Stobie
Bruce D. Bensinger
John D. Knapton**

BALLISTIC RESEARCH LABORATORY



OUTLINE

US ARMY
LABORATORY COMMAND

BALLISTIC RESEARCH LABORATORY

ASTM D2540

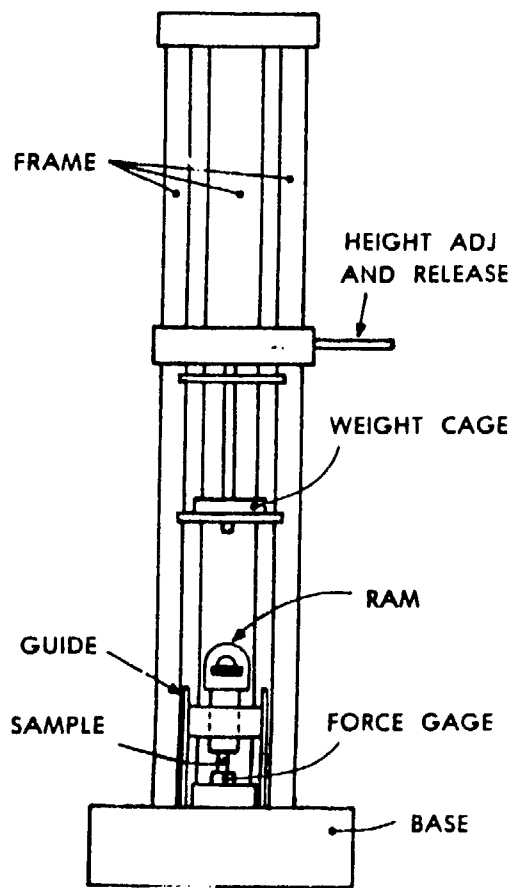
- NORMAL PROPYL NITRATE
CALIBRATION: TECHNOPRODUCTS INSTRUMENT
- AMBIENT LIQUID MONOPROPELLANTS
OTTO II
NOS-365
LP 1845
LP 1846
- TEMPERATURE SENSITIVITY
34 - 57 DEGREES C
- CONDITIONED TO SENSITIVITY CHANGE
OTTO II
LP 1846 TO 82 DEGREES C

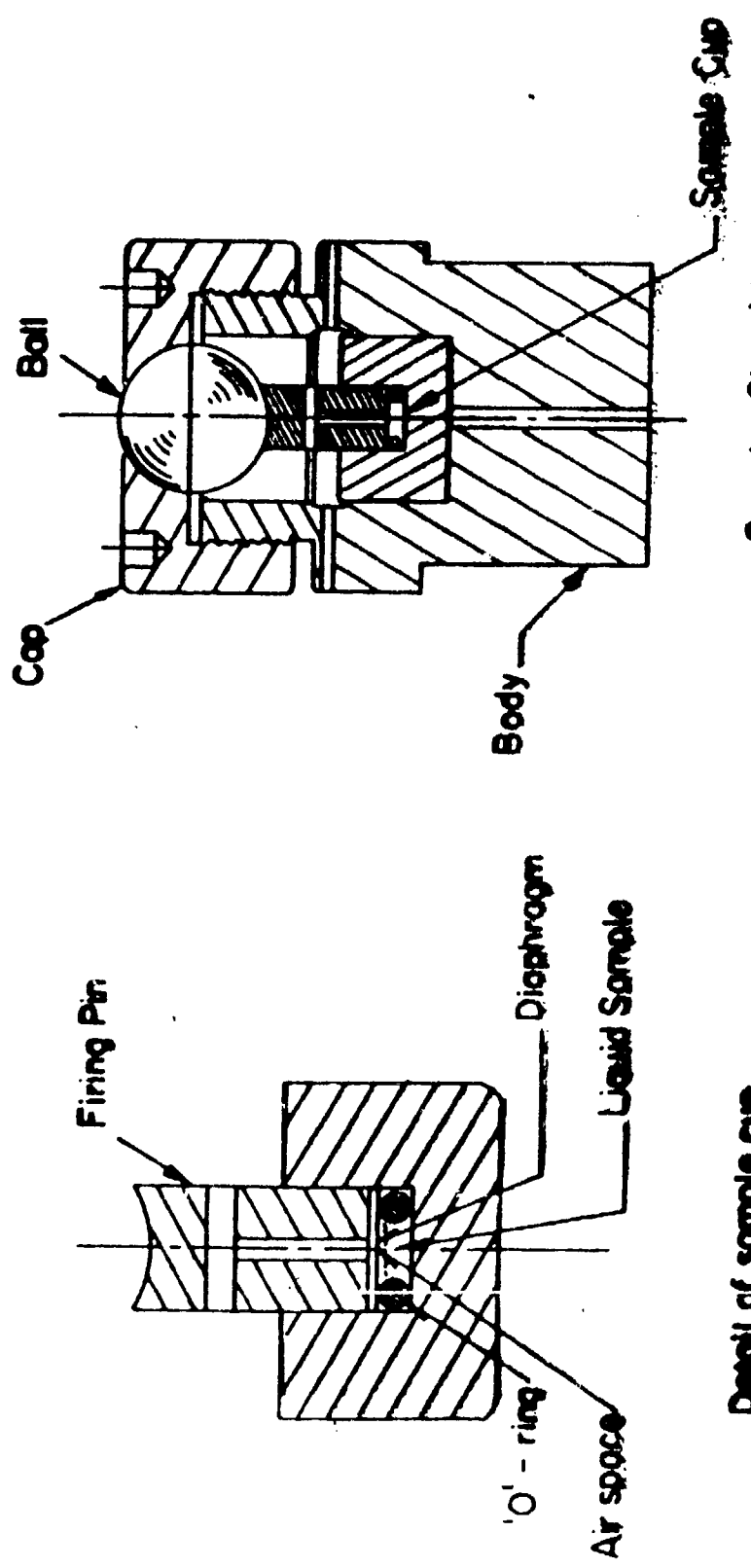
PCRL INCREASED ENERGY DROPWEIGHT

- CALIBRATION WITH NOS-365 AND LP 1845
- WATER CONTENT SENSITIVITY

High Rate Mechanical Response

Drop Weight Mechanical Properties Tester





NORMAL PROPYL NITRATE

SOURCE	50-% POSITIVE kg cm
ASTM D 2540	8.4
Mason et al.	17.3
BRL, 1982	12.8
BRL, 1986 (90% - 99.9%)	-
GC - Iso propyl nitrate	-

OTTO-I I 34-77 Nov 1976

NITRATE ESTER - DESENSITIZED - STABILIZER

9.5 - 70 kg cm - Mason, Ribovich, Weiss, Bureau of Mines

NOS-365 THIOKOL, Lot 240

HAN - IPAN

> 100 kg cm - Smith et al., NSWC

152 kg cm - Cruice, Hazards Research Corp.

LP-1845 THIOKOL, Lot 244

HAN - TEAN

152 kg cm - Cruice, Hazards Research Corp.

LP-1846 NOS, Lot 50-3

HAN - TEAN + 3 % Water

AMBIENT MONOPROPELLANT DROP WEIGHT TESTS

PROPELLANT	REFERENCE TEST 50% IGNITION (kg-cm)	PRESENT STUDY 50% IGNITION (kg-cm)
OTTO II	8.5-70	98
NOS-365	>100	98
LP 1845	152	33% @100
LP 1846	---	>100

ELEVATED TEMPERATURE TESTS

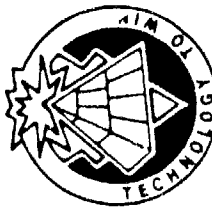
PROPELLANT	TEMPERATURE	50 % IGNITION
	°C	kg cm
Otto-II	ambient	98
	34 - 54	< 52
NOS-365	ambient	98
	34 - 49	93
LP 1845	ambient	(33 % - 100)
	37 - 57	88
LP 1846	ambient	> 100
	31 - 53	96

LP 1846 SENSITIVITY CONDITIONED LESS
THAN 82 DEGREES C

TEST NOS.	TEMPERATURE (degrees C)	ENERGY (kg-cm)	POSITIVE RESULTS
18 JUNE 51-57	54-62	100 98 96 80	2/4 1/1 1/1 1/1
20 JUNE 1-5	22	100	0/5
20 JUNE 8-15	44-48	100 94 92 90	1/1 2/2 2/4 0/2

TEMPERATURE SENSITIVITY OF OTTO II

TESTS	ENERGY (kg-cm)	TEMPERATURE (degrees C)	POSITIVE RESULTS
1-5	96-100	38-40	3/5
6-10	80-92	38-45	4/5
11-15	68-74	35-45	4/5



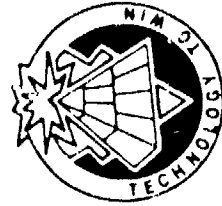
AMBIENT DROP WEIGHT RESULTS PCRL METHOD

BALLISTIC RESEARCH LABORATORY

US ARMY
LABORATORY COMMAND

PROPELLANT	REFERENCE	RESULTS (kg-cm)
NOS-365 (Lot 240)	140.8	152
LP1845 (Lot 292)	-	148
LP1845 (Lot 244)	154.6	-
LGP 1561	-	158
LGP 1654	-	164
LGP 1798	-	160
LGP 2099	-	152

CONCLUSIONS



BALLISTIC RESEARCH LABORATORY

US ARMY
LABORATORY COMMAND

- o The liquid propellants are insensitive to the maximum drop weight condition using ASTM 2540 at ambient temperatures.
- o The drop weight sensitivity increased slightly for the three HAN-based monopropellants at temperatures up to 57 degrees C.
- o The sensitivity of LP1346 increased at temperatures between 78 and 82 degrees C. This shift in drop weight sensitivity is believed to be due to loss of water in the liquid propellant.
- o Reasonable agreement with PCRL increased energy tests was observed with NOS 365 and LP 1845.
- o The water content difference of the new formulations could not be detected with the PCRL method.

Dr. Hans Joachim de Greiff
Fraunhofer-Institut für Chemische Technologie (ICT)
Joseph-von-Fraunhofer-Straße
P.O.Box 12 40
D-7507 Pfinztal 1 (Berghausen)
Phone: (0721)4640-321
Telex: 7 826 909 ict d
Telefax: (0721)46 40-111

Quantitative Analyses of HAN-Based Liquid Propellants

Abstract

This paper deals with quantitative analyses of HAN-Based monopropellants, in particular following stability tests. In the case of the propellant LP 1846, the compounds hydroxylamine nitrate and triethanolammonium nitrate are determined as the primary compounds, while free nitric acid and ammonium nitrate are considered as decomposition products.

As a determination method, potentiometric titration with water as solvent has been selected, using as apparatus a Metrohm "Titroprocessor 636" with a combined glass electrode as an indicator.

The propellant components were to be quantified by simultaneous titration in a sample. Therefore, the pK values of the different propellant components have been measured before starting the analytical work. HAN and AN had to be converted to derivates (acetoxim and formaldoxim) to enable the separation of the compounds.

As for triethanolammonium nitrate containing propellants such as LP 1846, AN can be titrated after steam distillation due to the nonvolatility of the free triethanolamine.

Table 1

Dissociation constants K_A as well as relevant pK_A^- and pK_B values in a number of propellant components in aqueous solution at 20 °C.

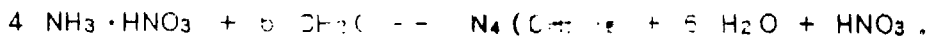
No.	Propellant Components	K_A mol x dm ⁻³	pK_A	pK_B
1	Hydroxylammonium nitrate (HAN) + formaldehyde --> formaldoxime	0.245×10^{-1}	1.61	12.56
2	Hydroxylammonium nitrate (HAN) + Acetone --> Acetoxime	0.191×10^{-1}	1.72	12.45
3	Ammonium nitrate (AN) + formaldehyde --> hexamethylene tetramine	0.141×10^{-5}	5.85	8.32
4	Hydroxylammonium nitrate (HAN)	0.733×10^{-6}	6.135	8.035
5	Triethanol ammonium nitrate (TEAN)	0.112×10^{-7}	7.95	6.22
6	Ammonium nitrate (AN)	0.331×10^{-9}	9.48	4.69
7	Isopropyl ammonium nitrate (IPAN)	0.138×10^{-10}	10.86	3.31

Determination of the pK value by potentiometric titration in accordance with the Henderson-Hasselbalch equation:

$$\text{pH} = \text{pK}_A - \log(C_{\text{acid}}/C_{\text{salt}}).$$

If the concentration of the acid is equal to that of the salt, the logarithmic term then becomes zero, and pK is equal to pH.

Ammonium salts react with formaldehyde to form the very weak base hexamethylen tetramine



Aldoxime or acetoxime is obtained from hydroxylammonium nitrate with formaldehyde or acetone:



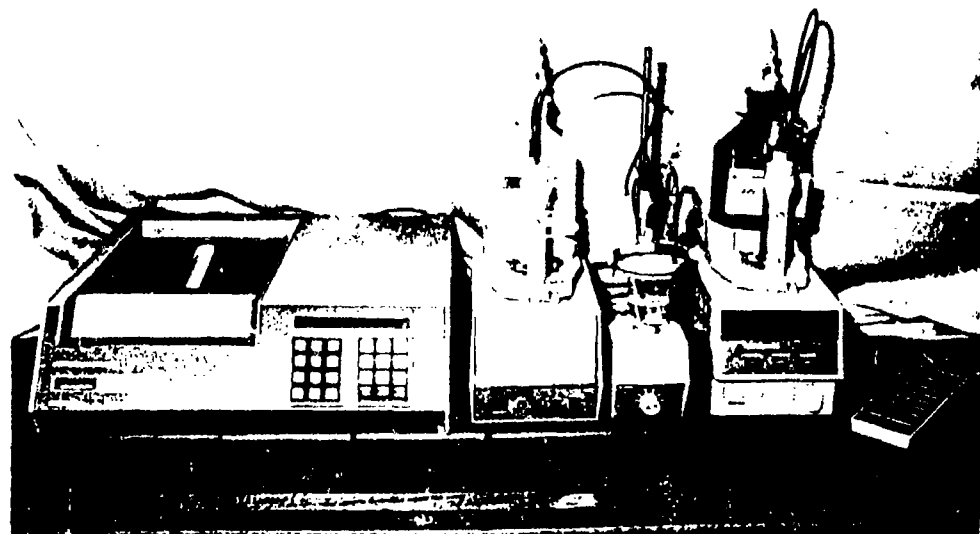


Fig. 1: Metrohm Titroprozessor 636

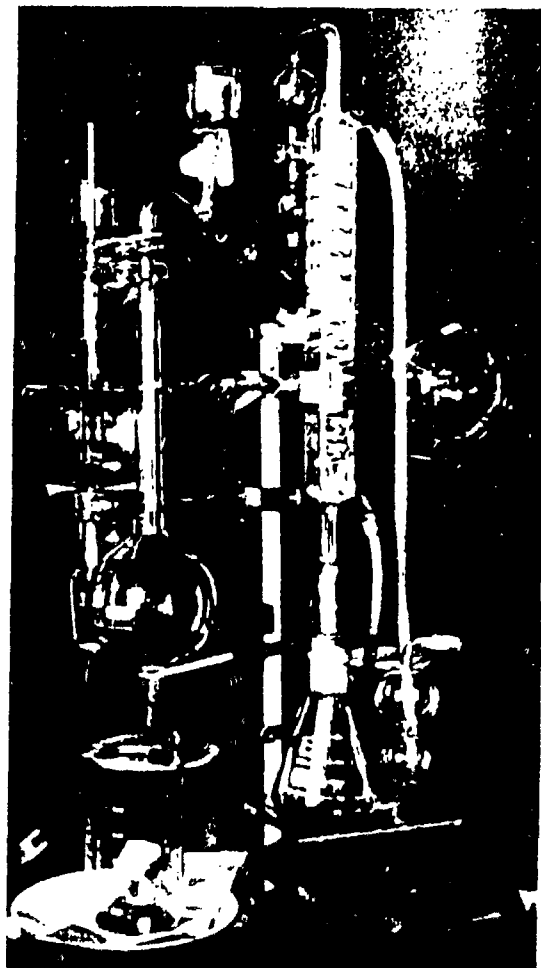


Fig. 21
Steam Distillation
Unit after Strohlein

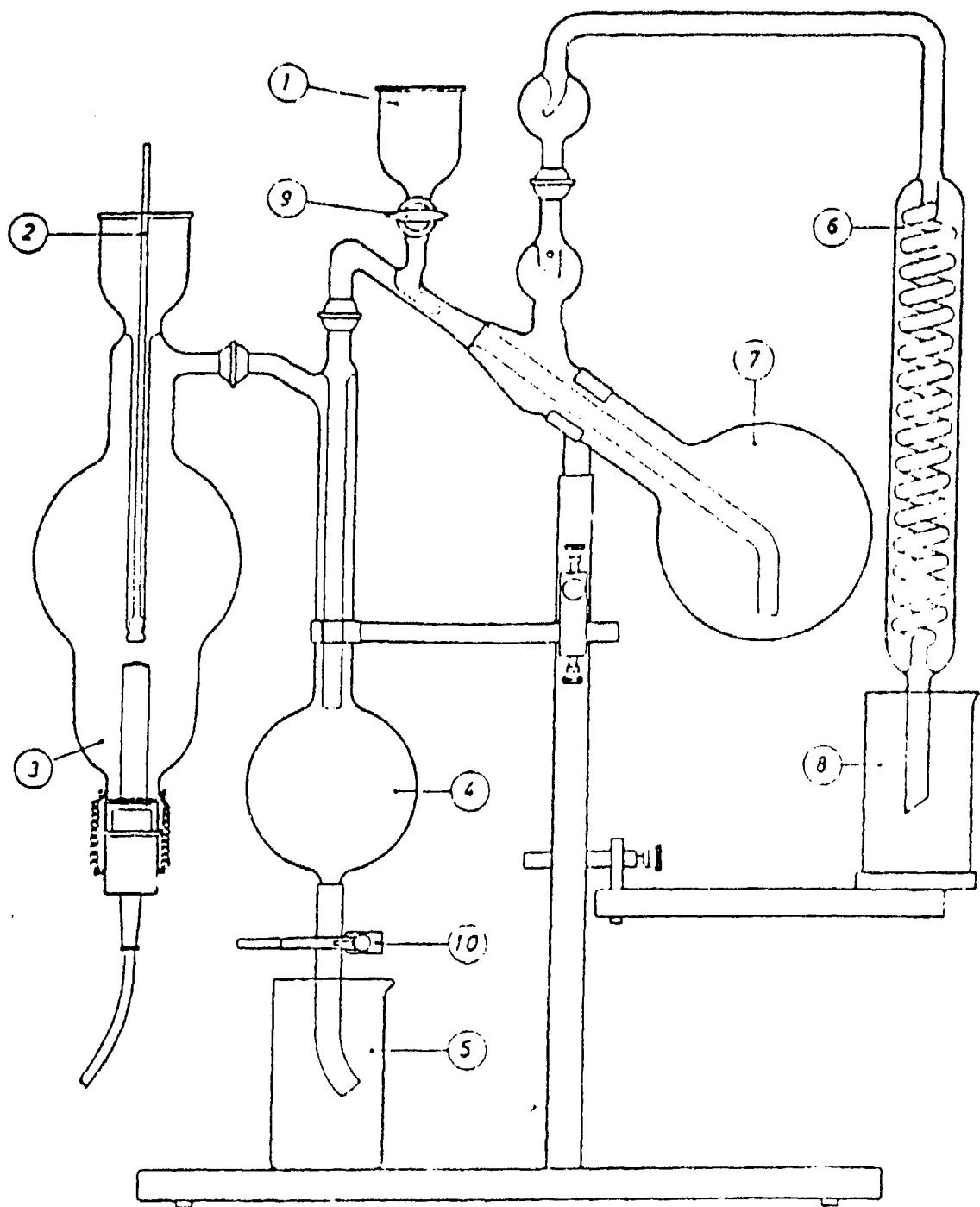
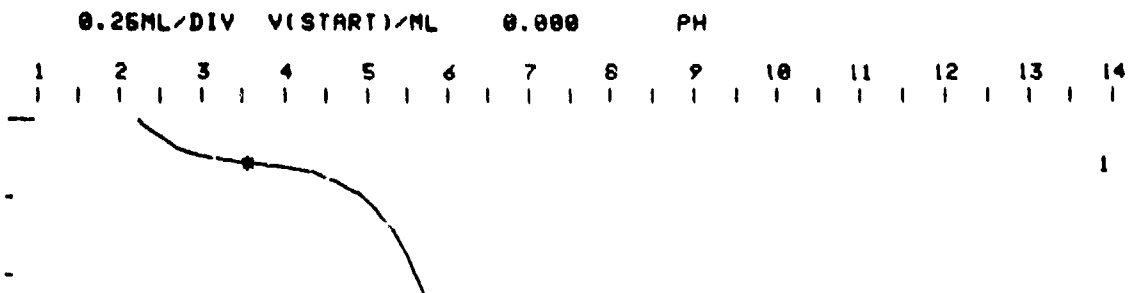
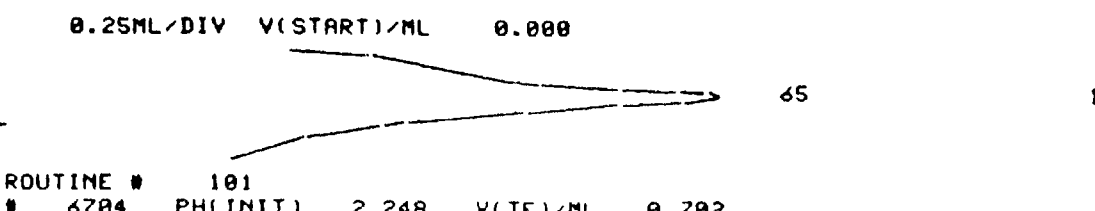


Fig. 3, Scheme of the Steam Distillation Unit

- (1) Inlet connection for the Sample, (3) Electric boiler,
- (4) Drop Separator, (6) Condenser, (7) Distilling flask,
- (8) Receiver.



DATE 17.12.87 NAME Martini



DATE 17.12.87 NAME Martini

BUR.1 V/ML	5.0	ROUTINE #	101
TEMP/C	22.0	REAGENT	0.0m KOH, aqueous, Titrisol
KINET D	8.0	TITER	1.0047
MPD VAR	8.0	ELECTRODES 1	(Metrohm) combined micro pH glass
START V/ML	0.000		electrode (type T)
STOP PH	100.000	SAMPLE	
STOP V/ML	5.000	563.6mg dilution (= 176.12mg propellant) were	
STOP # EP	9.0	added with 10ml H ₂ O and titrated.	
PAUSE/S	0.0		
EP-CRIT	5.0	REMARKS	
ADD V/ML	0.000	Determination of the concentration of nitric	
EP-W LIM1	0.000	acid (HNO ₃) in liquid propellant.	
PH LIM2	14.000	HNO ₃ = 2.62%	
0105			

Fig. 4: Analysis of LP 1846: Determination of free nitric acid: Titration curve (top) and 1st derivative (bottom)

0.25ML/DIV V(START)/ML 0.000 PH



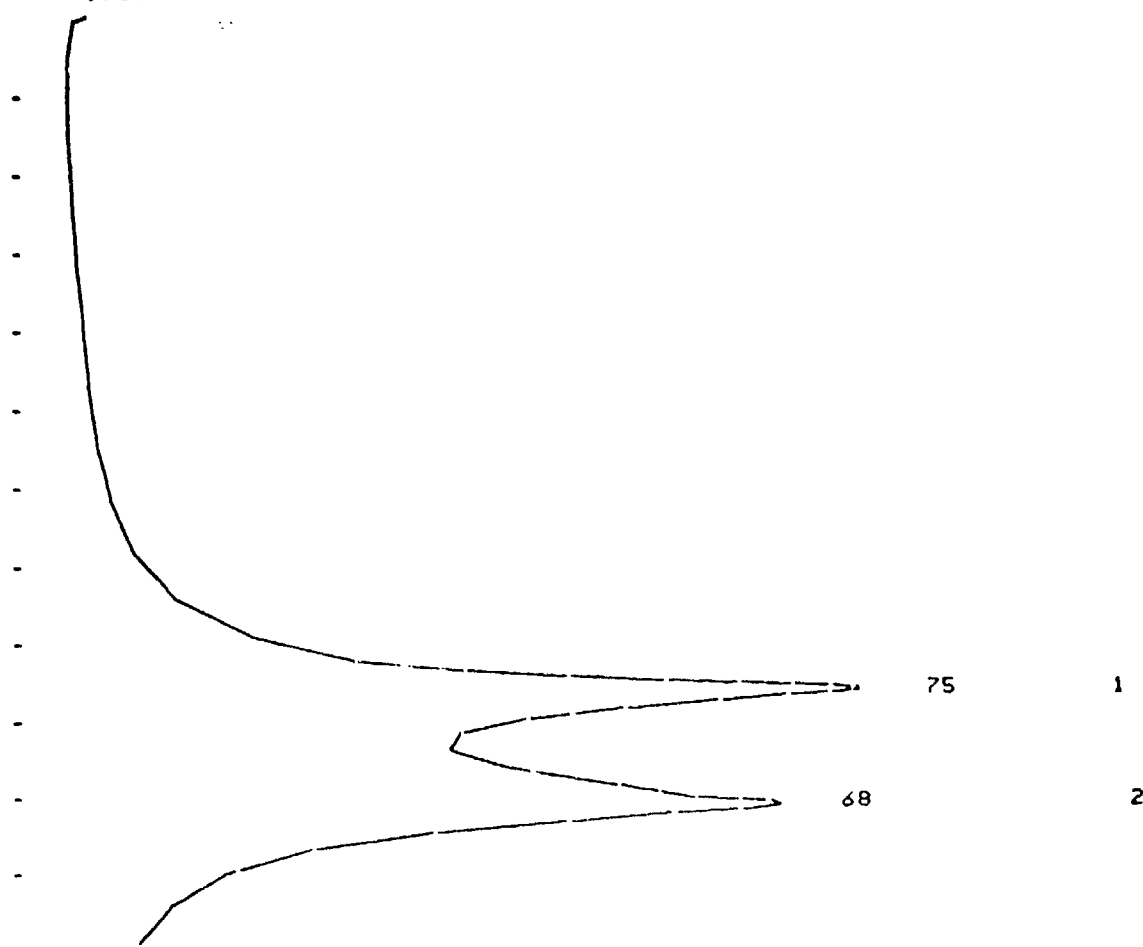
153

ROUTINE # 181
1706 PH(INIT) 1.410 V(TE)/ML 3.476
1 V/ML 2.181 PH(M) 5.048
2 V/ML 2.547 PH(M) 10.163

DATE 5.11.87 NAME Murtini

Fig. 5: Analysis of LP 1846: Simultaneous determination of HAN and TEAN by substitution titration: Titration curve.
Here: 1) Determination of HAN after acetoxime formation by the addition of acetone
2) Determination of TEAN

0.25ML/DIV V(START)/ML 8.000



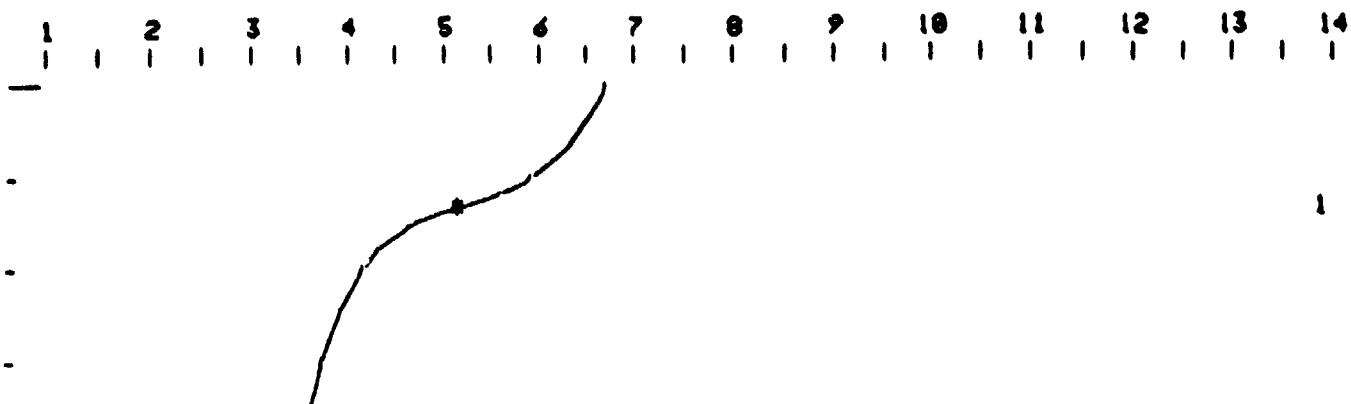
ROUTINE # 101
1706 PH(INIT) 1.410 V(TE)/ML 3.476
1 V/ML 2.184 PH(M) 5.048
2 V/ML 2.547 PH(M) 10.163

DATE 5.11.87 NAME Martini

BUR.1 V/ML	5.0	ROUTINE #	101
TEMP/C	23.0	REAGENT	0.5m KOH, aqueous, Titrisol
KIMET D	8.0	TITER	1.004
MPD VAR	8.0	ELECTRODES 1	(Metrohm) combined micro pH glass
START V/ML	0.000		electrode (type T)
STOP PH	100.000	SAMPLE	
STOP V/ML	5.000		358.1mg dilution (= 170.5mg propellant) were
STOP # EP	9.0		added with 10ml H ₂ O and 5ml acetone and titrated.
PAUSE/S	0.0		
EP-CRIT	5.0	REMARKS	
ADD V/ML	0.000		Determination of the concentration of hydroxyl-
EP-W LIM1	0.000		ammoniumnitrate (HAN) and triethanolammonium-
PH LIM2	14.000		nitrate (TEAN) in liquid propellant.
0105		HAN = 57.08%	TEAN = 17.15%

Fig. 6: Analysis of LP 1846: Simultaneous determination of HAN and TEAN by substitution titration: 1st derivative.
Here: 1) Determination of HAN after acetoxime formation by the addition of acetone
2) Determination of TEAN

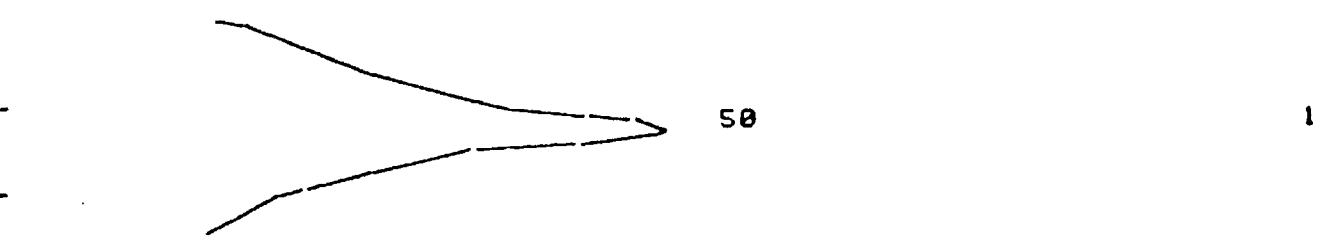
0.50ML/DIV V(START)/ML 0.000 PH



ROUTINE # 101
17102 PH(INIT) 6.781 V(TE)/ML 2.089
1 V/ML 0.680 PH(M) 5.165

DATE 10.03.88 NAME Martini

0.50ML/DIV V(START)/ML 0.000



ROUTINE # 101
17102 PH(INIT) 6.781 V(TE)/ML 2.089
1 V/ML 0.680 PH(M) 5.165

DATE 10.03.88 NAME Martini

BUR.1 V/ML	10.0	ROUTINE #	101
TEMP/C	23.5	REAGENT	0.05M HCl, aqueous, Titrisol
KINET D	8.0	TITER	0.4442
MPD VAR	8.0	ELECTRODES 1	(Metrohm) combined micro ph glass electrode (type T)
START V/ML	0.000	SAMPLE	105.3mg pure liquid propellant were added with
STOP PH	100.000		25ml Fehling I, 25ml Fehling II, 25ml H ₂ O,
STOP V/ML	10.000		distilled and titrated.
STOP # EP	9.0	REMARKS	receiver: 10ml 4% boric acid
PAUSE/S	0.0		Determination of the concentration of ammonium
EP-CRIT	5.0		nitrate (AN) in liquid propellant.
ADD V/ML	0.000		AN = 2.58%
EP-W LIM1	0.000		
PH LIM2	14.000		
0105			

Fig. 7: Analysis of LP 1846: Titration of Ammonia in diluted boric acid with 0.05 N hydrochloric acid, Titration curve (top) and 1st derivative (bottom)

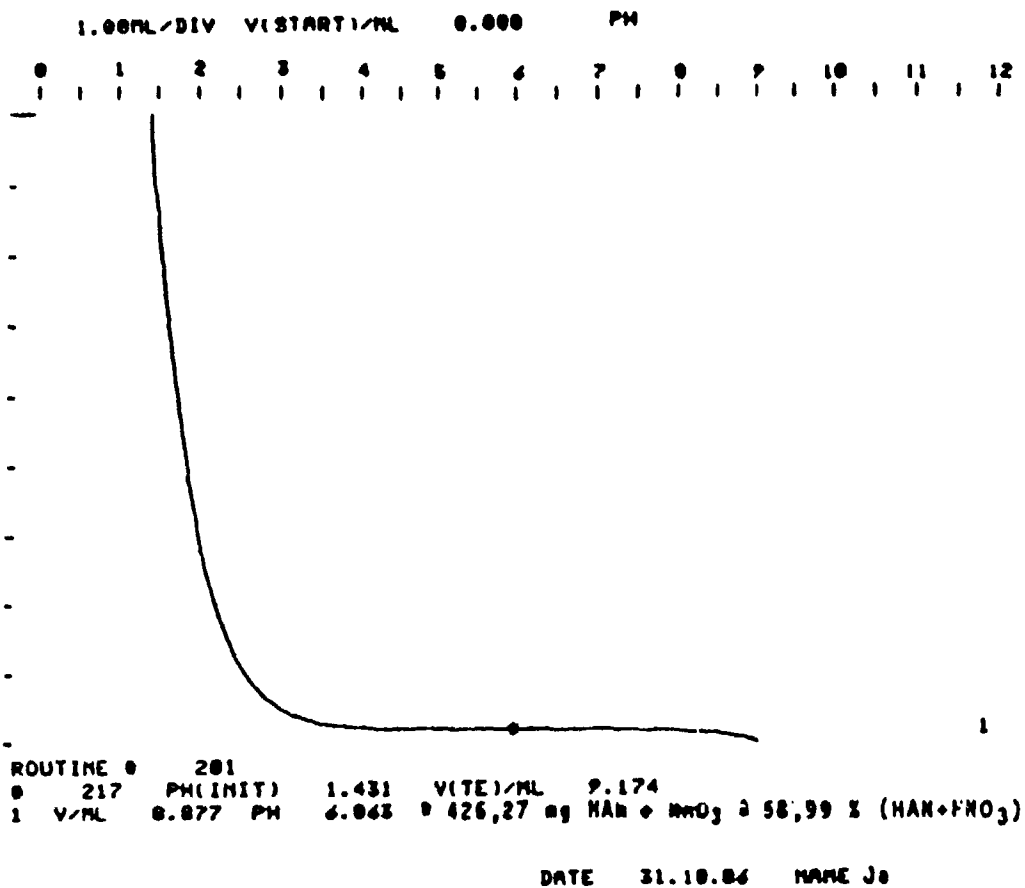
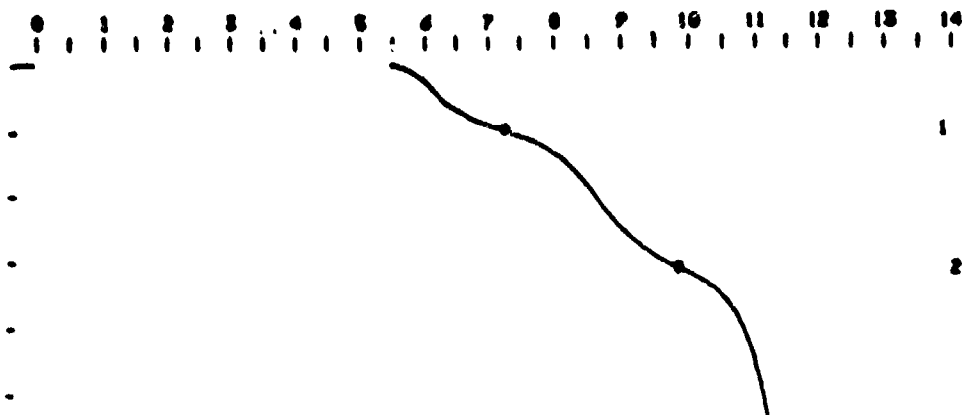


Fig. 8: Analysis of NOS-365:
 Simultaneous determination of HAN, IPAN and
 AN by substitution titration:
 Here: Determination of HAN after formation of
 acetoxime by the addition of acetone

1.00ML/BIV V(START)/ML

0.000

PH



ROUTINE 0

0 217 PH(INIT) 5.485 V(TE)/ML 5.868

1 V/ML 1.009 PH 7.311

2 V/ML 3.003 PH 2.074 ml + 126,64 mg IPAN + 17,53 x IPAN

DATE 31.10.86 NAME J.B.

BUR.2 V/ML 10.0

TEMP/C 25.0

KIMET D 0.0

MPD VAR 0.0

START V/ML 0.000

STOP PH 100.000

STOP V/ML 10.000

STOP 0 EP 0.0

PAUSE/S 0.0

EP-CRIT 5.0

ADD V/ML 0.000

EP-H LIM1 0.000

PH LIM2 14.000

0105

ROUTINE 0 201

REAGENT 0,5 n NaOH w&b. Titrisol

TITER 1.000

ELECTRODES 2 Kombinierte Glaselktrode Mettoba

SAMPLE 722,6 mg NOS 365 + 10 ml Aceton (Lan-Best.)

+ 5 ml Formaldehyd 37

+ 406,9 mg NH₄NO₃ lsg. (=3P,11 mg 10% Z)

REMARKS

1.00ML/BIV V(START)/ML 0.000



ROUTINE 0

0 217 PH(INIT) 5.485 V(TE)/ML 5.868

1 V/ML 1.009 PH 7.311 + 426,27 mg (HAN+HNO₃) + 58,99 x (HAN+HNO₃)

2 V/ML 3.003 PH 2.074 ml + 126,64 mg IPAN

+ 17,53 x IPAN

DATE 31.10.86 NAME J.B.

Fig. 9: Analysis of NOS-365:

Simultaneous determination of HAN, IPAN and AN by substitution titration: Titration curve (top) and 1st derivative (bottom).

Here:

- 1) Determination of AN after the addition of ammonium nitrate at a known quantity and the addition of formaldehyde (formation of hexamethylene tetramine)
- 2) Determination of IPAN

An Overview of the U.K. Approach to the Characterisation and Classification of the HAN-Based Liquid Propellant LP101.

S Westlake.

Royal Armaments Research and Development Establishment.
Powdermill Lane, Waltham Abbey, Essex EN9 1AX,
(United Kingdom).

Summary.

HAN-Based liquid propellant LP101, is currently being considered by the U.K. for use as a liquid propellant for guns. This paper summarises the initial assessment of LP101 for this use. It covers work connected with the manufacture and assay of the propellant and the assessment of its stability and compatibility with other materials it's likely to come into contact with during manufacture, storage and use. This paper will briefly outline some of the methods used in this assessment.

* * *

COPYRIGHT  CONTROLLER HMSO, LONDON 1988

CONTENTS.

1. Introduction.
2. Manufacture.
3. Compatibility and Stability.
4. Hazard Assessment.
5. Conclusions.
6. References.
7. Figure 1.

Problems have been encountered in finding a suitable method for assaying the propellant. It is very difficult to analyse HAN in the presence of TEAN. Chromatographic and titrimetric methods have been tried, but in both cases the results were non reproducible. The reaction between HAN and benzaldehyde was the basis of both methods.



In the titrimetric method the liberated nitric acid is titrated against ethanolic potassium hydroxide. In the chromatographic method the liberated water is detected by gas chromatography. It is believed that the reaction of benzaldehyde with HAN does not go to completion, hence the non reproducible results observed.

At the moment the propellant is blended by weight. The water content of the propellant is then determined by gas chromatography or Karl Fischer.

This situation is obviously not ideal and effort is being made to find a suitable method. However we have been assured that there has been good reproducibility between the blends that have been manufactured to-date.

The density, viscosity and refractive index of each blend is measured. Inorder to determine the effect of slight compositional changes on these parameters several small batches of modified composition have been made. These are shown in Table 1. along with their measured density, viscosity and refractive index.

COMPOSITION %HAN %TEAN %WATER	DENSITY 20°C	R.I. 24°C	VISCOSITY				
			-16	-10	0	10	20 °C
63.2 20.0 16.8	1.4555	1.4670	43.5	32.2	22.1	15.3	12.4
64.7 20.5 14.8	1.4748	1.4723	58.2	42.5	25.3	18.3	13.8
61.7 19.5 18.8	1.4409	1.4730	38.5	26.0	18.3	14.7	11.8
61.2 22.0 16.8	1.4482	1.4668	45.0	30.5	21.7	15.7	12.8
85.2 18.0 18.8	1.4824	1.4870	37.3	29.3	18.5	13.0	9.0

TABLE 1.

The different compositions represent propellants that are outside the specification limits and cover the variation of HAN/TEAN ratio at constant water and of water at constant

1. Introduction.

LP101 is currently being assessed by the U.K. as a liquid propellant for guns, with the emphasis being on its ultimate use as a tank gun propellant. The U.S. have spent many years researching the possibilities of using liquid propellants for both artillery and tank guns and have produced several viable propellants. LP101 is equivalent to American LPG 1845, but has been given a U.K. designation for specification purposes and to avoid confusion with propellant of U.S. origin. Like LPG 1845, LP101 is a solution of Hydroxylammonium nitrate (HAN) and triethanolammonium nitrate (TEAN) in water.

Prior to the start of this project U.K. experience with liquid propellants had been concentrated on packaged systems and confined to very specialist use. The gun propellant being proposed was unlike any propellant currently in service use in the U.K. and so a programme was set up to establish its characteristics and suitability for service use. The U.K. had access to a certain amount of U.S. data, but as LP101 was manufactured in the U.K., using ingredients from British suppliers, it was necessary to characterise the propellant, as made, to ensure that LP101 was indeed comparable to LPG 1845.

Royal Ordnance were contracted to manufacture the propellant and to determine its compatibility with other materials likely to come into contact with it.

2. Manufacture.

LP101 is a solution of hydroxylammonium nitrate (HAN) and triethanolammonium nitrate (TEAN) in water. The TEAN is manufactured from Triethanolamine and nitric acid and purified by crystallisation. The HAN is currently manufactured by a chemical method (which is commercial-in-confidence) and supplied as a 40% solution in water. However, HAN, from an alternative supplier, is in the process of being assessed. This HAN is supplied as a 24% solution. The HAN from both suppliers requires concentrating before blending. Concentration takes place under vacuum and the temperature is not allowed to exceed 80°C. This requires a vacuum of about 5mm of mercury to remove the last few percent of water and still keep the temperature below 80°C.

The HAN and TEAN are blended together and the percentage of water adjusted to give a suitable propellant.

HAN/TEAN ratio. This was to determine the effect a variation from specification had on these physical properties.

The refractive index varied linearly with water content but not with the HAN/TEAN ratio in the range studied. The low temperature viscosity increased markedly as water content decreased but only slightly as the TEAN is increased. The density varies linearly with respect to TEAN but is non linear with respect to water. The density variation is shown graphically in figure 1.

Density and refractive index are now being used to monitor the blending process.

It is known that the stability of HAN based propellants is seriously affected by metal ion contamination, particularly iron and copper. Therefore each batch of propellant has been screened for iron using atomic adsorption. The results are shown in table 2.

Blend No:	ppm wt/wt	
	Copper	Iron
2	0.03	0.3
4	0.10	0.4
5	N.D.	0.3
6	0.17	0.3

Table 2.

3. Compatibility and Stability.

As part of the propellant assessment programme a test procedure has been developed to screen all materials that are likely to come into contact with the propellant during manufacture, storage and life.

Candidate materials are initially checked for possible severe incompatibility using a splash and immersion test. A few drops of propellant are placed in contact with the candidate material so that the surface is just wetted. Observations are made over one hour. If no rapid reaction or decomposition occurs then more propellant is added such that the sample is just submerged. The test is examined after a further hour, after 5 hours, 24 hours and 7 days. All observations are recorded.

If no rapid reaction or decomposition occurs the test is repeated at 60°C. These tests can warn of severe incompatibility and screen materials for short term exposure and accidental contact.

Materials under consideration for long term contact are subjected to further tests to establish their long term compatibility. In this test aging is accelerated by using elevated temperatures. Most monopropellants are inherently thermally unstable and give rise to gaseous products when heated. This decomposition can be catalysed by contamination or contact with foreign material.

The test to establish long term stability compares gas evolution of propellant in contact with candidate material, when held at an elevated temperature, with that of control samples. The gas evolved is monitored for up to 6 months using a pressure transducer and the temperature of the test is 69°C. This temperature was the lowest temperature at which measurable levels of gas could be detected from the control samples. On completion of the test the propellant is analysed for dissolved and particulate matter and the candidate materials are tested for any changes in physical properties. Full details of both the short and long term stability tests are given in reference 1 and 2.

These tests are not totally satisfactory. They are not general enough to detect all types of incompatibility reaction; for example a non gas producing reaction or one with an initial induction period. However virtually all reactions are accompanied by heat generation. A test method has been developed using heat flow calorimetry to determine if the propellant is thermally stable. This test will show if any treatment of the propellant, such as heating or contact with a suspect material, has affected its chemical stability. Full details of the test are given in reference 3 and will be described in the following paper.

The test has also been used to screen the batches of propellant that have so far been manufactured. Good correlation has been found between iron content and thermal stability, as demonstrated by this method.

An example where gas generation can be misleading was observed during some work designed to measure the rates of gas evolution from samples of LP101 heavily contaminated with metal ions (reference 4). Samples of LP101 containing 0.5 g/litre of Cu^{2+} were heated at 50, 60 and 70°C for up to 4 days. The sample heated at 70°C gave an initial gas evolution rate of 1.48 cc/hour. This steadily decreased and after 3 days the rate had reduced to 0.67 cc/hour. After 4 days the sample "boiled off" and the contents of the container were ejected with some violence. This experiment gave strong indication that the reactions taking place during the decomposition of LP101 are not simple. It is obvious that there are at least two different reactions occurring in this case.

4. Hazard Assessment.

As part of the qualification procedure, a new propellant needs to be screened to establish whether or not it is a candidate for inclusion in UN Class 1, ie whether it needs to be treated as an explosive or not. This screening is required for transport and storage purposes. It was hoped that LP101, if suitably packaged, would not fall into this category and be classed as non explosive. In order to establish this LP101 was subjected to UN series 1 and 2 tests. These tests are described in detail in reference 5 but are described briefly below:-

BAM 50/60 Steel Tube. Propellant is placed in a steel tube of 50mm i.d. and 60mm external diameter and subjected to the detonative shock from a 50g Debrix 13 high explosive booster and a No 8 aluminium concave-based detonator in series 1 and 2 respectively. The number and size of the tube fragments determines whether the propellant is class 1 or not.

Koenen Steel Tube. Propellant is placed in a 24mm diameter steel tube of 70mm length, closed at one end with an orifice plate. The tube is heated and in consecutive tests the orifice is reduced until fragmentation of the tube occurs. The size of the orifice that causes fragmentation determines whether the propellant is class 1 or not.

The results of these tests classified the propellant as UN Class 1. These tests do not allow for differentiation between high explosive (1.1) or propellant (1.3) so the propellant was given a temporary 1.1 classification.

Results from further testing using the Large Sealed Vessel Test (reference 6) indicated that hazard division 1.3 was appropriate for LP101. The next series of tests (reference 7) confirmed this for the proposed method of packing. The single package test showed that, if confined in a 5 litre rigid polythene, narrow necked screw top containers, explosion did not propagate in the package and surrounding packages would not be endangered.

LP101 was finally given a 1.3L classification i.e. Propellant to be stored and transported separate from other propellants. Isolation is necessary because of the corrosive and oxidative nature of LP101.

5. Conclusions.

Manufacture.

The method of manufacture of LP101 has been fairly well established, but problems in assaying the propellant have been encountered. Work in this area is about to commence and it is hoped that a full assay method should be available in the near future. Refractive index or density measurement are being used for monitoring the blending procedure.

Compatibility and Stability.

The splash and immersion test, gas evolution test and heat generation test are currently being used to screen materials for use with LP101. The information from all these tests are used when making a sentencing decision.

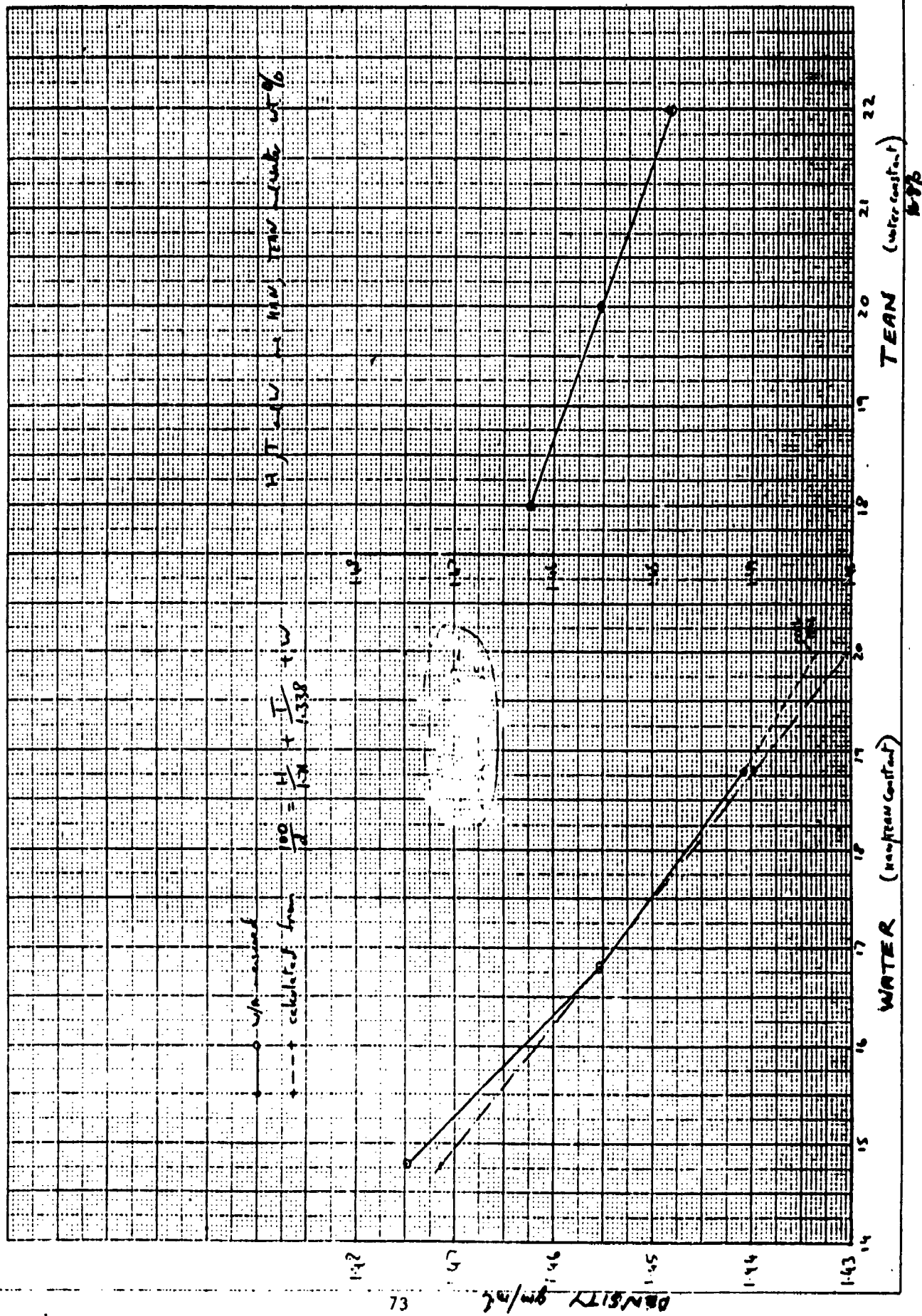
Hazard Assessment.

UN series 1 and 2 tests and supporting tests have classified LP101 as 1.3L. This only applies to propellant stored in 5 litre lots or less and in the specified packaging. Further testing will be required before the propellant can be transported or stored in bulk containers.

REFERENCES.

1. D. Sutton. Royal Ordnance R&D Centre, Westcott Report. RO(W)/LTM/LPG/STT. May 1987.
2. D. Sutton. Royal Ordnance R&D Centre, Westcott Report. RO(W)/LTM/LPG/MLTT. May 1987.
3. P.F. Bunyan. RARDE Memorandum 4/88, 1988.
4. N. Lynch. Royal Ordnance R&D Centre, Westcott. D. Sutton. Internal Memorandum LST-IM-1/88. Feb. 1988.
5. Recommendations on the Transport of Dangerous Goods, Tests & Criteria, First Edition. United Nations Publication ST/SG/AC.10/11, 1986. Part 1.
6. Explosives Hazard Assessment, Manual of Tests, SCC No 3, MOD, Waltham Abbey 1972.
7. Recommendations on the Transport of Dangerous Goods, Tests & Criteria, First Edition. UN Publication ST/SG/AC.10/11, 1986. Test 6 (a).

Figure 1



Possible Test Methods to Study The Thermal Stability
of Hydroxylammonium Nitrate Based Liquid Gun Propellant

P F Bunyan
S Westlake

Royal Armament Research and Development Establishment,
Powdermill Lane, Waltham Abbey, Essex EN9 1AX,
(United Kingdom).

Summary

The effect of contamination of a hydroxylammonium nitrate based liquid gun propellant with various metal ions has been studied using the techniques of heat flow calorimetry, thermogravimetry and a simple time to pressure burst test. All three tests showed a destabilising effect of dissolved copper and iron on this propellant. The three approaches are compared and their relative merits and disadvantages are discussed. It is concluded that heat flow calorimetry would provide the most suitable method for detailed compatibility studies, while a pressure burst test could be used for routine surveillance checks.

* * *

N.B. This document is intended to support a verbal presentation to be given at the 4th Annual Conference on HAN-Based Liquid Propellants, Structure and Properties at the Ballistics Research Laboratory, Aberdeen Proving Ground, Maryland. It reproduces the information reported in RARDE Memorandum 4/88, but includes some additional results that have been gathered since that Memorandum went to press.

COPYRIGHT C CONTROLLER HMSO, LONDON 1988

CONTENTS

1	Introduction	3
2	Laboratory Work	4
2.1	Heat Flow Calorimetry	4
2.2	Thermogravimetry	6
2.3	Time to Pressure Burst Test	6
3	Discussion and Conclusions	8
4	References	9
5	Symbols and abbreviations	9
Tables 1-3		
Figures 1-3		
Annex A	Sample Preparation Procedures	

INTRODUCTION

Following several years of investigation into the use of liquid gun propellants in the USA, a programme of work has recently commenced in the UK to develop a gun system employing a liquid monopropellant based on Hydroxylammonium nitrate (HAN).

This material is unlike any other propellant currently being used in British service and it can be expected to behave differently from conventional solid gun propellants based on NG/NC/nitroguanidine.

It has been reported that the stability of this class of propellant deteriorates if contaminated with trace quantities of certain metal ions, particularly iron and copper (Ref 1).

When left in contact with many metal components commonly found in gun systems, this type of propellant has been found, by experience, both to corrode the metal surface and to take metal ions into solution in appreciable quantities (up to several hundred ppm).

In order to investigate the effect of various treatments on the propellant (age, temperature, contact with other components of the gun system etc) it is necessary to have methods of measuring the decomposition rate of the propellant. In the case of conventional single, double and triple base solid gun propellants, this has usually been done by measuring the rate of stabiliser consumption either directly (eg by quantitative chromatographic determination of stabiliser degradation products) or indirectly (eg by measuring the time delay before brown fumes are visible as in the heat test).

Since HAN based propellants contain no stabiliser, these traditional tests are obviously of no use and alternative means of characterising them are required.

Tests are needed to fulfil 2 requirements:

a. Requirement 1

A reproducible, discerning, sensitive test to measure the effect on stability of various forms of contamination quantitatively, to provide information to help with the selection of suitable construction materials for guns and storage vessels, ie to perform the role that accelerated ageing followed by quantitative stabiliser analysis currently fulfils for conventional gun propellants.

b. Requirement 2

A quick stability check to be used as an indication of

useful life remaining and to give early warning of contamination with incompatible materials. This test may be qualitative but it must be simple to perform and use inexpensive, universally available equipment, ie to perform the role that Abel's heat test currently fulfils for conventional solid gun propellants.

2 LABORATORY WORK

2.1 Heat Flow Calorimetry

2.1.1 Equipment and Materials

Heat generation was monitored using an LKB 2277 microcalorimeter ("bioactivity monitor"). Its instrumentation and detection principle are described in reference 2.

Samples were contained in 3cm³ glass ampoules and sealed with Teflon lined rubber seals (LKB part no. 2277-303). Data were recorded using the microcomputer logging system described previously (Ref 3).

A sufficiently large sample of the liquid propellant designated LP101 was obtained from a single batch of experimental propellant (batch 2) to enable all experiments in this investigation to be completed on the same material. (LP101 is a British copy of the US propellant LP1845. It is an aqueous solution of HAN and triethanolammonium nitrate [TEAN])

Analytical reagent grade metal nitrate salts were used to prepare contaminated propellant samples.

2.1.2 Experimentation and Results

Samples containing known concentrations of metal ions were prepared by adding the appropriate metal nitrate salt to the mixed propellant, or to aqueous solutions of its components (HAN or TEAN).

Heat generation was measured by following the experimental procedure described in Annex A.

Heat evolution rates after 3 hours at 77°C associated with various treatments of the propellant are shown in Table 1.

2.1.3 Observations and Remarks

Iron

It can be seen that the presence of trace quantities of dissolved iron causes a large increase in the heat generation rate of the propellant. The effect appears to be a linear function of concentration under the conditions investigated (Fig 1).

The presence of copper also causes a large increase in the heat generation rate of the propellant. The effect is again a linear function of concentration and the rate is about an order of magnitude greater than for a similar concentration of iron.

Nickel

The presence of nickel increased the heat generation rate slightly, but the effect was far smaller than that seen with either iron or copper.

Aluminum

It can be seen that aluminum has very little effect on heat generation rate from the propellant when in solution compared with other metals investigated. (However, this propellant is known to be very incompatible with solid metallic aluminum)

Chromium

The presence of chromium increased the heat generation rate slightly, but the effect was far smaller than that seen with iron or copper.

Silver

It can be seen that the presence of silver had very little effect on the heat generation rate given by the propellant.

Propellant Components

No heat generation was detected from aqueous solutions of TEAN whether contaminated or not.

Aqueous solutions of HAN can be seen to be exhibiting a similar enhancement in their heat generation rate when contaminated by iron or copper as was seen with the intact propellant when similarly treated.

It would appear that the heat generation enhancement observed is the result of a reaction between the HAN and the metal ions. TEAN appears to neither react with the metal ions itself, nor to influence their reaction with HAN.

LP101 - Blend 4

When heat flow calorimetry was performed on a new batch of propellant (blend 4) it was found to be generating about twice as much heat as the original blend 2. It was shown subsequently that the new propellant contained a trace impurity of about 1.5 ppm of iron, compared with the 0.5 ppm present in the old propellant (Ref 5). This finding is consistent with the higher heat generation rate reported here.

2.2 Thermogravimetry

2.2.1 Equipment and Materials

Weight loss curves were recorded using a Mettler TG50 thermobalance.

Samples were contained in 150 µl alumina crucibles (Mettler part no. ME 24124)

2.2.2 Experimental and Results

Propellant samples containing known concentrations of metal ions were prepared by weighing in the appropriate metal nitrate salt.

Weight loss curves were recorded on propellants containing different contaminants using the experimental procedure and conditions described in Annex A. A typical weight loss curve for an uncontaminated sample is shown in figure 2. All curves were of this general shape, but with the step tending to be displaced to lower temperatures when the sample was contaminated.

A summary of the temperature at which a 50% reduction of weight had occurred for each treatment is shown in table 2.

2.2.3 Observations and Remarks

It can be seen that a significant reduction in the mean temperature of 50% weight loss could be demonstrated if 10 runs each of uncontaminated propellant and either 5 ppm (or greater) of iron contamination or 1 ppm (or greater) of copper contamination were considered.

The results are not quantitative, but agree qualitatively with the HFC results as follows:

- a Copper and iron appear to cause thermal instability.
- b The effect of copper is greater than that of iron for similar concentrations.

2.3 Time to Pressure Burst Test

2.3.1 Equipment and Materials

Liquid propellant samples were sealed in 3cm³ glass ampoules, identical with those used for the HFC tests (LKB part no. 2277-303).

An elevated temperature was maintained in the sample using an electrically heated, cylindrical, aluminium block with 20x100mm cylindrical holes cut into the plane surface to contain the samples (Fig 3). Isothermal temperature control of the block was achieved with an AEI platinum resistance thermometer controller. All experiments reported here were performed at a block temperature of 118°C.

2.3.2 Experimentation and Results

The pressure required to rupture the ampoule cover was found by sealing distilled water inside the glass ampoules and increasing the temperature slowly. Rupture of the seals occurred between 160 and 170°C, implying a bursting pressure of between 6 and 8 atmospheres (Ref 3).

Time to pressure burst was recorded by monitoring, with a potentiometric chart recorder, the voltage from a thermocouple embedded in a cork bung used to seal the cylindrical hole in the heating block containing the sample ampoule. When a pressure burst occurred, the bung was forced out of the hot block and the thermocouple cooled, causing a deflection on the recorder.

Details of sample preparation and experimental procedure are described in Annex A.

Pressure burst times for propellant samples contaminated in a variety of ways are summarised in Table 3.

2.3.3 Observations and Remarks

It can be seen that contamination of the propellant with copper and iron causes a large decrease in time to pressure burst while nickel, aluminum, chromium and silver have little or no effect.

Duplicate results are variable, as would be expected from the 6 to 8 atmosphere variation in rupture pressure of these ampoules. However, the effect due to contamination with traces of iron and copper is sufficiently pronounced to be seen above random variation, even on single results.

As with the TGA test, the results are not quantitative, but agree qualitatively with the HFC results.

3 DISCUSSION AND CONCLUSIONS

All three types of test show the destabilising effect of traces of certain metals in solution on this type of propellant and agree qualitatively on the ranking order of magnitude of effect of those metals.

The HFC method gives the most sensitive, discerning and reproducible information of the three, is quantitative and operates at a temperature closer to that which the propellant is likely to encounter during manufacture and use than the other two. It would therefore appear to be an acceptable technique for performing sophisticated tests to allow decisions about suitable construction materials to be used for storage vessels and gun systems etc (Requirement 1). However, the equipment is expensive, requires a skilled operator and carefully controlled laboratory conditions and is not widely available. It would not appear practicable to use it as a quick, cheap, simple surveillance check.

The time to pressure burst test gives semi-quantitative information and the results are too variable to be used for exact work. However, it requires simple, cheap, universally available equipment and little training. This type of test could thus fulfil the need for a quick stability test (Requirement 2).

The thermogravimetric method does show a decrease in stability caused by copper and iron contamination and agrees qualitatively with the other two tests. It would therefore be conceivable to employ such a test as a stability check for these types of propellants. However, it shares the disadvantages of the HFC test of requiring carefully controlled laboratory conditions, expensive equipment and a skilled operator, without offering the advantages of measuring any single recognised feature of the decomposition reaction quantitatively. It is therefore not proposed to pursue this approach any further.

Future work will concentrate on employing the HFC test described here to study the effect on thermal stability of various treatments of HAN-based liquid propellants.

1 Klein N BRL Report No 1876, 1976.
Wellman C R

2 Wadso I *Thermochimica Acta* 96, pp313-325, 1985.

3 Bunyan P F RARDE Memorandum 43/86, 1987.

4 Handbook of Chemistry and Physics,
65th. Edition, D-193.

5 Phillips M Private Communication.

5 SYMBOLS AND ABBREVIATIONS

BAM Bioactivity Monitor

HFC Heat Flow Calorimetry

HAN Hydroxylammonium Nitrate

TEAN Triethanolammonium Nitrate

W Watts

g Grammes

ppm Parts per million (weight/weight)

**TABLE 1 Heat Evolution Rates of Liquid Propellants
Measured Using The Bioactivity Monitor**

SAMPLE	HEAT GENERATION RATE ($\mu\text{W/g}$)
LP101 (uncontaminated blend 2)	1.2
LP101 (uncontaminated blend 4)	2.4
LP101 + 8.4 ppm iron	13.2
LP101 + 18.7 ppm iron	33.4
LP101 + 50 ppm iron	96
LP101 + 82 ppm iron	171
LP101 + 100 ppm iron	208
LP101 + 3.8 ppm copper	26.8
LP101 + 8 ppm copper	70
LP101 + 100 ppm copper	>1000*
LP101 + 50 ppm nickel	3.2
LP101 + 100 ppm nickel	5
LP101 + 50 ppm aluminum	1.6
LP101 + 100 ppm aluminum	1.6
LP101 + 100 ppm chromium	6.8
LP101 + 50 ppm chromium	5.0
LP101 + 100 ppm silver	2.5
LP101 + 50 ppm silver	2.2
80.3% HAN (uncontaminated)	2.8
80.3% HAN + 8.3 ppm iron	11.5
80.3% HAN + 8.8 ppm copper	55

* Generating heat at a rate above the maximum range of the equipment. Sample removed to prevent damage.

CONDITIONS Samples contained in sealed 3 cm³ glass ampoules at 77°C. Heat generation rate reported after 3 hours.

TABLE 2 Thermogravimetric Analysis of Liquid Gun Propellant

PROPELLANT SAMPLE	MEAN TEMPERATURE WHEN HALF WEIGHT LOSS RECORDED* (°C)	STANDARD DEVIATION IN BRACKETS	DIFFERENCE OF MEAN TEMPERATURE AT HALF WEIGHT LOSS FROM THAT OF UNCONTAMINATED PROPELLANT	
			95%CL	99%CL
Uncontaminated	209.6	(7.63)	-	-
+ 100 ppm iron	180.9	(7.85)	-28.7	± 7.27
+ 100 ppm copper	170.8	(4.71)	-38.8	± 5.95
+ 5 ppm iron	189.7	(15.74)	-18.9	± 11.61
+ 5 ppm copper	182.5	(10.44)	-27.1	± 8.59
+ 1 ppm iron	203.4	(18.82)	-6.2!	± 13.49
+ 1 ppm copper	183.0	(10.73)	-26.6	± 8.75

* Based on 10 analyses in each case

! No significant difference demonstrated (p=0.05)

TABLE 3 Time To Pressure Burst Of Liquid Gun Propellant Contaminated With Metal Ions

SAMPLE	TIME TO PRESSURE BURST (HOURS)	
Uncontaminated LP101	45, 38, 35, 39, 41, 43, 48	41!
LP101 + 100 ppm iron	2, 2	2!
LP101 + 50 ppm iron	3.75, 3	3.375!
LP101 + 20 ppm iron	8, 7.5	7.75!
LP101 + 10 ppm iron	12.5, 12.5	12.5!
LP101 + 5 ppm iron	13, 18	14.5!
LP101 + 100 ppm copper	0.5, 0.75	0.825!
LP101 + 50 ppm copper	1, 1	1!
LP101 + 20 ppm copper	4, 4.5	4.25!
LP101 + 10 ppm copper	7, 7	7!
LP101 + 5 ppm copper	10.5, 8	8.75!
LP101 + 100 ppm aluminum	34, 32	33!
LP101 + 50 ppm aluminum	34, 45	38.5!
LP101 + 100 ppm nickel	17, 18	17.5!
LP101 + 50 ppm nickel	19, 20	19.5!
LP101 + 100 ppm chromium	24, 38	30!
LP101 + 50 ppm chromium	28, 38	34!
LP101 + 200 ppm silver	37, 44	40.5!
LP101 + 100 ppm silver	35, 40	37.5!
80.3% HAN (in water)	17, 17	17!

! Mean value (hours)

CONDITIONS: 3g samples of propellant sealed in 3cm³ glass ampoules held isothermally at 118°C

Seals burst between 8 and 8 atmospheres

FIG. 1

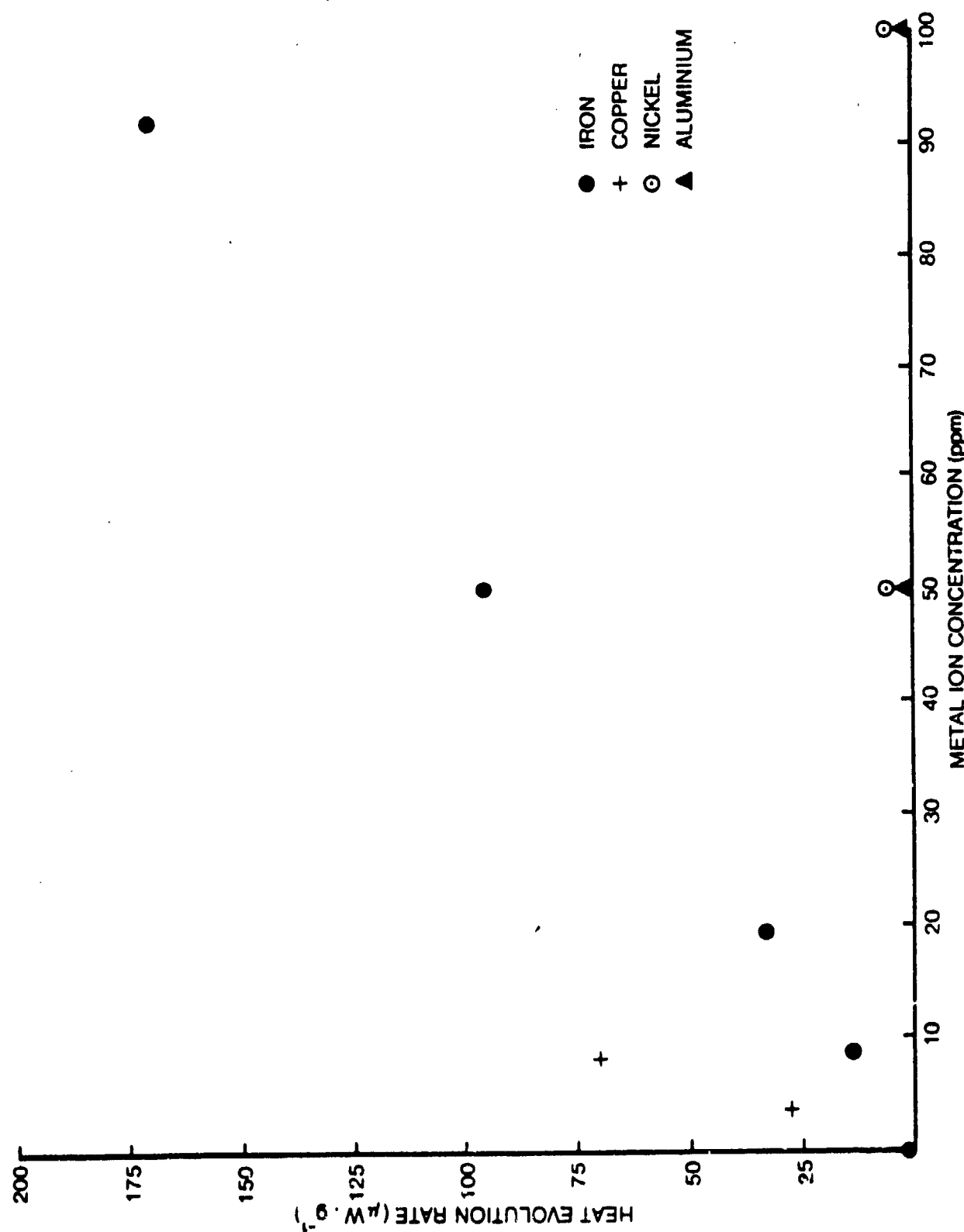


FIG. 1 HEAT EVOLUTION FROM CONTAMINATED LP101 SAMPLES

FIG. 2

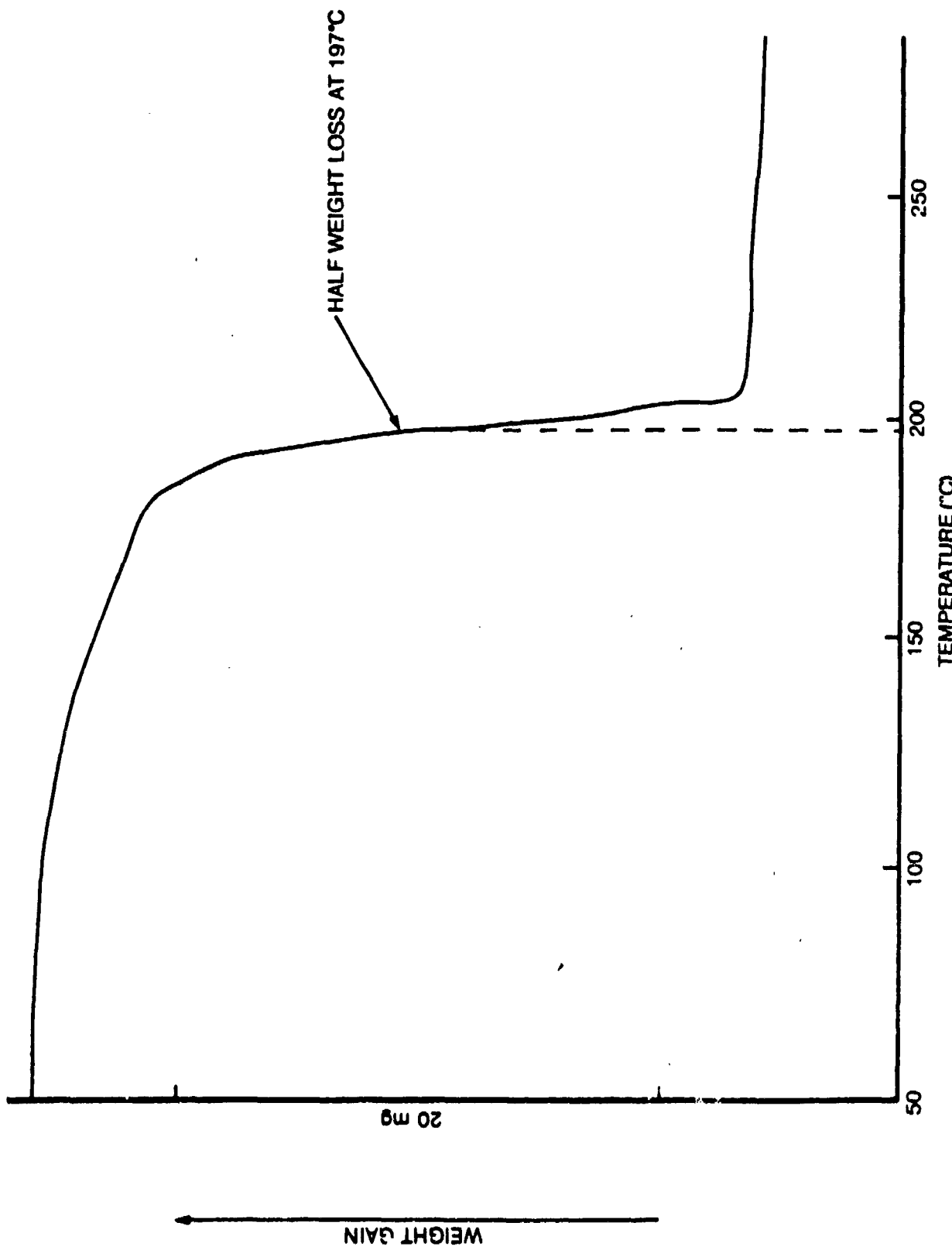


FIG. 2 WEIGHT LOSS CURVE (UNCONTAMINATED LP101)

FIG. 3

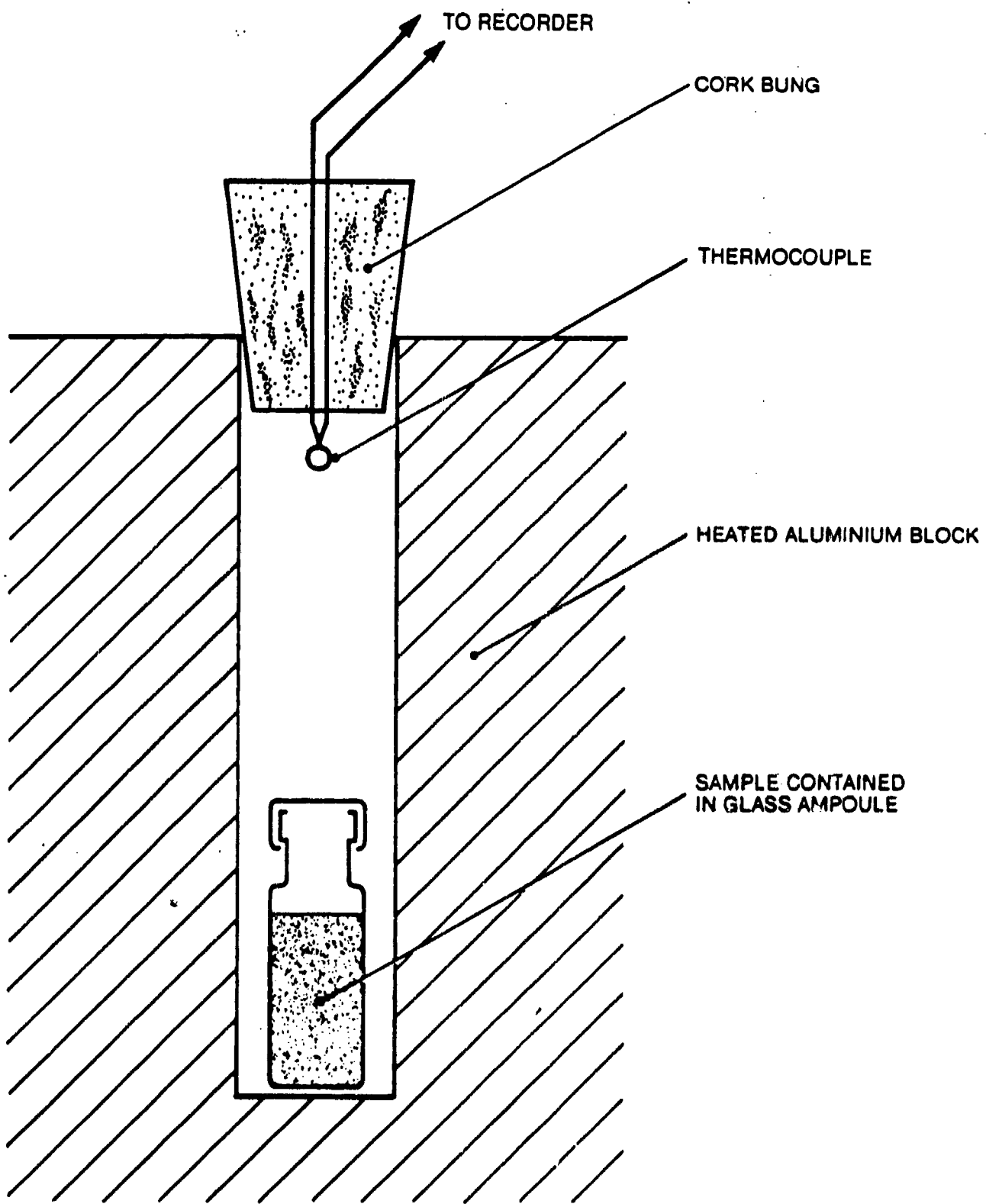


FIG. 3 PRESSURE BURST TEST - SAMPLE CONFIGURATION

SAMPLE PREPARATION PROCEDURES

A1 HEAT FLOW CALORIMETRY

- 1 Heat new glass ampoules and lids for 24 hours at 80°C in a vacuum oven. Store in a desiccator over P₂O₅ until ready for use.
- 2 Set the BAM bath to the desired temperature and allow 24 hours for the cylinder to equilibrate.
- 3 Adjust the output to zero volts using the potentiometer on the BAM, with thermally balanced, inert ampoules in both the sample and reference wells.
- 4 When the output becomes constant, record the blank signal for 1 hour.
- 5 Subject the sample well to an appropriate, known calibrating power, supplied by resistive heating of the calibration element around the sample detection zone.
- 6 Record the calibration signal, when constant.
- 7 Fill a glass sample ampoule with uncontaminated propellant using a Pasteur pipette. This step is to remove any source of contamination present in the ampoule as supplied.
- 8 Discard the uncontaminated propellant.
- 9 Place between 3.5 and 4g of propellant which has received the treatment of interest into the sample ampoule and record the sample weight.
- 10 Seal the ampoule with a Teflon-lined aluminium cap.
- 11 Lower the ampoule into the equilibration region of the BAM cylinder. Retain the sample in this region until temperature equilibrium is achieved (this will take about 30 minutes)
- 12 Lower the sample into the detection region of the cylinder and commence measurement of power output.

A2 THERMOGRAVIMETRY

- 1 Weigh between 25 and 35mg of the sample of liquid propellant into a clean 150ul alumina crucible (Mettler part no 24124).
- 2 Place on the balance pan of a calibrated Mettler TG50 thermobalance. Do not cover the crucible with a lid, since this would be pushed off by the foaming, decomposing propellant.

3 Increase the temperature experienced by the sample from 50 to 300°C at a linear rate of 20 degrees per minute in an atmosphere of nitrogen flowing at 200 ml/minute and record the sample weight as a function of temperature throughout the analysis.

4 Record the temperature at the point where the sample had experienced a 50% weight loss.

A3 TIME TO PRESSURE BURST

1 Clean a 3cm³ glass ampoule with uncontaminated liquid propellant as for steps 7 and 8 of the HFC method.

2 Transfer 3g of treated propellant sample into the sample ampoule and seal with a Teflon-lined aluminum cap.

3 Heat the ampoule and sample to 118°C by placing them inside a cylindrical hole drilled into a heated aluminum block.

4 Seal the entrance to the heating block well with a cork bung containing a chromel/aluminel thermocouple.

5 Monitor the voltage from the thermocouple as a function of time using a potentiometric chart recorder.

6 When the ampoule seal ruptures, the cork bung is blown out of the hot block allowing the thermocouple to cool down. the time to pressure burst may be deduced from the associated pen deflection on the chart recorder.

Possible Test Methods To Study The
Thermal Stability of Hydroxylammonium

Nitrate Based Liquid Gun Propellants

P F Bunyan

S Westlake

Royal Armament Research and Development Establishment,
Powdermill Lane, Waltham Abbey, Essex EN9 1AX
(United Kingdom)

PROBLEM DEFINITION

EXISTING TESTS NOT SUITABLE

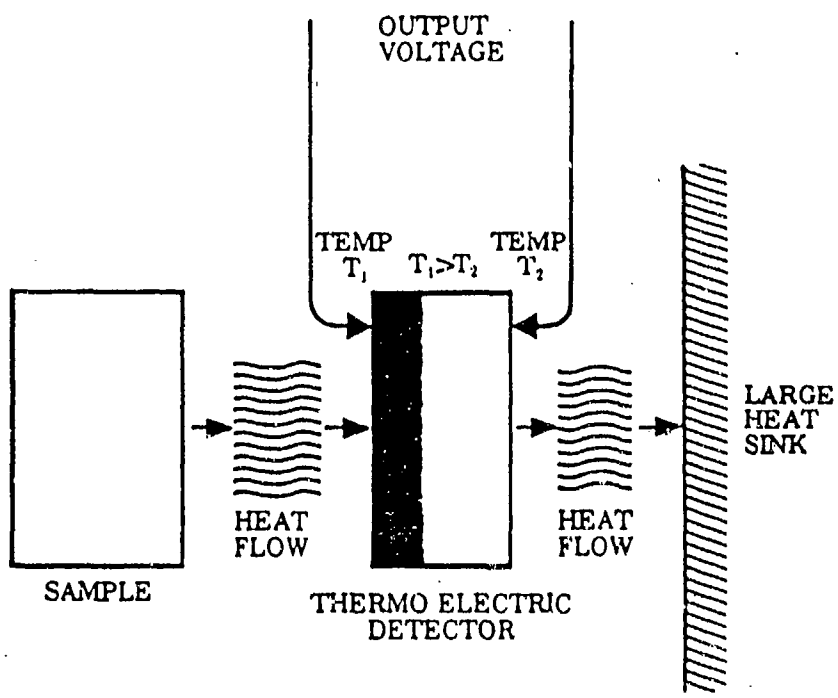
: NEW TESTS REQUIRED

2 MAIN REQUIREMENTS ..

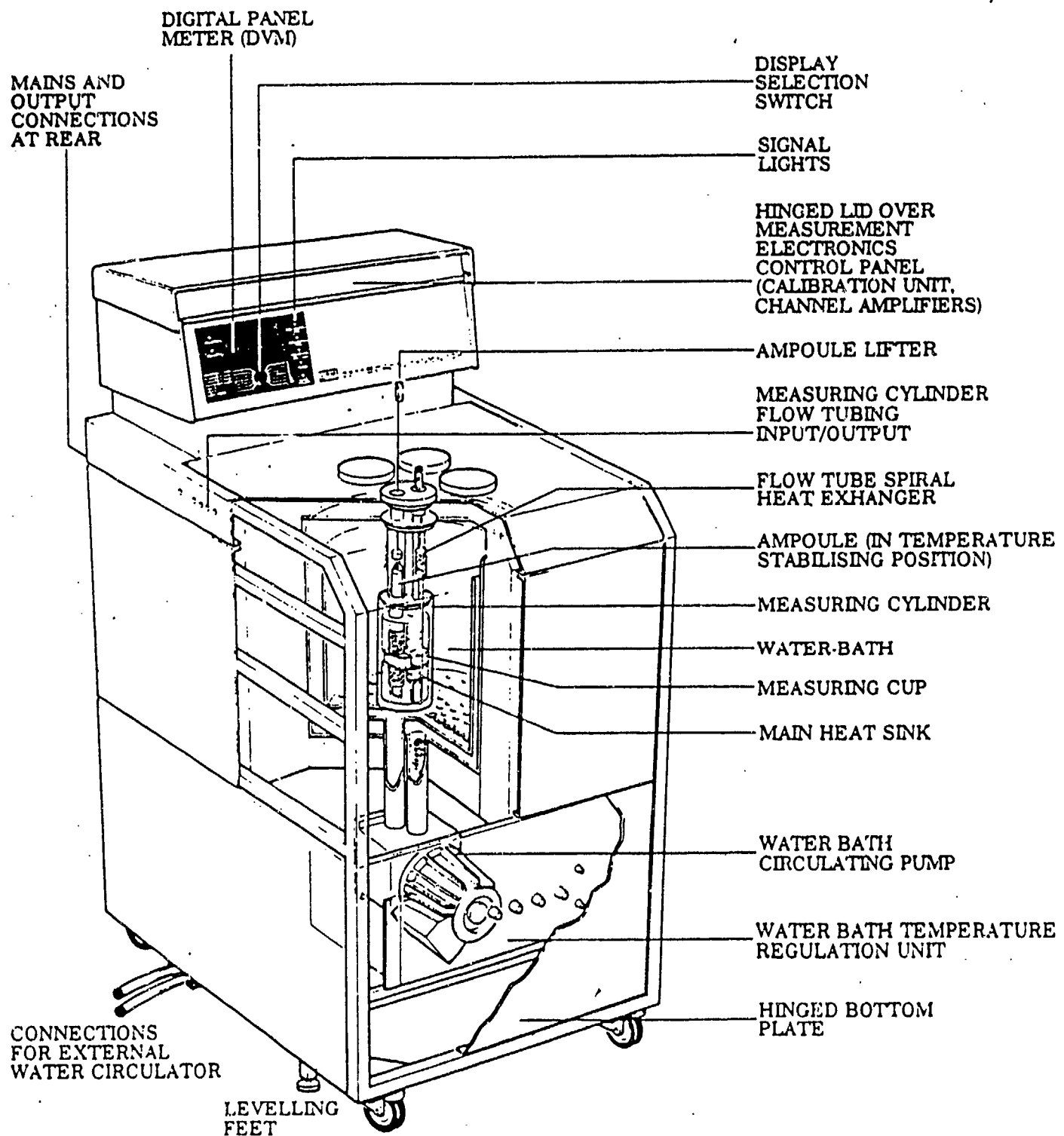
- 1. QUANTITATIVE**
- 2. QUALITATIVE**

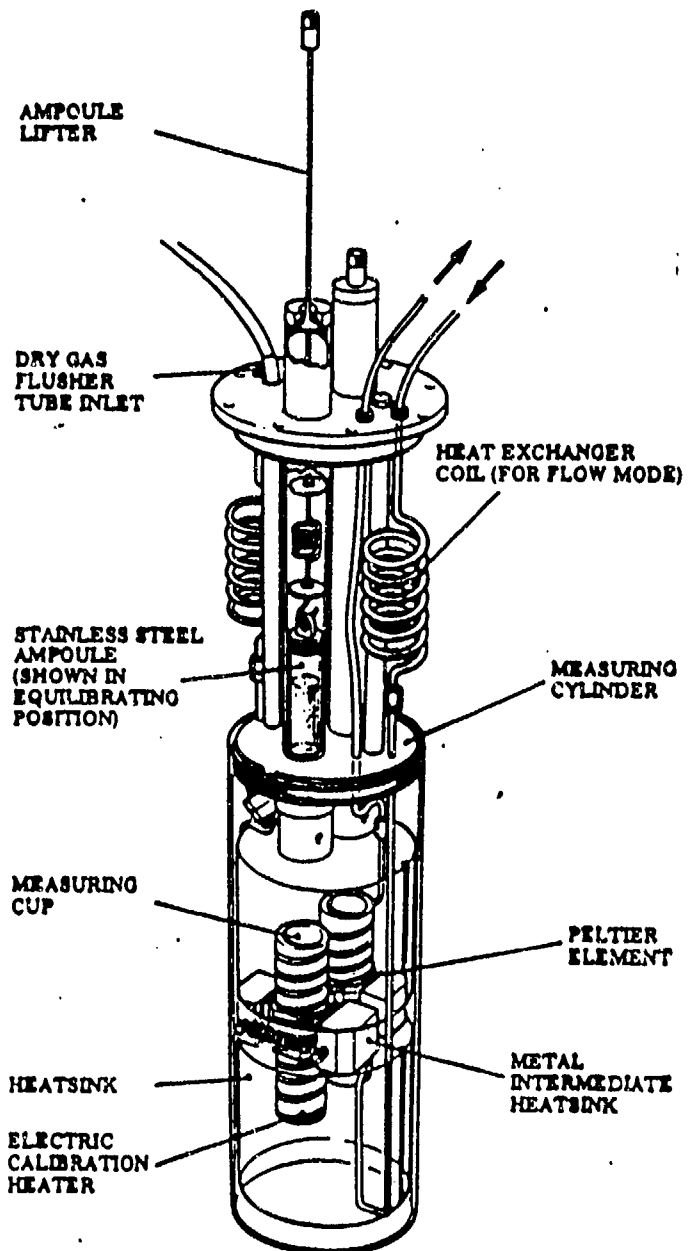
ADVANTAGES OF HFC

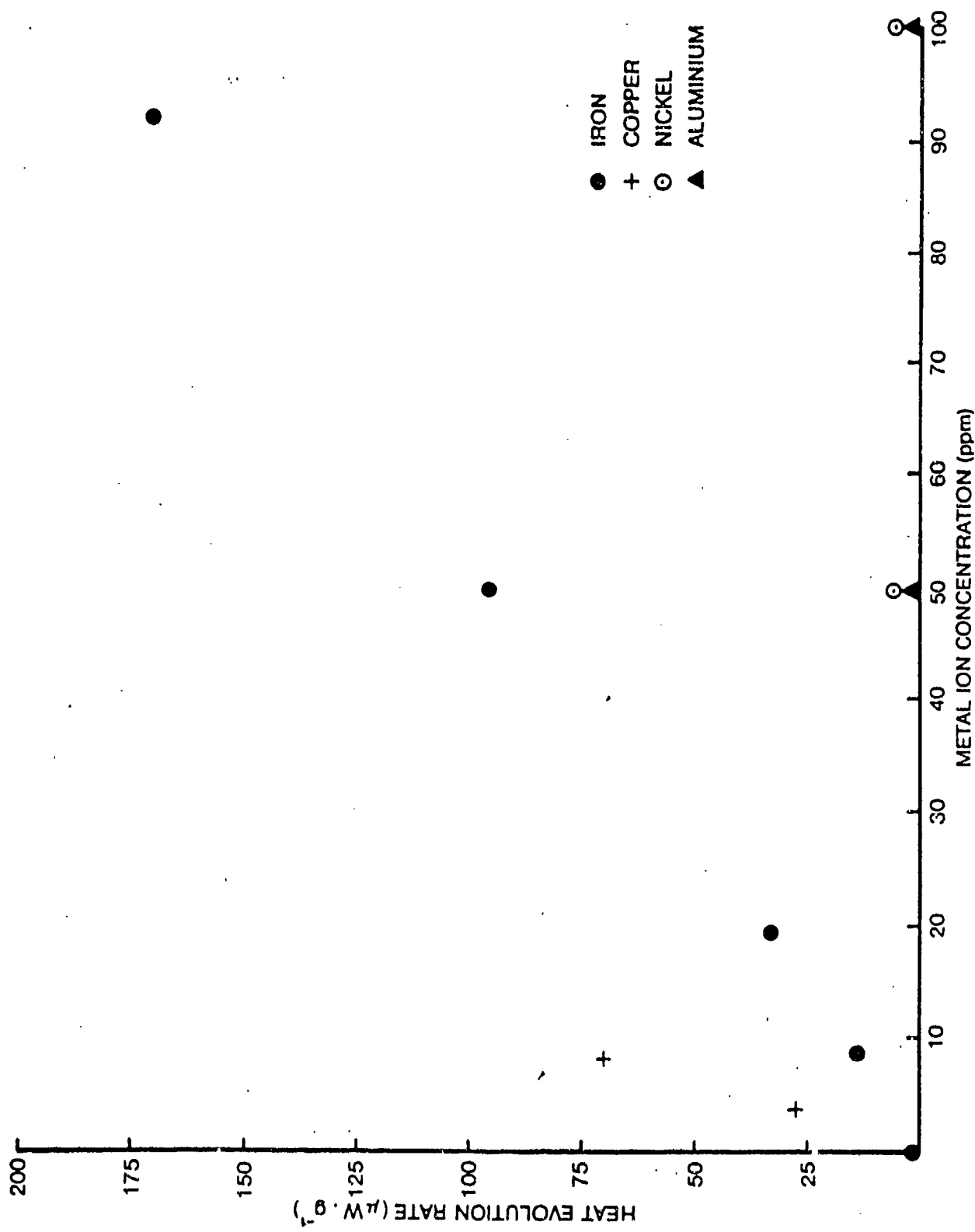
1. DOES NOT RELY ON STABILISER
2. SAMPLE HOLDERS ARE COMPATIBLE
3. FAIRLY LOW TEMPERATURE
4. QUANTITATIVE
5. SAMPLE SIZE
6. AVAILABILITY

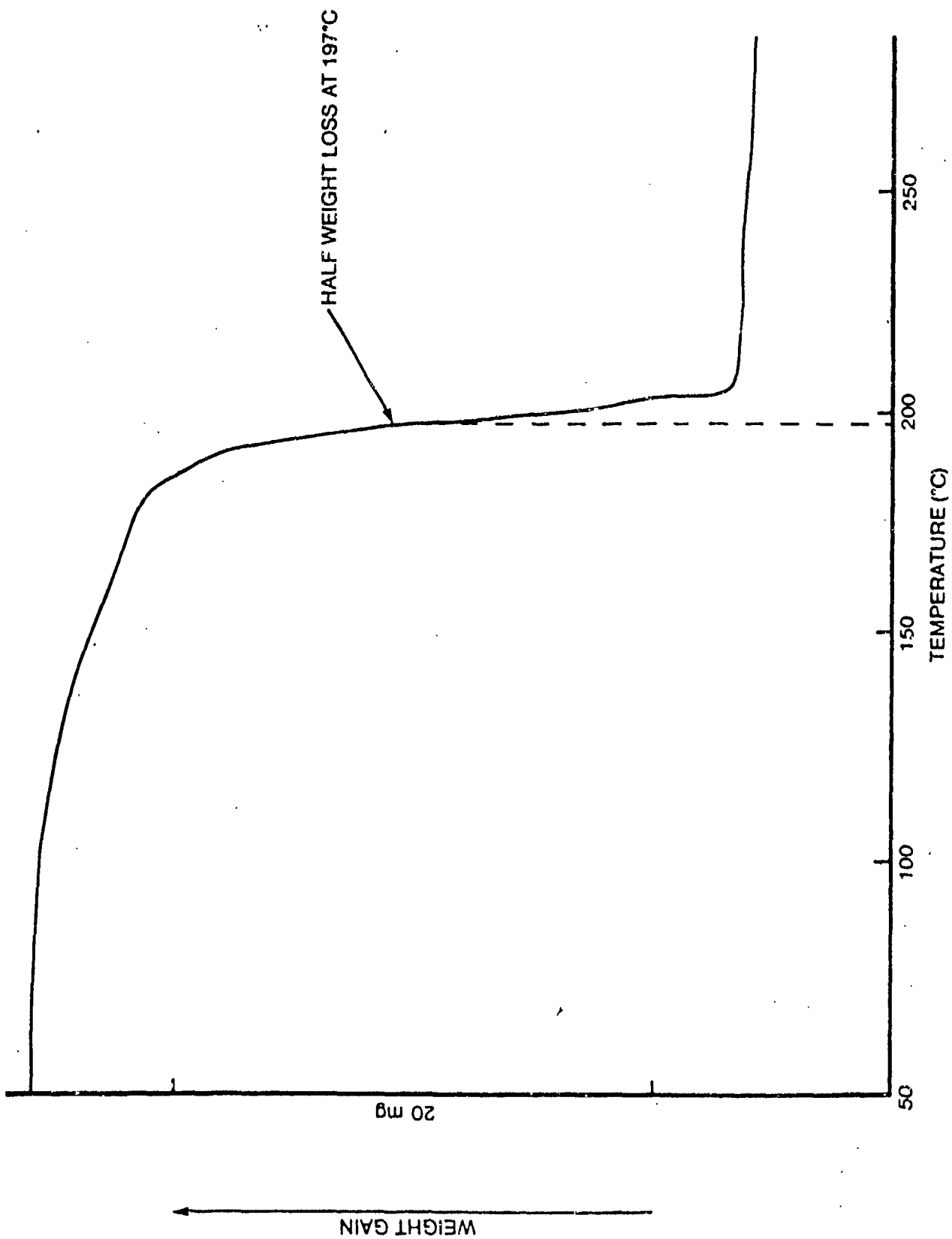


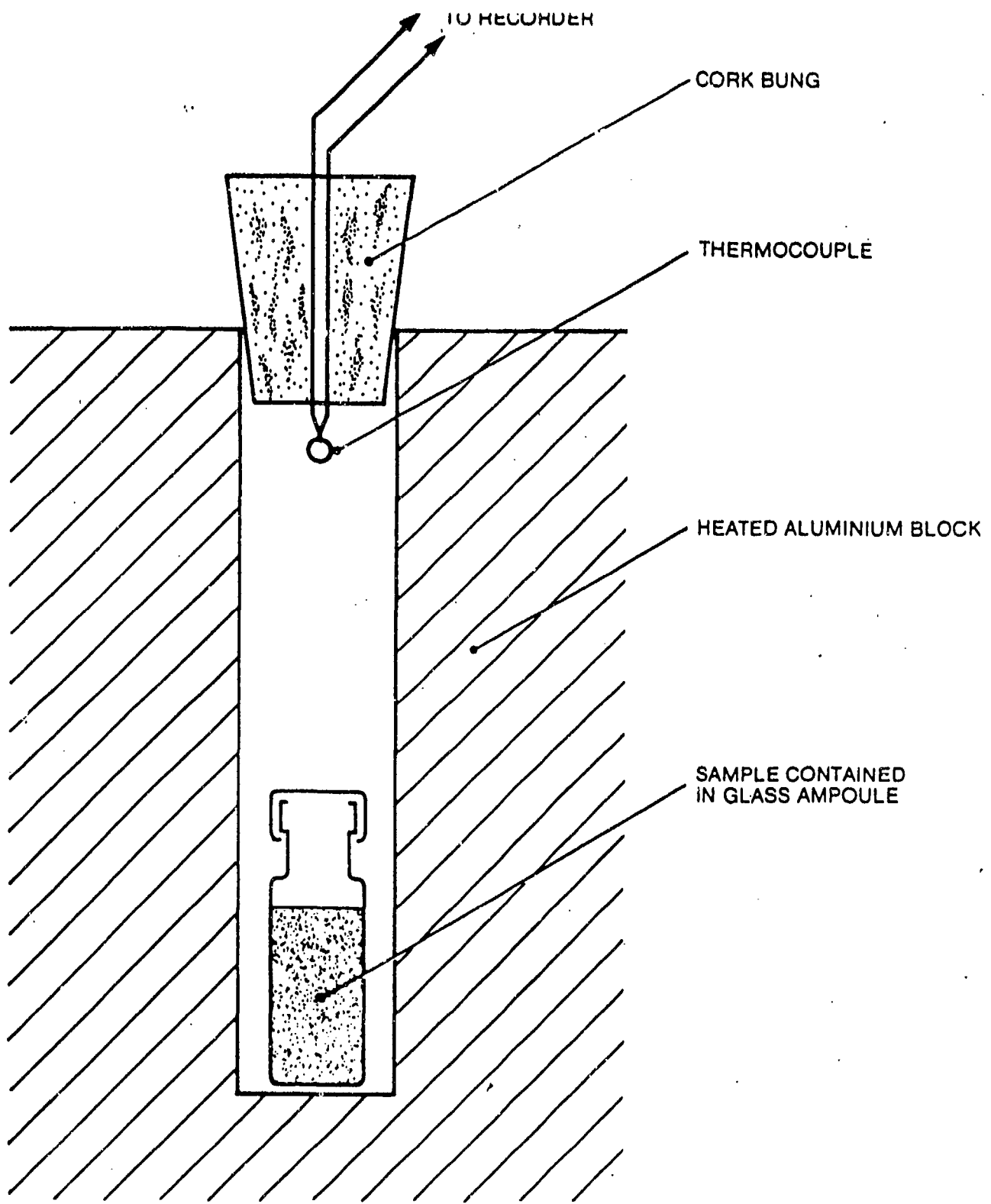
NOTE: HEAT FLOW IS ACTUALLY THREE DIMENSIONAL











PRESSURE BURST TEST - SAMPLE CONFIGURATION

TIME TO PRESSURE BURST

SAMPLE TTPB (HOURS)

UNCONTAMINATED

+ 100 PPM COPPER	0.5
+ 100 PPM IRON	2
+ 100 PPM ALUMINIUM	33
+ 100 PPM NICKEL	17.5
+ 100 PPM CHROMIUM	30
+ 100 PPM SILVER	37.5

CONCLUSIONS

1. HFC TEST SUITABLE FOR
REQUIREMENT 1
2. TPPB TEST SUITABLE FOR
REQUIREMENT 2
3. TGA TEST NOT SUITABLE
FOR EITHER REQUIREMENT

HYDRODYNAMIC THEORY OF LIQUID PROPELLANT DYNAMICS

J.W. Haus and F. Chung-Yau
Rensselaer Polytechnic Institute
Troy, New York 12180-3590

1. Linearized Hydrodynamics
 - A. Three component fluid
 - i) light scattering spectra
 - ii) sound absorption and dispersion
 - B. Chemical reactions in Equilibrium
2. Continuing Research
 - A. Instabilities
 - i) Thermodynamic
 - ii) Chemical
 - B. Inhomogeneous distribution of gases
 - C. Thermal effects of inhomogeneities on instabilities

supported by U.S. Army Watervliet Arsenal, Grant No. DAAA 22-85-C-0218

1. Linearized Hydrodynamic equations for
a three-component mixture

HAN + TEAN + water

Continuity equation $\rho = \rho_0 + \rho_1$

$$\frac{\partial \rho_1}{\partial t} = -\rho_0 \vec{\nabla} \cdot \vec{v}$$

Navier-Stokes equation

$$\rho_0 \frac{\partial \vec{v}}{\partial t} = \vec{\nabla} \cdot \vec{T} = -\vec{\nabla} p + \eta_s \nabla^2 \vec{v} + \eta_b \vec{\nabla} (\vec{\nabla} \cdot \vec{v})$$

Conservation of energy $T = T_0 + T_1$

$$\rho_0 \left[C_p \frac{\partial T_1}{\partial t} - K_{T1} \frac{\partial \mu_1}{\partial c_1} \frac{\partial c_1}{\partial t} - K_{T2} \frac{\partial \mu_2}{\partial c_2} \frac{\partial c_2}{\partial t} + T_0 \frac{\partial S}{\partial \rho} \frac{\partial \rho_1}{\partial t} \right] = K \nabla^2 T_1$$

Conservation of particle species

$$\frac{\partial c_i}{\partial t} = \vec{\nabla} \cdot \vec{f}_i = D_i \left[\nabla^2 c_i + \frac{K_{Ti}}{T_0} \nabla^2 T_1 + \frac{K_{Pi}}{P_0} \nabla^2 P \right]$$

$$i=1, 2$$

Parameters for three component fluid

Thermodynamic

C_p, C_v, α, χ_T

$$\frac{\partial \mu_1}{\partial C_1}, \frac{\partial \mu_2}{\partial C_2}$$

thermal ratios: K_{T1}, K_{T2}

baricentric ratios: K_{P1}, K_{P2}

Transport

viscosities:

$$\eta_B = \left(\frac{4}{3} \eta_s + \eta_v \right), \eta_s$$

thermal diffusion:

$$K/g_0 C_p = D_T$$

chemical diffusion:

$$D_1, D_2$$

Chemical Reactions

relaxation times:

$$\tau_1, \tau_2$$

enthalpic changes:

$$\frac{\partial h}{\partial C_1}, \frac{\partial h}{\partial C_2}$$

thermodynamic:

$$\frac{\partial C_1}{\partial T}, \frac{\partial C_2}{\partial T}$$

A. Three-component fluid

solution of equations via Fourier-Laplace transform methods

$$t \rightarrow z$$

$$\vec{x} \rightarrow \vec{k}$$

R.D. Mountain, J. Res. NBS A72, 95(1968).

R.D. Mountain and J.M. Deutch, J. Chem. Phys. 50, 1103(1969).

J.W. Haus, J. Chem. Phys. 60, 2638(1974).

5-component vector for the thermodynamic state variables

$$\overset{\Delta}{\vec{N}}(\vec{k}, z) = (\hat{C}_1, \hat{C}_2, \hat{P}, \hat{\psi}, \hat{\phi})$$

$$\psi = \vec{\nabla} \cdot \vec{v} \Rightarrow \hat{\psi} = -i \vec{k} \cdot \vec{\nabla}$$

$$\phi = T_1 - \frac{T_0 \alpha}{C_p S_0} P$$

The probability distribution for fluctuations
is statistically independent

$$W(\vec{N}(\vec{k}, 0)) = h_1(c_1) h_2(c_2) h_3(p) h_4(\psi) h_5(\phi) = e^{\frac{\Delta S}{k_B}}$$

the functions $h(Q)$ are Gaussian:

$$\text{e.g. } h_1(c_1) = N \exp\left\{-\frac{\partial \mu_1}{\partial c_1} \delta c_1^2 / 2k_B T\right\}, -\frac{\partial \mu_1}{\partial c_1} < 0$$

The linearized hydrodynamic equations are
written in matrix form:

$$\overset{\Delta}{\tilde{N}}(\vec{k}, z) = \overset{\approx}{M}^{-1}(\vec{k}, z) \cdot \vec{N}(\vec{k}, 0)$$

$\overset{\approx}{M}(k, z)$ is the matrix of coefficients of
the variables in $\overset{\Delta}{\tilde{N}}(\vec{k}, z)$.

$\det(\overset{\approx}{M})$ is a polynomial of order 5 in z .
It contains only even orders in k .

$$\det(\overset{\approx}{M}) = (z - \lambda_1)(z - \lambda_2) \cdots (z - \lambda_5)$$

The determinant of \tilde{M} has the following roots:

2 roots are complex, these are associated with the propagating modes

$$\lambda_{\pm} = \pm i c_0 k - \Gamma k^2$$

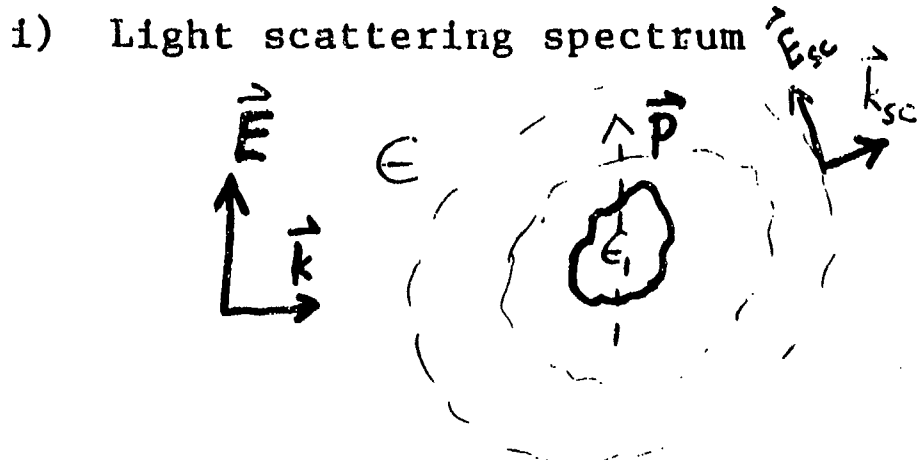
3 roots are real, these are diffusion modes

$$\lambda_1 \approx k^2 \left(\frac{1}{D_1} + \frac{1}{D_2} \right)^{-1}$$

$$\lambda_{2/3} = \frac{k^2}{2} \left[(D_T + D_1 + D_2) \pm \left[(D_T + D_1 + D_2)^2 - 4 D_T (D_1 + D_2) \right]^{1/2} \right]$$

$$\Gamma = \frac{1}{2} \left\{ \frac{\eta_B}{S_0} + \frac{K(\gamma-1)}{C_P S_0} + \sum_{i=1}^2 \frac{D_i}{S_0^2} \left(\frac{\partial \varphi}{\partial C_i} + \frac{\partial \mu_i}{\partial C_i} \frac{K_{Ti}}{C_P S_0} \right)^2 \right\},$$

$$D_i' = D_i \left(1 + \frac{K_{Ti}^2}{C_P T_0} \frac{\partial \mu_i}{\partial C_i} \right)$$



structure factor is the spectral density of dielectric constant fluctuations.

$$S_{\epsilon}(\vec{k}, \omega) = \langle \Delta \epsilon(\vec{k}, \omega) \Delta \epsilon(\vec{k}, 0) \rangle$$

$$= \sum_{i,j} \frac{\partial \epsilon}{\partial N_i} \frac{\partial \epsilon}{\partial N_j} S_{ij}(\vec{k}, \omega)$$

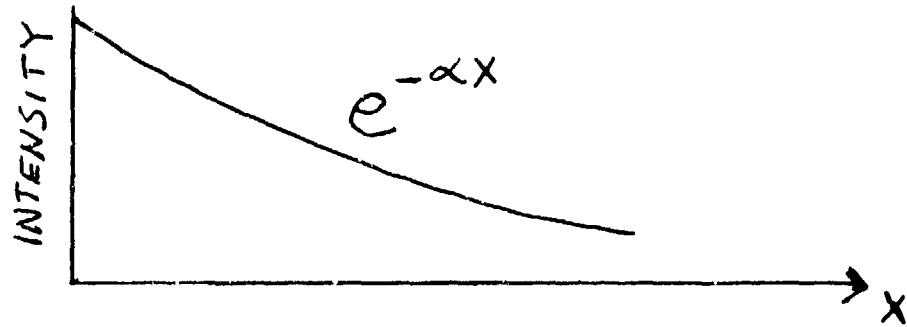
spectrum of fluctuations in the state variables $Z = -i\omega$

$$S_{ij}(\vec{k}, \omega) = \frac{1}{\pi} \text{Re} \left\{ \left\langle \left(\begin{smallmatrix} M & \vec{N}_d \\ \approx & i \end{smallmatrix} \right)_i N_d^{(0)} \right\rangle_w \right\}$$

$$= \frac{1}{\pi} \text{Re} \left\{ \sum_e \frac{V_{ie} V_{je}}{i\omega + \lambda_e} \right\}$$

ii) Ultrasonics

Frequency imposed by transducer,
akin to light transmission experiment



absorption: wave intensity diminishes
with distance

dispersion: "time-of-flight" after
launching acoustic wave

$\det(M)$ gives solution for plane-
wave propagation

$$\rho_i(\vec{x}, t) = \rho_i^{(0)} e^{i(\vec{k} \cdot \vec{x} - \omega t)}$$

$$\vec{k} = k \hat{e}_x \quad k = k_R + i k_I$$

in limit $\omega \rightarrow 0$

dispersion: $k_R = \frac{\omega}{C_0}$

absorption $k_I^2 = \frac{\Gamma^2 \omega^4}{4 C_0^6}$

B. Chemically reacting fluid near equilibrium

$$\frac{\partial \vec{v}}{\partial t} = - \rho_0 \vec{\nabla} \cdot \vec{v}$$

$$\rho_0 \frac{\partial \vec{v}}{\partial t} = \vec{\nabla} \cdot \vec{T}$$

$$\frac{\partial C_i}{\partial t} = \vec{\nabla} \cdot \vec{f}_i - \frac{1}{\tau_i} \left(\delta C_i - \frac{\partial C_i}{\partial T} T_1 - \frac{\partial C_i}{\partial P} P_1 \right)$$

$$\frac{\partial}{\partial t} \{ \dots \} = K \nabla^2 T + \sum_i \frac{\partial h_i}{\partial C_i} \frac{1}{\tau_i} \left\{ \delta C_i - \frac{\partial C_i}{\partial T} T_1 - \frac{\partial C_i}{\partial P} P_1 \right\}$$

eigenvalues of $\det(M)$

$$\lambda_1 \approx \lambda^\circ$$

$$\lambda_{2/3} \approx \lambda_{2/3}^\circ + \sum_i \frac{1}{\tau_i} \left(1 + \frac{1}{T_0} \frac{\partial h_i}{\partial C_i} \frac{\partial T}{\partial S} \frac{\partial C_i}{\partial T} \right)$$

propagating modes also affected.
 The real part is altered, the imaginary part is unchanged.

2. Continuing research

A. Instabilities

I) Thermodynamic, spinodal decomposition

liquid-gas transition

$$\chi_T < 0 \quad \text{no propagating modes}$$

phase separation of fluid components

$$\frac{\partial \mu_i}{\partial c_i} < 0, \quad \text{uphill diffusion}$$

II) Chemical

model: change of activation energy with pressure:

$$\tau_i^{-1} = \frac{1}{\tau_i^0} e^{-E(P)/k_b T}$$

Equations of motion

$$\frac{\partial \vec{p}_1}{\partial t} = -\rho_0 \vec{\nabla} \cdot \vec{v}$$

$$\rho_0 \frac{\partial \vec{v}}{\partial t} = -\vec{\nabla} \cdot \vec{J}$$

$$\frac{\partial}{\partial t} \{ \dots \} = k \nabla^2 T + \left(\frac{A}{\zeta_0} e^{-E(P)/k_B T} - B \right)$$

$k \rightarrow 0$ two roots vanish

third root

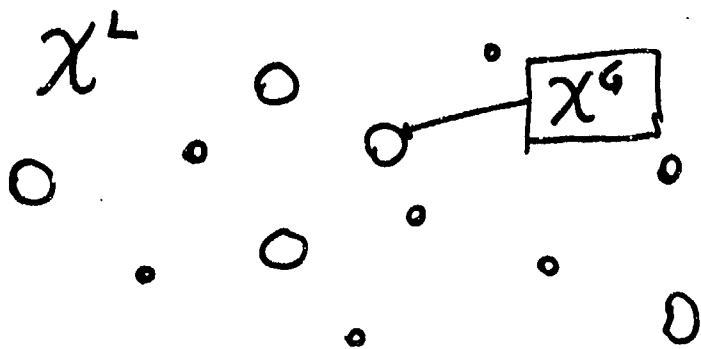
$$z = \frac{-A}{k_B T \chi'_0 \rho_0 \zeta_p} \left(\frac{E}{T} + \frac{\chi_T}{\alpha} \frac{\partial E}{\partial P} \right)$$

The fluid is unstable when

$$\frac{E}{T} + \frac{\chi_T}{\alpha} \frac{\partial E}{\partial P} < 0$$

The activation energy must decrease with pressure increase and be of sufficient magnitude in its change.

Inhomogeneous distribution of gases



$\chi^G \gg \chi^L$ gas is easily compressed

- a. large change of volume on compression
- b. hot spots. They affect the chemical stability.

CONCLUSIONS

- A. Hydrodynamic theory gives a complete description that can unify both light scattering and ultrasonic experiments under a single formalism.
- B. The hydrodynamic theory provides insight into modelling instabilities in fluid mixtures.
- C. Chemical reactions change the light scattering spectra, especially in the forward scattering direction, and the ultrasonic absorption.
- D. An inhomogeneous distribution of reaction products could be modelled within this formalism.

4th ANNUAL CONFERENCE ON HAN-BASED LIQUID PROPELLANT
STRUCTURE AND PROPERTIES
US ARMY BALLISTIC RESEARCH LABORATORY
ABERDEEN PROVING GROUND, MD
30 AUG - 1 SEP 88

Title of Paper Ionic Aspects of the Decomposition of HAN Solution

Presentation Time Request 20 (min)

Type of Paper: Progress; Summary; State-of-art; Other

Speaker's Name Walter S. Koski Phone Number (301)338-7418

Affiliation/address Department of Chemistry, The Johns Hopkins University,
Baltimore, Maryland 21218

Co-author(s) name(s) none

ABSTRACT (Use reverse side if necessary)

Abstract.

HAN aqueous solutions are stable at room temperature however application of an appropriate stimulus either thermal or chemical can initiate the decomposition of the HAN to produce N₂O, NO, N₂, NO₂, etc. Since HAN solutions are highly ionic it is reasonable to examine the role that ion-molecule reactions may play in the decomposition process. It is believed that the initial step is a proton transfer reaction from the hydroxylammonium ion so to this end the proton affinities of NH₂OH, NH₃, H₂O and nitric acid will be discussed and a chemical mechanistic scenario will be developed which is consistent with the known experimental facts of HAN decomposition.

4th ANNUAL CONFERENCE ON HAN-BASED LIQUID PROPELLANT
STRUCTURE AND PROPERTIES
US ARMY BALLISTIC RESEARCH LABORATORY
ABERDEEN PROVING GROUND, MD
30 AUG - 1 SEP 88

Title of Paper Reaction Kinetics of HAN, TEAN and Water Mixtures Using a Personal Computer

Presentation Time Request 20 (min)

Type of Paper: X Progress; Summary; State-of-art; Other

Speaker's Name A.K. Macpherson Phone Number (215) 758-4105

Affiliation/address Dept. of Mech. Engg. and Mechanics, Bethlehem, PA 18015

Co-author(s) name(s) A.J. Bracuti

ABSTRACT (Use reverse side if necessary)

A program has been developed to study the reaction kinetics of gun propellants such as the HAN based liquids using a personal computer. These HAN based systems can be studied using a mainframe computer but often require long run times. In order to eventually model the liquid propellant guns, including the fluid flow, it was necessary to develop a fast reacting program which would form part of the final system. In addition, a reaction program which could run on a PC is convenient for initial testing of possible fuels. The main problem with any such system is that the equations are stiff with ideal time steps varying from 10E-18 seconds to 10E+03 seconds. Under these conditions many integration schemes become unstable. An additional problem of using a PC is that the accuracy is limited and with long runs, the atom conservation can become badly in error.

A semi-implicit time advance scheme was used to obtain stability. The time step was varied through a prescribed regime and equations were included or eliminated depending on the particular part of the regime in operation. By varying the time step pattern, the accuracy could always be improved at the expense of increased computer time. The equilibrium conditions were calculated using the MCVECE code. Using the equilibrium conditions, the reaction kinetic code was used to study various HAN, HAN-water, TEAN and TEAN-Water and the results compared with available experimental data.

ELECTRICAL IGNITION OF HAN-BASED LIQUID GUN PROPELLANTS

G. Klingenberg*, H. J. Frieske**, and H. Rockstroh*

* Fraunhofer-Institut für Kurzzeitdynamik, Ernst-Mach-Institut,
Abteilung für Ballistik (EMI-AFB), Weil am Rhein, FRG

** Dynamit Nobel AG, Werk Dellbrück, Abteilung Grundlagen und
Zukunftstechnik, Köln, FRG

ABSTRACT

The present paper reports on progress achieved in the study of the electrical ignition of the hydroxylammonium nitrate (HAN) based liquid gun propellant LP 1846. The goal of the present work is to develop an igniter system suitable for regenerative liquid propellant guns. Several igniter configurations, designed by the Ballistic Research Laboratory (BRL) and the Ernst-Mach-Institute (EMI-AFB), have been tested. Voltage and current as well as the pressure histories were measured for each discharge. The electrostatic field distribution was calculated by a finite element code implemented at Dynamit Nobel. The theoretical analysis yielded improved electrode designs for future testing.

1. INTRODUCTION

The discharge by an igniter system into the combustion chamber of a regenerative liquid propellant gun (RLPG) builds up the pressure required to set the injector piston into motion and to generate the energy for igniting the liquid propellant (LP) thus injected. Solid propellant igniters are currently being used to initiate the combustion in medium and large caliber RLPGs. However, the goal of the future RLPG development is to incorporate a liquid propellant ignition system eliminating solid propellants from the logistic train [1]. One LP used for the tests is LGP 1846, which contains hydroxylammonium nitrate (HAN), triethanolammonium nitrate (TEAN), and water [2]. Since LGP 1846 is an electrolyte, primarily electrical ignition has been studied so far.

2. EXPERIMENTAL

The ignition experiments were conducted with two different ignition test fixture types used in the closed bomb mode.

2.1 Test Fixture No. 1

A view of the first test chamber is shown in Figure 1. It comprises the isochoric test chamber equipped with pressure gage and rupture disk or sapphire window and the center electrode assembly. The test chamber volume can be preselected, via an insert, to 60. or 101 cm³.

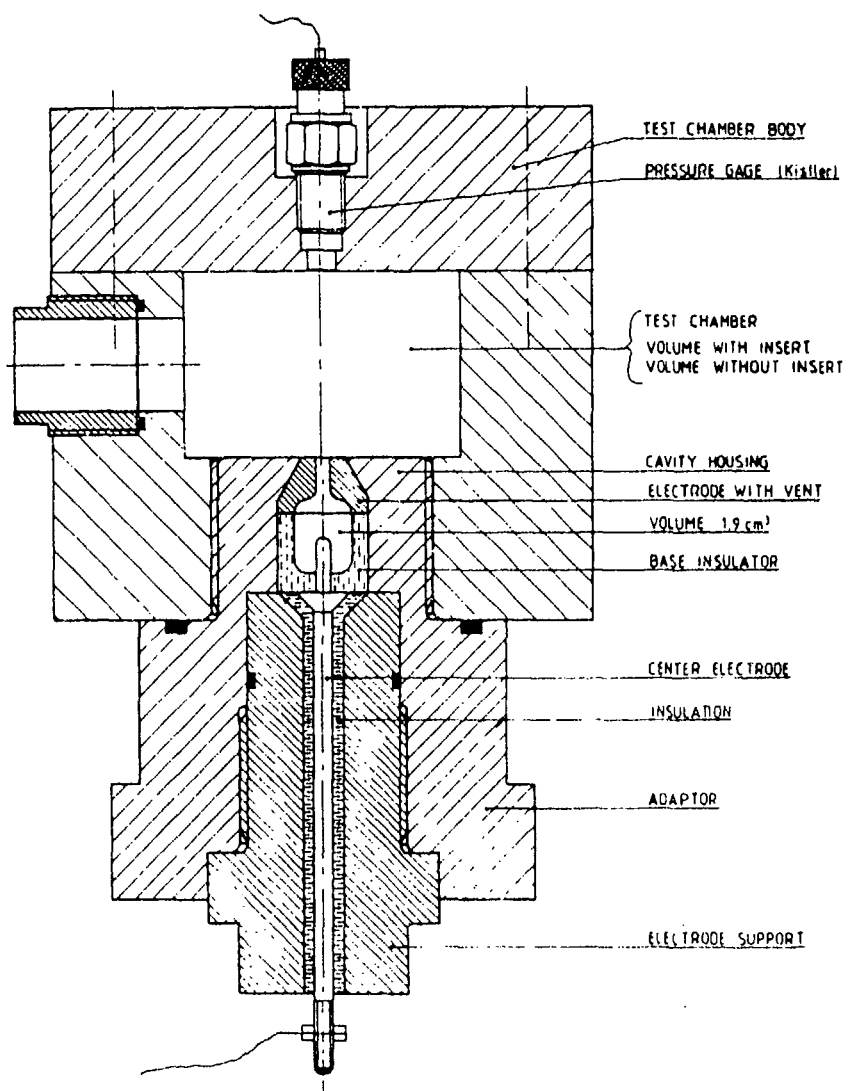


Fig. 1. EMI-AFB test chamber (first design)

The center electrode assembly is depicted in somewhat greater detail in Figure 2. The principle structural features of this

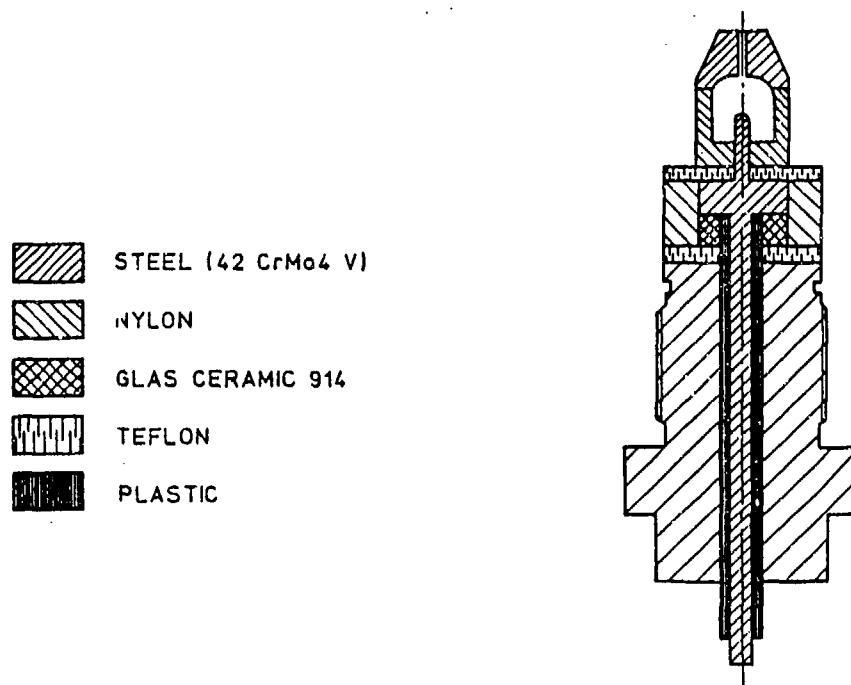


Fig. 2. Center electrode assembly

assembly are the center electrode, the vented outer electrode and the base insulator. Figure 2 displays a more recent design than Figure 1. Two igniter cavity configurations were investigated: One, a design introduced by BRL; the other developed by EMI-AFB (Figs. 3 and 4).

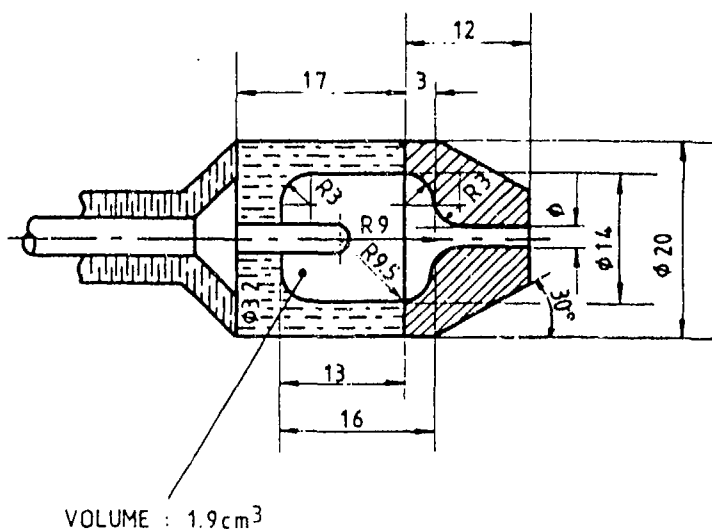


Fig. 3. BRL type igniter cavity

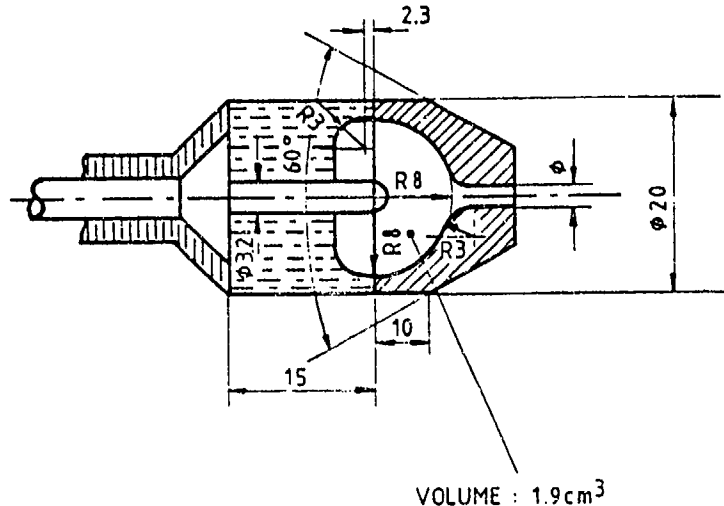


Fig. 4. EMI-AFB type igniter cavity

The cavity volume was 1.9 cm^3 in both cases. During the course of the experiments, the vent diameters were narrowed from 2 to 1.6 mm thus improving the confinement of the liquid propellant fill.

2.1.1 BRL Igniter Configuration

The study commenced with one of the BRL type [1] configurations (Fig. 3) according to the request of the contracting agency. The design tested at EMI-AFB is characterized by its cylindrical cavity and the fact that the center electrode ends well below the insulator's upper edge.

2.1.2 EMI-AFB Igniter Configuration

Figure 4 shows the igniter configuration designed at EMI-AFB. The cavity is circular rather than cylindrical; in addition, the center electrode protrudes further upward into the cavity.

2.2 Test Fixture No. 2

A special test chamber has been designed and built at EMI-AFB (Fig. 5). This chamber includes sapphire windows for monitoring the ignition process by optical techniques and a measuring port for

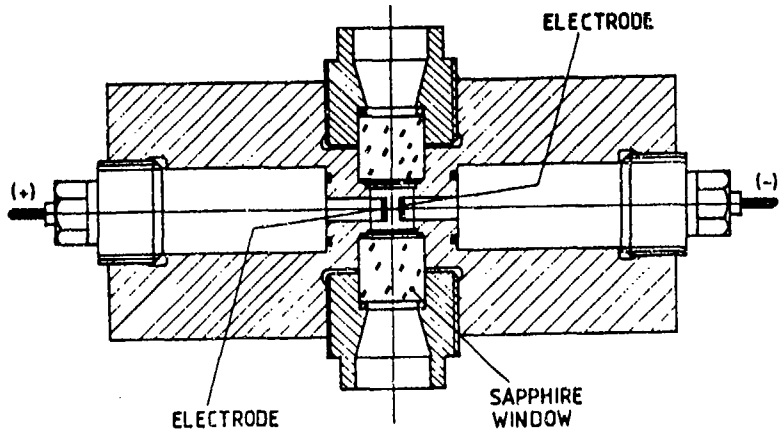


Fig. 5. EMI-AFB test chamber (second design)

recording the pressure or temperature history. The fill volume of 20 cm^3 can be reduced by appropriate inserts. In our current experiments a volume of 6.7 cm^3 was used. Various electrode configurations can be built into the chamber. The configurations tested so far include plate, sphere, and needle electrodes (Fig. 6). The maximum pressure is limited to 60 MPa by the rupture disk.

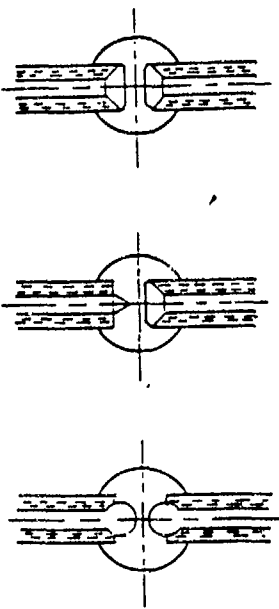


Fig. 6. Basic electrode configurations

3. SAMPLE RESULTS

3.1 BRL Igniter Configuration

Tests were conducted with the test fixture number 1 using both the 101 and 60 cm³ volumes. In the latter tests the vent diameters were 2.0, 1.8, and 1.6 mm, respectively; some of the data measured are summarized in Table 1. Note, that the maximum pressure is determined by the rupture disk to $p_{max} = 16 \text{ MPa}$.

Table 1. Tests of BRL igniter cavity; chamber volume: 60 cm³

Test No.	Vent Orifice Diam. [mm]	Volume of LP [cm ³]	Current I [A]	Voltage U [Volt]	Power P [kW]	Energy E [Joule]	Pressure p _{max} [MPa]	Ignition Delay [ms]
1	1.6	1.9	132	1700	192	79	16.4	1.6
2	1.6	1.9	147	1660	225	88	15.1	1.6
3	1.8	1.9	128	1600	184	101	16.5	2.9
4	1.8	1.9	127	1620	184	94	16.0	2.8
5	1.8	1.9	130	1660	193	91	15.9	2.9

For a vent diameter of 2.0 mm, the ignition characteristics was poor. In several cases there was no ignition of the LP. In other cases substantial amounts of LP were expelled prematurely into the test chamber. The shortest ignition delays were obtained with the highest confinement of 1.6 mm vent diameter. Generally, the reproducibility of the tests was unsatisfactory. A possible explanation for this will be given in the theoretical section.

In view of the above results the subsequent tests with the chamber volume of 101 cm³ were performed using the 1.6 mm vent diameter exclusively (Table 2). The scatter of the ignition delay is not really improved.

Table 2. Tests of BRL igniter cavity; chamber volume: 101 cm³

Test No.	Vent Orifice Diam. [mm]	Volume of LP [cm ³]	Current I [A]	Voltage U [Volt]	Power P [kW]	Energy E [Joule]	Pressure P _{max} [MPa]	Ignition Delay [ms]
6	1.6	1.9	140	1560	200	85	9.0	1.7
7	1.6	1.9	130	1650	194	63	12.0	1.3
8	1.6	1.9	145	1580	208	78	12.5	1.0
9	1.6	1.9	153	1560	210	84	9.5	2.2
10		1.9	133	1650	195	60	8.5	1.9

3.2 EMI-AFB Igniter Configuration

The EMI-AFB cavity configuration is essentially a geometrically compressed version of the BRL design. The basic idea was to produce an even spacing in the field lines centered at the tip of the inner electrode. It was assumed that this would ensure improved ignition behavior. Sample results of these experiments are summarized in Table 3. When compared with the data of Table 1, less electrical energy is required to achieve sustained ignition with the EMI-AFB configuration. Also, the ignition delay is significantly reduced.

Table 3. Tests of EMI-AFB igniter cavity; chamber volume: 60 cm³

Test No.	Vent Orifice Diam. [mm]	Volume of LP [cm ³]	Current I [A]	Voltage U [Volt]	Power P [kW]	Energy E [Joule]	Pressure P _{max} [MPa]	Ignition Delay [ms]
11	1.6	1.9	180	1500	215	66	11.6	1.2
12	1.6	1.9	175	1550	225	62	11.5	1.2
13	1.6	1.9	170	1550	215	56	12.5	1.1
14	1.6	1.9	180	1700	250	59	11.5	0.9
15	1.6	1.9	170	1500	220	68	12.0	1.2

3.3 Test Fixture No. 2

This design permits the investigation of both conductive and non-conductive LPs, by generating either a plasma through an arc discharge or by electrochemical initiation. The following anode-cathode configurations have been tested so far: (1) plate-plate, (2) sphere-plate, (3) needle-plate, and (4) sphere-sphere.

Preliminary results indicate that at the selected electrode distance of 7.2 mm the configuration (3) yields an arc discharge but no ignition. Comparatively, the other configurations gave electrochemical ignition. However, extremely long and inconsistent ignition delays were observed. Generally, ignition took place well after the current had been shut off (30 ms - 1.5 min). The investigation of the physical and chemical processes involved by optical means, starting with high-speed camera recordings, has begun.

4. CALCULATION OF ELECTRICAL FIELD

The calculation of the electrical field between the electrodes was made by means of a finite element code for the electrostatic case. This work was carried out for the BRL and EMI-AFB igniter cavity configurations. In addition, a modified version is proposed aiming at an optimal field distribution.

The calculated field lines for the BRL and EMI-AFB configurations are drawn in Figures 7 and 8. The spaces or segments between individual field lines are numbered 1 to 11. The segment sizes were chosen for convenience. Figure 9 depicts the change of electrode surface areas and the segment volume versus the segment number. No distinct differences are seen for the center electrode surface area curves (Fig. 9 A). Comparatively, the outer electrode surface area curves are characterized by the existence of a maximum. The maximum surface for the BRL configuration is to be found at segment number 4, that for the EMI-AFB type at segment number 8

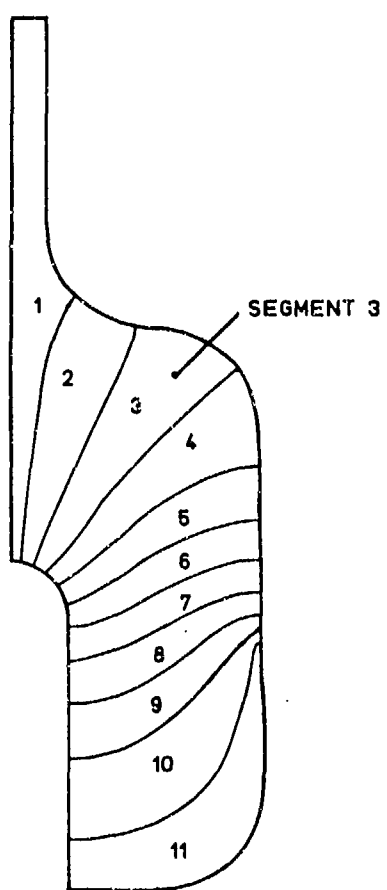


Fig. 7. Field lines calculated for BRL type igniter cavity

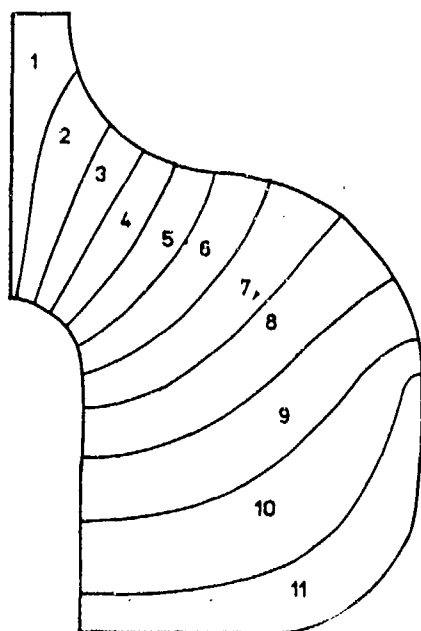


Fig. 8. Field lines calculated for EMI-AFB type igniter cavity

EVALUATION FROM PREDICTED FIELD LINES

— EMI TYPE IGNITER CAVITY
- - - BRL TYPE IGNITER CAVITY

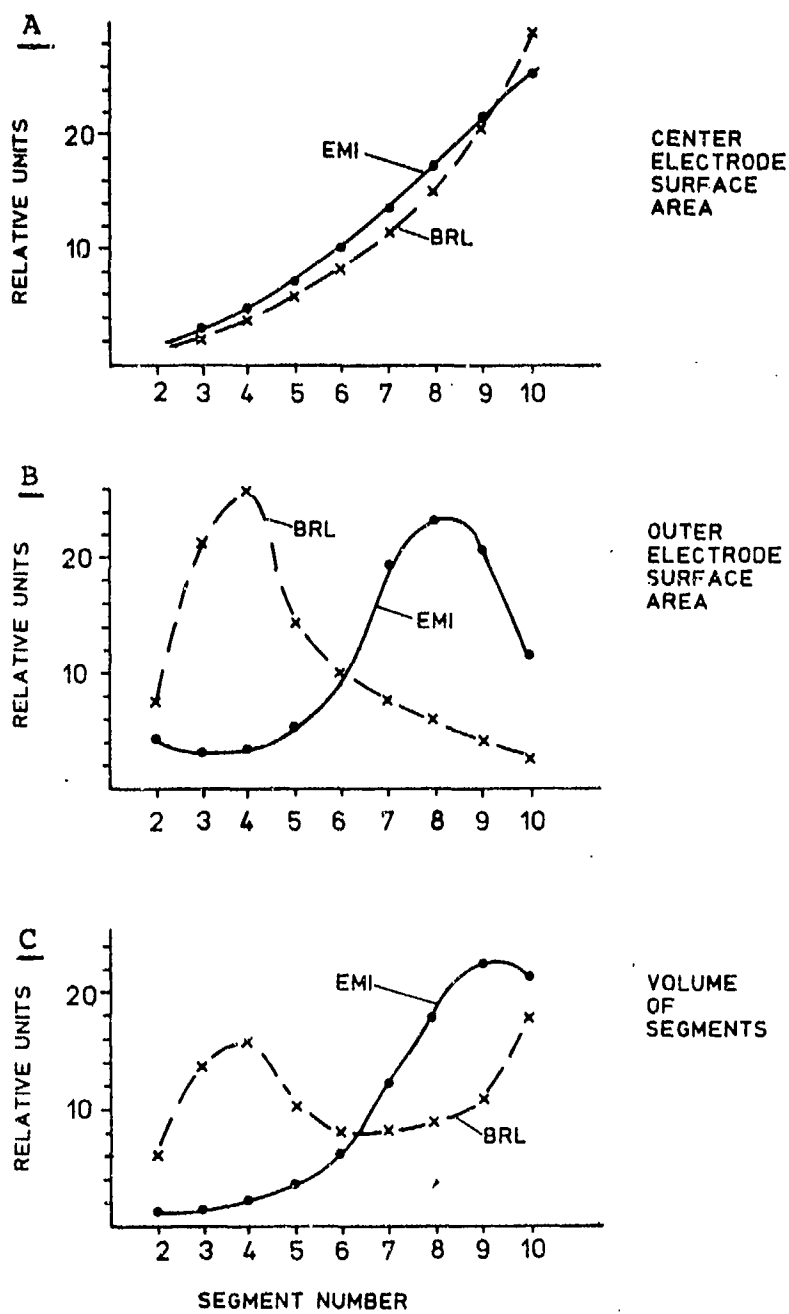


Fig. 9. Electrode surface area and volume of segments versus segment number for BRL and EMI-AFB type igniter cavities

(Fig. 9 B). The corresponding volume curves, whose maxima are at segments numbers 4 and 9, respectively, are shown in Figure 9 C.

Ignition is expected to be favored in the vicinities of the minima of the curves in Figure 9. That is, for the BRL design there are two such regions, one at the inner electrode in segments 2, 3, 4, the other at the outer electrode in segments 8, 9, 10 (Fig. 7). Contrarily, the EMI-AFB design has only one such favored region, namely in segments 2, 3, 4 for both electrodes (Fig. 8).

The points made above suggest that an optimized cavity geometry should feature both an even spacing of the field lines and a narrow surface/volume minimum at or near the tip of the center electrode. Figure 10 shows such a configuration, obtained from the computer calculations. The corresponding surface area/volume versus segment number curves are drawn in Figure 11.

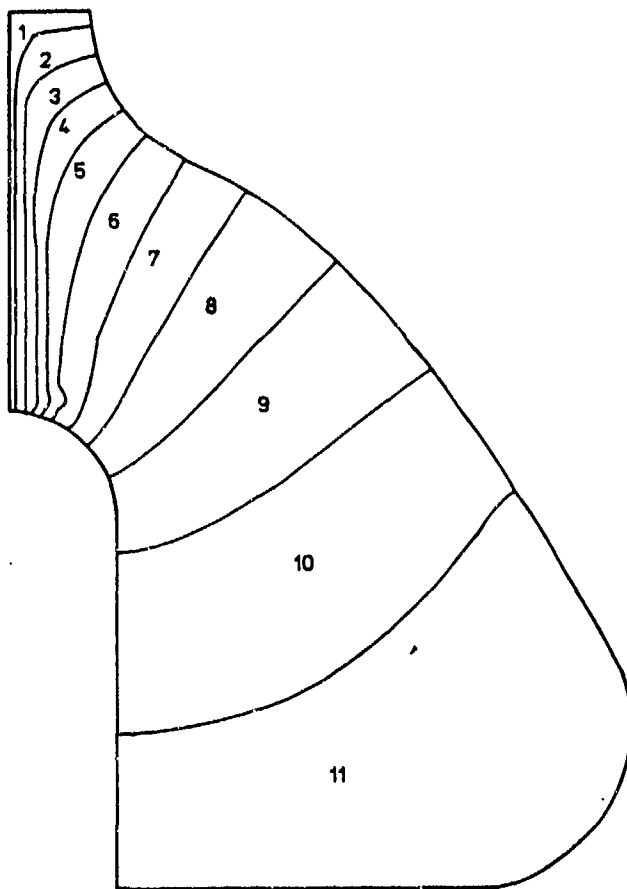


Fig. 10. Field lines calculated for optimized version of igniter cavity

EVALUATION FROM PREDICTED FIELD LINES
(OPTIMIZED IGNITER CAVITY)

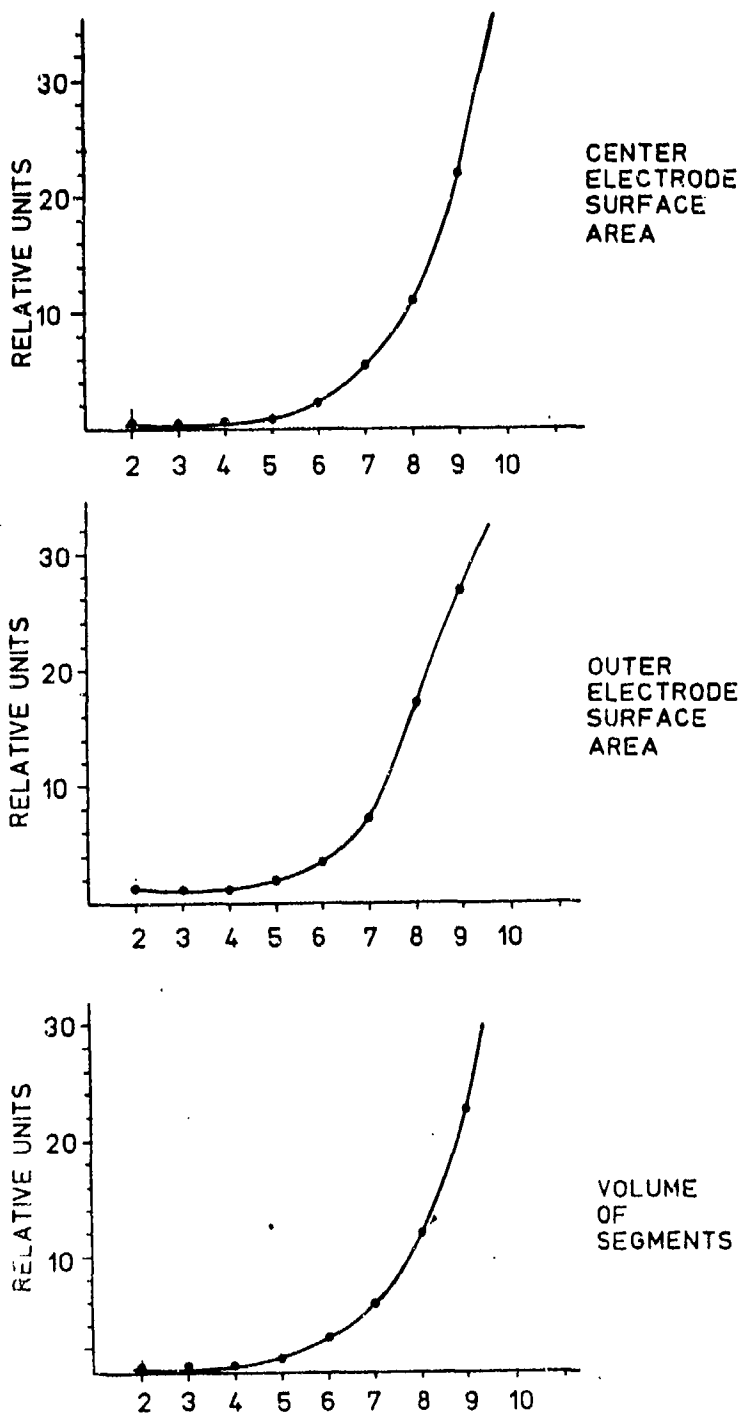


Fig. 11. Surface area and volume of segments versus segment number for optimized version of igniter cavity

5. CONCLUDING REMARKS

Although it is tempting to speculate on the connection between the experimental data in Tables 1 and 3 and the theoretical results in the last section, we prefer to wait for the test results of the modified chamber. We do not expect to find a simple connection between the electrostatic field line distribution and the ignition behavior. In reality, a non-uniform time-varying electrical field develops in the liquid propellant charge interacting with the electrolyte.

Our scepticism is reinforced by the preliminary results obtained with the EMI-AFB test fixture (Section 3.3). Apart from the, unsurprising, occurrence of an arc discharge for the needle-plate geometry, the ignition delays did not seem to follow any pattern. However, it may well be that electrode surface uniformity plays a more important role than previously appreciated. In this case, the conventional finishing procedure will prove to have been inadequate. The extreme scatter of the ignition delays indicates that factors other than the basic electrochemistry may come into play.

ACKNOWLEDGEMENT

The authors would like to acknowledge that the research work reported in this paper has been made possible through the support and sponsorship of both the Ministry of Defence of the Federal Republic of Germany and the U.S. Government through its Ballistic Research Laboratory via its European Research Office as well as through the inhouse funding of the Dynamit Nobel AG. Also, the authors would like to thank Messrs. O. Wieland and R. Roschig for their assistance in this work.

REFERENCES

- [1] J. DeSpirito, J. D. Knapton, and I. C. Stobie, "Progress on Electrical Ignition of Liquid Gun Propellants for Application in Regenerative Liquid Propellant Guns", Proceedings of the 24th JANNAF Combustion Meeting, Monterey, CA, October 1982.
- [2] W. F. Morrison, J. D. Knapton, and G. Klingenberg, "Regenerative Injection Liquid Propellant Guns", Journal of Ballistics, Vol. 8, No. 3, July 1985, pp. 2026-2060.

4th ANNUAL CONFERENCE ON HAN-BASED LIQUID PROPELLANT
STRUCTURE AND PROPERTIES
US ARMY BALLISTIC RESEARCH LABORATORY
ABERDEEN PROVING GROUND, MD
30 AUG - 1 SEP 88

Title of Paper The Burning Rate of HAN-Based Liquid Propellants: The Effect of HAN Concentration on Burning Rates

Presentation Time Request 20 (min)

Type of Paper: Progress; Summary; State-of-art; Other
Speaker's Name Steven R. Vosen Phone Number (415) 294-3434

Affiliation/address Sandia National Laboratories
Livermore, CA 94550

Co-author(s) name(s) _____

ABSTRACT (Use reverse side if necessary)

Propellants being considered for use in liquid propellant (LP) guns consist of a stoichiometric mixture of the salts hydroxylammonium nitrate (HAN) and triethanolammonium nitrate (TEAN) in water. The flame structure at pressures of less than 34 MPa has been shown¹ to consist of a HAN decomposition reaction followed by a TEAN decomposition reaction. The burning rate of the propellant has been shown to be limited by the decomposition rate of HAN, to the extent that HAN decomposition may occur in the absence of TEAN. One implication of this is that it may be possible to sustain a "fume-off" in which HAN decomposes (releasing 20% of the heat of reaction), resulting in a highly explosive mixture. In an attempt to better understand the initial reactions which occur during LP combustion, previous experiments were conducted on HAN-water mixtures which have the same HAN concentration as does LP. This provides one with information on the initial reactions which occur in an LP flame and also closely approximates the burning rate of the propellant.

To obtain more information on the HAN decomposition reaction as it occurs in a flame, a series of experiments will be conducted on HAN-water mixtures of varying concentrations at various pressures. Specifically, HAN-water concentrations of 13, 11, 9, 7 and 5 molar will be conducted at pressures of 6 MPa to 34 MPa. (For comparison, LP 1846 is 9.1 molar HAN and burns at these pressures during the ignition of LP guns.) The mixtures will be contained in a strand burner while undergoing combustion at approximately constant pressure (less than 1% pressure increase during combustion) and will be observed by shadowgraph photography. This will provide information on the importance of HAN decomposition on the burning rates of LP, on the presence of drops in the region above the decomposing liquid, and on the stability of the liquid-gas interface. In addition, the relationship between HAN concentration and pressure on the decomposition rate will be indicative of the importance of condensed phase reactions in the decomposition of HAN.

* This work is sponsored at Sandia National Laboratories by a cooperative research and development program funded by the Department of Energy and the Department of Army.

¹ Vosen, S. R. "The Burning Rate of HAN-Based Liquid Propellants." To appear in the Twenty-second (International) Symposium on Combustion, also in the Twenty-fourth JANNAF Combustion Meeting, October 1987.

The Decomposition Rate of HAN / Water Mixtures

Steven R. Vosen

**Combustion Research Facility
Sandia National Laboratories
Livermore, California**

**Work supported by a Memorandum of
Understanding between DOA and DOE**

Objectives

- Determine the cause of the "negative pressure exponent" observed for LP combustion
- Investigate the role of interfacial instabilities on decomposition rates
- Determine the importance of gas and / or liquid phase chemistry on HAN decomposition

Approach

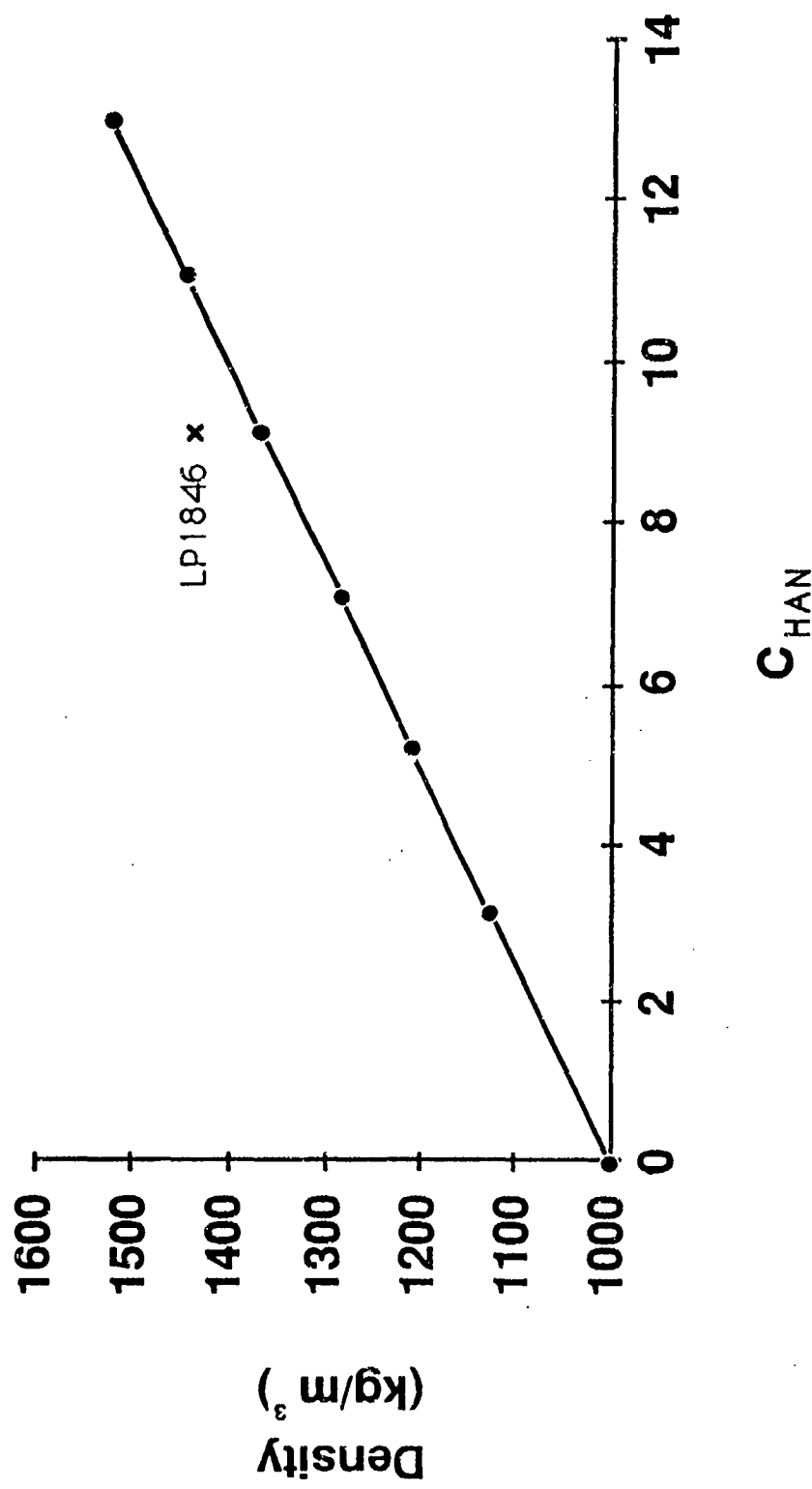
**Study the effect of HAN concentration and pressure
on the decomposition of HAN / water mixtures in a
"strand burner" to determine:**

- Decomposition rates
- Interfacial dynamics

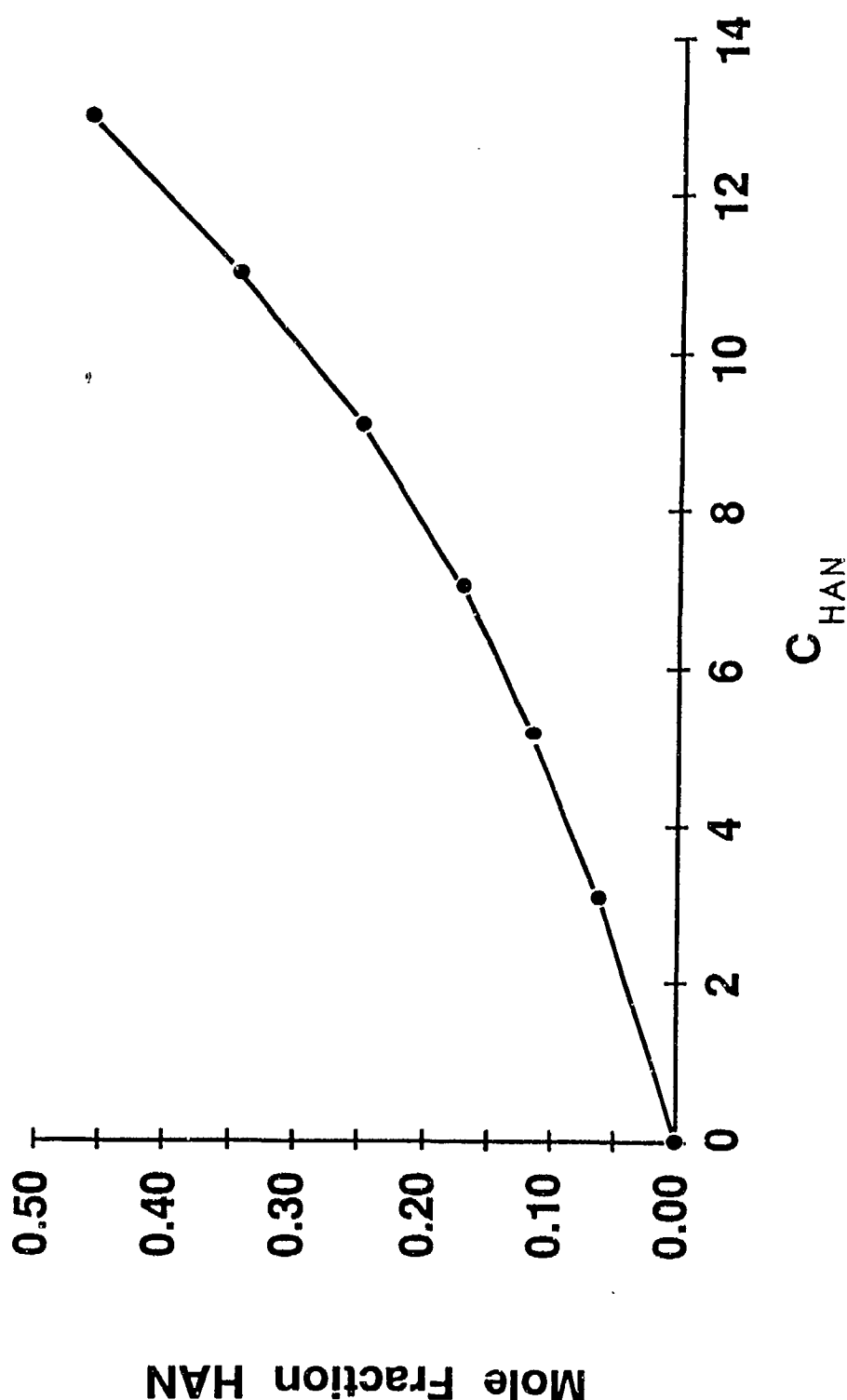
Experimental Conditions

- Constant pressure (5 - 35 MPa)
- Burn column of fluid (1 to 7 mm cross section, 40 mm deep)
- Electric discharge initiation of reaction (joules in μ s)

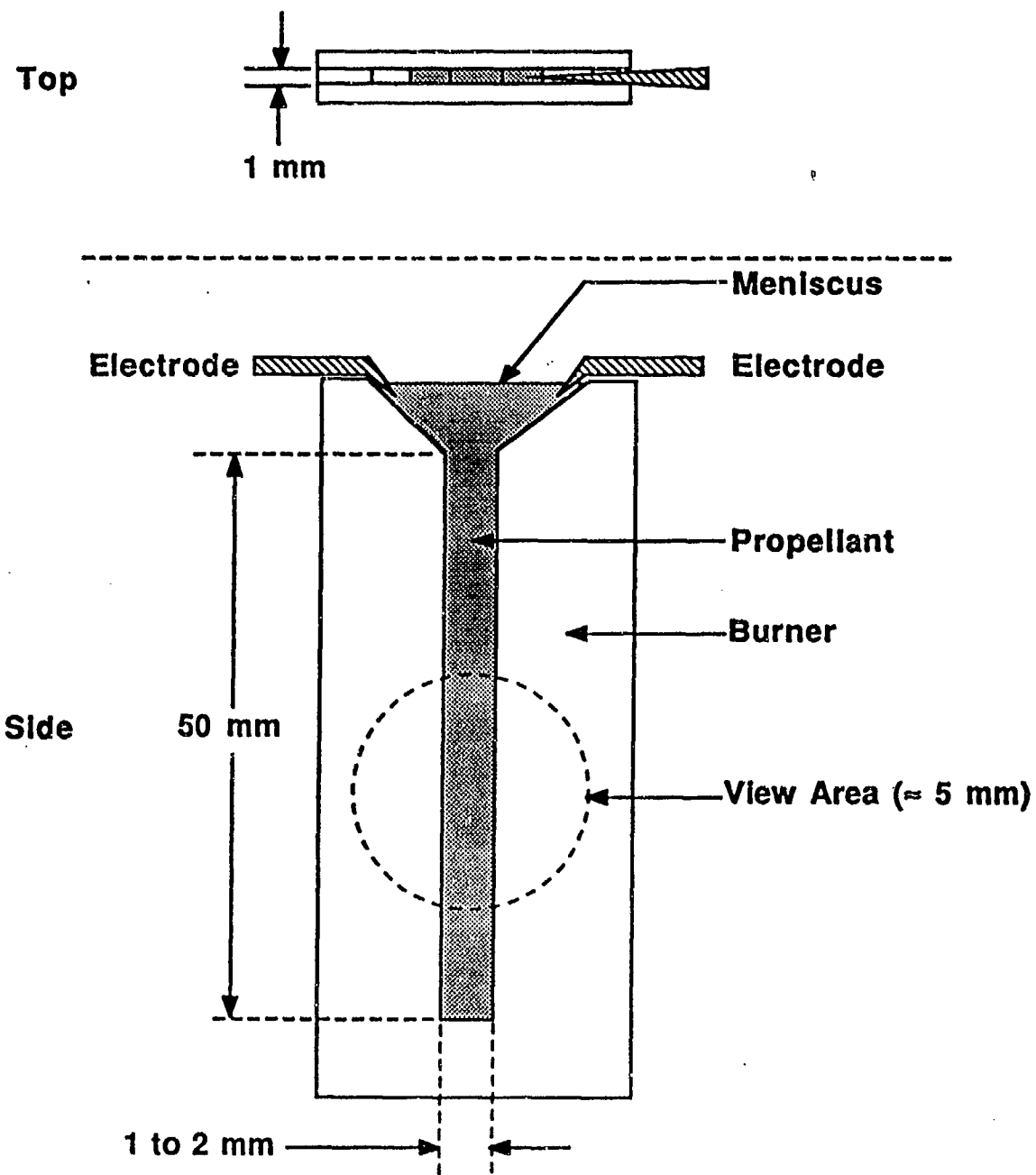
HAN / Water Mixture Density



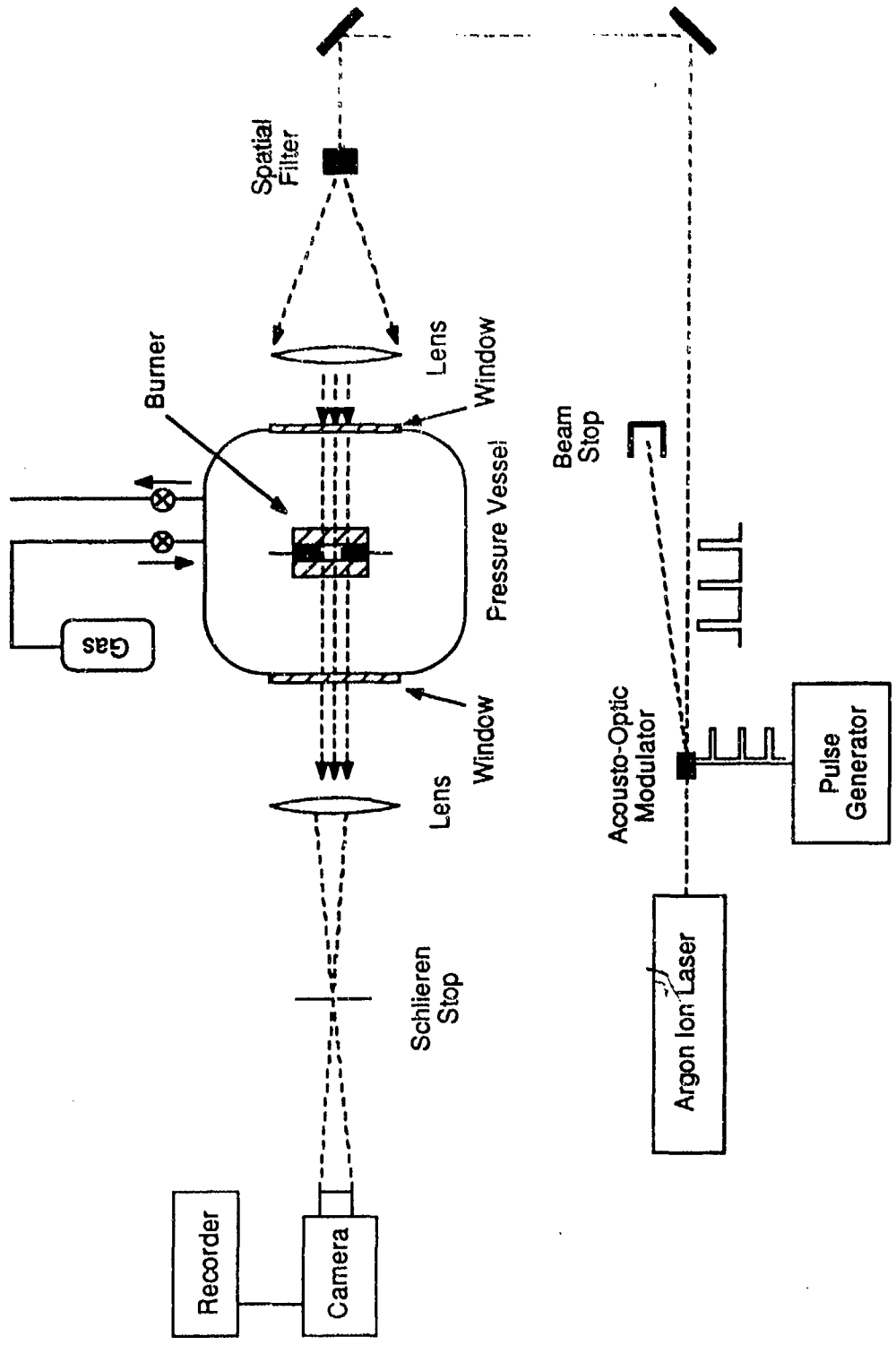
HAN Mole Fraction in HAN / Water Mixtures



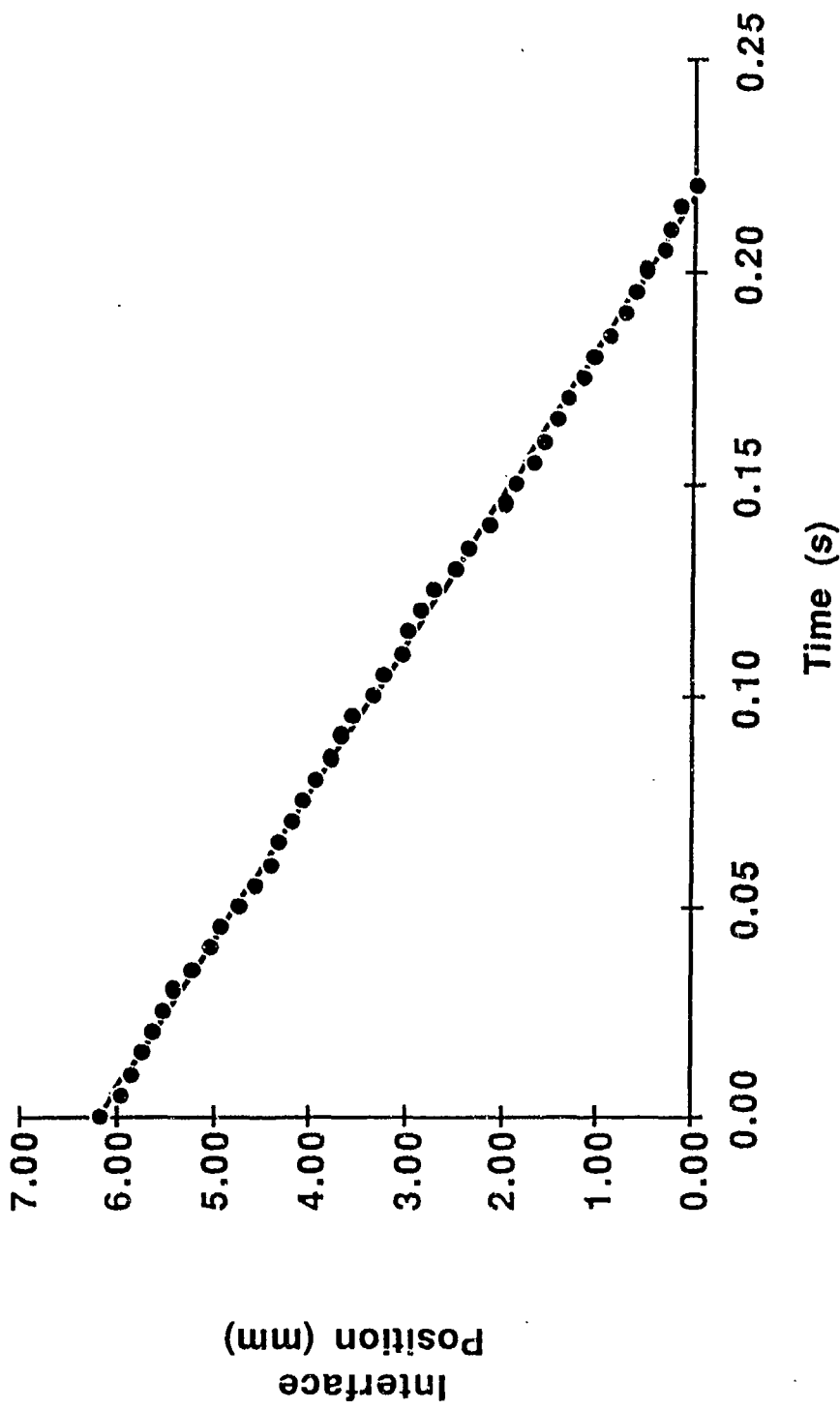
Burner



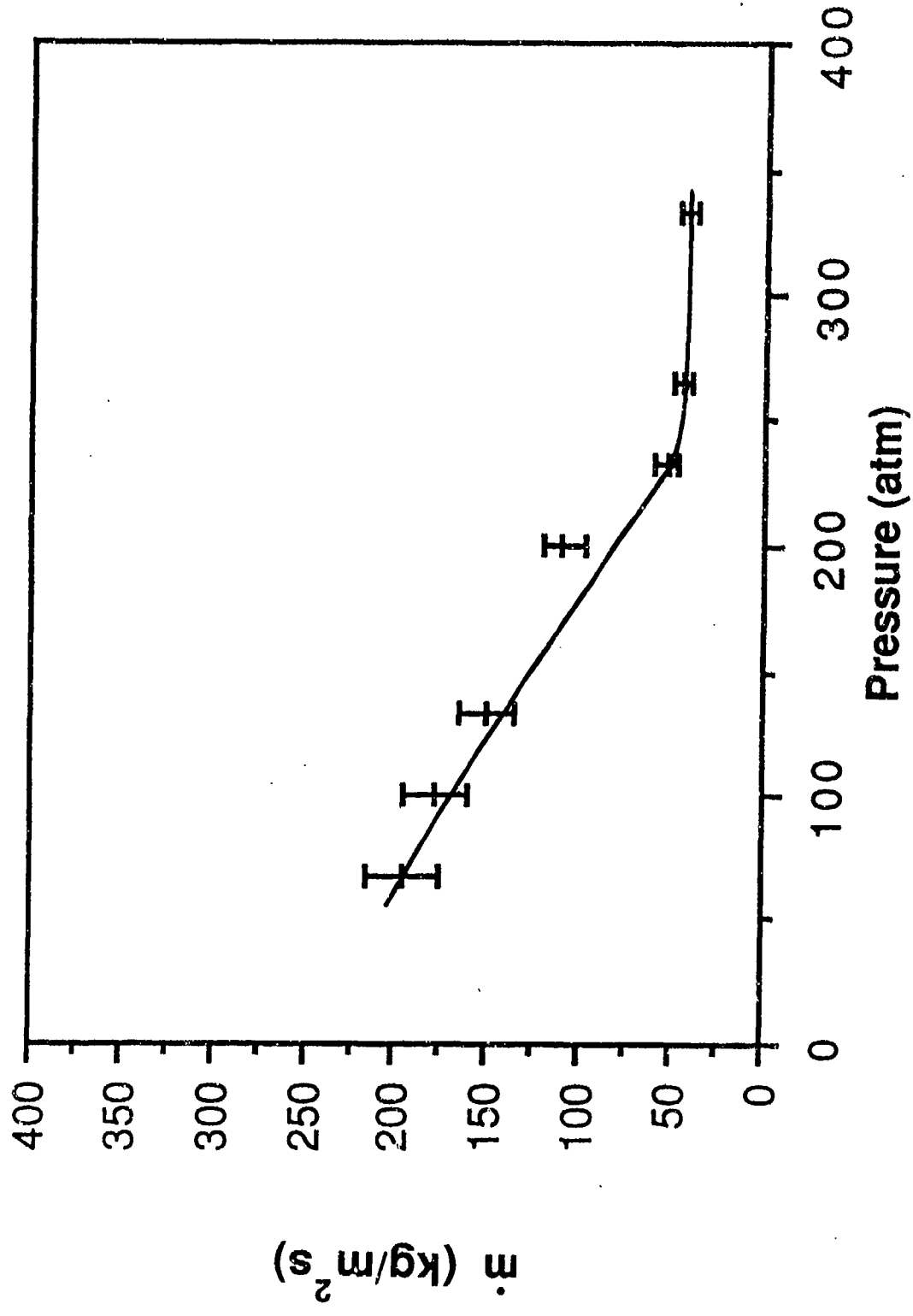
Schematic of Experiment



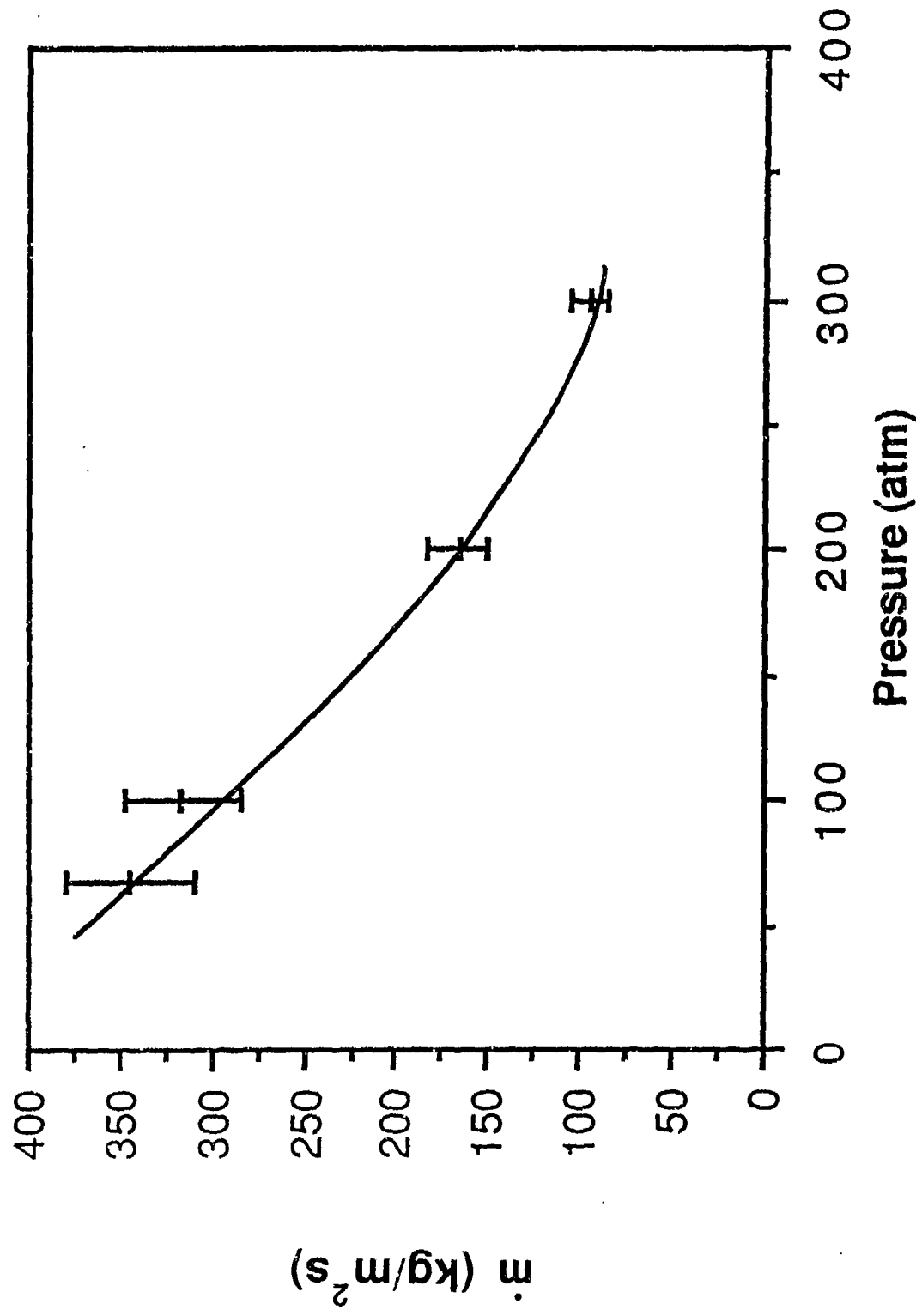
Interface Velocity Determination



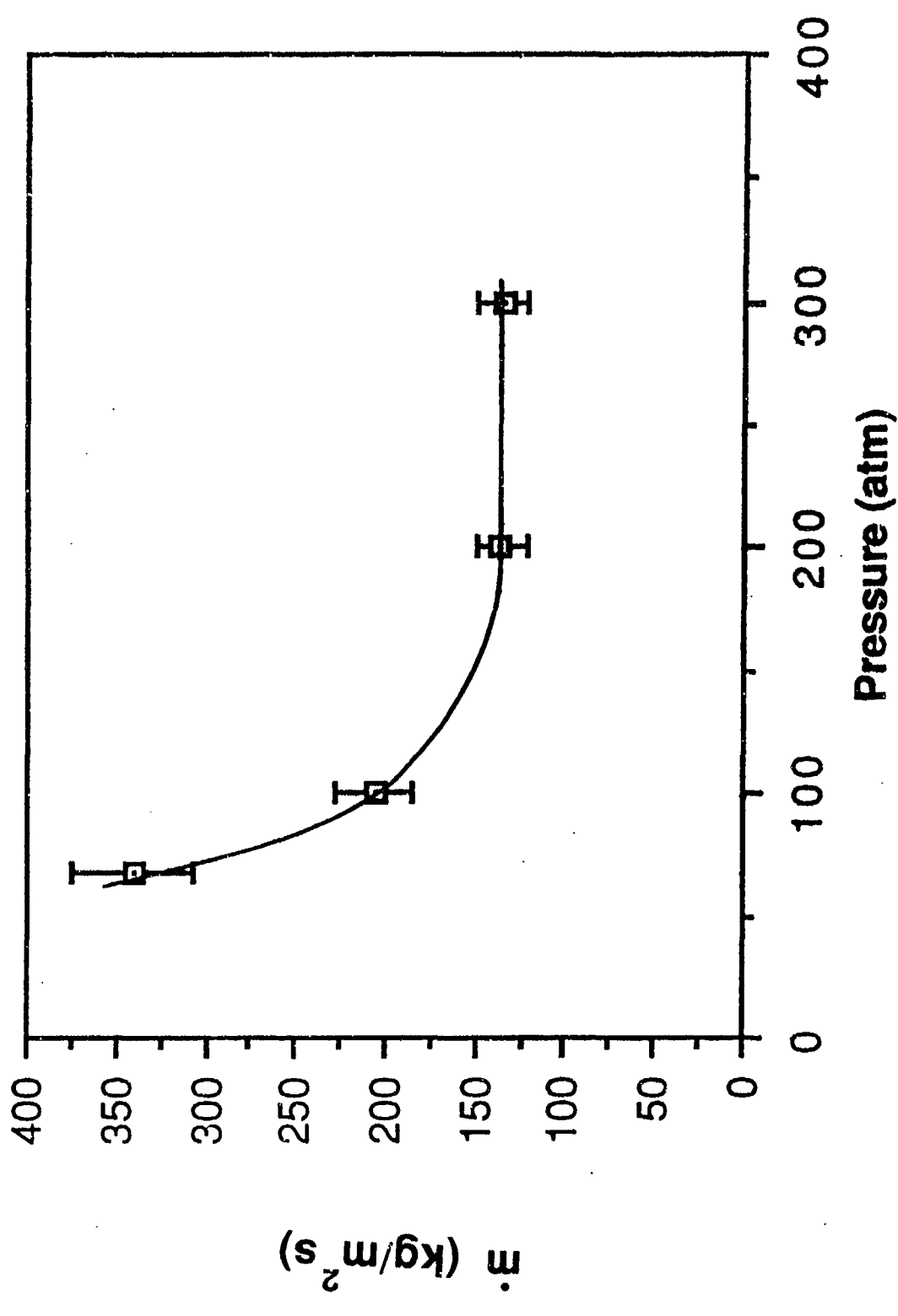
LP1846 Regression Rate Data - 1.8 mm Burner



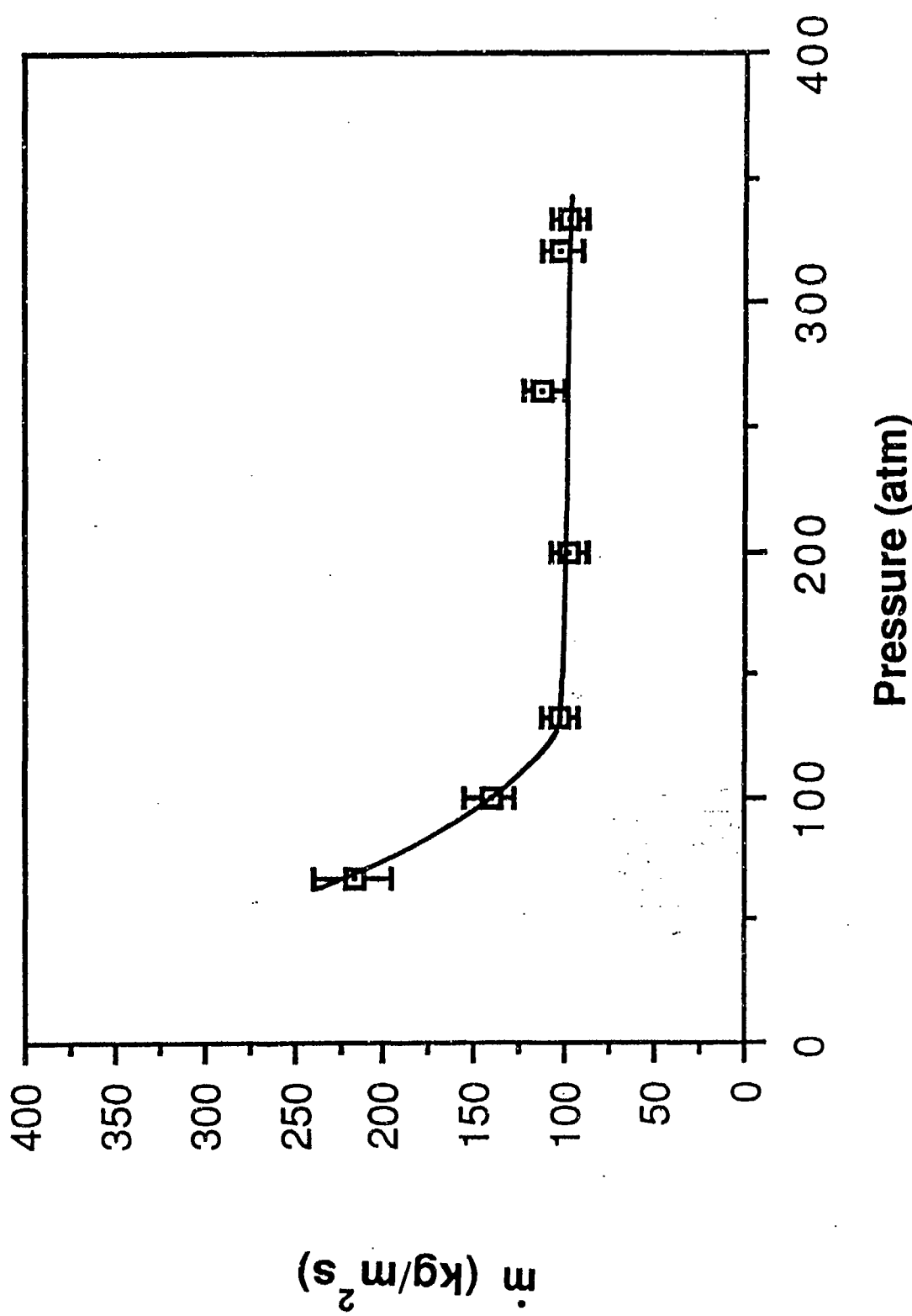
LP1846 Regression Rate Data - 5 mm Burner



9.1 molar HAN Regression Rate Data - 5 mm Burner



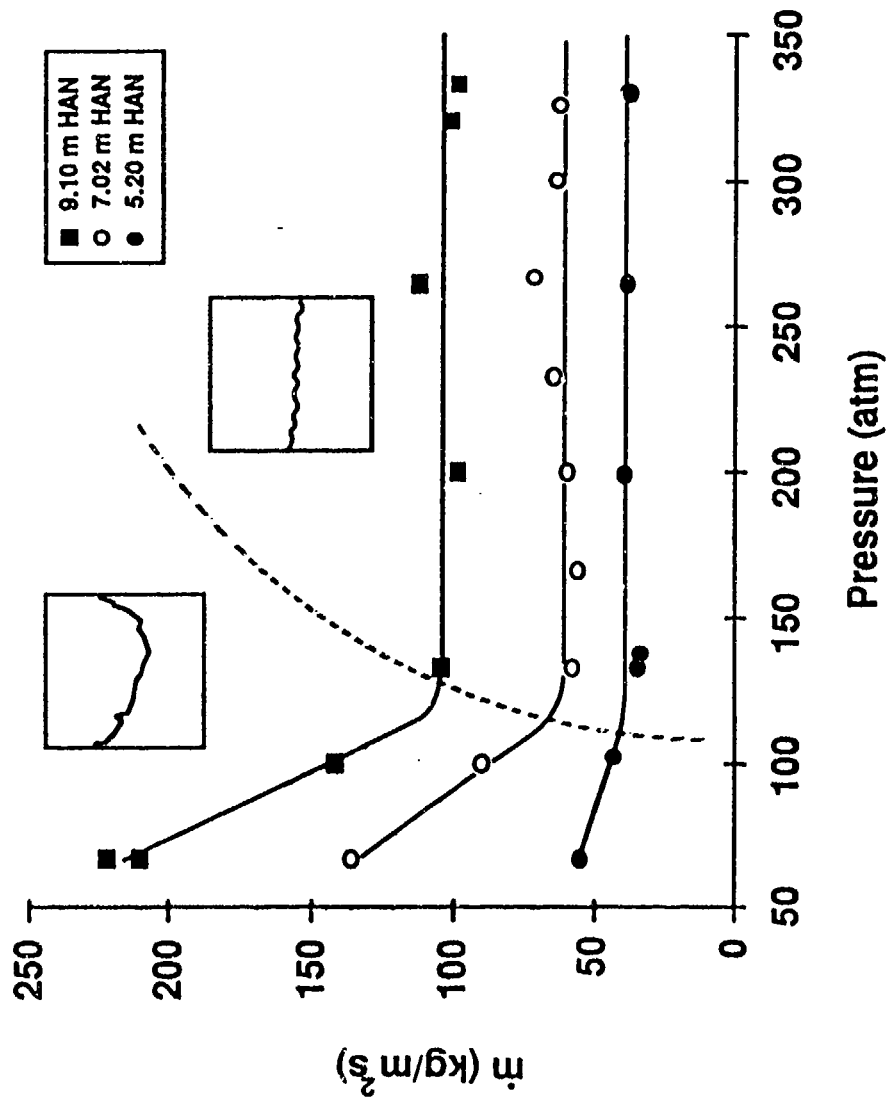
9.1 molar HAN Regression Rate Data - 1.8 mm Burner



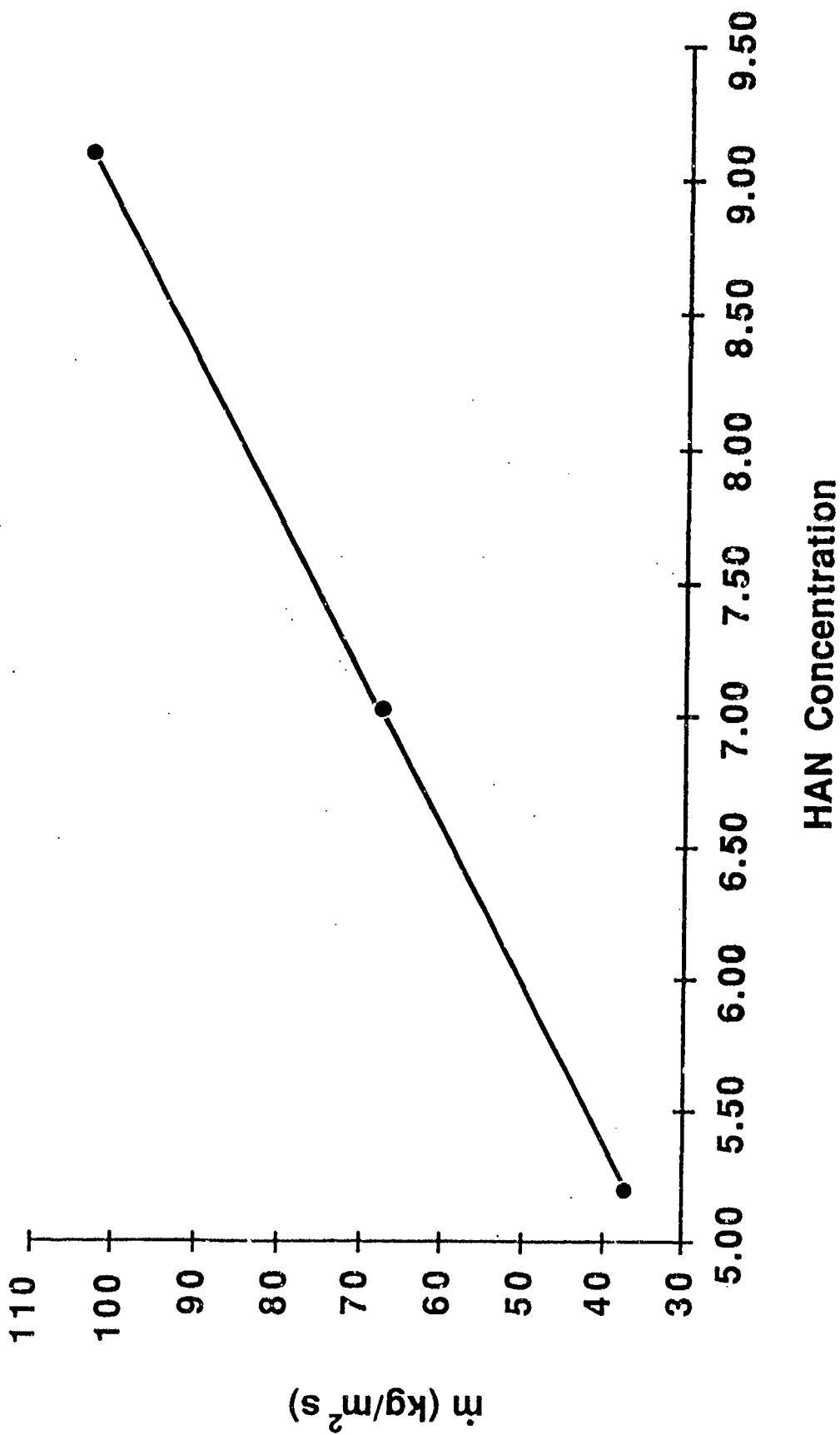
Observations

- Can not sustain decomposition in 3 molar HAN
- The water in the decomposition products of 5, 7 and 9 molar HAN is mainly in the liquid phase
- The water in the decomposition products of 11 and 13 molar HAN is mainly in the vapor phase

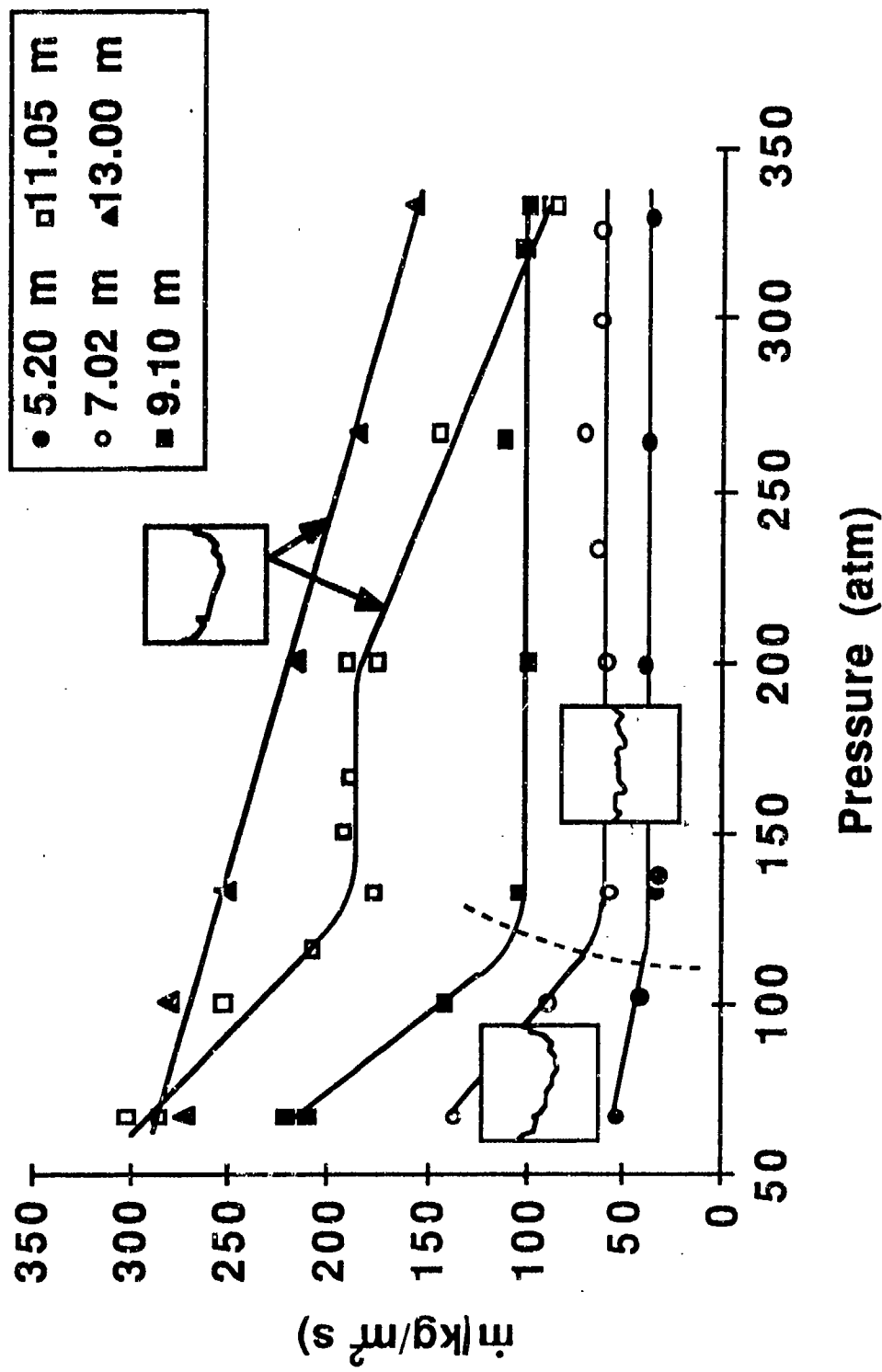
Apparent Mass Burning Rate - 1.8 mm Burner



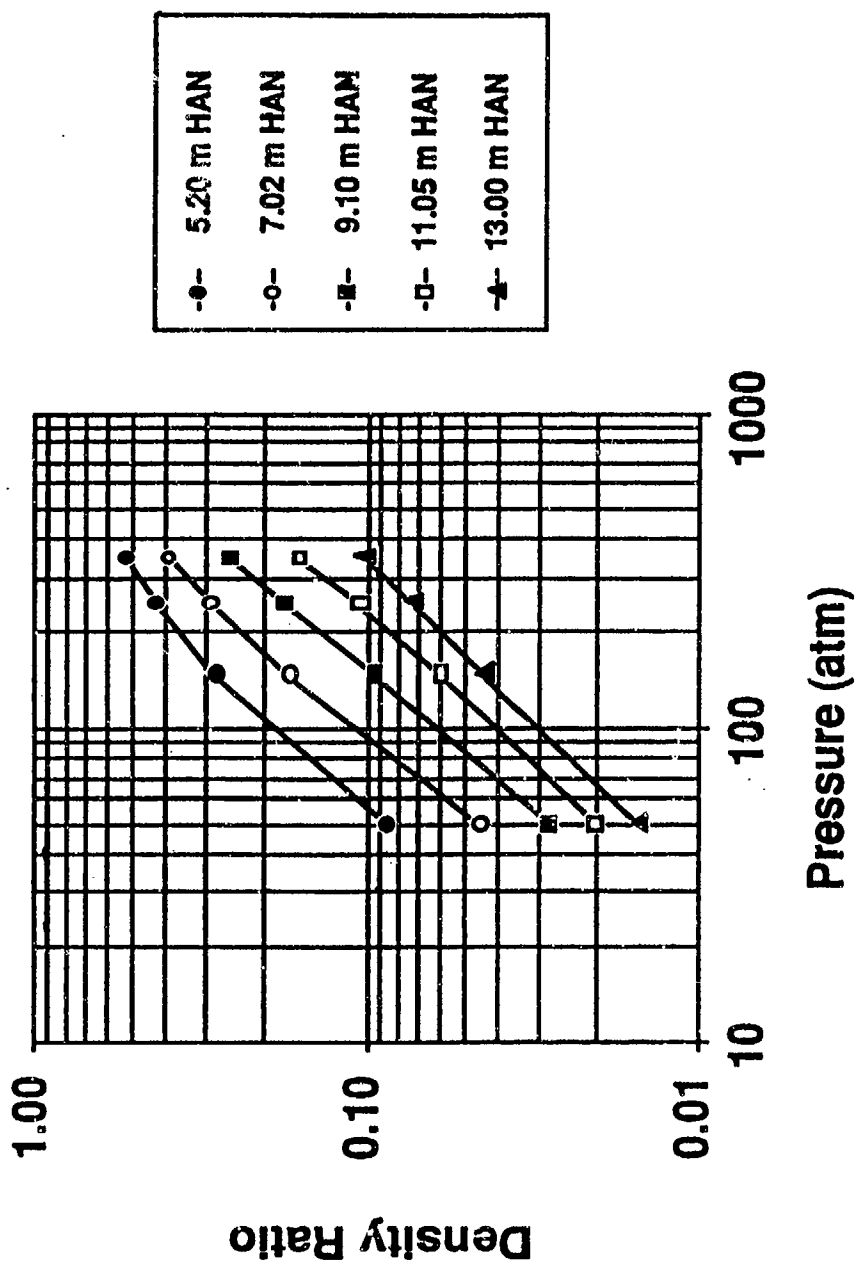
Apparent Burning Rate vs. HAN Concentration



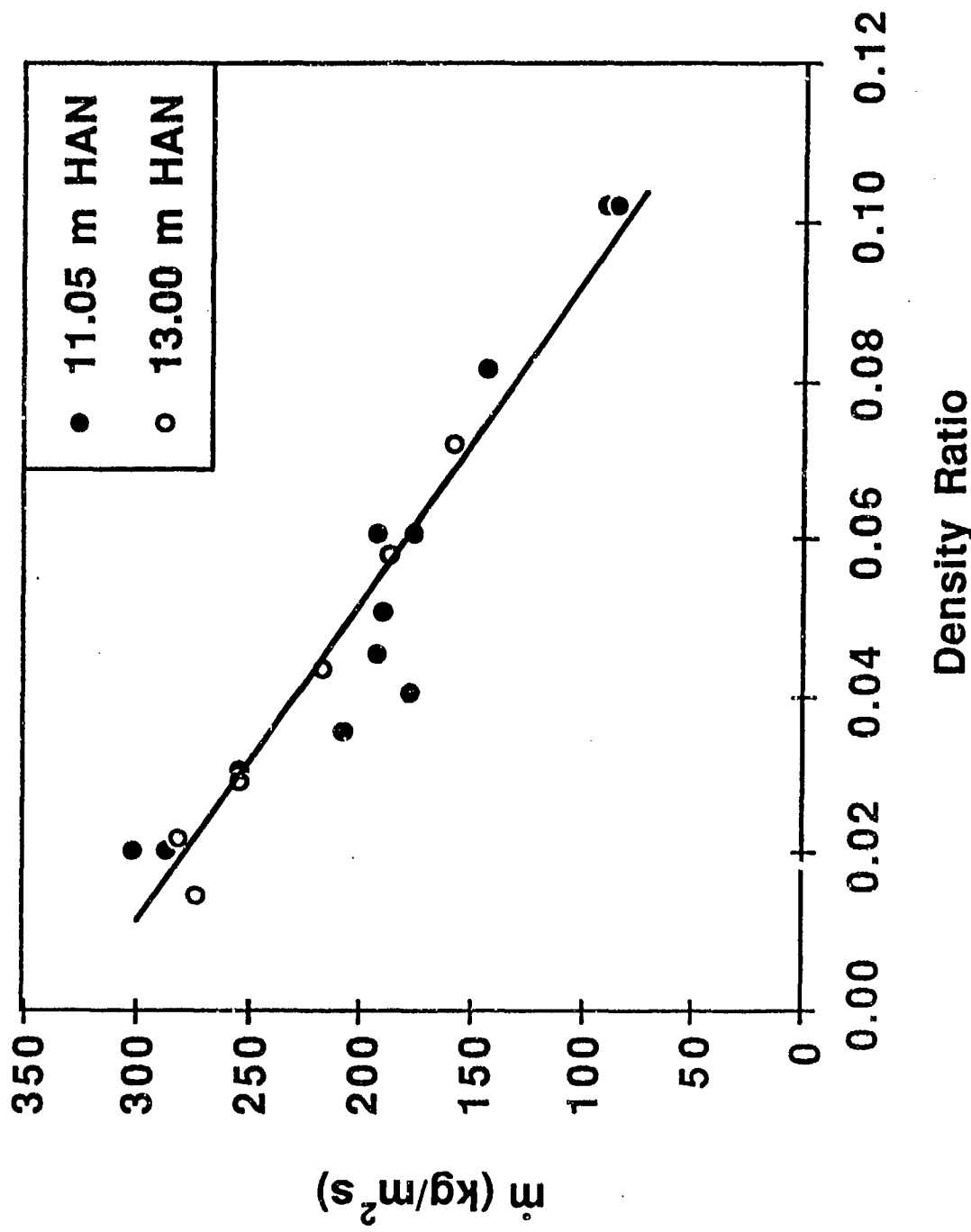
Apparent Mass Burning Rate - 1.8 mm Burner



Decomposition / Initial Density Ratio



Mass Burning Rate vs. Density Ratio (11 & 13 m HAN)



Conclusions

- HAN / water apparent decomposition rates are similar to LP1846 apparent burning rates
- Repeatable measurements of the decomposition rate can be made
- Accomplished by judicious choice of burner geometry, ignition location and viewing location
- In burners of less than 7 mm diameter, the dominant length scales for instabilities are several mm and tens of μm

Conclusions (2)

- There are two identifiable regimes of HAN decomposition:
 - At low pressure, the apparent decomposition rate $\approx 1/P$ (due to hydrodynamic instabilities)
 - At higher pressure, the apparent decomposition rate $\approx \text{HAN concentration}$
- There is strong evidence for condensed phase reactions being the rate limiting step in HAN decomposition and LP combustion
- The unusual apparent burning rate dependence on pressure is the result of:
 - a pressure independent burning rate, and
 - hydrodynamic instabilities which become less important at higher pressures

Current and Future Work

- Effect of additives on the decomposition of HAN
Modification of fluid properties and chemistry
- Image analysis of photographs
Information on interface length scales
- Emission Spectroscopy from LP flames
Identification of gas phase species

4th ANNUAL CONFERENCE ON HAN-BASED LIQUID PROPELLANT
STRUCTURE AND PROPERTIES
US ARMY BALLISTIC RESEARCH LABORATORY
ABERDEEN PROVING GROUND, MD
30 AUG - 1 SEP 88

Title of Paper Study of Thermal Diffusive-Reactive Instability in Liquid Propellants: The Effects of Surface Tension and Gravity

Presentation Time Request 20 (min)

Type of Paper: Progress; Summary; State-of-art; Other

Speaker's Name Robert C. Armstrong Phone Number (415) 294-2470

Affiliation/address Sandia National Laboratories
Livermore, CA 94551

Co-author(s) name(s) S. B. Margolis

ABSTRACT (Use reverse side if necessary)

We have extended previous work by considering a thermal and pressure dependence to the reaction dynamics. We predict that, in addition to the well-known cellular instabilities first found by Landau, pulsating instabilities will be found associated with flame interaction with the thermal and pressure (hydrodynamic) fields. These results are found in the limit of small gas-phase density and are related to similar results found for solid propellants. As a consequence of this discovery, it is predicted that there are regimes of instability under conditions that would have been predicted stable by previous work. Entirely different behavior is found for a relatively dense gas phase. We predict a separate new mechanism for instability that is a direct interaction between convection cooling of the flame and the thermal field's ability to restore itself via thermal diffusion.

It becomes evident from this and previous work that many regimes of instability in liquid propellant combustion are possible and even likely. Some direction from experiment is necessary to make the best use of theoretical effort. We will discuss the ways in which stability analyses can be used to interpret liquid propellant experimental data for the purpose of uncovering which of the proposed mechanisms of instability are present in physical systems.

This work sponsored at Sandia National Laboratories by a cooperative research and development program funded by the Department of Energy and the Department of Army.

Title of Paper: The Response of an LP to Heating at High Pressure

Presentation Time Requested: 15 min.

Type of Paper: Progress

Speaker's Name: Richard A. Beyer

Affiliation: US Army Ballistic Research Laboratory

SLCBR-IB-I

APG, MD 21005-5066

A series of experiments has been performed with the goal of understanding the rate and phenomenology of the energy release of drops of a liquid monopropellant when subjected to hot, high pressure flows. The propellant studied was LP 1846.

The studies to be reported has involved the application of increased pressure, up to 4000 psi (28 MPa). Although incomplete, several interesting observations have been made. The primary diagnostic has been high speed photography. Drops have been heated either by placing them in electrically heated regions while suspended on 10 μm diameter carbon fibers, or by directly heating the wire holding them. In the first case, helium gas was used to maximize thermal conductivity to the drops and to maintain good visualization of event. Over a range from 2000 to 4000 psi, the drops were found to appear quiescent for a time up to 500 msec, with no change in transmission (the liquid is transparent until reactions begin) or diameter; they then gassify in a time on the order of 1 millisecond. The evolved gases are relatively transparent. Any light emission would probably not be detected. If a drop is similarly suspended a few drop diameters from a heating wire, the time to drop gasification is shorter, as expected, and results in a cloud of high optical density gas. This difference suggests that significant liquid phase reactions are taking place in the first case.

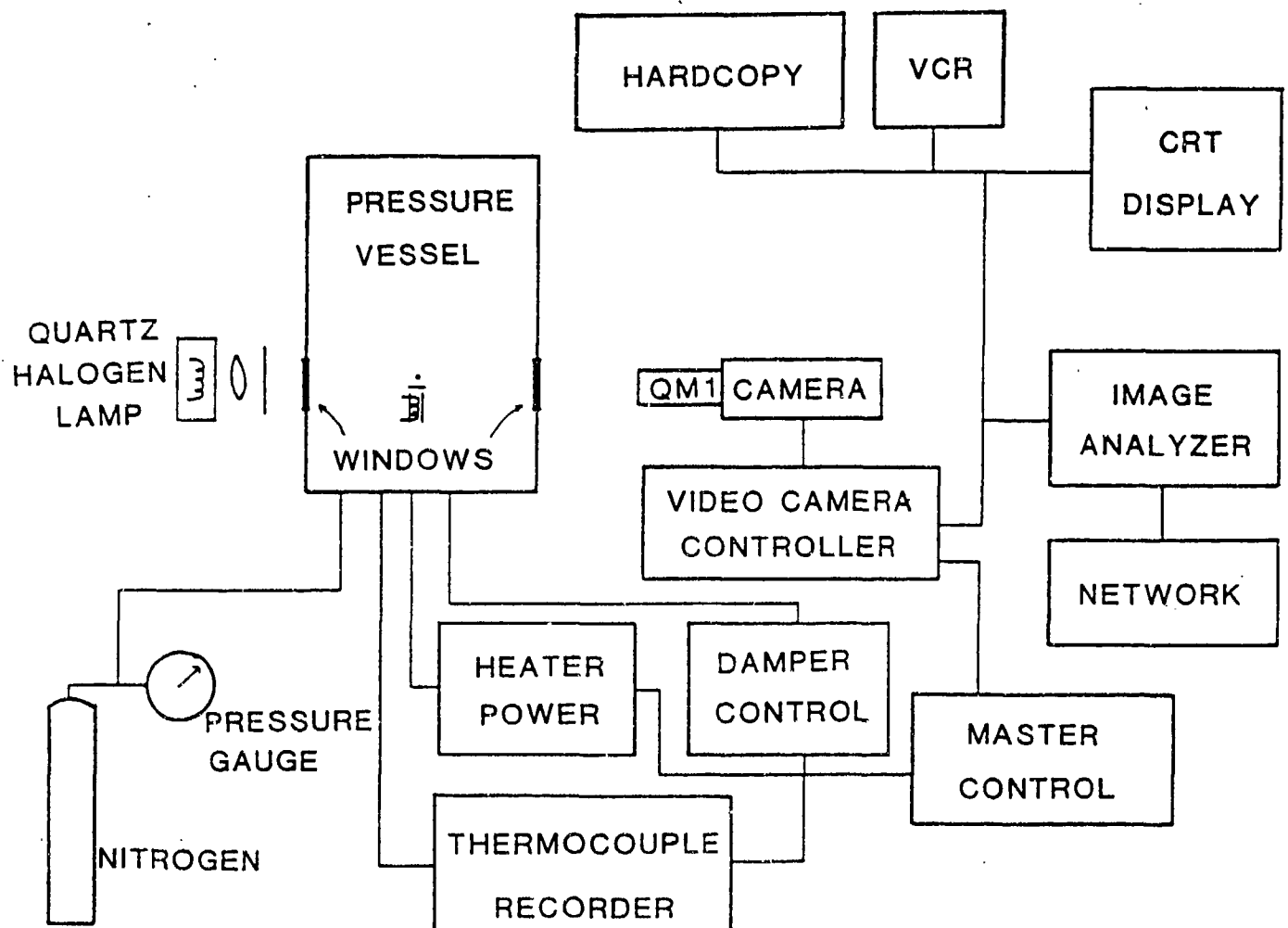
Drops have also been studied by directly heating the suspending wire. In studies with fine (25 μm) diameter wires, there appears to be an important pressure effect on behavior. In all cases the evolve gases are very dense. At pressures below a threshold which is near 1500 psi (10 MPa), gases evolve from the contact point of the wire with the drop for up to ten milliseconds or more, and the process stops if the current is turned off to the wire. Above the apparent threshold the gasification of the drop is rapid (ca. 1 msec) and irreversible; in events where the drop was thrown from the wire by motion upon heating, the drop gasified rapidly while free at higher pressures, but merely emitted a small puff of gas and then stabilized until leaving the field of view (several msec) at lower pressures. Studies are under way to determine if this threshold is as sharp as preliminary work indicates.

Studies into the mechanism of drop ignition are also of interest. These have been pursued by placing a somewhat larger drop (1 mm dia.) on 22 ga. nichrome wire. Imaging of emitted light shows that a flame is present in the gas phase well away from the wire, suggesting that the drop completely gasifies and then ignites and burns as a premixed gas phase flame. Present efforts are to identify and time resolve the emission from this flame to identify possible roles of the various LP components.

THE RESPONSE OF
LP1846 TO
HEATING AT
HIGH PRESSURE

RICHARD BEYER

USA BRL



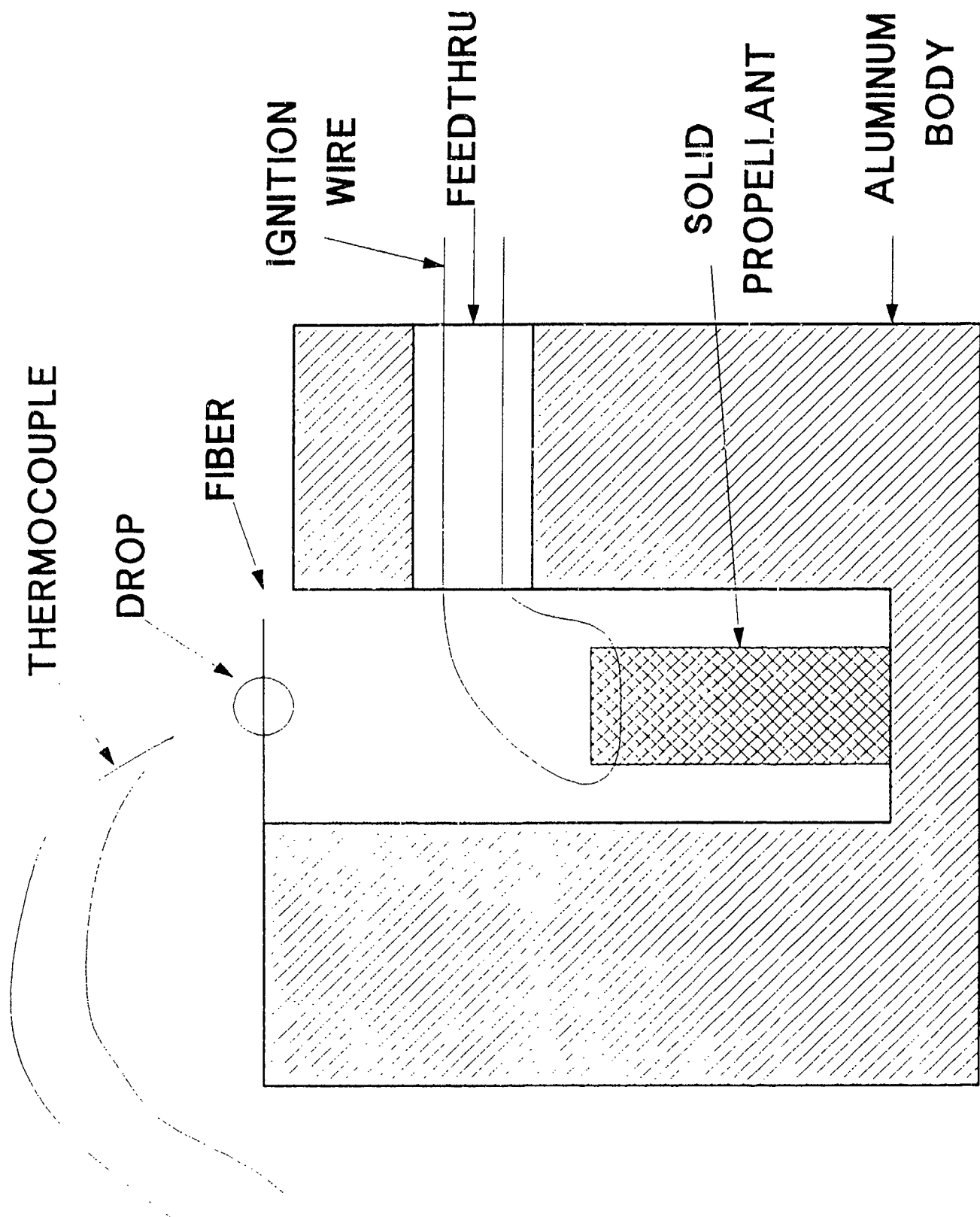
**DROPS HEATED
BY BURNING
SOLID PROPELANT**

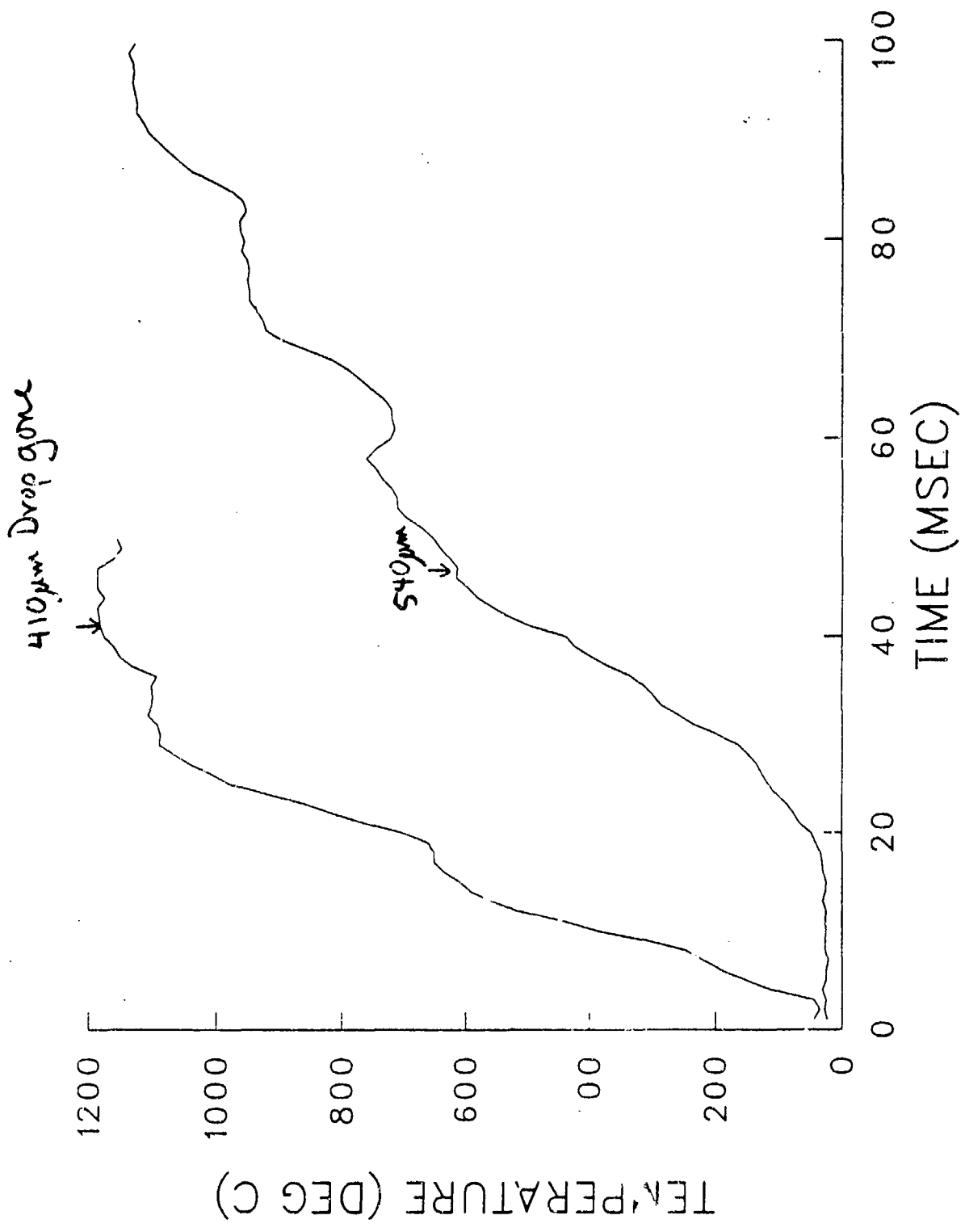
GOALS OF NEXT PHASE

IGNITION OF DROPS

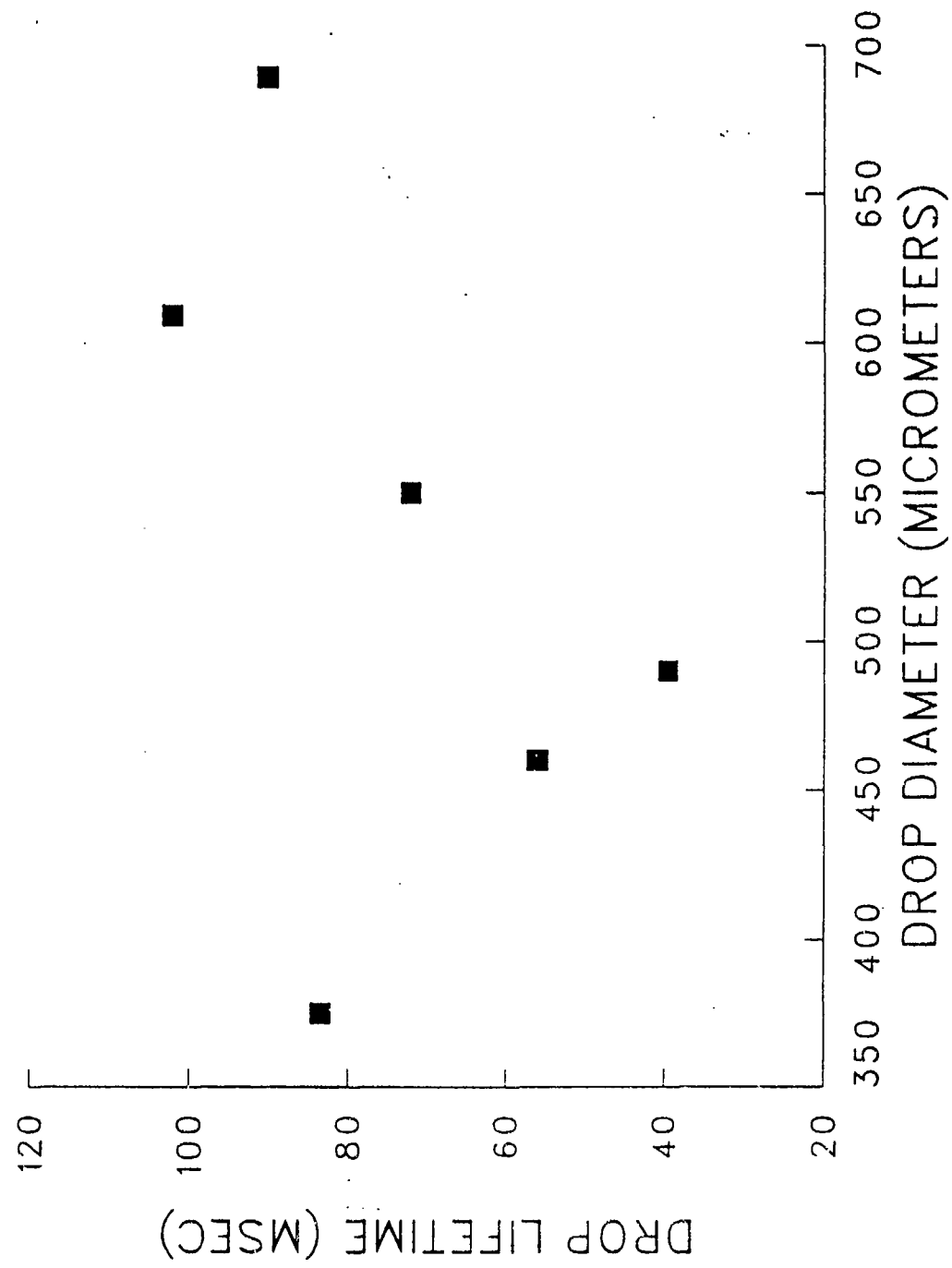
- HOT FLOW
- HIGH PRESSURE
- LARGE DROPS

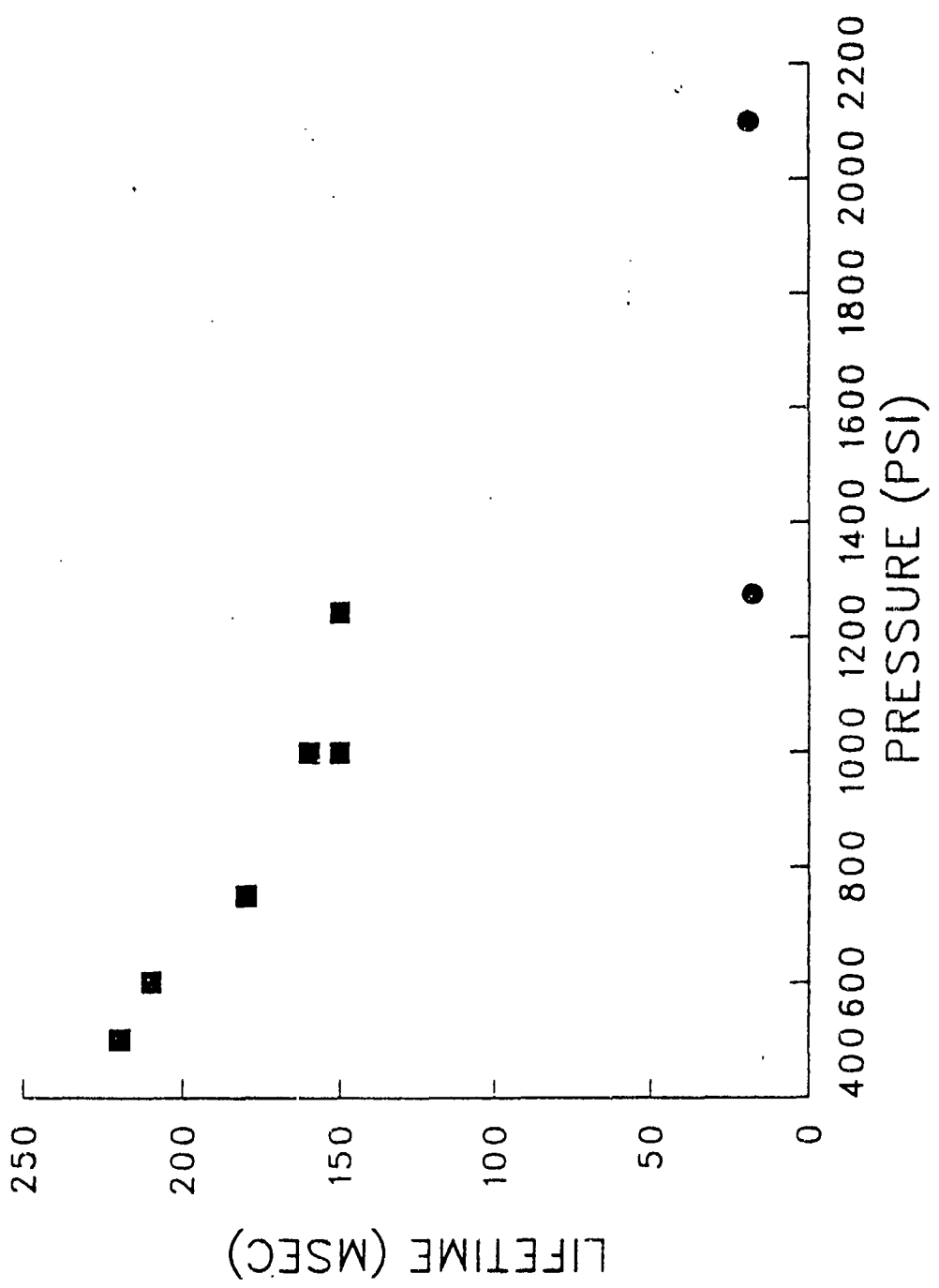
COMPARE WITH DRY HEAT





$A \sim 8.8 \text{ MPa}$
 $\sim 1295 \text{ ps}$





SUMMARY

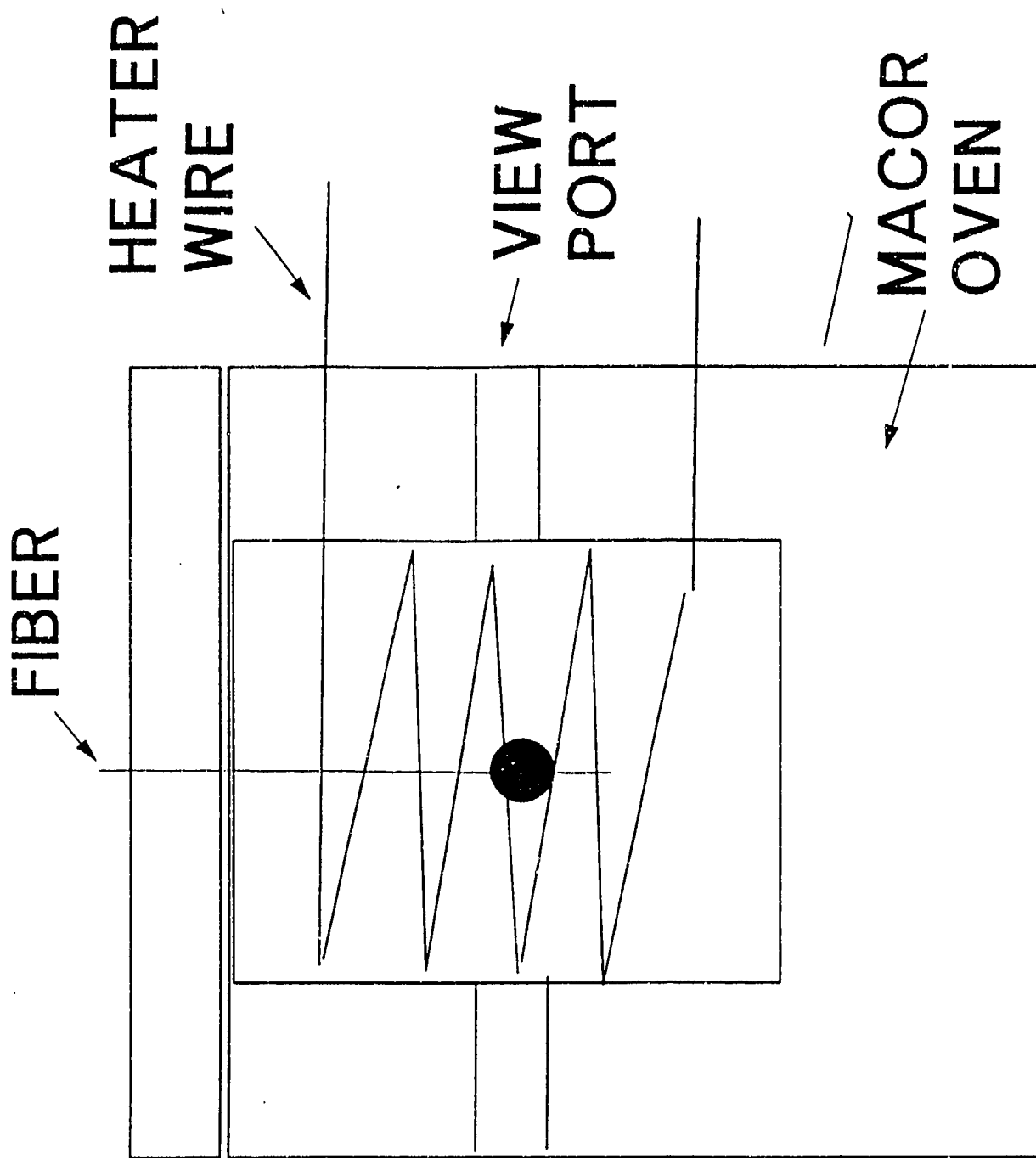
VISUALIZATION POSSIBLE

VISIBLE LIGHT OBSERVED

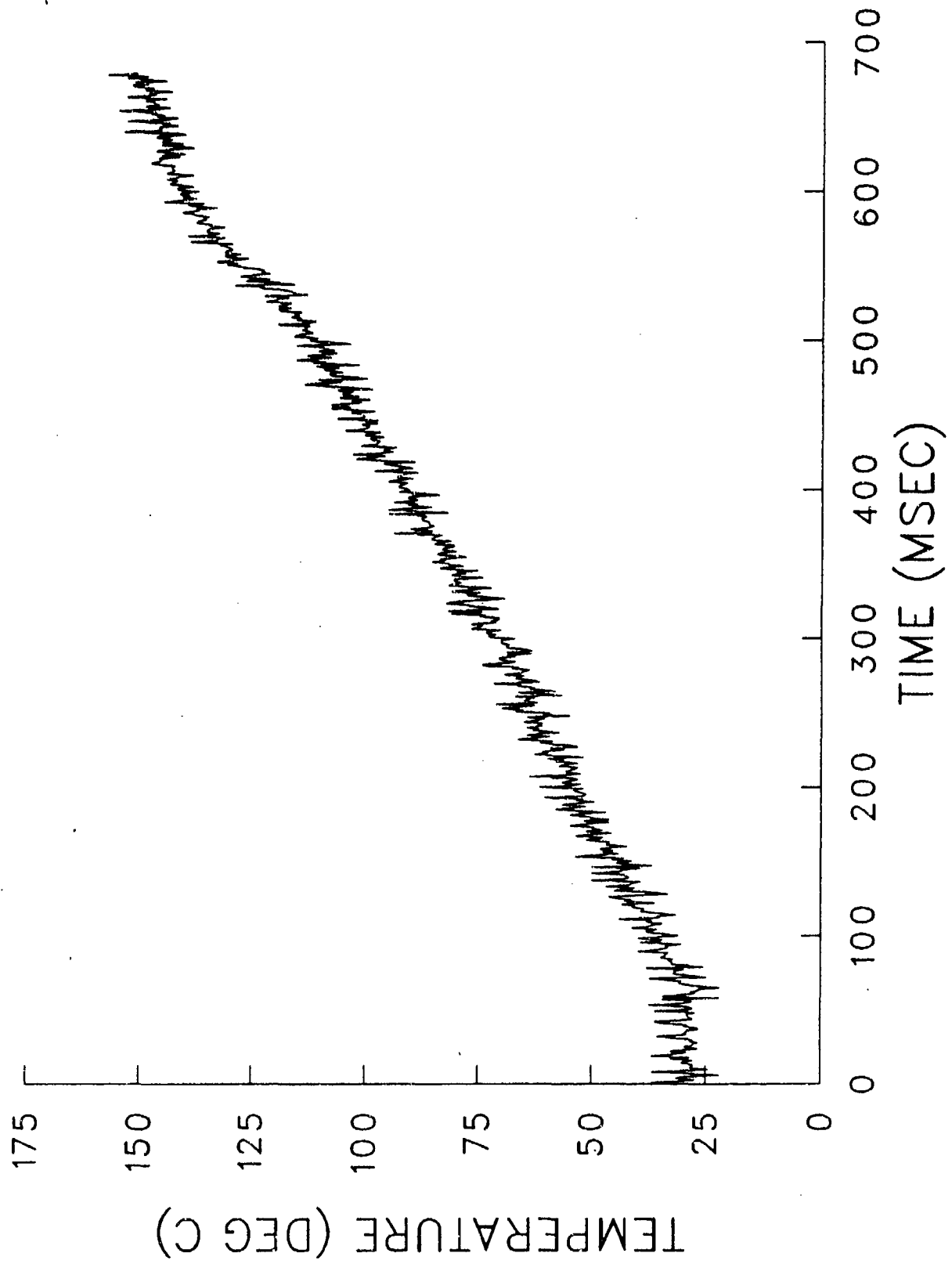
LIFETIMES SHORTER

THAN PREVIOUSLY

**HEATING IN
"OVEN"**



Thermocouple at drop position.



OVEN HEATER

LONG DELAYS

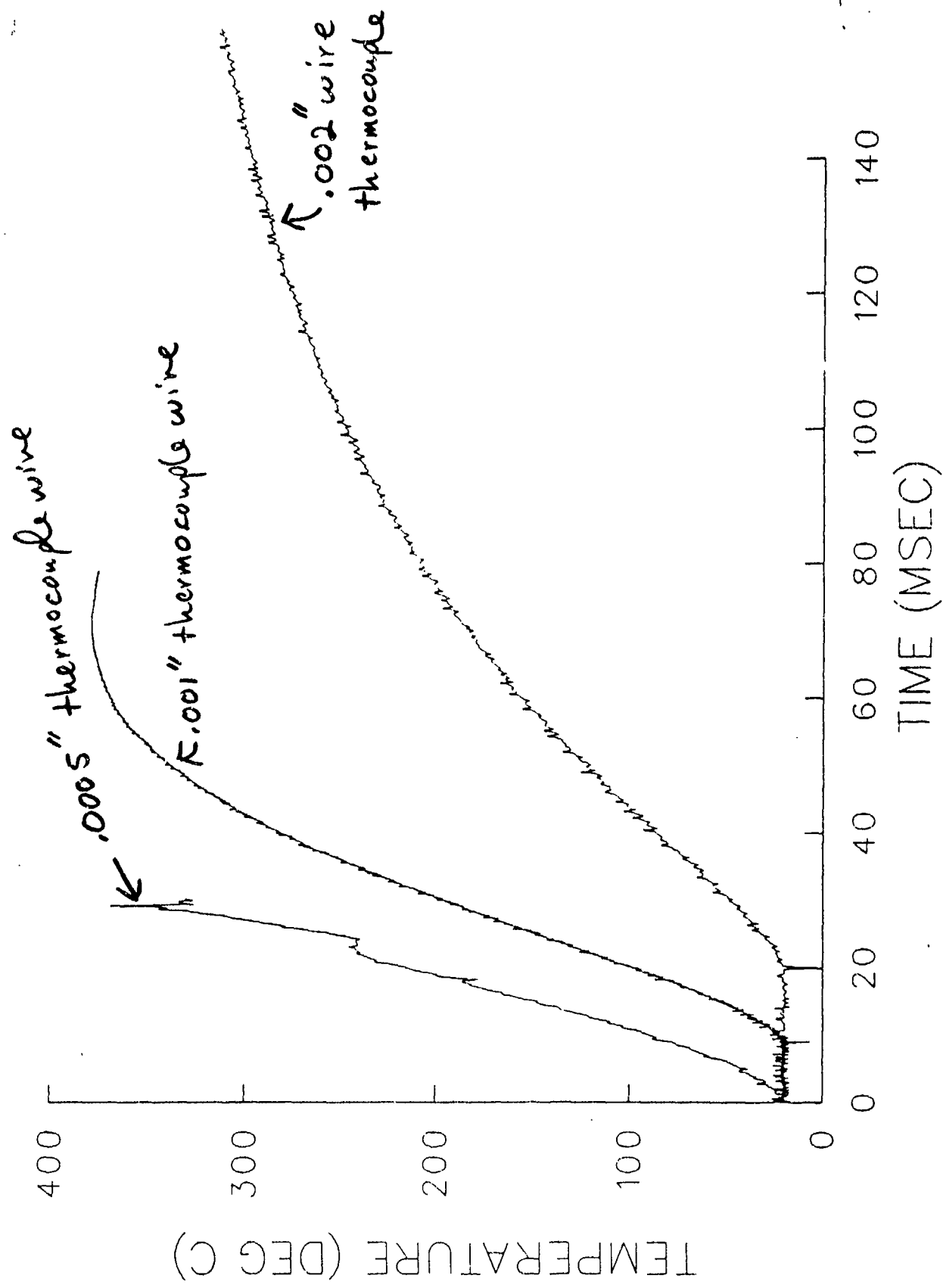
NON-REPRODUCIBLE

CLEAR GAS-PHASE
PRODUCTS

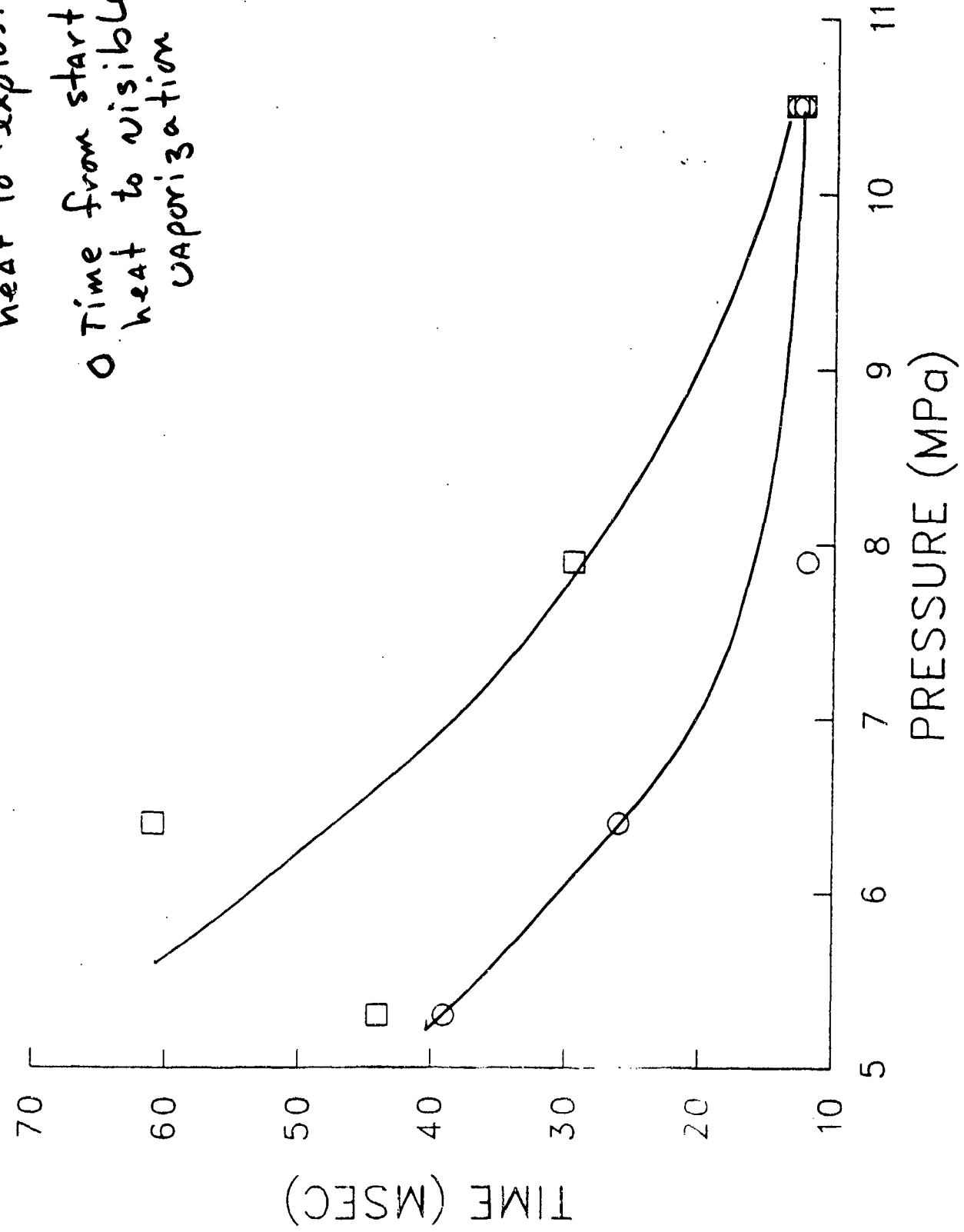
HEATING RATE
DEPENDENCE

**DROPS ON
HOT WIRE**

THERMOCOUPLE RESPONSE - 1 MIL HEATER



□ Time from start of
heat to "explosion"
○ Time from start of
heat to visible
vaporization



DROP ON HOT WIRE

- RAPID VAPORIZATION
- DENSE CLOUD
- PRESSURE DEPENDENCE
- CONCENTRATION
DEPENDENCE

SUMMARY OF HEATING OBSERVATIONS

- AT HIGHER PRESSURES DROPS VAPORIZIZE RAPIDLY
- PRESSURE OF RAPID VAPORIZATION IS CONCENTRATION DEPENDENT
- DENSITY OF GAS PRODUCTS IS DIFFERENT IN PRESENCE OF A CONDUCTING WIRE

FUTURE EFFORTS

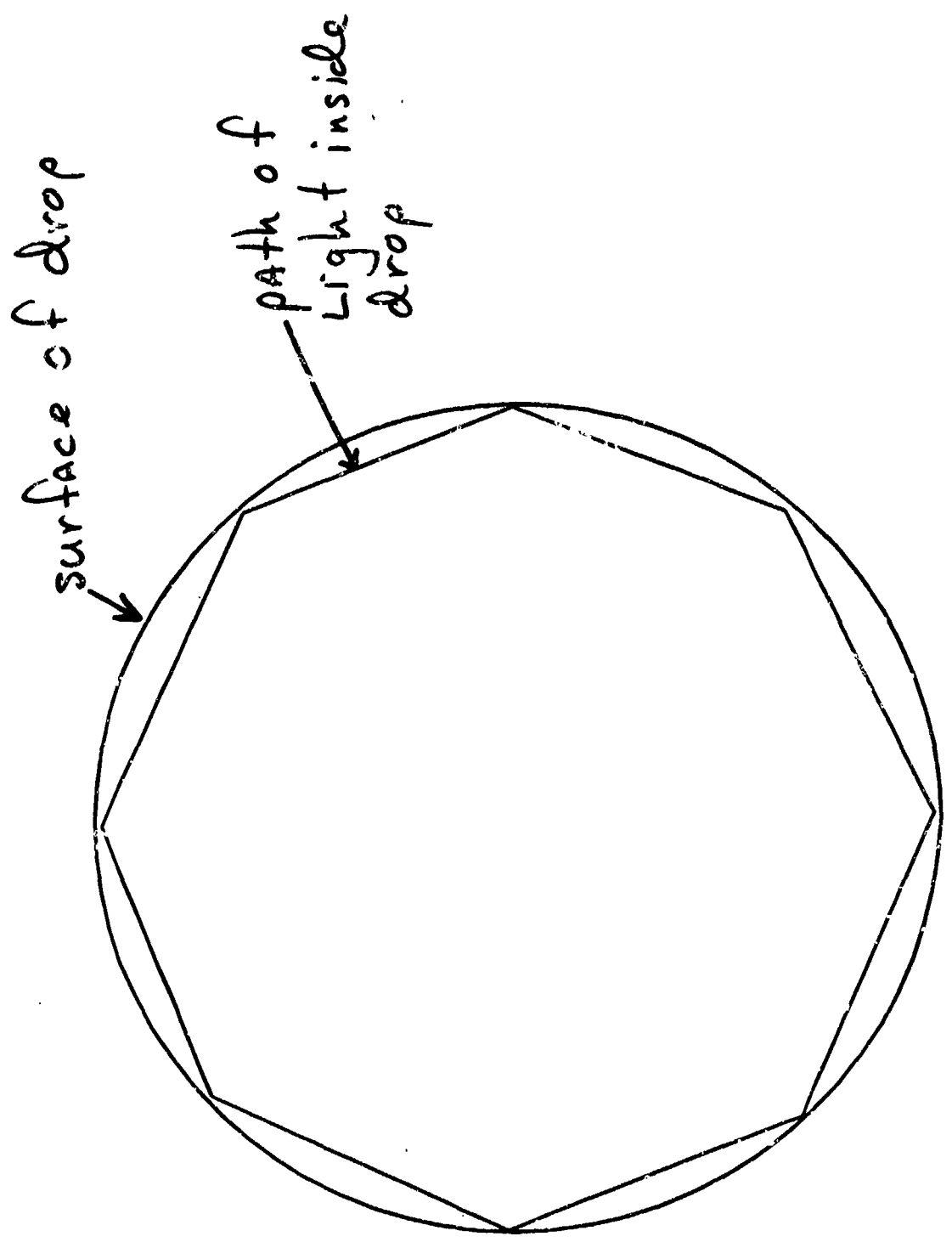
SPECTROSCOPIC PROBES

GAS PHASE

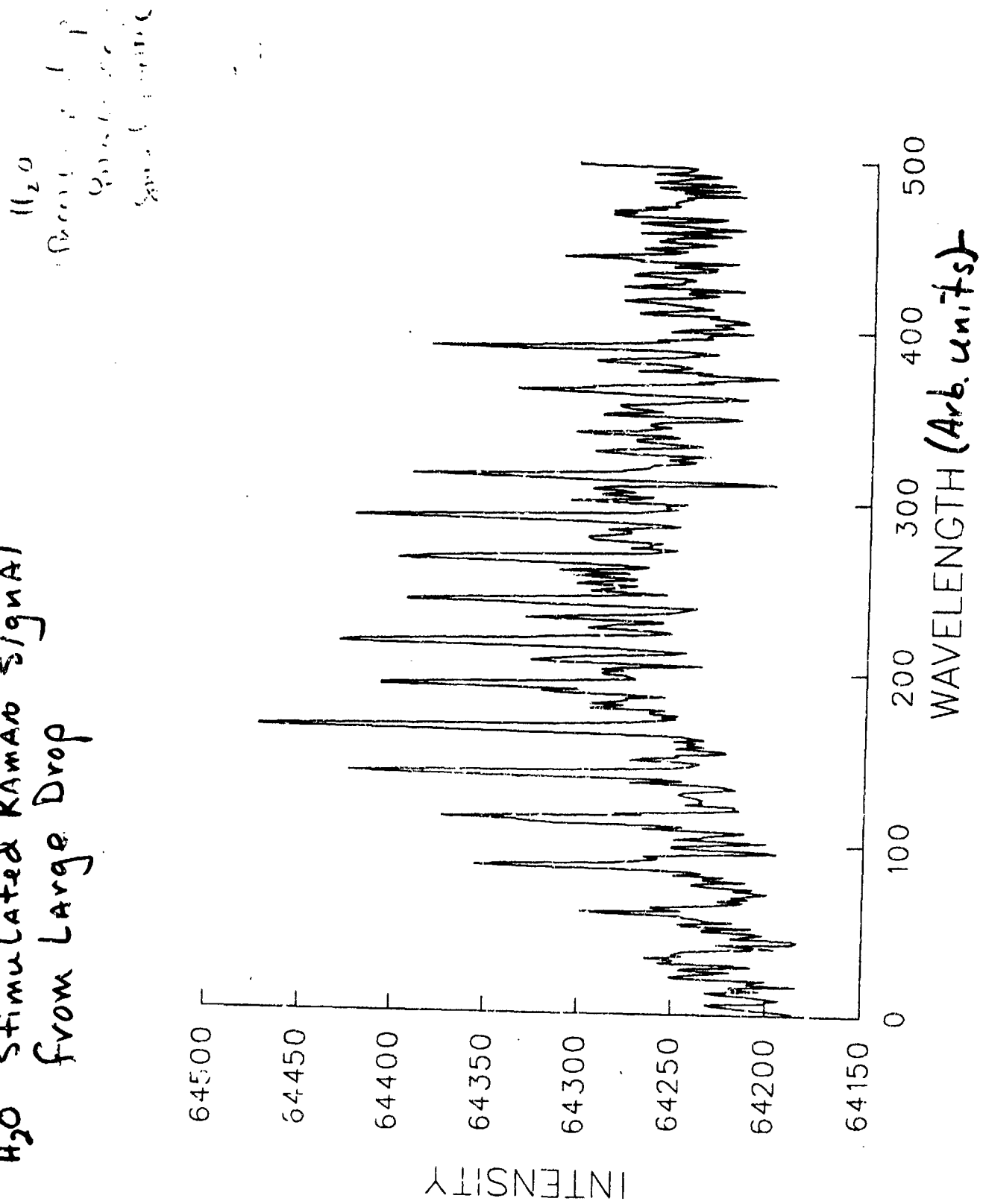
LIQUID PHASE

TEMPERATURE

DETERMINE VARIABLES



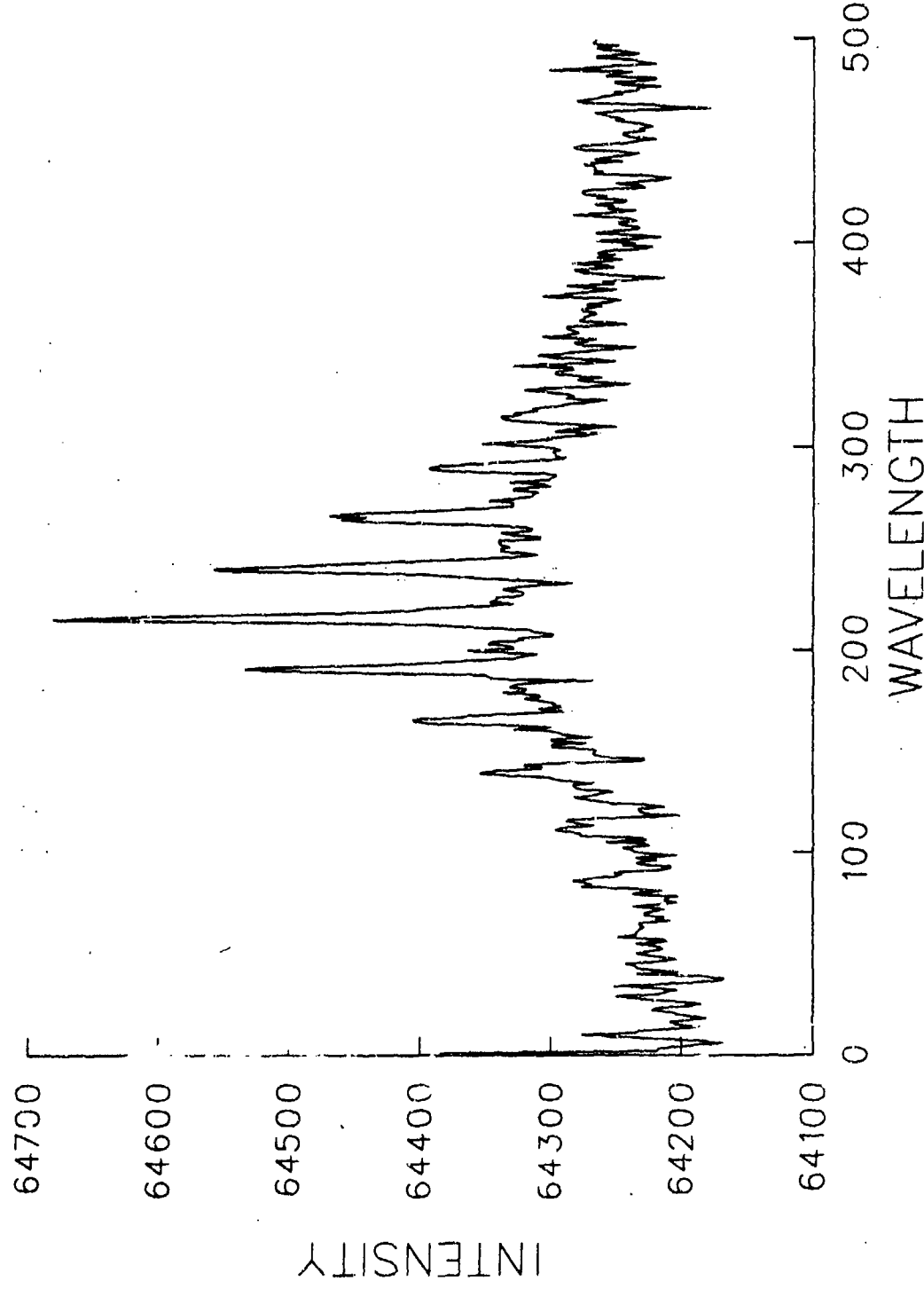
H_2O Stimulated Raman Signal
from Large Drop



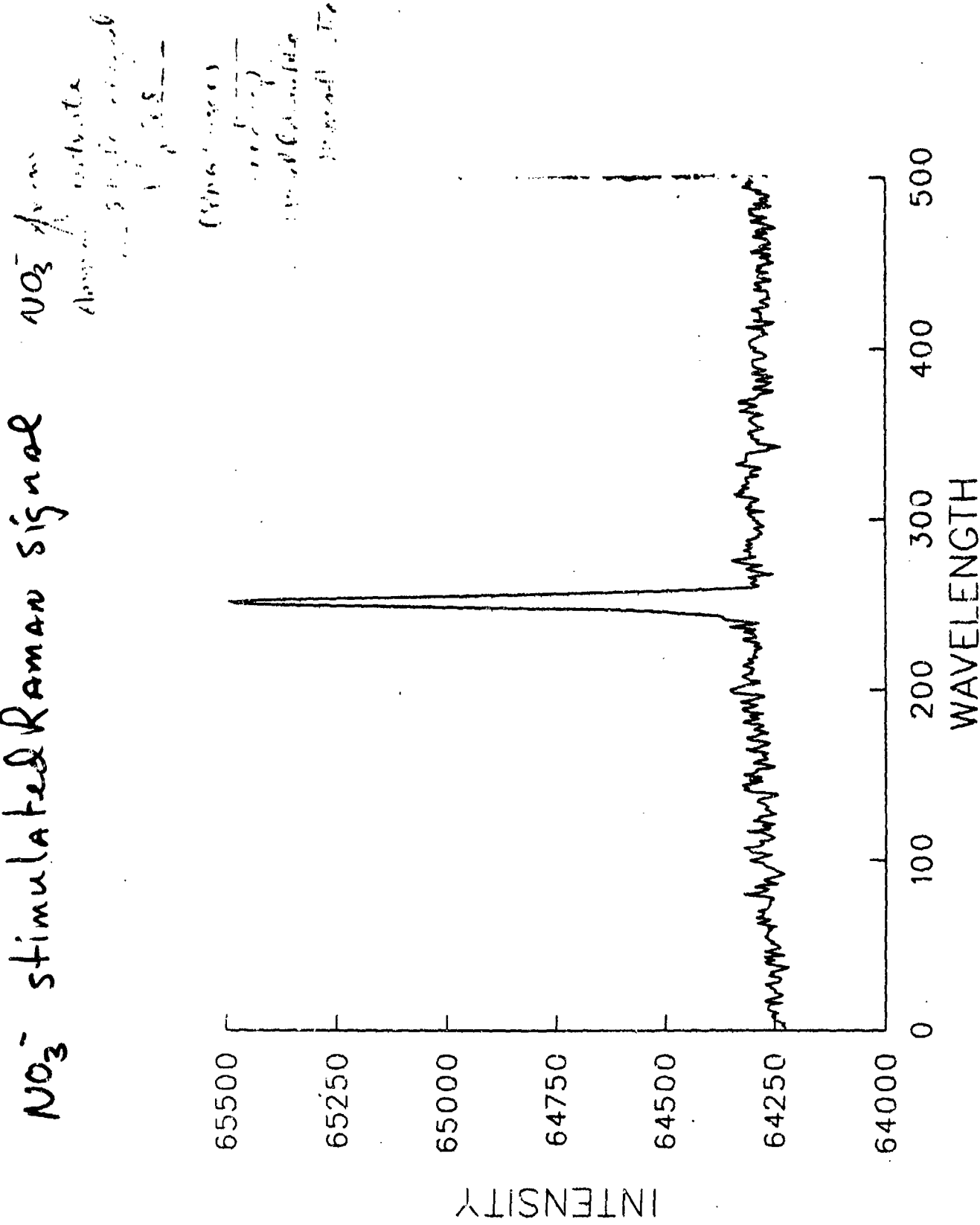
H_2O

Stimulated Raman Signal
Smaller drop

A_2 Stimulated Raman
(Free Space, 1000 Hz)
Wavelength



NO_3^- stimulated Raman signal



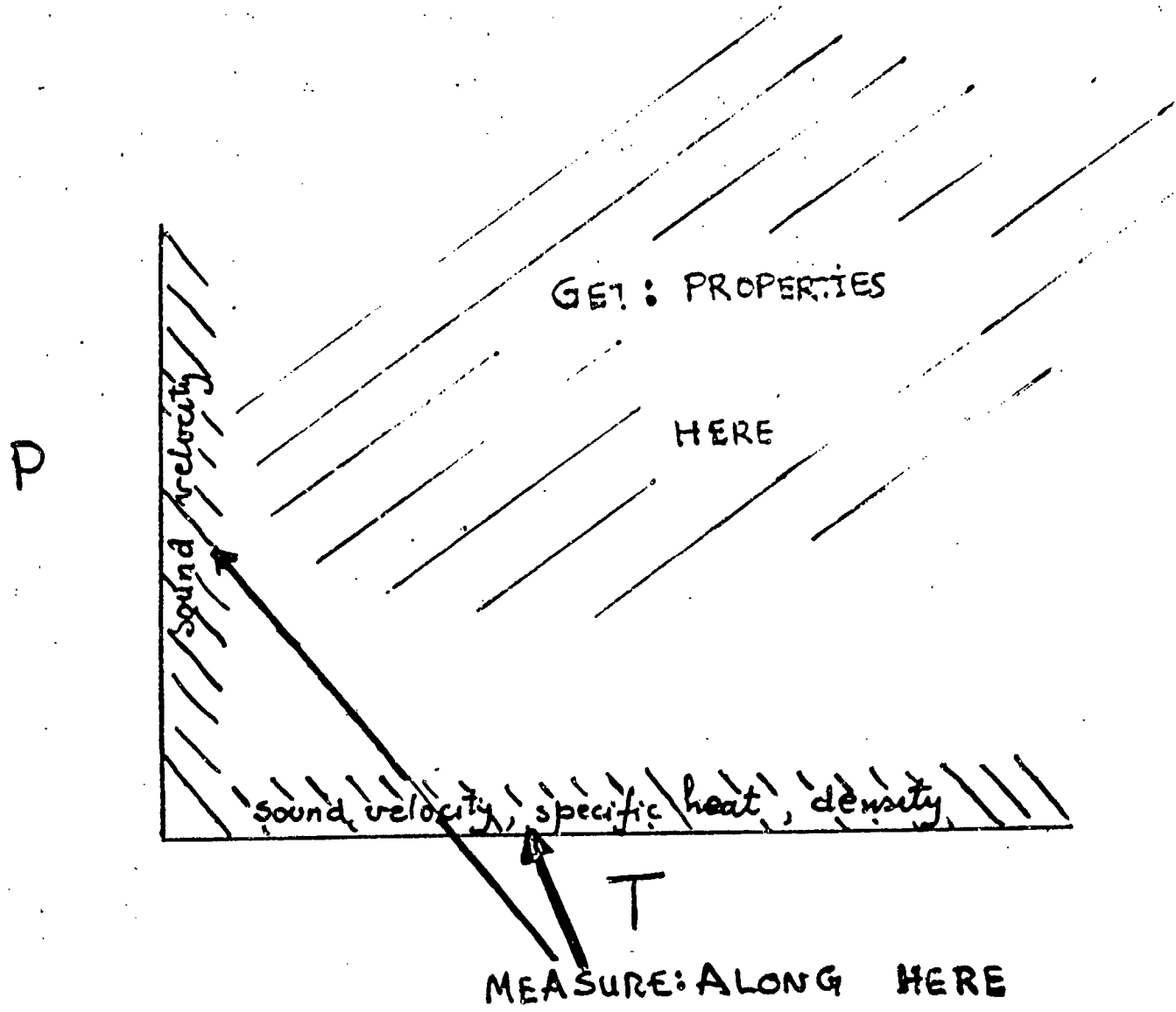
EQUATION OF STATE AND THERMODYNAMIC PROPERTIES OF THE HAN-EAN-WATER SYSTEM

J. FRANKEL, W. SCHOLZ, J.F. COX
U.S. ARMY, ARDEC, CCAC, BENET LABORATORIES
WATERVLIET, NY 12189-4050

- * PREVIOUS WORK
- COMPLETE "MACRO" THERMODYNAMIC DESCRIPTION OF LP.
- EQUATION OF STATE (EOS) AND THERMODYNAMIC PROPERTIES FOR LIQUID AS LONG AS NO PHASE CHANGES OCCURRED.
- * NOW
- MODEL THE SYSTEM FROM A "MICRO" POINT OF VIEW, TO PREDICT PHASE BOUNDARIES, SURFACE TENSIONS, FREE ENERGIES.
- * METHOD
- USE HARD SPHERE MODEL FOR LIQUIDS. MATCH THE RESULTING EOS IN LIQUID STATE WITH THE EOS OBTAINED FROM OUR PREVIOUS TECHNIQUES.

PREVIOUS MEASUREMENTS IN LP

- * SOUND VELOCITY WITH PRESSURE
- * SOUND VELOCITY WITH TEMPERATURE
- * C_p WITH TEMPERATURE



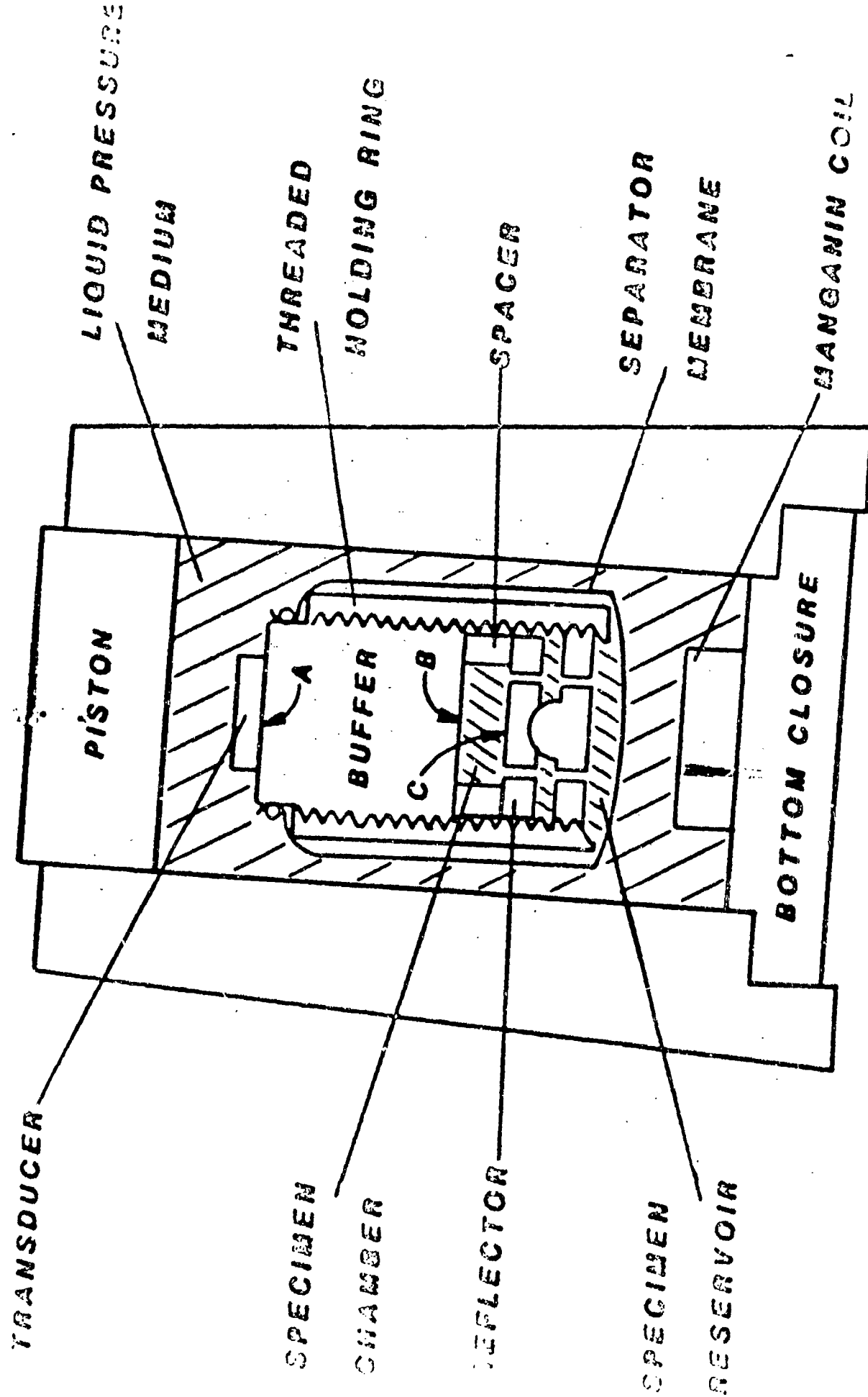
FROM: CLASSICAL THERMODYNAMICS

FOR: HOMOGENEOUS, ISOTROPIC PHASE

Pressure and Temperature Dependence of Thermodynamic Quantities* (Obtained Here)

Equation	Units
$v(T) = 1966 - 1.703T$	m/sec, °C
$K_T(P) = 1.954 \times 10^{-8} + 5.200 \times 10^{-6}T$	bar ⁻¹ , °C
$v(P) = 1942.79 + 0.154P - 6.482 \times 10^{-6}P^2 - 1.638 \times 10^{-10}P^3$	m/sec, bar
$P(P) = 1.4532 + 2.9387 \times 10^{-6}P - 2.1711 \times 10^{-9}P^2 + 1.2192 \times 10^{-13}P^3$	gm/cm ³ , bar
$\beta(P) = 48679 + 10.848P$ (Tait Equation)	bar, bar
$C_p(P) = 2.29 + 9.78 \times 10^{-6}P$	joules/gm K, bar
$\beta(P) = 4.898 \times 10^{-4} - 5.20 \times 10^{-9}P$	K ⁻¹ , bar
$K_T(P) = 2.02 \times 10^{-8} - 3.38 \times 10^{-9}P + 3.36 \times 10^{-13}P^2$	bar ⁻¹ , bar

*Pressure dependence found at room temperature (23°C).
Temperature dependence found at one atmosphere.



PRESENT MEASUREMENT IN HAN-WATER, TEAN-WATER SYSTEMS

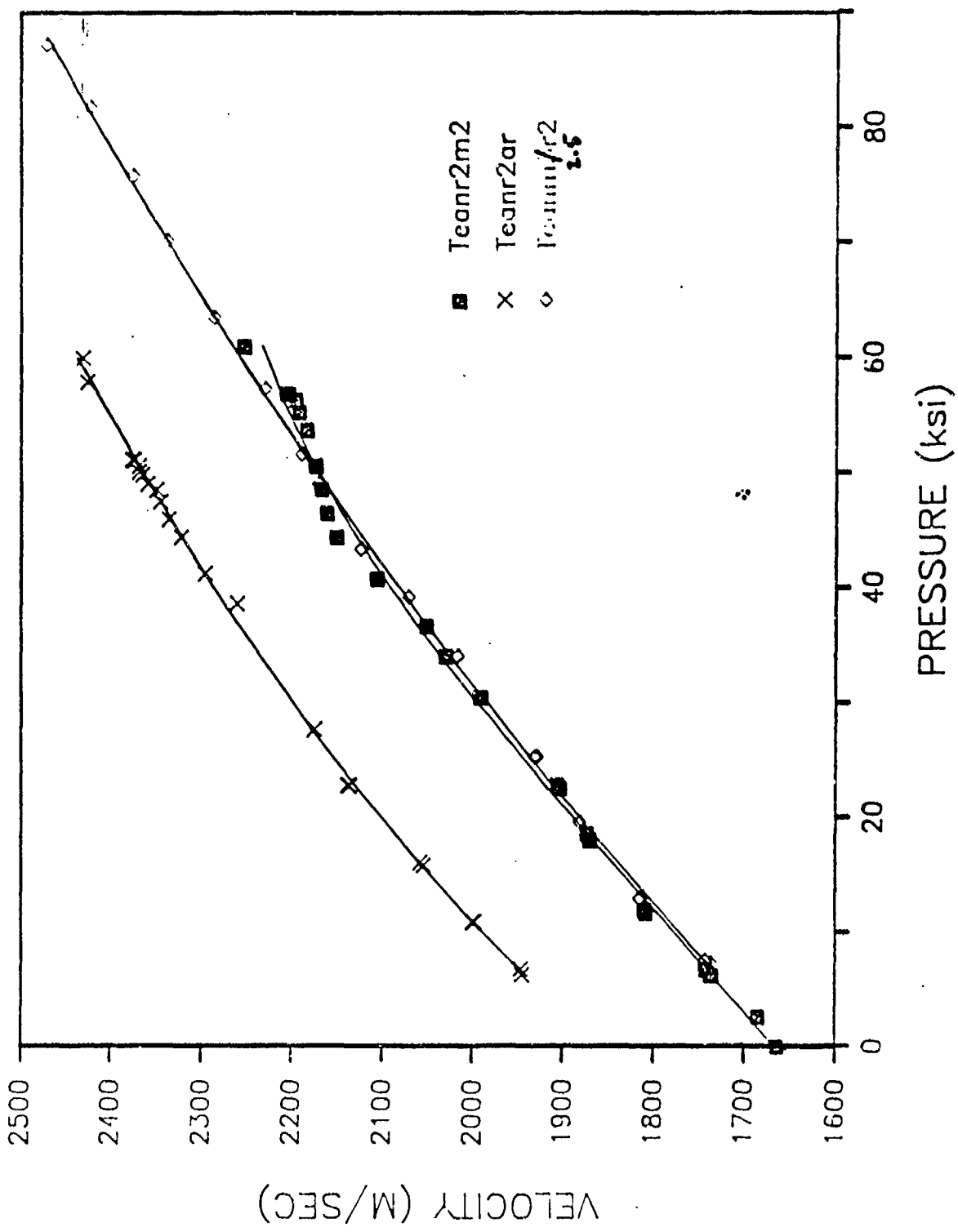
- * SOUND VELOCITY WITH PRESSURE.
- * SOUND VELOCITY WITH TEMPERATURE.
- * DENSITY WITH TEMPERATURE
- * CP WITH TEMPERATURE

TO OBTAIN:

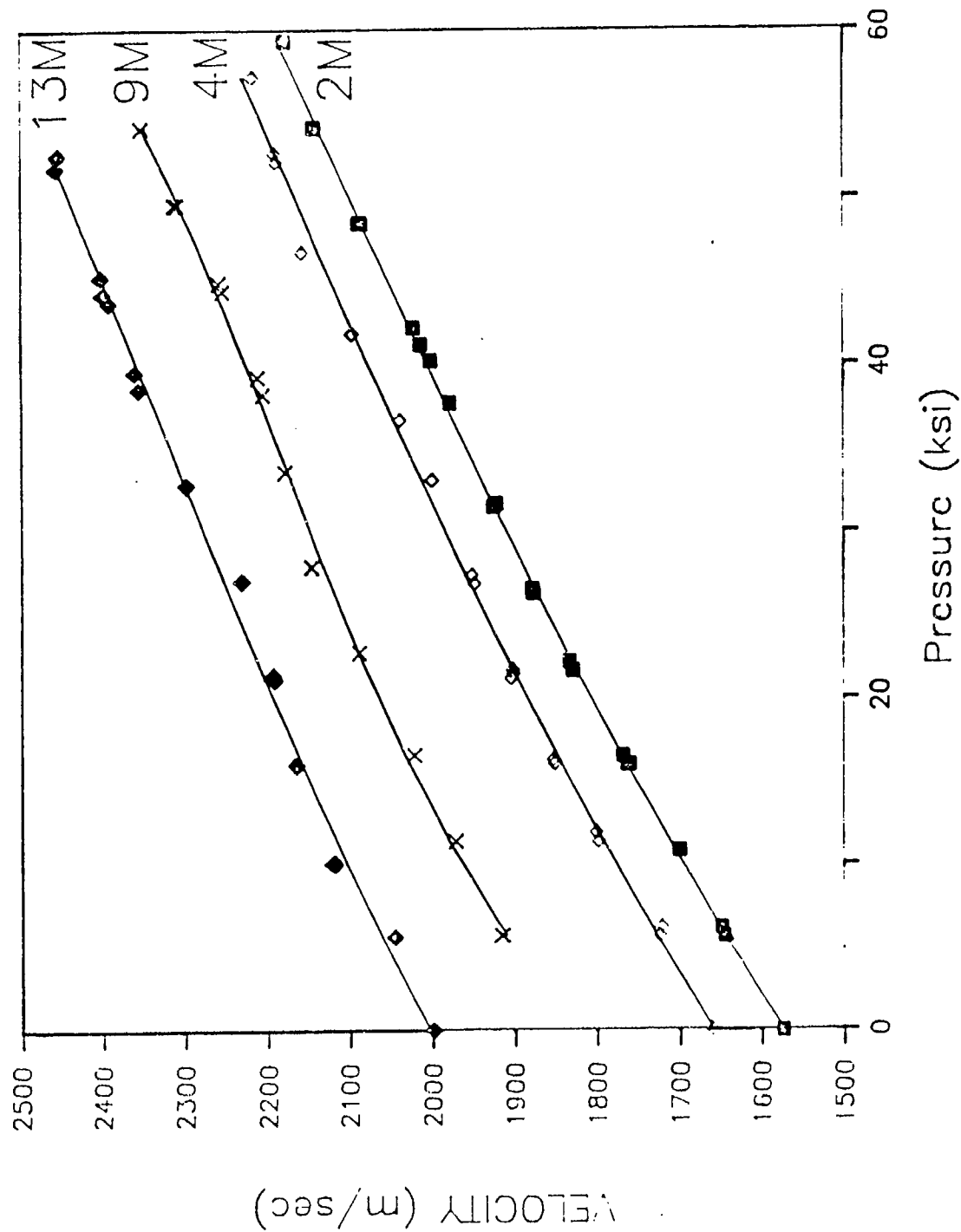
- * FULL THERMODYNAMIC DESCRIPTION OF EACH SYSTEM
- * VARIOUS CHEMICAL POTENTIALS DISCERNABLE FROM CONCENTRATION AND TEMPERATURE DEPENDENT DATA.
- * MATCH RESULTS OF HARD SPHERE EOS FOR EACH SYSTEM WITH RESULTS OBTAINED FROM ABOVE.

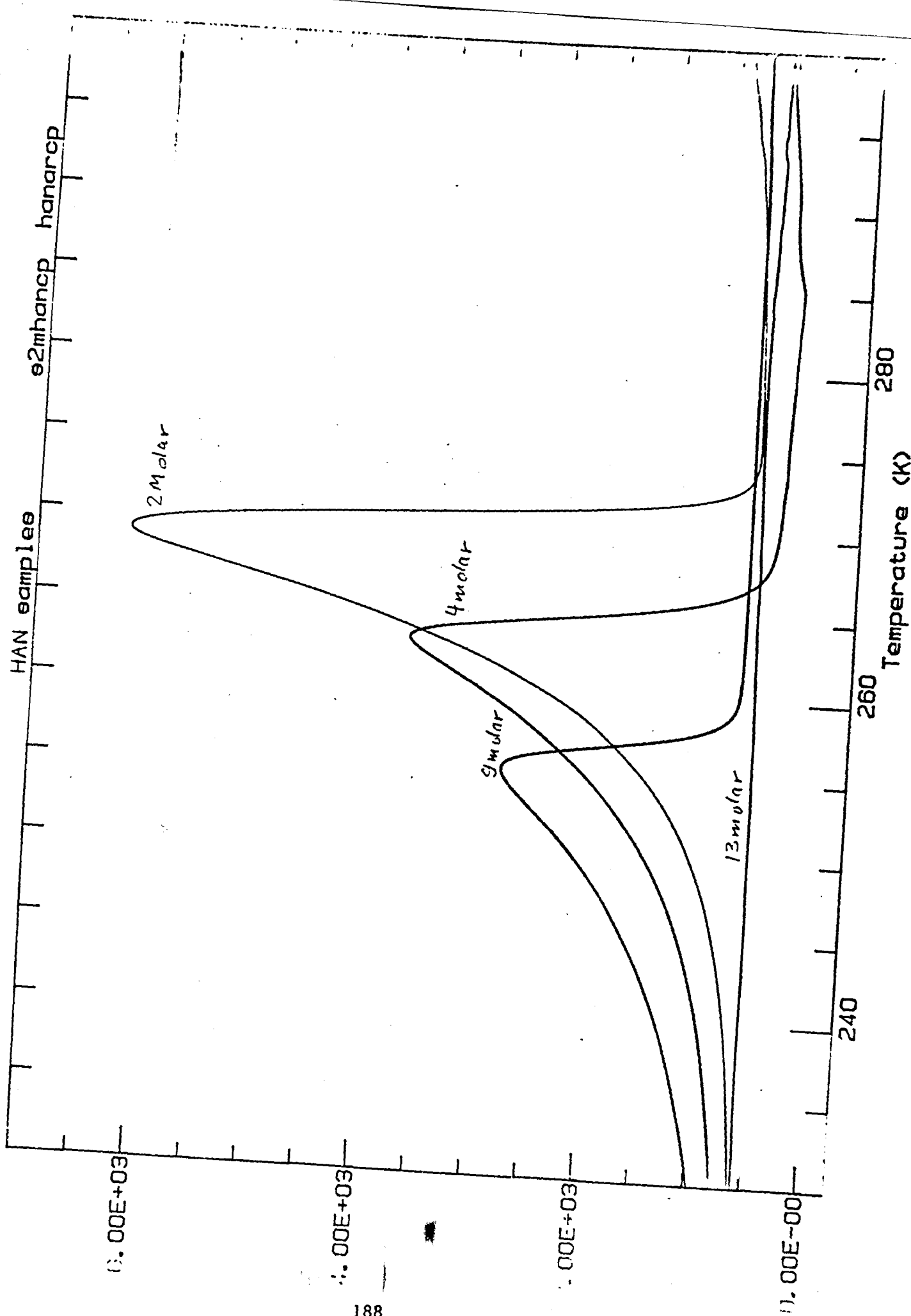
THE CORROSIONIC PROPERTIES OF AQUEOUS MITURES 2553

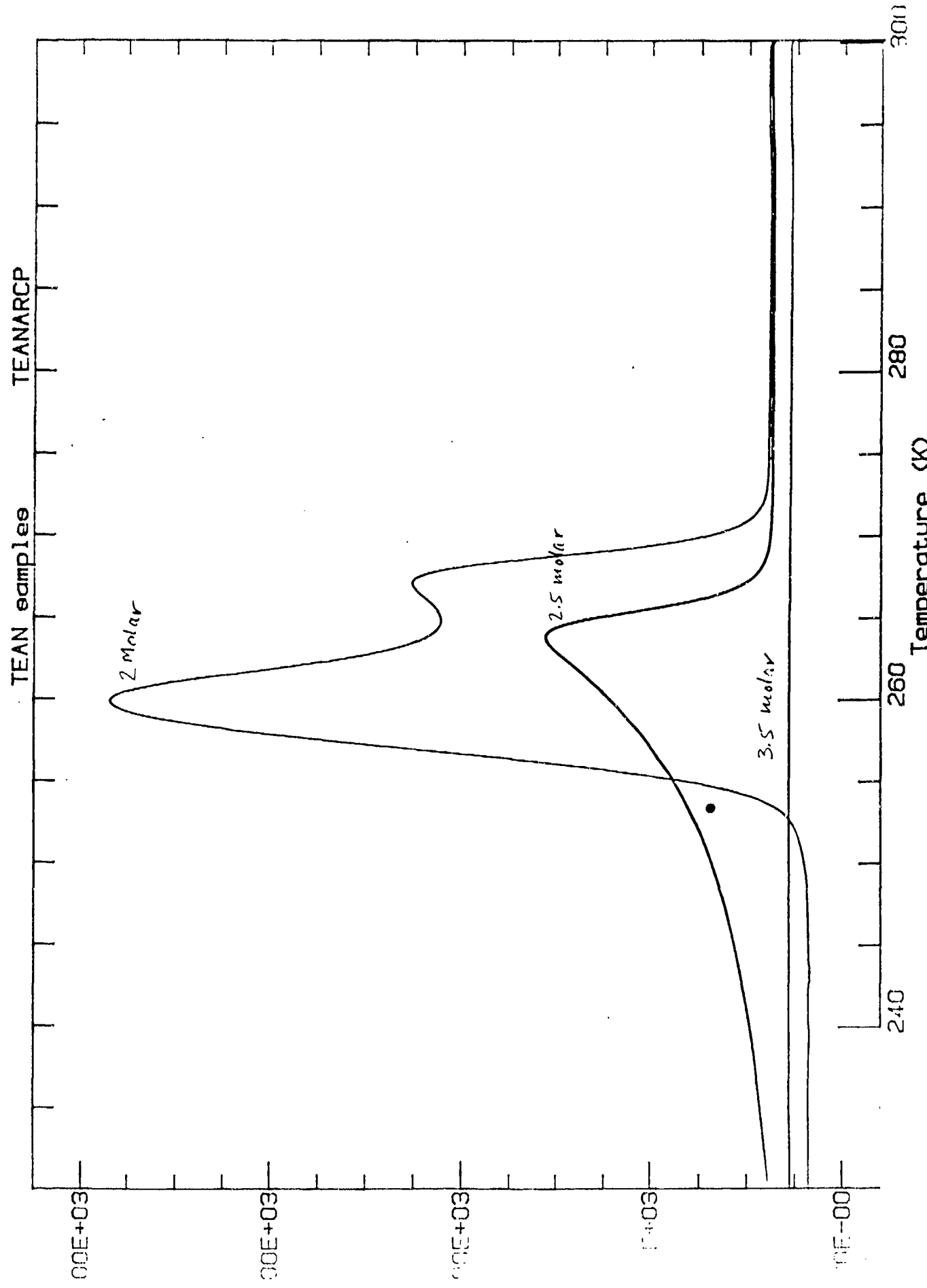
AQUEOUS TEAIN SOLUTIONS



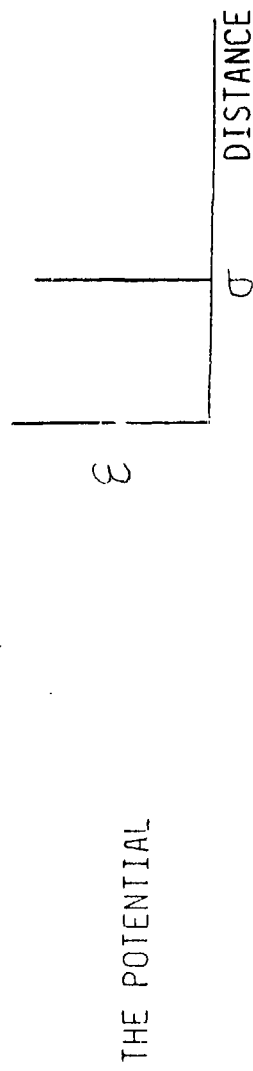
AQUEOUS HAN MIXTURES







THE HARD SPHERE MODEL HAS BEEN WELL STUDIED.



ENERGY OF THE SYSTEM IS ONLY KINETIC.

THE LIQUID EQUIVALENT OF THE IDEAL GAS MODEL.

TO HAVE THE MODEL CONFORM TO THE REALITY THAT THE MOLECULES THAT MAKE UP A LIQUID HAVE AN ATTRACTION FOR EACH OTHER.

USE THE CONCEPT OF "INTERNAL PRESSURE" $A(v)$

WE USE THE CARNahan-STARLING VERSION OF THE HARD SPHERE EOS.

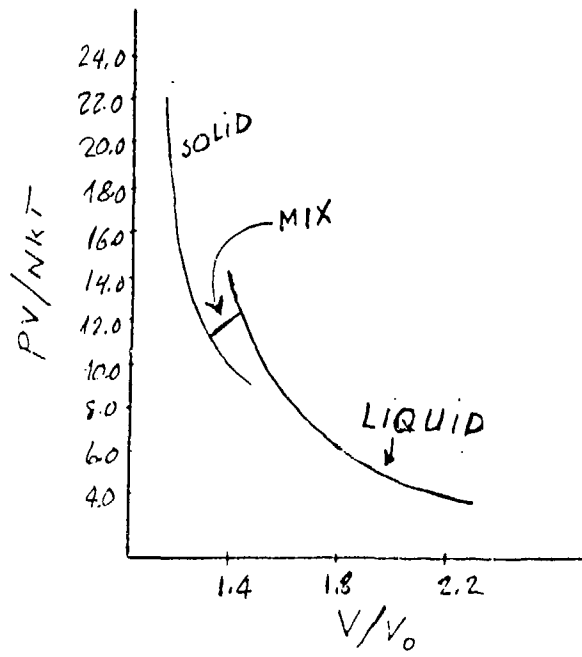
USE THE CO

v - SPECIFIC VOLUME

v_0 - SPECIFIC VOLUME AT CLOSEST PACKING = N MOLECULES $\cdot \frac{\sigma^3}{\sqrt{2}}$

N - MOLES/GM

$$\sigma = \text{HARD SPHERE DIAM.}$$



EQUATION OF STATE FOR HARD SPHERE MODEL

CAN BE REWRITTEN

$$\left(\frac{P + A(V)}{N R T} \right) V_B = n f(\eta)$$

THE SPECIFIC VOLUME IS OBTAINED FROM THE LIQUID EOS WHICH WE ALREADY HAVE. V_B IS NOW A PARAMETER CHOSEN TO OPTIMIZE THE FIT.

$$A_{\text{Vapor}}(V) = \frac{N R T}{V_B} n f(\eta) - P \quad \left. \begin{array}{l} \text{THIS IS THE INTERNAL PRESSURE WHICH} \\ \text{CAN BE CALCULATED FROM THE MODEL.} \end{array} \right\}$$

$$(\text{in } \text{ft}) \quad V_B = 0.423 / P$$

THE "EXPERIMENTAL" INTERNAL PRESSURE:

WE CAN OBTAIN THE EOS FROM THE HELMHOLTZ FREE ENERGY H

$$(1) \quad P = -\left(\frac{\partial H}{\partial V}\right)_T = -\left(\frac{\partial U}{\partial V}\right)_T + T\left(\frac{\partial S}{\partial V}\right)_T$$

$$(2) \quad U = \text{INTERNAL ENERGY AND } \left(\frac{\partial S}{\partial V}\right)_T = \left(\frac{\partial P}{\partial T}\right)_V$$

BUT $\left(\frac{\partial U}{\partial V}\right)_T dV$ IS A MEASURE OF THE WORK BEING DONE IN OVERCOMING THE INTERNAL PRESSURE DURING A VOLUME CHANGE IN LIQUID.

$$\Lambda(V) dV = \left(\frac{\partial U}{\partial V}\right)_T dV$$

$$\text{AND } \Lambda(V) = \left(\frac{\partial U}{\partial V}\right)_T$$

FROM (1), (2) AND (3)

$$\Lambda(V)_{\text{exp}} = \left(\frac{\partial U}{\partial V}\right)_T = -P + T\left(\frac{\partial P}{\partial T}\right)_V = -P + \frac{T\beta}{K_T} = \frac{C_P \beta \rho V^2}{C_P + TV^2 \beta^2} - P$$

$\Lambda(V)$ CAN BE CALCULATED SINCE β = VOLUME EXPANSIVITY OR κ = SOUND VELOCITY K_T = ISOTHERMAL COMPRESSIBILITY; ARE AVAILABLE FROM OUR EXPERIMENT.

1846

P(BAR)	EXP A(V) (BAR)	THEORY A(V) (BAR)	$\eta \times 10^3$
0	7139.2	6843.3	474.5
500	6929.7	6625.4	479.0
1000	6665.9	6398.0	483.6
1500	6344.6	6162.1	487.6
2000	5962.5	5918.5	491.4
2500	5516.9	5667.8	494.9
3000	5005.2	5411.0	498.3
3500	4425.1	5148.6	501.5
4000	3775.0	4881.3	504.0
4500	3053.7	4609.7	507.0
5000	2260.7	4334.5	510.0

COMPARISON OF INTERNAL PRESSURE OBTAINED WITH MODEL
AND FROM MEASUREMENT.

AGREEMENT IS SURPRISINGLY GOOD, BEFORE SOLIDIFICATION
STARTS IN MODEL.

WARRANTS CONTINUED STUDY FOR WHOLE WATER-HAN-TEAN SYSTEM.

Physical Properties of Liquid Propellants:
Measurements of Shear Viscosity, Volume Viscosity and Density

J. Schroeder*, C.S. Choi*, Y.T. Lee*

Department of Physics

Rensselaer Polytechnic Institute

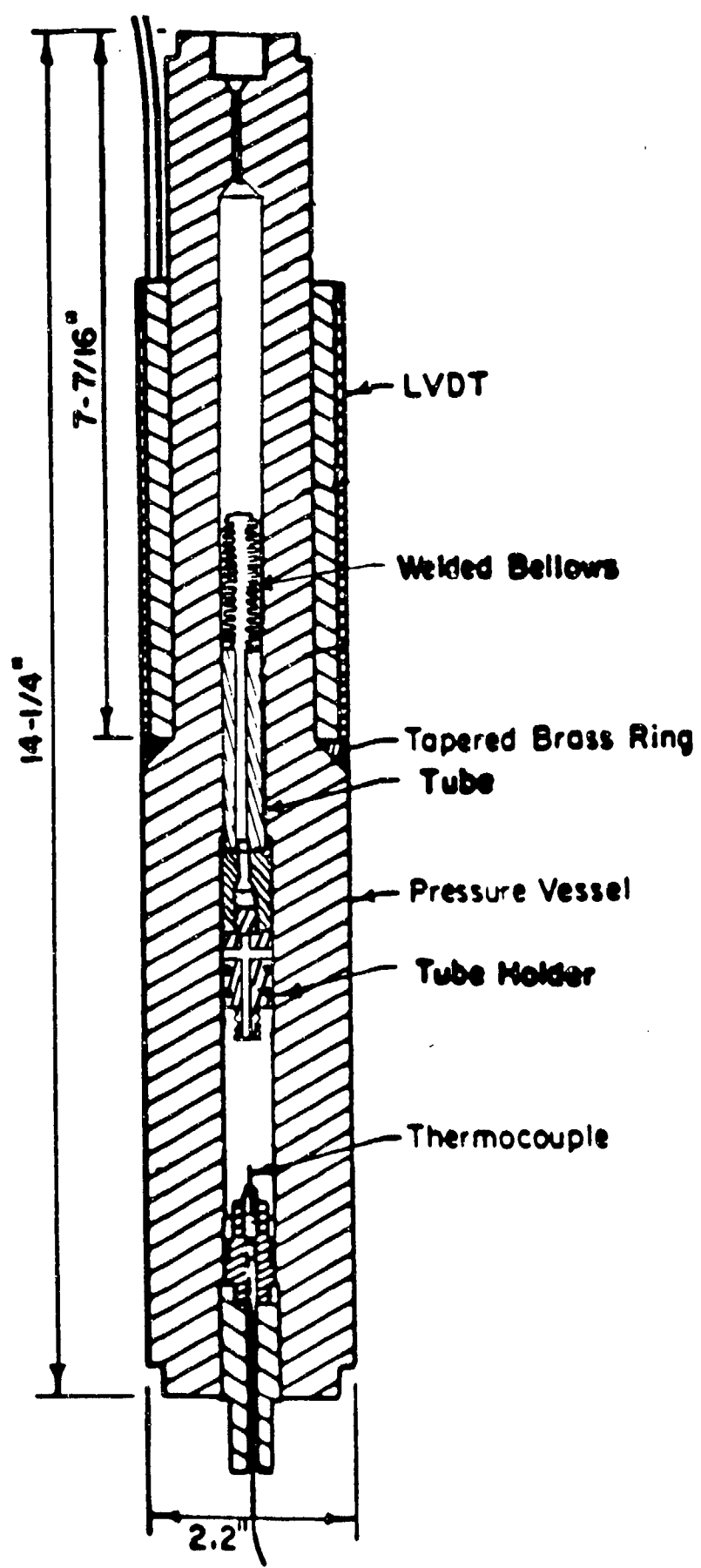
Troy, NY

J. Frankel

Watervliet Arsenal

Watervliet, NY

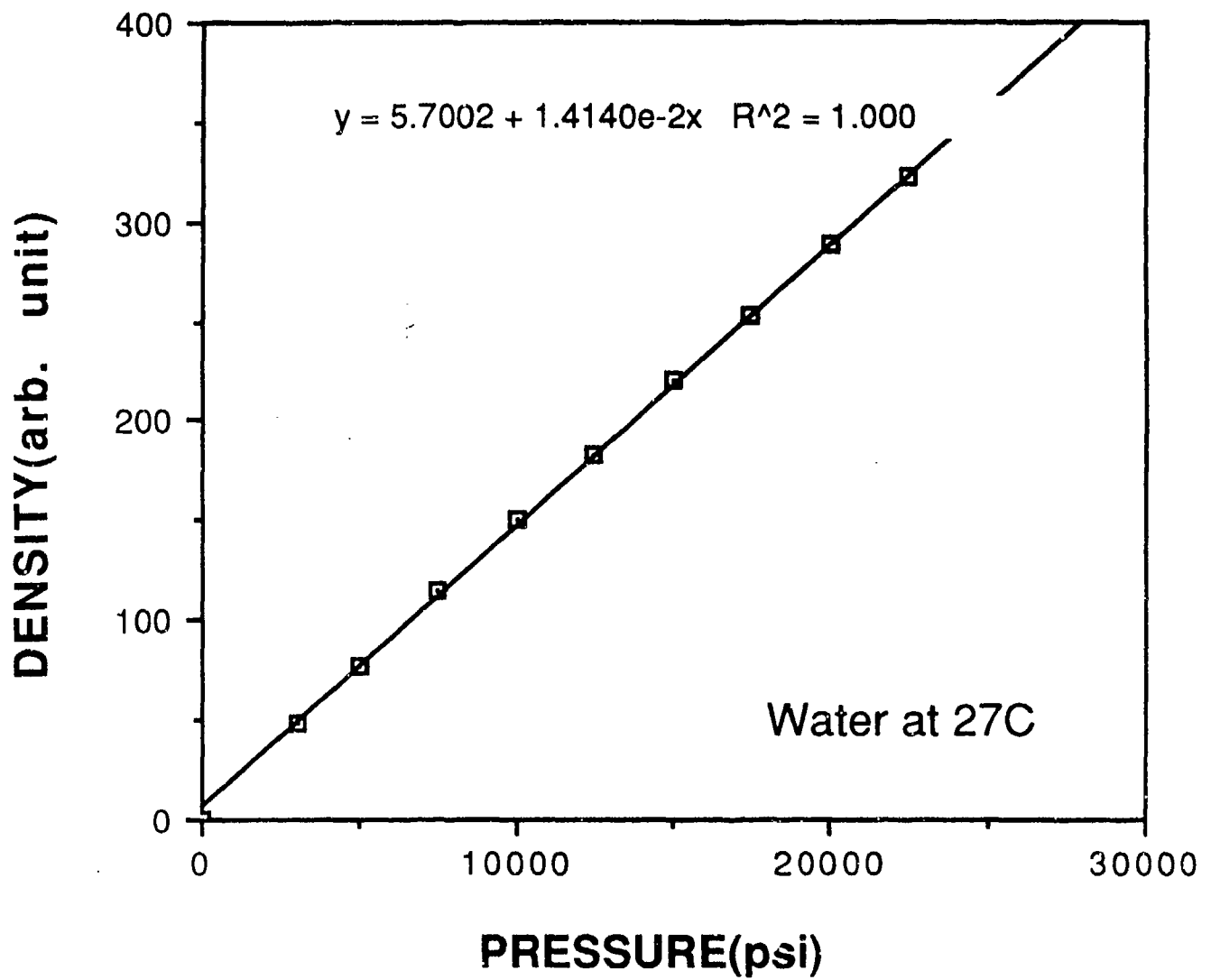
*Supported in part by U.S. Army, Watervliet Arsenal, Grant No. DAAA
22-85-C-0218.



The density $\rho_{T,P}$ can be obtained from the following equation

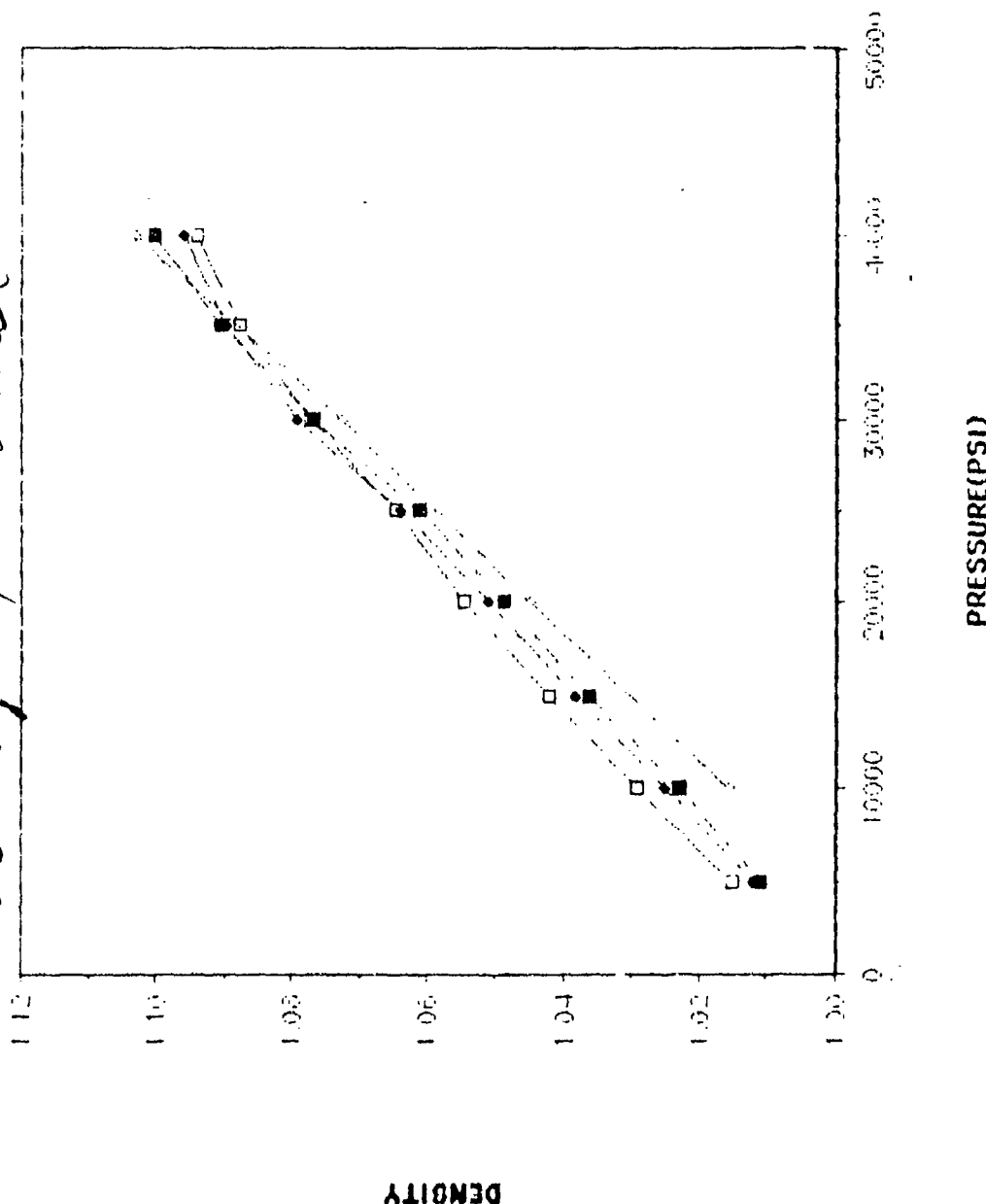
$$\rho_{T,P} = \frac{M}{M/\rho_0 - A_0 [1 + 2\alpha(T - T_0)] [1 - 2\beta(P - P_0)] (r_0 - r)}$$

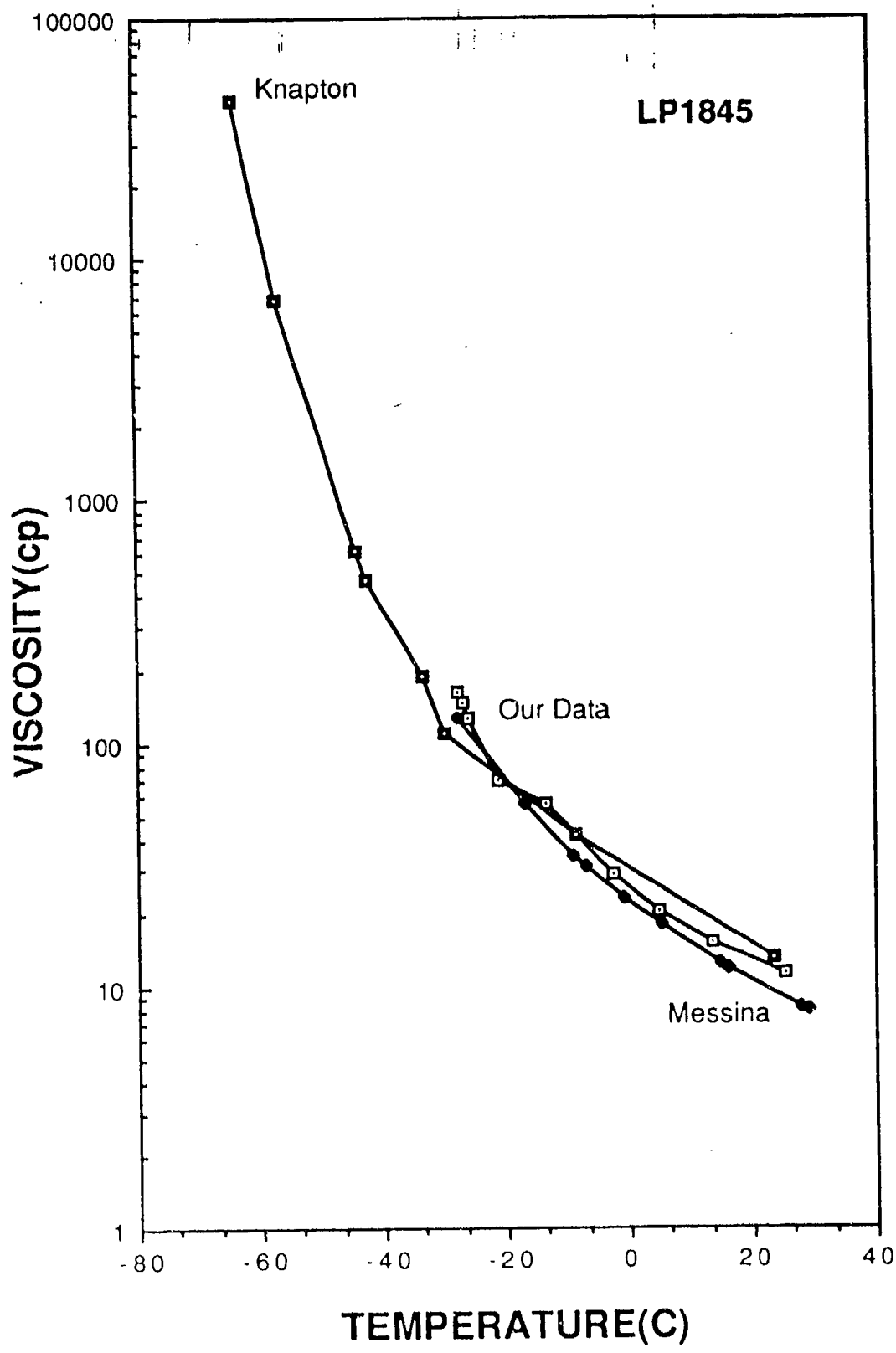
where M is the mass of fluid in the bellows, ρ_0 is the fluid density at temperature T and atmospheric pressure, A_0 is the bellows cross-sectional area at reference temperature T_0 and atmospheric pressure. α is the linear coefficient of compressibility of stainless steel, $r_0 - r$ is the change of bellows length. The bellows cross-sectional area A_0 is determined by calibration with distilled water.

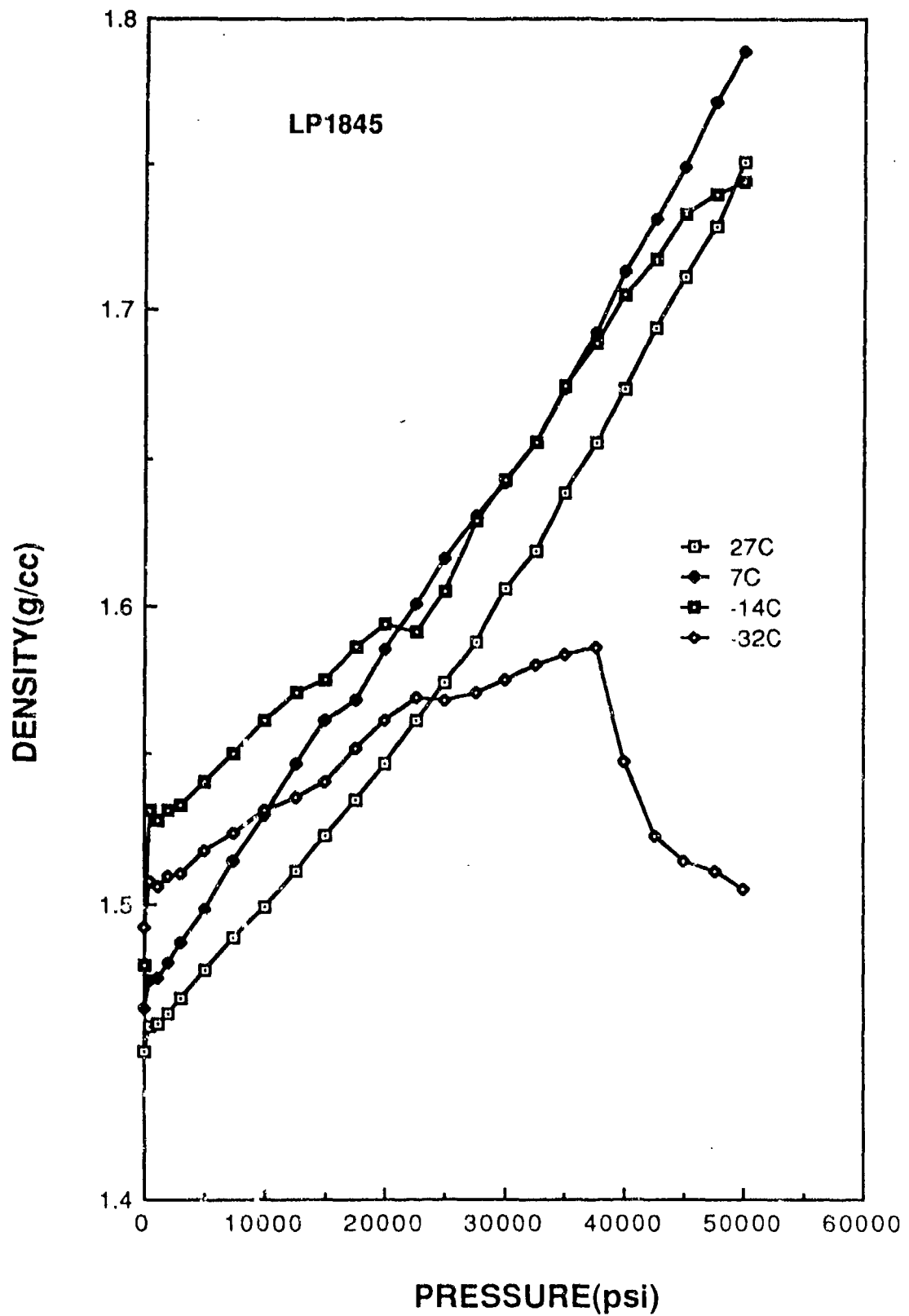


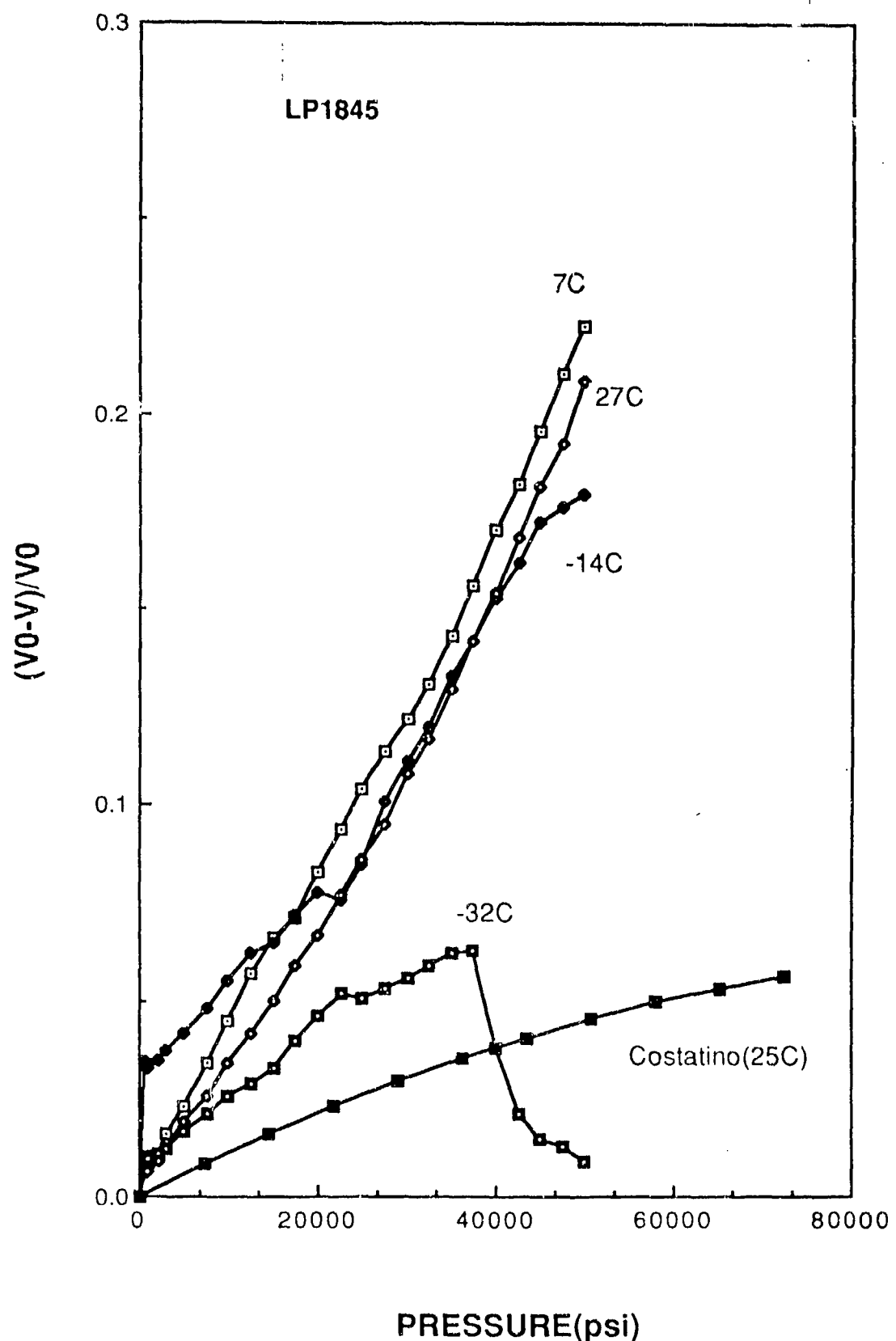
June 10, 1988

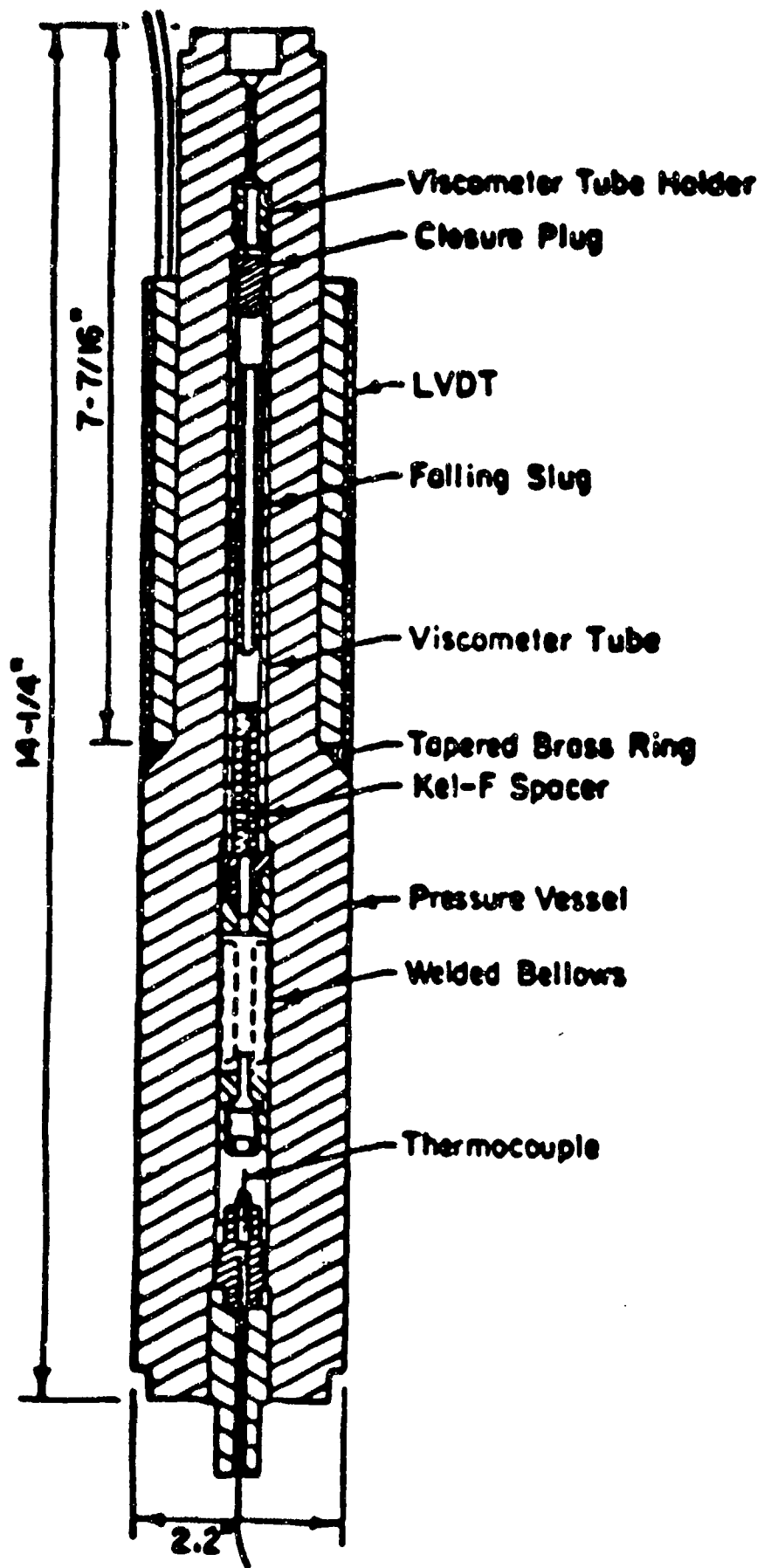
Data from "Untitled Data"
Density of Water





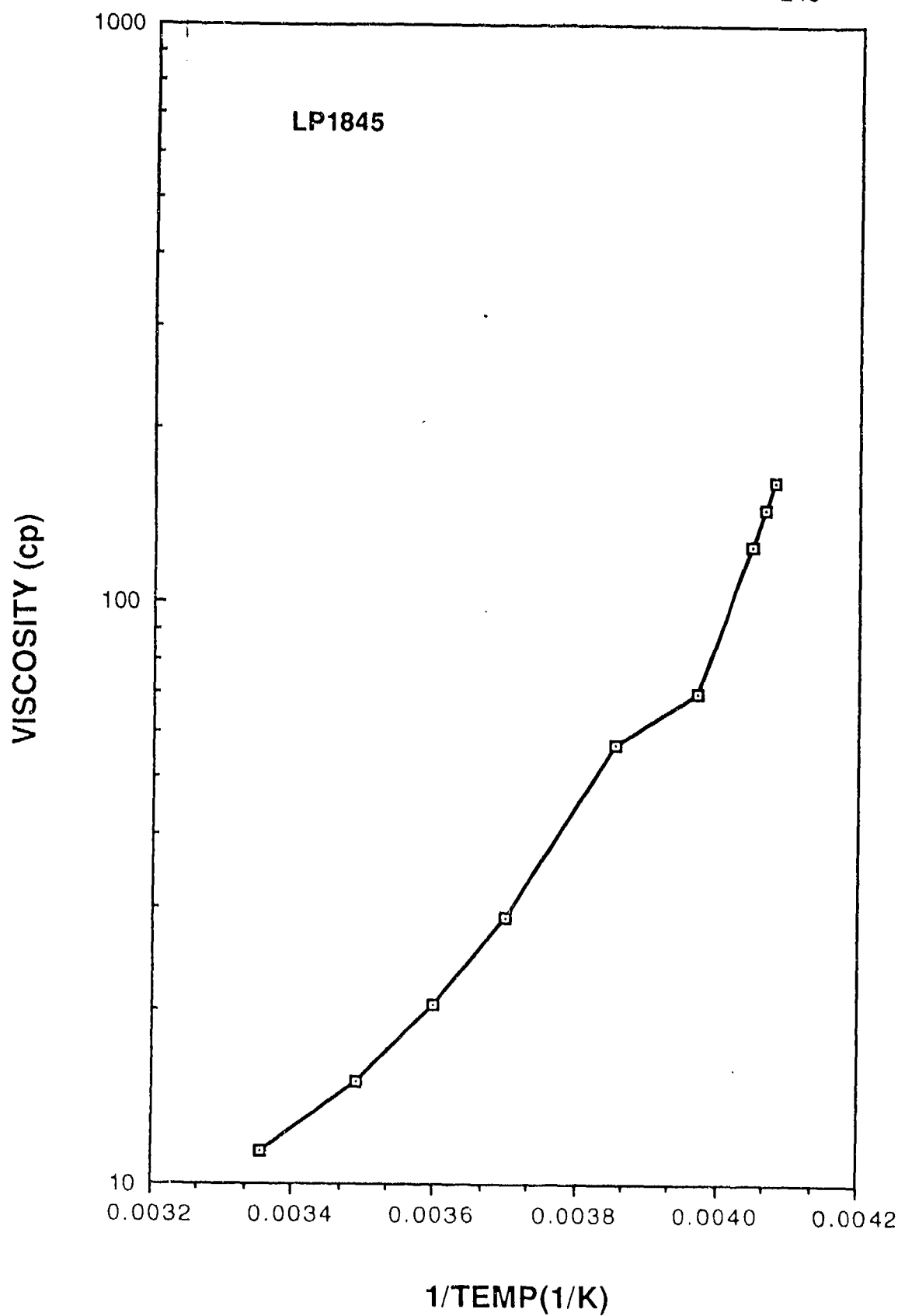






TEMP(K)

300 280 260 240



1/TEMP(1/K)

Viscosity measurements

Viscosities of LP1845 as a function of temperature and pressure were measured by a high pressure falling slug viscometer of similiar design as that described by R.J. McLachlan¹⁾. To detect the falling time exactly a linear variable differential transformer(LVDT) was used. The viscosity η of the liquid at a given temperature and pressure for a right circular cylinder of radius r falling vertically for a distance of L in a tube of radius R , is proportional to the falling time T of the slug and is given by the equation^{1),2)}

$$\eta = \frac{T(\rho_1 - \rho_2)r^2 g((R^2 + r^2)\ln(R/r) - (R^2 - r^2)^2)}{2L(R^2 + r^2)}$$

where ρ_1 and ρ_2 are densities of the slug and liquid respectively, and g is the acceleration due to gravity. In deviations of above equation end effects have been neglected and it can be simplified as

$$\eta = c (\rho_1 - \rho_2) T$$

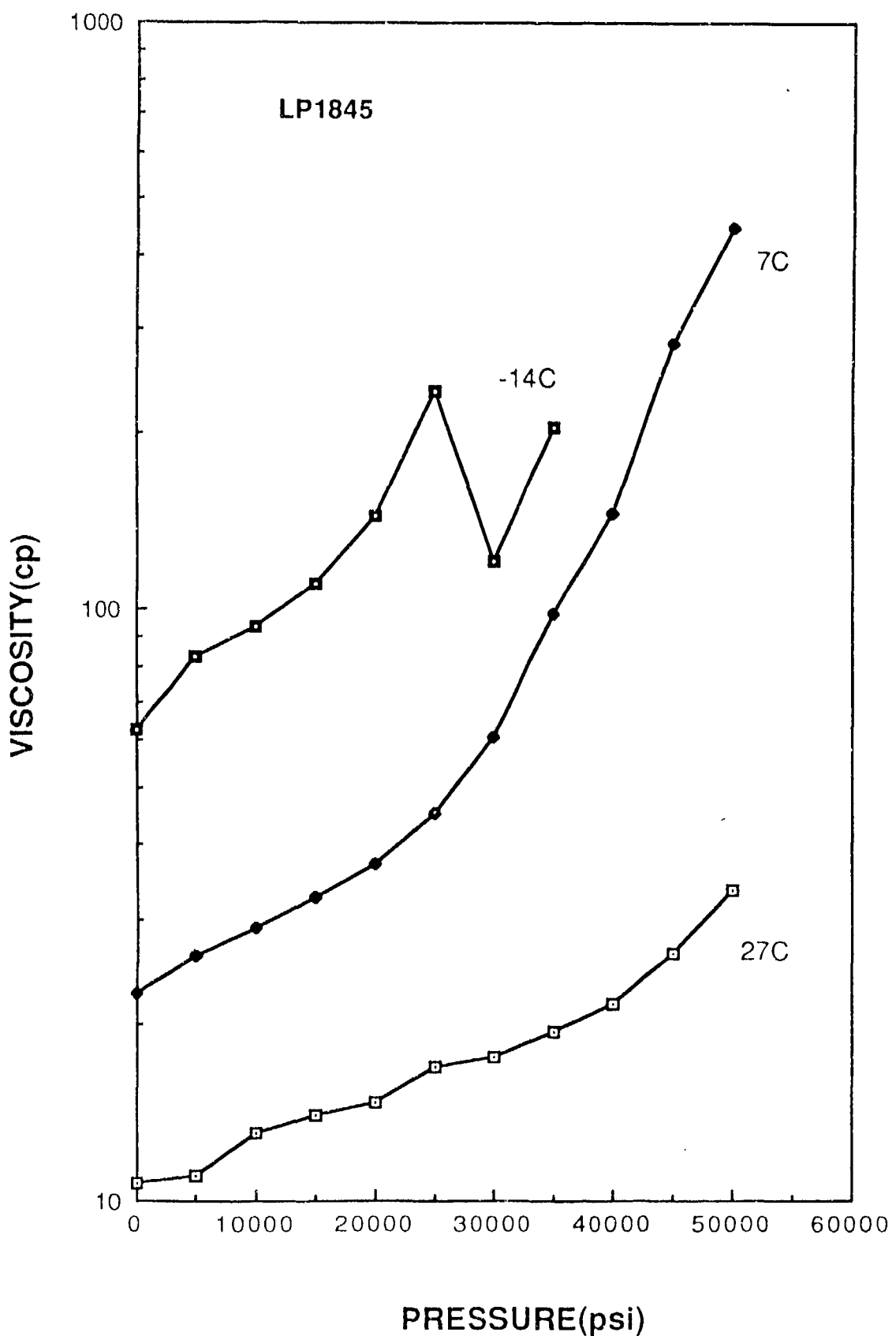
where c is the proportionality constant. The proportionality constant was determined experimentally by using Brookfield viscosity standard fluid(50.5 cp, 0.960 g/ml at 25 C). All measurements for calibration were made at constant temperature within 0.1 C and atmospheric pressure. Special attention was paid to cleanliness of the viscometer and removal of air bubbles in the liquid. Viscosity measurements of LP1845 were performed at various temperatures and pressures. To reduce the experimental error, the falling time was measured at least six times at same condition. The results are shown in the table.

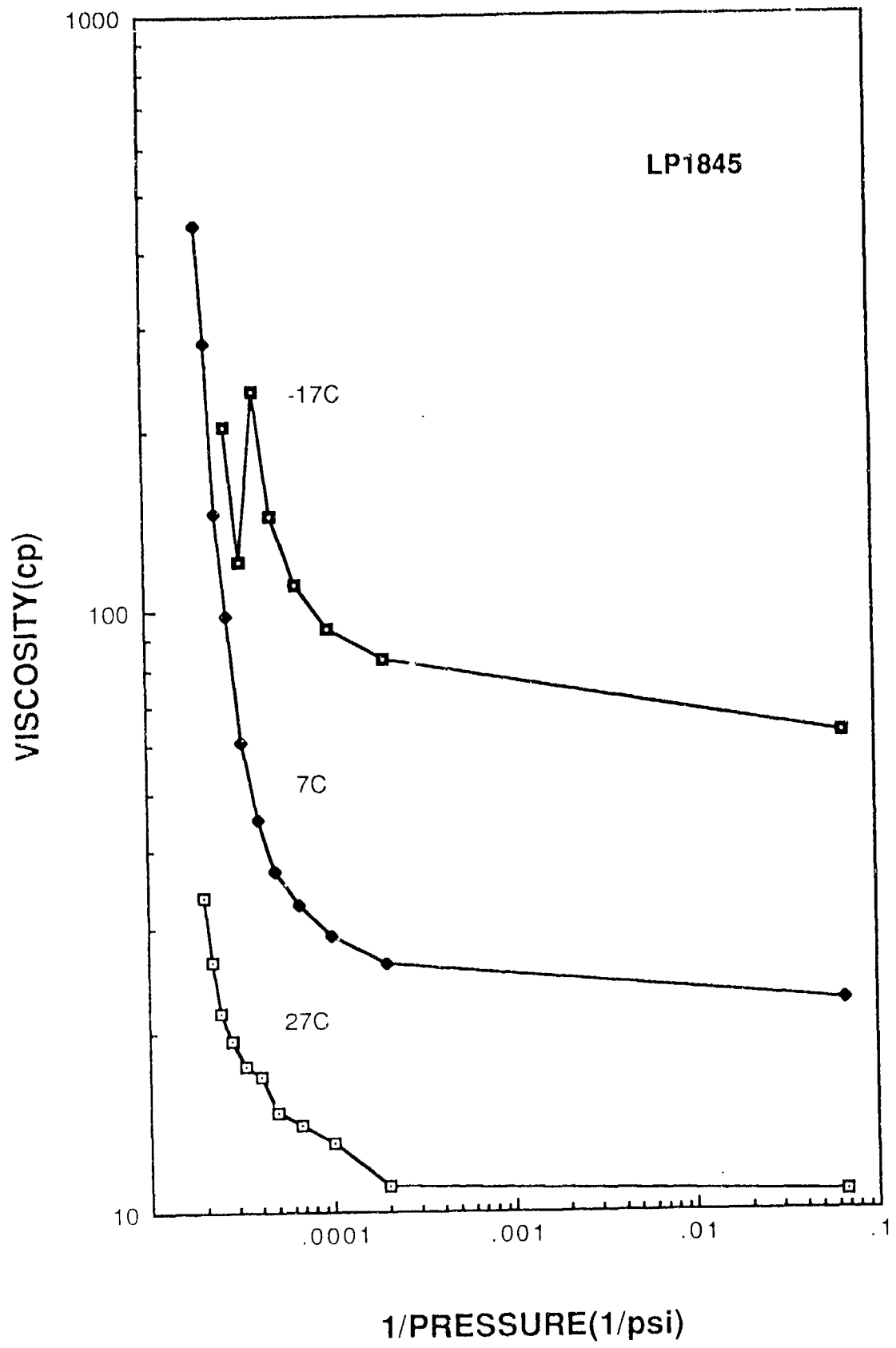
Table. Viscosity of LP-1845		
Temperature (C)	Density * (g/ml)	Viscosity (cp)
25.0	1.4515	11.33
13.4	1.4596	15.03
4.9	1.4657	20.36
-2.8	1.4712	28.65
-13.6	1.4786	56.74
-21.2	1.4846	70.12
-28.0	1.4893	161.66

*Extrapolated value from N.A. Messina et. al 3)

o. Reference

- 1) R.J. Melachlan, Journal of physics E; Scientific Instruments, 1976, vol.9, p391-394.
- 2) J.B. Irving and A.J. Barlow, Journal of physics E; Scientific Instruments, 1971, vol4, p232-236.
- 3) N.A. Messina et. al., Preceedongs of the 21st JANNAF Combustion Meeting, vol.II, CPIA Publication 412, Oct. 1984, p515.





**BRILLOUIN SCATTERING SYSTEM WITH STABLE 5-PASS
FABRY-PEROT INTERFEROMETEP**

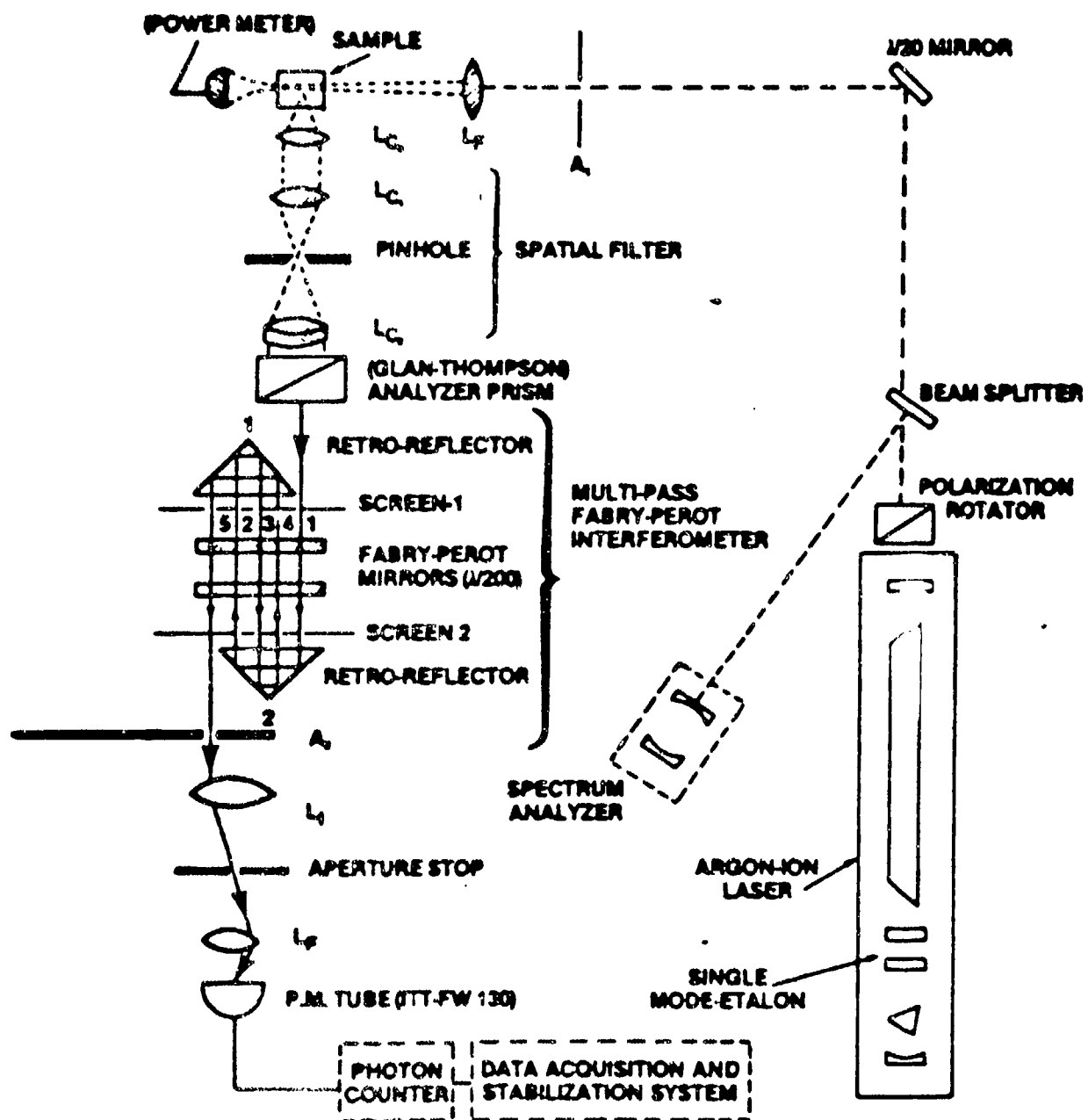


TABLE 1

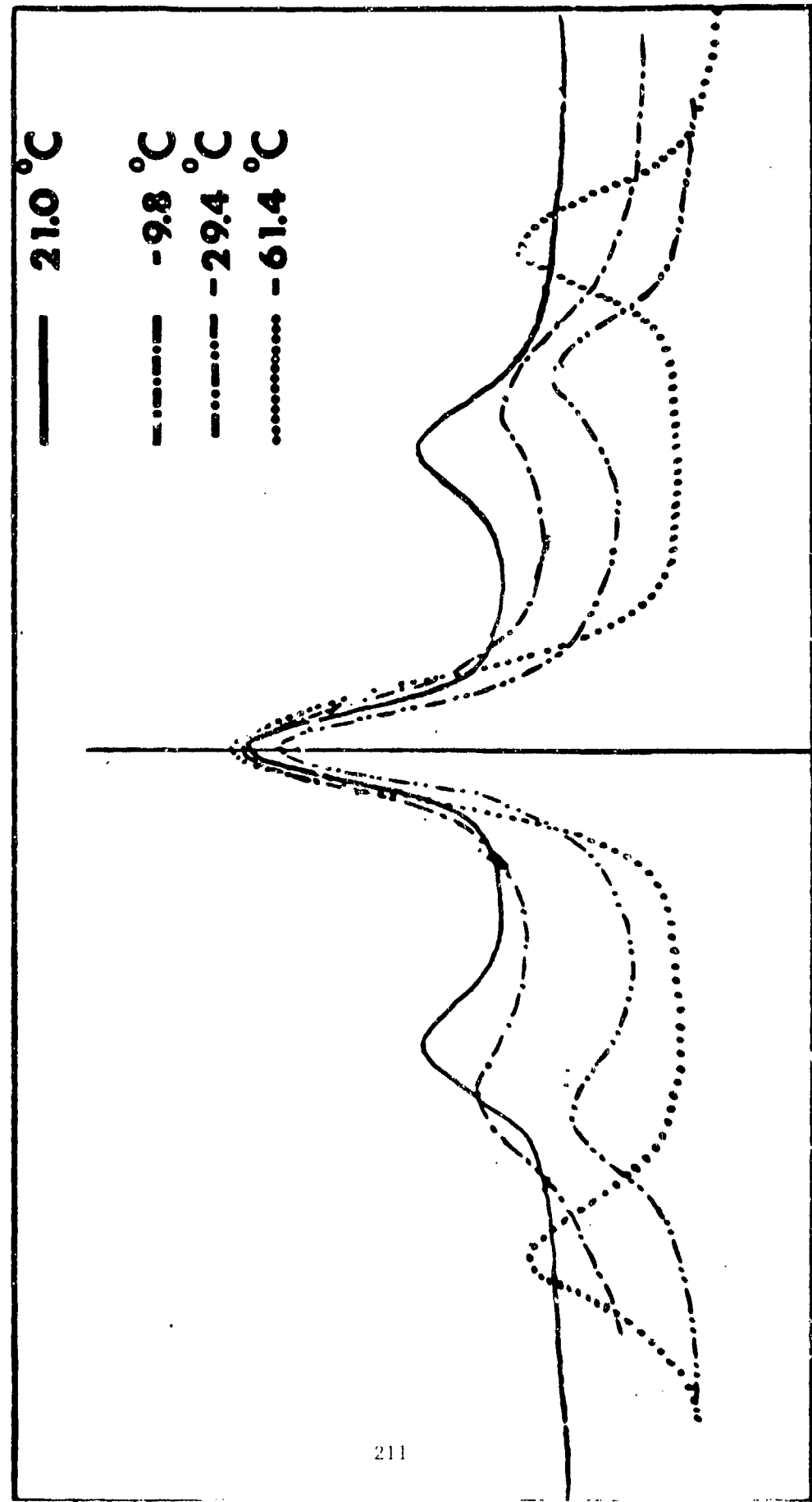
PHYSICAL PROPERTIES STUDIED BY RAYLEIGH-BRILLOUIN SCATTERING
FROM SINGLE-COMPONENT AND BINARY LIQUIDS

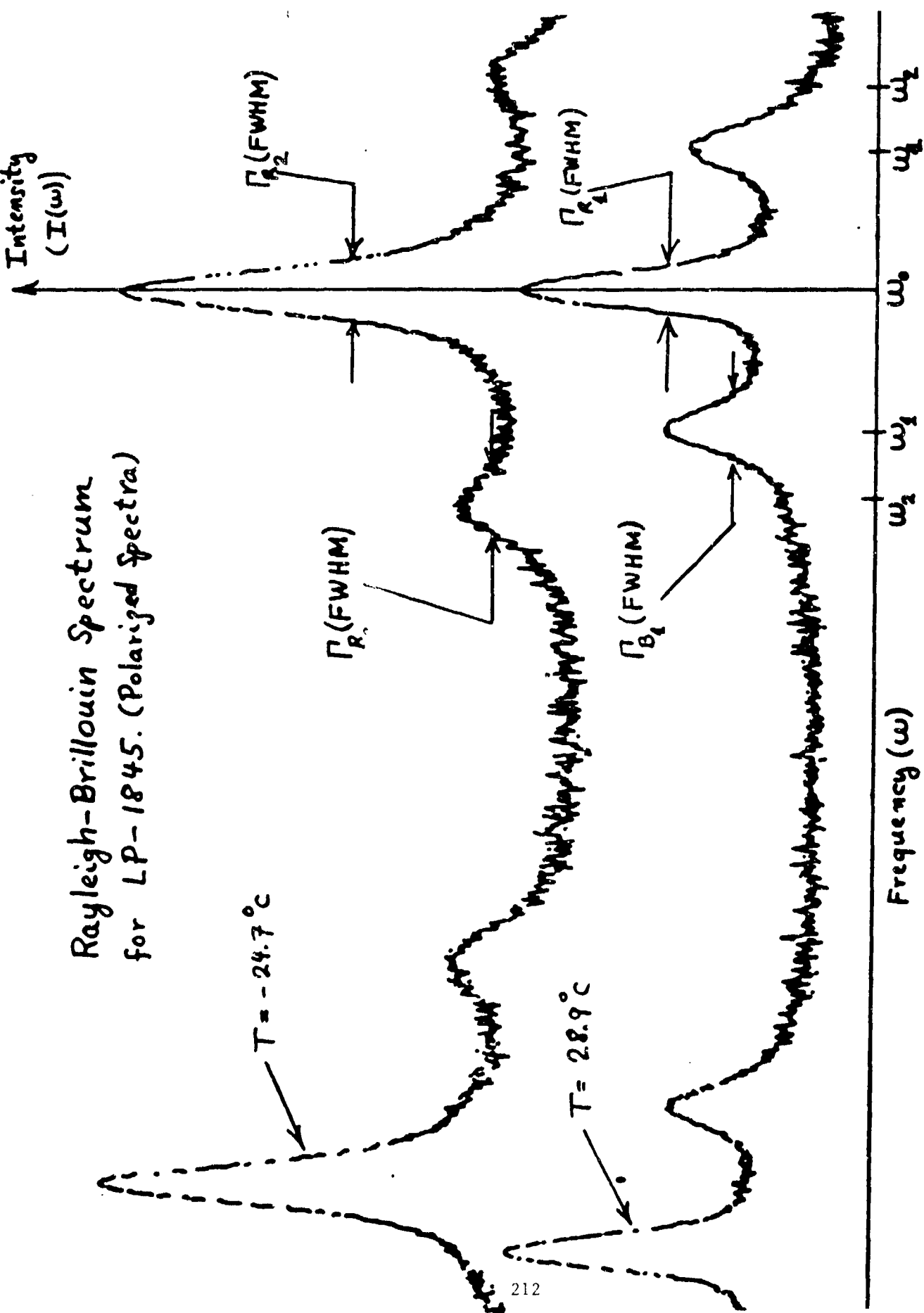
MEASURED QUANTITY	SINGLE COMPONENT LIQUID	BINARY MIXTURE
TOTAL INTENSITY	κ_T	ACTIVITY COEFFICIENTS $(\partial \mu / \partial x)_{P,T}$
LANDAU-PLACZEK RATIO	κ_T	ACTIVITY COEFFICIENTS $(\partial \mu / \partial x)_{P,T}$
RAYLEIGH LINEWIDTH	$\chi = (\lambda / \rho c_p)$	ISOTHERMIC DIFFUSION CONSTANT (D) for $\chi (> D)$
BRILLOUIN INTENSITY	POCKELS' COEFFICIENT (P_{ij})	POCKELS' COEFFICIENT (P_{ij})
SHIFT OF BRILLOUIN LINE	HYPersonic VELOCITY (v_L , [∞]) AND ELASTIC CONSTANT C_{ij}	HYPersonic VELOCITY (v_L , [∞]) AND ELASTIC CONSTANT C_{ij}
WIDTH OF BRILLOUIN LINE	SOUND ATTENUATION (PHONON LIFETIMES) LONGITUDINAL VISCOSITY ($\eta_\nu + 4/3 \eta_s$)	SOUND ATTENUATION (PHONON LIFETIMES) LONGITUDINAL VISCOSITY ($\eta_\nu + 4/3 \eta_s$)

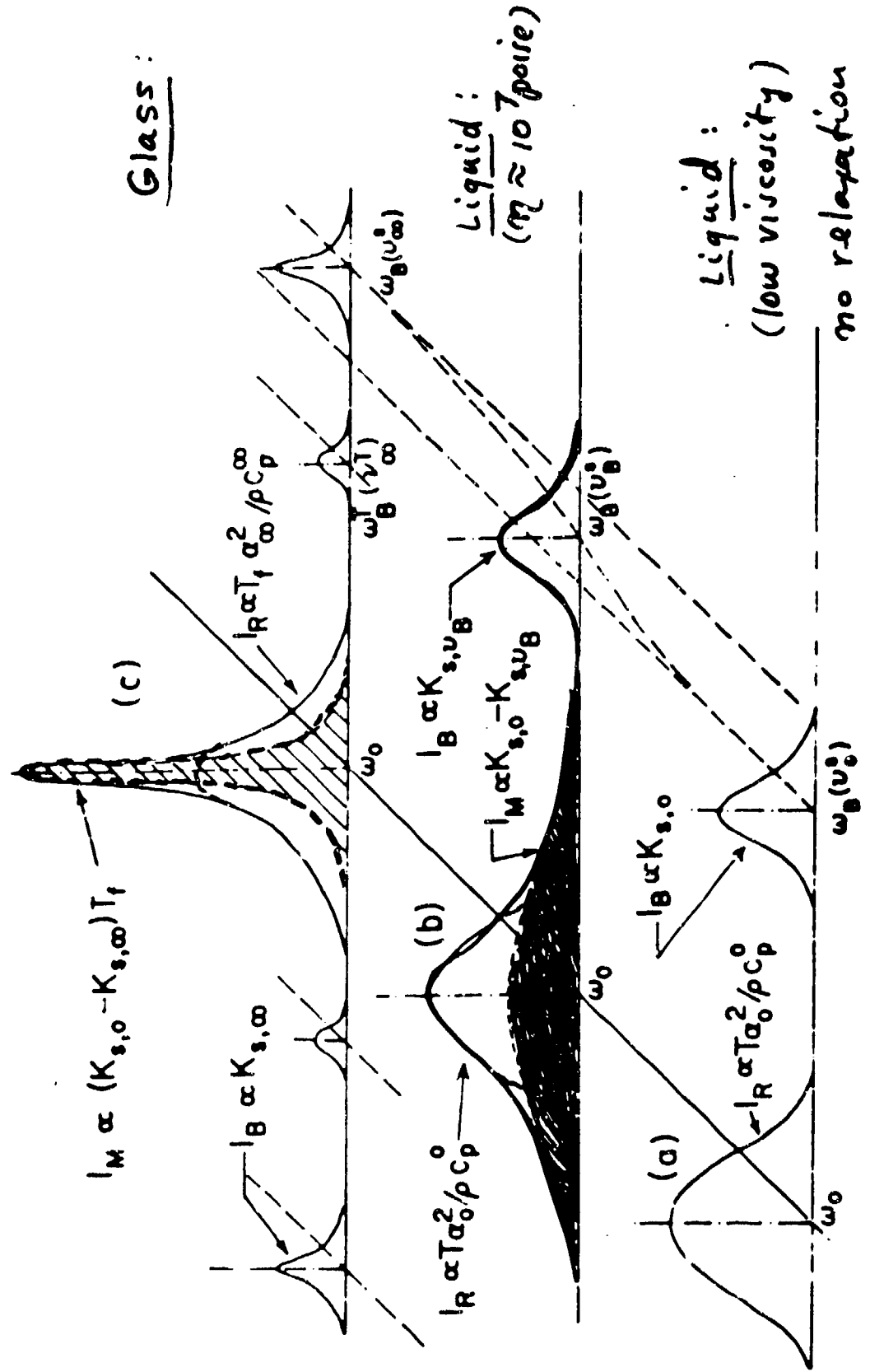
LTP-1845:

{
2.3% HAN/
19.6% TGAU/
18.1% Water.

LTP-1845 (HAN, TGAU, Water)







RAYLEIGH - BRILLOUIN LIGHT SCATTERING

$$I \propto \left[\rho \frac{\partial \epsilon}{\partial p} \right]^2 \langle \Delta \rho^2 \rangle + \left[\frac{\partial \epsilon}{\partial c} \right]^2 \langle \Delta c^2 \rangle$$

$$\propto \left(\frac{k_B T \beta_T}{V} \right)$$

Density Fluctuations:



$$\propto \left(\frac{k_B T}{V} \right)^{1/2} \left(\frac{\partial \mu}{\partial c} \right)_{P,T}$$

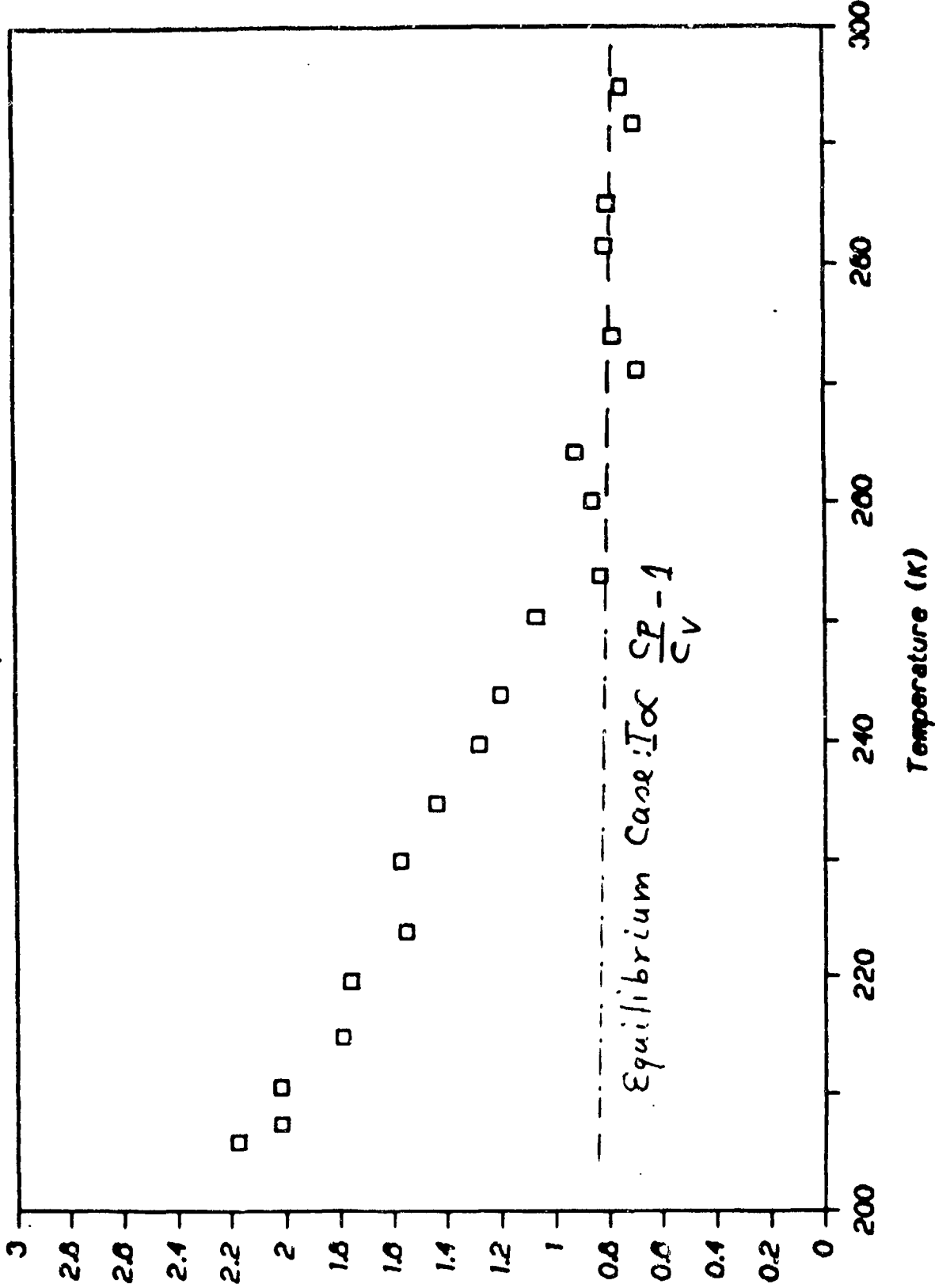
Concentration flucutations:



Determine from Ultrasonic
Hypersonic Measurements

Measurement of this quantity as a function of T, P or Concentration will allow the study of the critical point of phase separation. Rayleigh Linewidth becomes very narrow, and Rayleigh line becomes very intense. Hence, study stability of Binary fluid mixtures.

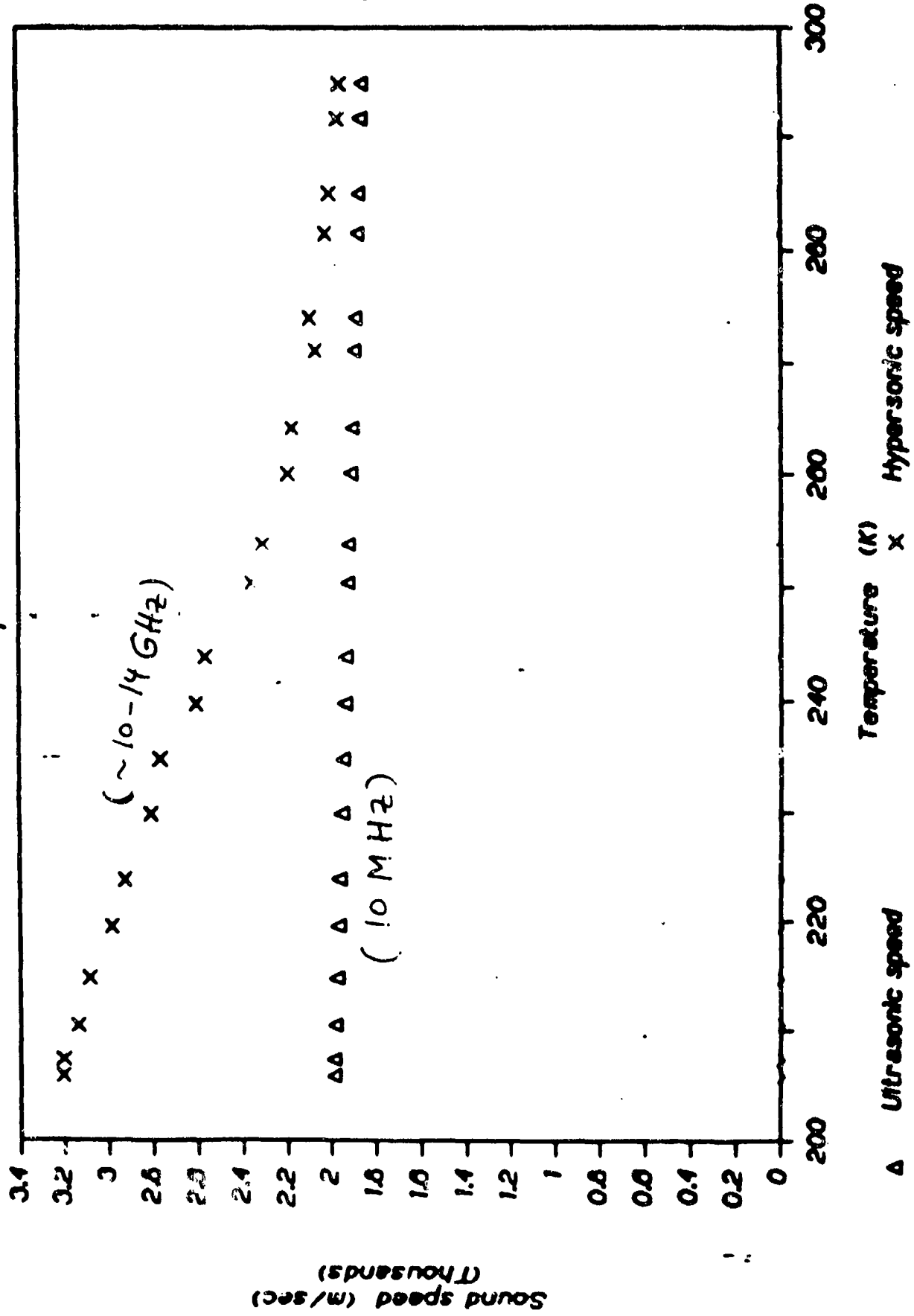
Landau-Placzek Ratio of LP1845
12th Sept. 1987

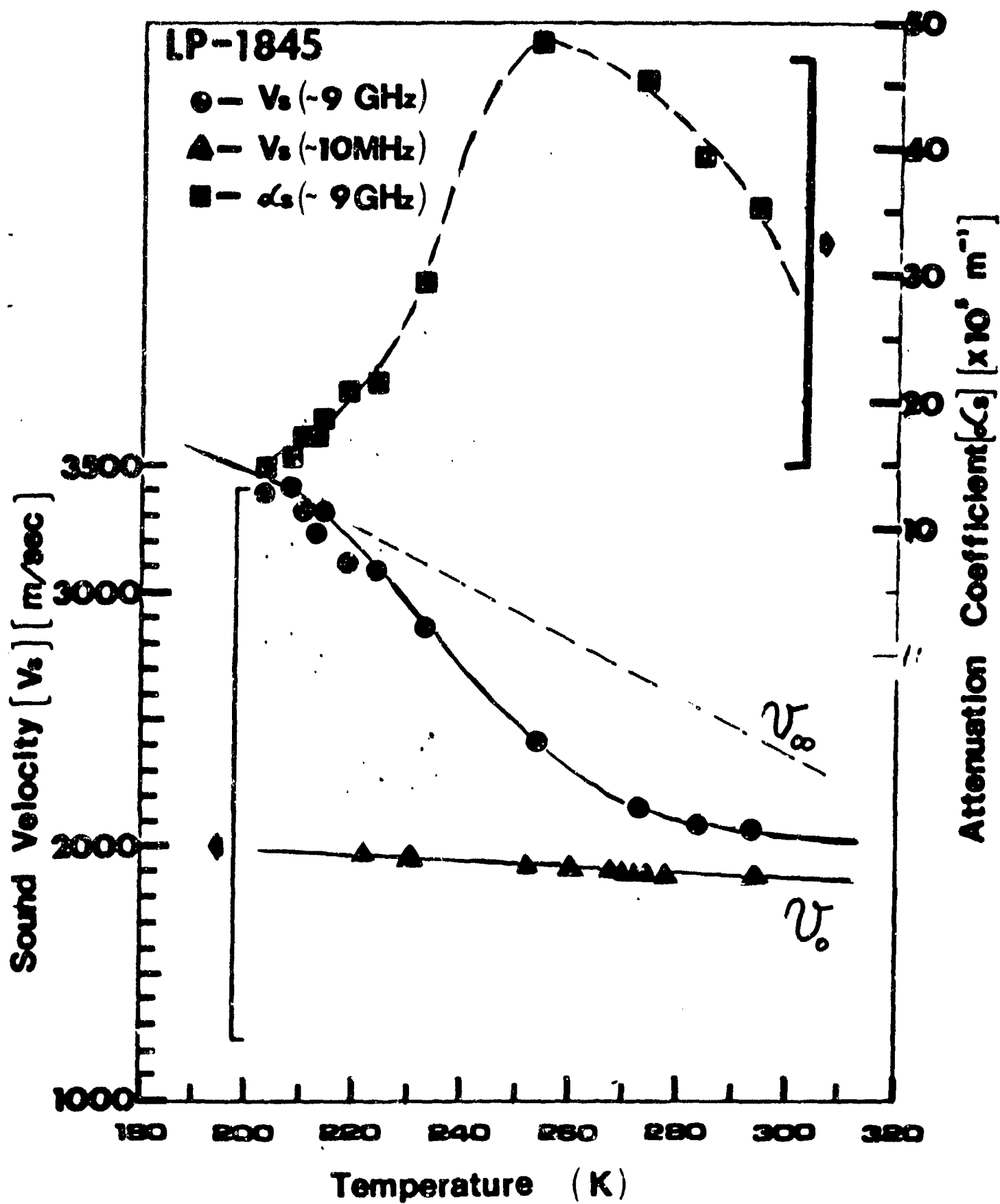


Landau-Placzek Ratio

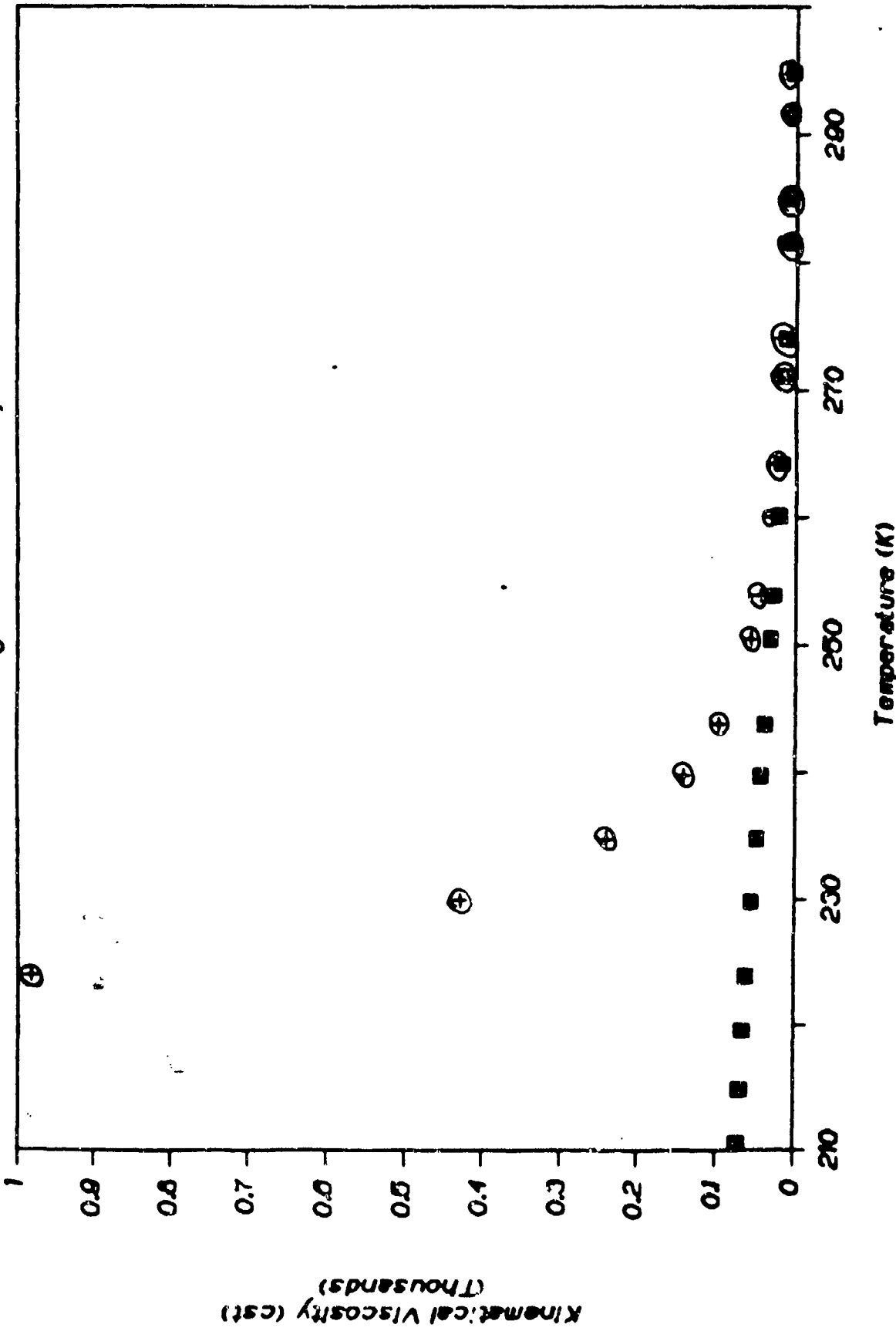
Hyperersonic & Ultrasonic speed of LP1845

10th Sept. 1967





Kinematical Viscosity of LP-1845
shear (⊖) and longitudinal (⊕) viscosity



Kinematical Viscosity (cSt)
(Thousands)

BRILLOUIN SCATTERING AT HIGH PRESSURE

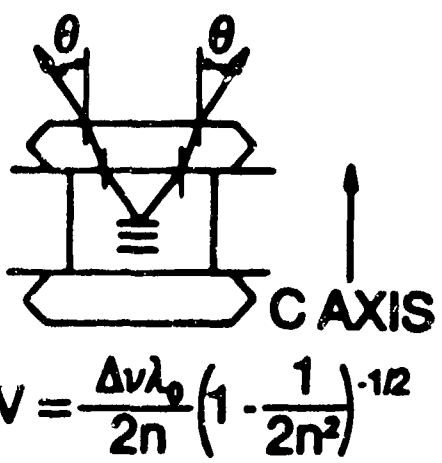
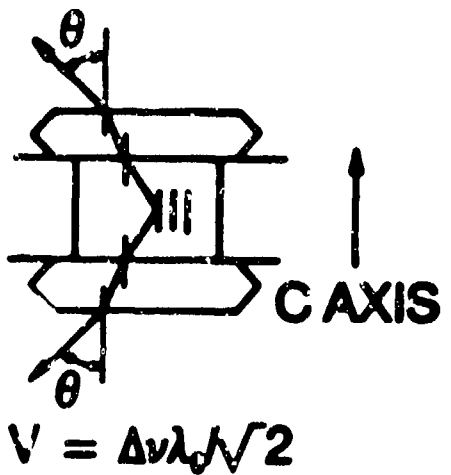
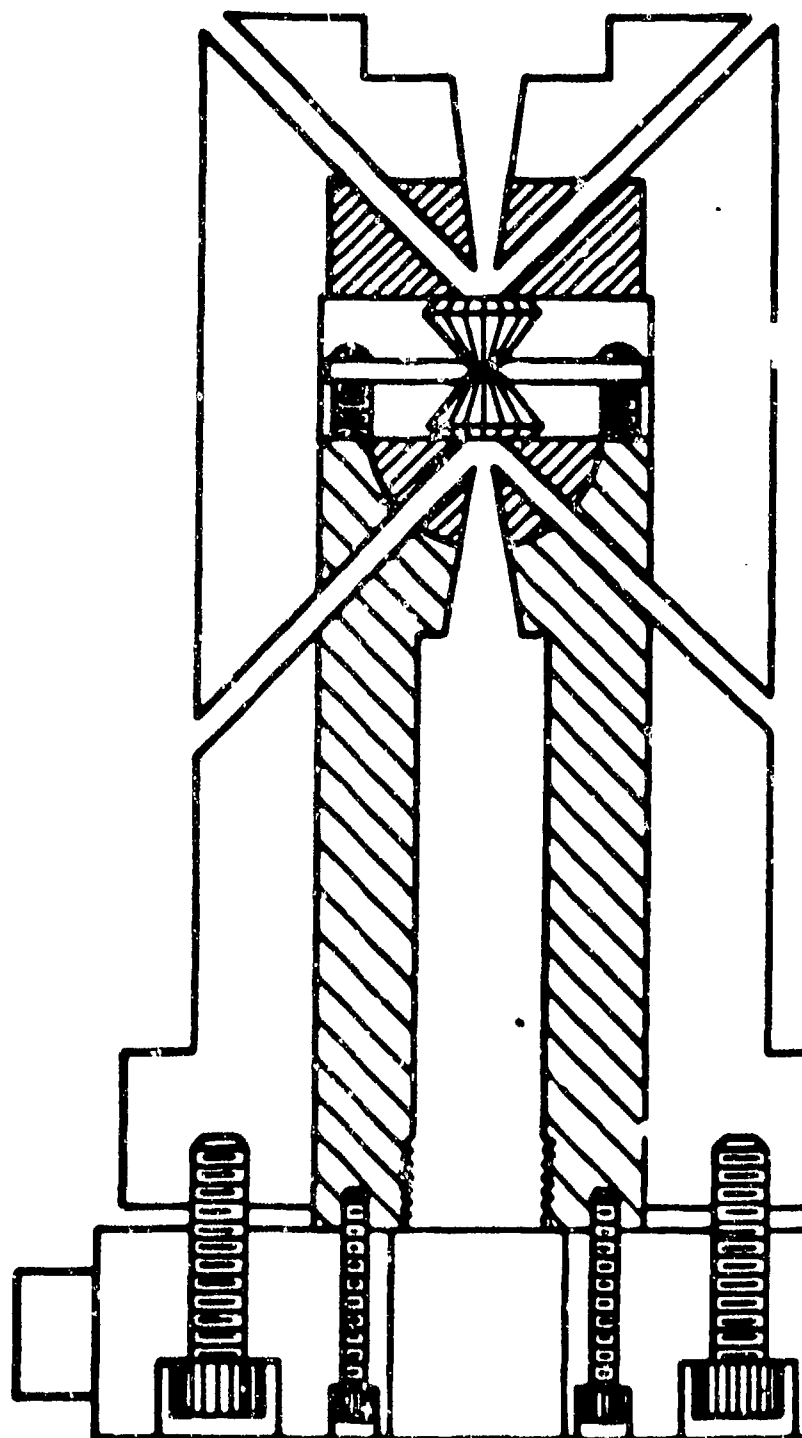
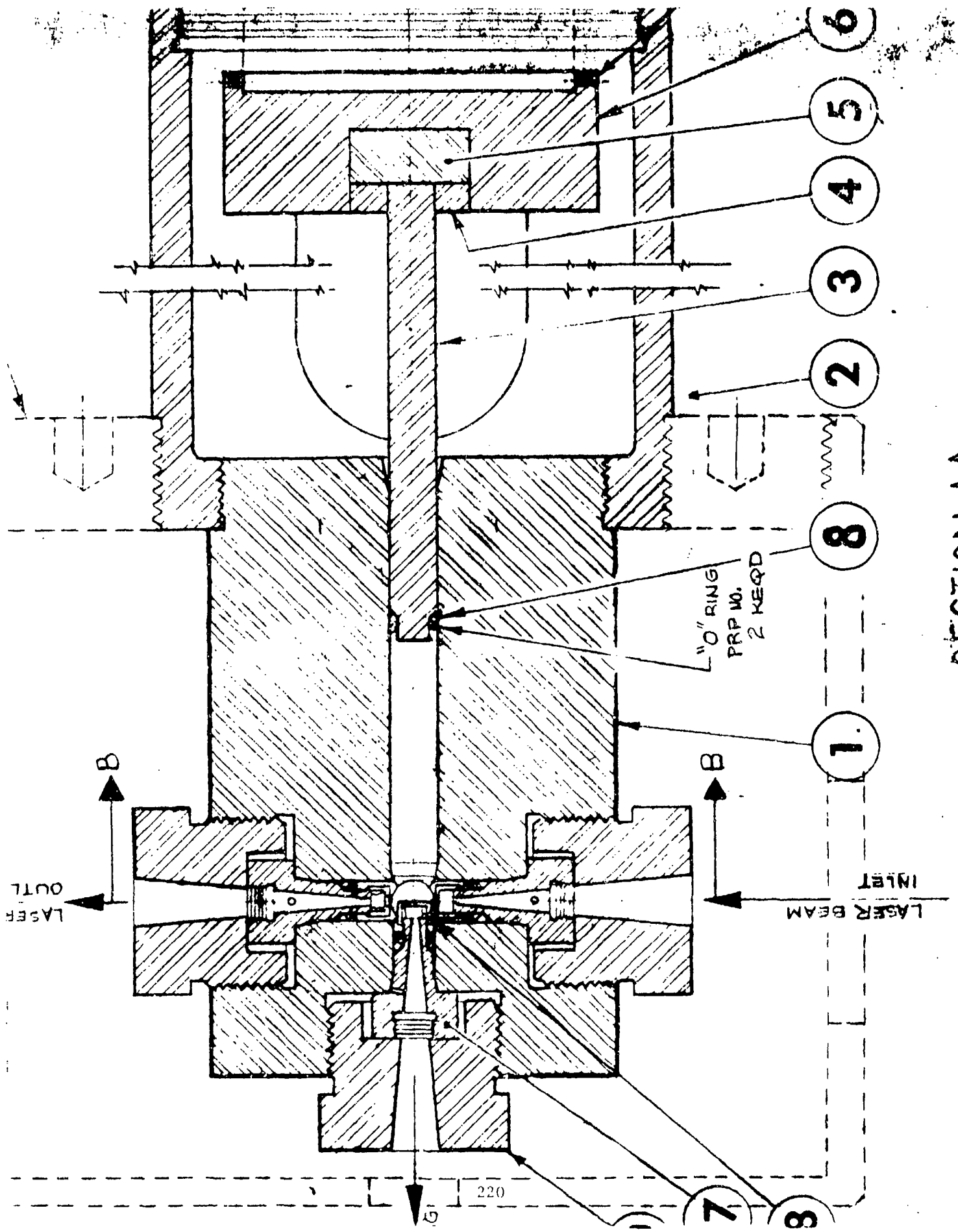
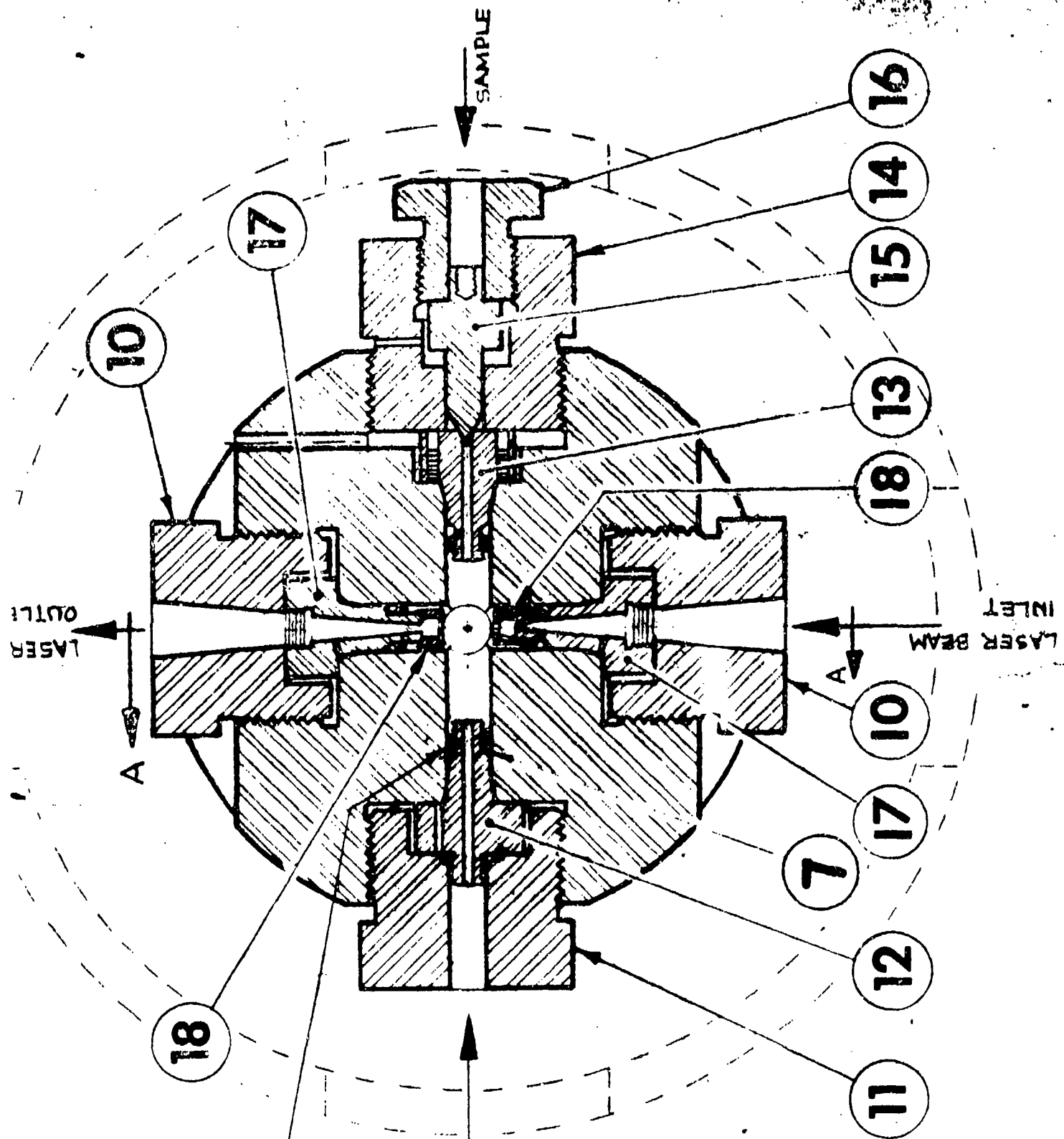


FIG. 4





5" RINGS
PK# N.C. 008
O REQD

SURE
SUREMENT
IGANIN
GE 221

**THE SOLUBILITY OF GASES UNDER PRESSURE
IN LIQUID PROPELLANTS**

**S. MURAD / P. RAVI
UNIVERSITY OF ILLINOIS
CHICAGO**

AUGUST 1988

ABSTRACT

A corresponding states correlation has been developed for the solubility of pure gases and mixtures in LGP 1846, a HAN based liquid propellant [1]. For nitrogen, methane, xenon, krypton, and argon, and their mixtures the correlation can be used to estimate gas solubilities for pressures upto 100 MPa in the temperature range $258 < T < 303$ K. The correlation is in satisfactory agreement with all available experimental data for these systems. Dissolved gases are expected to significantly effect many physical and chemical properties of liquid propellant systems.

INTRODUCTION

Aqueous solutions of hydroxyl ammonium nitrate (HAN), and aliphatic amine nitrates (AAN), posses excellent potential for use as high performance liquid propellants. One such propellant being actively considered is LGP 1846, which consists of 60.79, 19.19, and 20.02 weight percent of HAN, triethanol ammonium nitrate (TEAN), and water, respectively.[2]. The physical properties of these propellants are needed to model their behavior in the gun, where they can be under high pressures, and in contact with combustion gases. Since such gases can in general be expected to be soluble to some extent in the propellants, there is a need for a reliable method for predicting such solubilities, especially under high pressures. Dissolved gases are known to significantly affect many physical and chemical properties of aqueous solutions.

The corresponding states theory is a powerful tool for predicting thermodynamic and transport properties of fluids. However, the conditions that must be satisfied for the simple corresponding states principle to be valid are only obeyed by simple molecules like pure argon , krypton, and xenon [3]. In this paper we extend the simple corresponding states theory to include more complex substances that do not satisfy these conditions. This has been accomplished by replacing the critical parameters (usually temperature and volume) generally used in corresponding states, by two adjustable parameters. These parameters can be obtained from very limited experimental data. The technique used is similar in spirit to the shape factor method which has been widely used to predict thermodynamic and transport properties for a wide range of substances [4,5].

THEORY

The solubility of a gas in a liquid can be conveniently estimated via its fugacity. At equilibrium the fugacity of any component i must be equal in both the gas and liquid phases [6].

$$f_i^{(G)} = f_i^{(L)} \quad (1)$$

The fugacity in the gas phase can usually be estimated using generalized corresponding states charts, which are widely available [7], although if necessary it can be directly obtained from the relationship

$$RT \ln \left(\frac{f_i^{(G)}}{y_i P} \right) = \int_0^P \left(\bar{v}_i - \frac{RT}{P} \right) \frac{dP}{P} \quad (2)$$

where R is the universal gas constant, T the temperature, P the pressure, y_i the mole fraction of i in the gas phase, and \bar{v}_i the partial molar volume of i. The integral in eqn. (2) can be evaluated using a suitable equation of state. For the more common substances, such equations of state are available [8].

For the liquid phase the fugacity can be estimated from [9],

$$f_i^{(L)} = \gamma_i x_i H_{i,S}^0 \exp \left(\int_0^P \frac{\bar{v}_i dP}{RT} \right) \quad (3)$$

where $H_{i,S}^0$ is the Henry's constant in the solvent, γ_i the activity coefficient, and x_i the mole fraction of i in the solution. When $x_i \rightarrow 0$ (in practice less than 0.1), $\gamma_i \rightarrow 1$. Since we expect our solubilities to be rather low, and assuming \bar{v}_i to be independent of pressure (an assumption generally acceptable up to 100 MPa), eqn. (3) can be simplified to

$$f_i^{(L)} = H_{i,S}^0 \exp\left(\frac{P\bar{v}_i^\infty}{RT}\right) \quad (4)$$

From eqns. (1) & (4), the solubility of the gas can be estimated as

$$x_i = f_i^{(G)} / H_{i,S}^0 \exp\left(\frac{P\bar{v}_i^\infty}{RT}\right) \quad (5)$$

Thus in addition to $f_i^{(Q)}$, to predict the solubility of gases in liquid propellants, data is needed on $H_{i,S}^0$ and \bar{v}_i^∞ . In the next section we describe how these can be estimated using corresponding states.

RESULTS

The fugacity of component i in the gas phase can be obtained using generalized corresponding states tables or charts, e.g., those provided in Lewis and Randall [7]. For pure gases,

$$(f/P)_i^{\text{Pure}} = (f/P)^0 [(f/P)^1]^\omega \quad (6)$$

where $(f/P)^0$ and $(f/P)^1$ are generally given as a function of reduced temperature and pressure, and ω is the Pitzer acentricity factor [9]. For mixtures, one can generally make the assumption of ideal mixing, especially when the constituents of the mixture have similar chemical structure. In such cases the fugacity of component i in a mixture is given by

$$f_i^{(G)} = y_i f_i^{\text{Pure}} \quad (7)$$

To test the accuracy of this generalized corresponding states method for fugacity for the gases of interest to us, we also calculated fugacities using the rigorous definition of eqn. (2), using accurate equations of state. Both the methods showed excellent agreement. For mixtures we used a revised Redlich - Kwong equation [10] with eqn. (2).

Henry's constants for gases in solvents can be estimated from solubility data at atmospheric pressure and eqn. (5).

$$H_{i,S}^0 = P/x_i, \quad (8)$$

since at low pressures $f_i^{(Q)} \rightarrow P$ and $PV_i^{\infty}/RT \rightarrow 0$. Experimental data on the solubility of various simple gases in LGP 1846 has been measured recently by Koski [11]. We have used this data to obtain a generalized correlation for Henry's constant,

$$H_{i,S}^0 = -206.7 + 3.992 T - 0.0126 T^2, \quad (9)$$

where $H_{i,S}^0 = H_{i,S}^0/\beta_i$ and $T = T/\alpha_i$. Values of α_i and β_i for various gases in LGP 1846 are given in Table 1. Figure 1 shows a comparison of values for Henry's constants from the corresponding states correlation given by eqn (9), and the available experimental data. As can be seen, the correlation represents the data quite accurately.

There are no experimental measurements available for \bar{V}_i of the gases studied here in LGP 1846. However experimental data is

available for \bar{V}_i^∞ in water and other concentrated aqueous electrolyte solutions. Eqn. (2) applied to the solubility of gases in water and electrolyte solutions leads to the expression

$$\frac{x_i^w}{x_i^{ES}} = \frac{H_{i,ES}^0}{H_{i,W}^0} \exp\left(\frac{P\bar{V}_{i,ES}^\infty - \bar{V}_{i,W}^\infty}{RT}\right) \quad (10)$$

An examination of experimental data [12,13] on gas solubilities in water, and aqueous electrolyte solutions at pressures between 0.1 and 60 MPa, clearly shows that although x_i^w/x_i^{ES} is a function of temperature, it is independent of pressure. From the form of eqn (10), this can only be possible if $\bar{V}_{i,ES}^\infty = \bar{V}_{i,W}^\infty$. We have extended this result to LGP 1846 and approximated \bar{V}_i^∞ data in water as \bar{V}_i^∞ for these gases in LGP 1846. Such "experimental data" for \bar{V}_i^∞ was then fitted to a generalized corresponding states correlation,

$$\bar{V}_i^\infty = -0.0156 + 33.26T^\infty, \quad (11)$$

where $T^\infty = \bar{V}_i^\infty P_i^c / RT_i^c$ and $P_i^c = T P_i^c / C_s T_i^c$.

Here P_i^c and T_i^c are the critical pressure and temperature of i , and C_s is the cohesive energy density of LGP 1846, originally introduced by Scatchard and Hildebrand in developing the regular solution theory [6]. Since water is the only volatile substance in LGP 1846 at temperatures of interest to us, this would essentially be the value for water. Figure 2 shows a comparison of \bar{V}_i^∞ values predicted using the corresponding states correlation of eqn. (11), and available experimental data [12,13]. In view of the relatively large uncertainties in such experimental measurements, the correlation is quite satisfactory.

The solubility of gases under pressure can now be obtained by using eqn (5). The fugacity in the gas phase can be obtained using the correlations available in the literature (see eqns 6 and 7). The Henry's constants required in eqn (5), can be obtained from the correlation developed here (eqn 9), and the partial molar volumes from eqn (11). Experimental data is not available for the solubility of gases in liquid propellants, at high pressures. It is therefore not possible to test our method for liquid propellants. However, limited data is available on gases in aqueous solutions such as sodium chloride. In Figure 2A we have compared results obtained using the technique outlined above with experimental data for N₂ in aqueous sodium chloride [12]. The results confirm the general validity of assumptions we have made for a wide range of pressures.

The results for five pure gases (Ar, Kr, Xe, N₂ and CH₄) are shown in Figures 3 to 7. The solubility increases with pressure, but the rate of increase of solubility with pressure decreases with increasing pressure. The solubility also increases with temperature at low and moderate pressures, but it appears that there may be an inversion in this temperature dependence at high pressures (around 100 MPa). Although, this inversion is within the estimated accuracy of our predictions, it is clear, that the temperature dependence of solubility varies considerably over the pressure range 0 to 100 MPa. The behavior of xenon is somewhat different from that of the other simple gases. This is because the critical temperature of xenon is 289.7 K, which is close to the ambient temperatures studied here.

The solubility of simple gas mixtures in LGP 1846 is shown in Figures 8 and 9 for N₂-CH₄ and Ar-CH₄, respectively, for three compositions. The solubility of the mixture as a function of pressure increases as the mole fraction of the component with the higher critical pressure increases. The solubility of the Ar-CH₄ mixture does not vary much with composition, as the critical pressures of the two are very close to each other, although there seems to be an inversion in the composition dependence at around 700 atm. This again is within the estimated accuracy of our predictions. The pressure dependence of the solubility is similar and the temperature dependence is expected to be the same as for

the pure gases. Similar results are obtained for Ar-N₂ and Kr-CH₄ mixtures.

CONCLUSIONS

We have developed a technique for predicting solubilities of gases in LGP 1846. This technique could be extended to other aqueous electrolyte solutions, and work is currently in progress to enable such an extension. All the correlations used are based on the corresponding states principle, which has been found to be a very powerful method for such predictions by us and others [4,5]

ACKNOWLEDGEMENTS

The authors would like to thank Prof. W. Koski, for supplying his experimental results prior to publication. This research was sponsored by the U. S. Army Ballistics Research Laboratory (J. Q. Wojciechowski, technical monitor). The authors would like to thank E. Freedman, N. Klein, C. Leveritt, W. Morrison, and J. Wojciechowski, for their helpful comments and encouragement. Computing Services were provided by the University of Illinois Computer Center.

REFERENCES

1. Decker, M.M., Freedman, E., Klein, N., Leveritt, C.S., and Wojciechowski, J.Q., "HAN-Based Liquid Propellants : Physical Properties", Ballistic Research Laboratory, Technical Report (1988).
2. Klein, N., "Liquid Propellants for use in Gun - A Review", Rept. BRL-TR-2641, U.S. Army Ballistic Research Laboratory, Aberdeen Proving Grounds, Maryland, 1983.
3. Reed,T.M., and Gubbins, K.E., "Applied Statistical Mechanics", McGraw Hill, New York, 1973.
4. Rowlinson, J.S., and Watson, I.D, Chem. Eng. Sci., 24, 1565, 1969.
5. Brucks, M.G., and Murad, S., Chem. Eng. Commun., 40, 345, 1986.
6. Prausnitz, J.M., Lichtenhaler, R.N., and Azevedo, E.G., "Molecular Thermodynamics of Fluid Phase Equilibria", Prentice Hall, New Jersey, 1986.
7. Lewis, G.N., Randall, M., Pitzer, K.S., and Brewer, L., "Thermodynamics", McGraw Hill, 1961.
8. Reid,R.C., Prausnitz, J.M., and Poling, B.E., "The Properties of Gases and Liquids", McGraw Hill, New York, 1986.
9. Ref. 6, Page 87.
10. Prausnitz,J.M., and Chueh, P.L., "Computer Calculations for High-Pressure Vapor - Liquid Equilibria", Prentice Hall, New Jersey, 1968.
11. Koski, W., private communications, 1987.
12. O'Sullivan, T.D., and Smith, N.O, J. Phys. Chem., 74, 1460, 1970.
13. Gardiner, G.E., and Smith, N.O., J. Phys. Chem., 76, 8, 1972.

Table 1

<u>GAS</u>	<u>α_1</u>	<u>$10^{-3}\beta_1$</u>
Nitrogen	1.52	3.220
Methane	1.64	1.220
Xenon	2.64	0.373
Krypton	1.99	0.566
Argon	1.74	1.350

FIGURE CAPTIONS

Fig. 1: The calculated (eqn. 9) and experimental values of Henry's constants; ____ calculated, • experimental.

Fig. 2: The calculated (eqn. 11) and experimental values of partial molar volumes; ____ calculated, • experimental.

Fig. 2A: The calculated and experimental solubilities of nitrogen in 1 m aqueous sodium chloride ~~X~~ ____ calculated, ■ experimental [12].

at 51°C

Fig. 3: The estimated solubility of argon in LGP 1846; ____ 30,
--- 15, ____ 0 Deg. C.

Fig. 4: The estimated solubility of krypton in LGP 1846; ---25,
____ 0 Deg. C.

Fig. 5: The estimated solubility of xenon in LGP 1846 at 30 Deg. C.

Fig. 6: The estimated solubility of nitrogen in LGP 1846; ____ 30,
--- 15, ____ 0 Deg. C.

Fig. 7: The estimated solubility of methane in LGP 1846; ____ 30,
--- 15, ____ 0 Deg. C.

Fig. 8: The estimated solubility of nitrogen-methane mixture in LGP 1846 at 30 Deg. C; ____ 75, --- 50, ____ 25 mole% methane.

Fig. 9: The estimated solubility of argon-methane mixture in LGP 1846 at 30 Deg. C. ____ 75, --- 50, ____ 25 mole% methane.

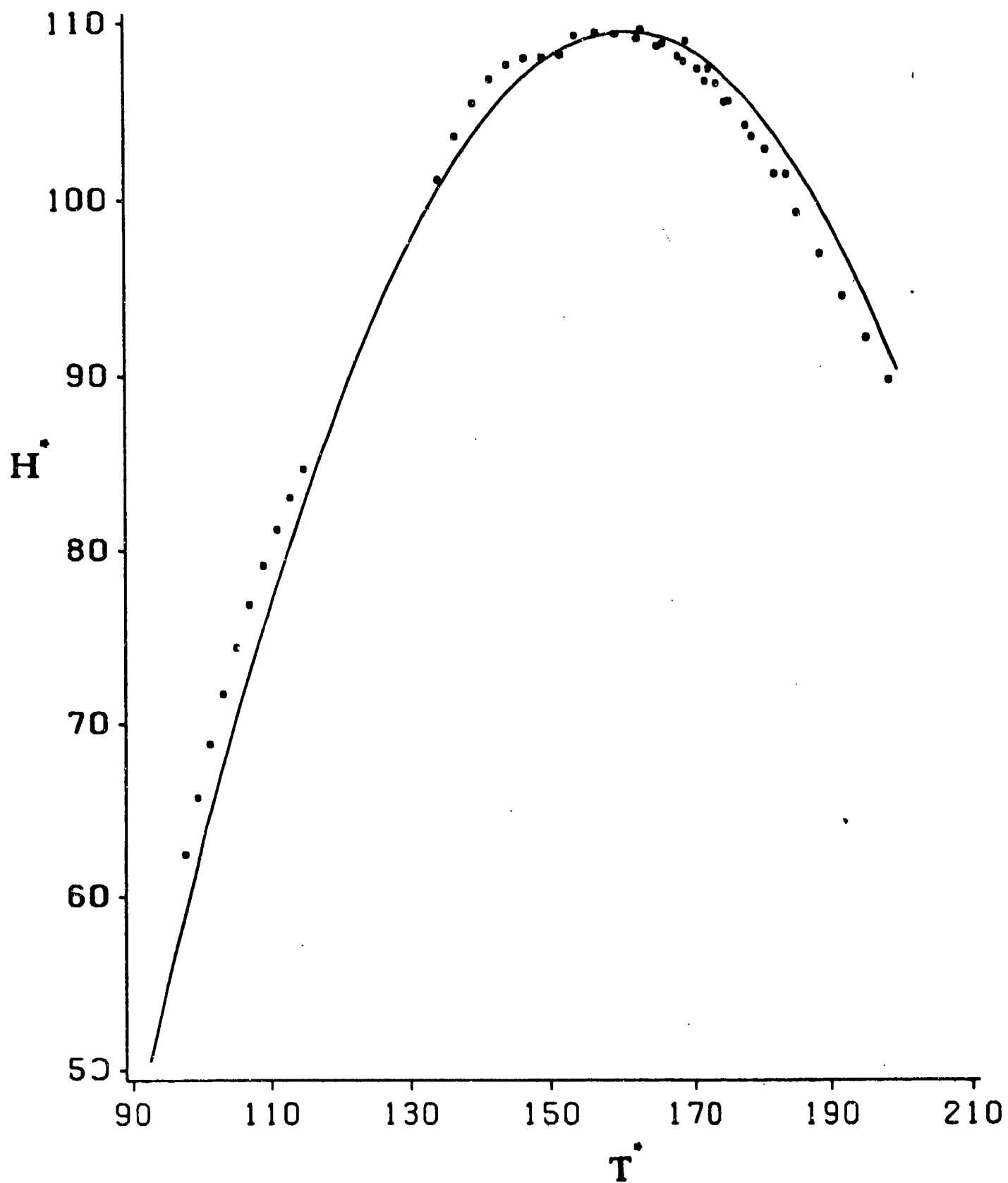


FIG. 1

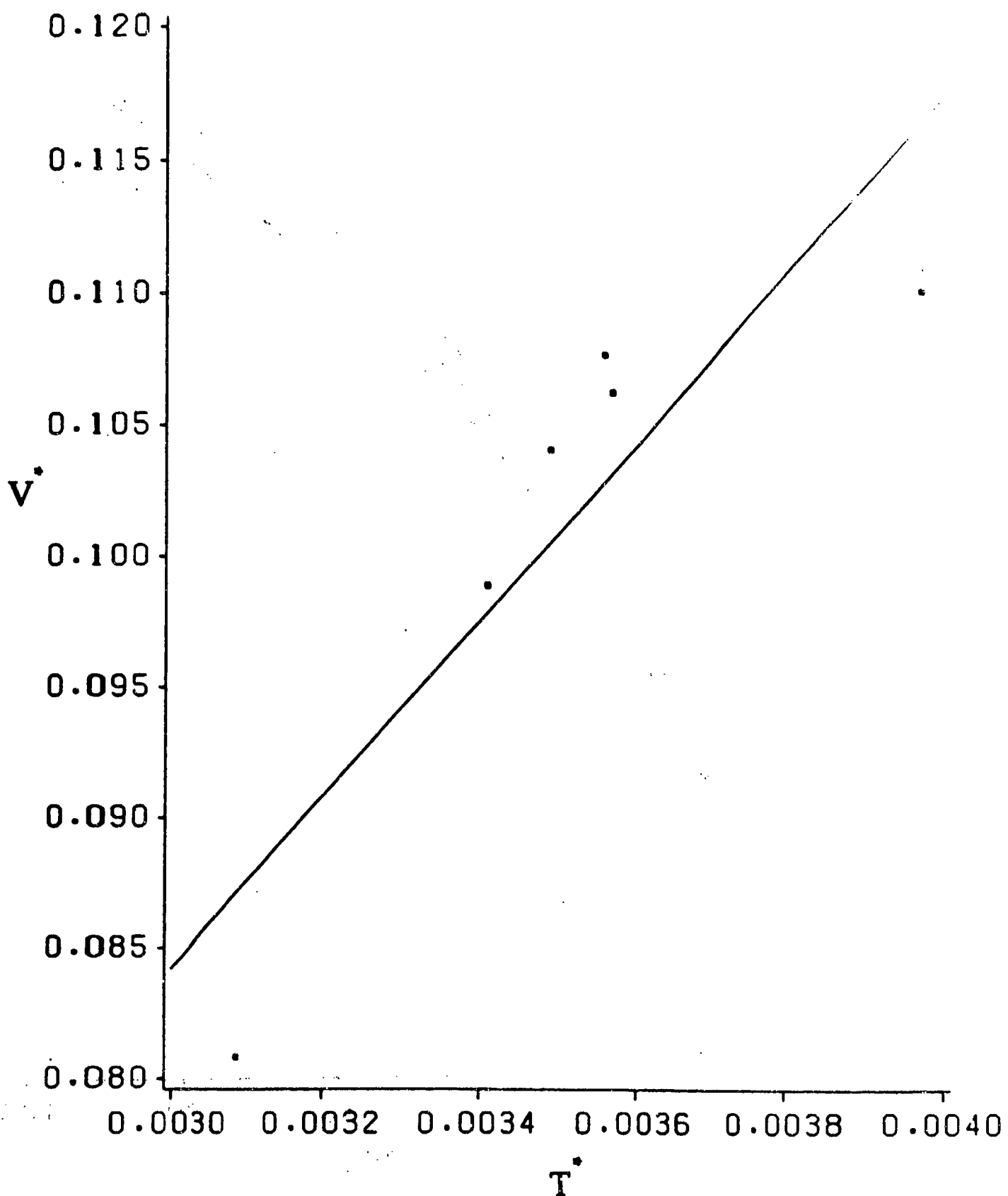


FIG. 2

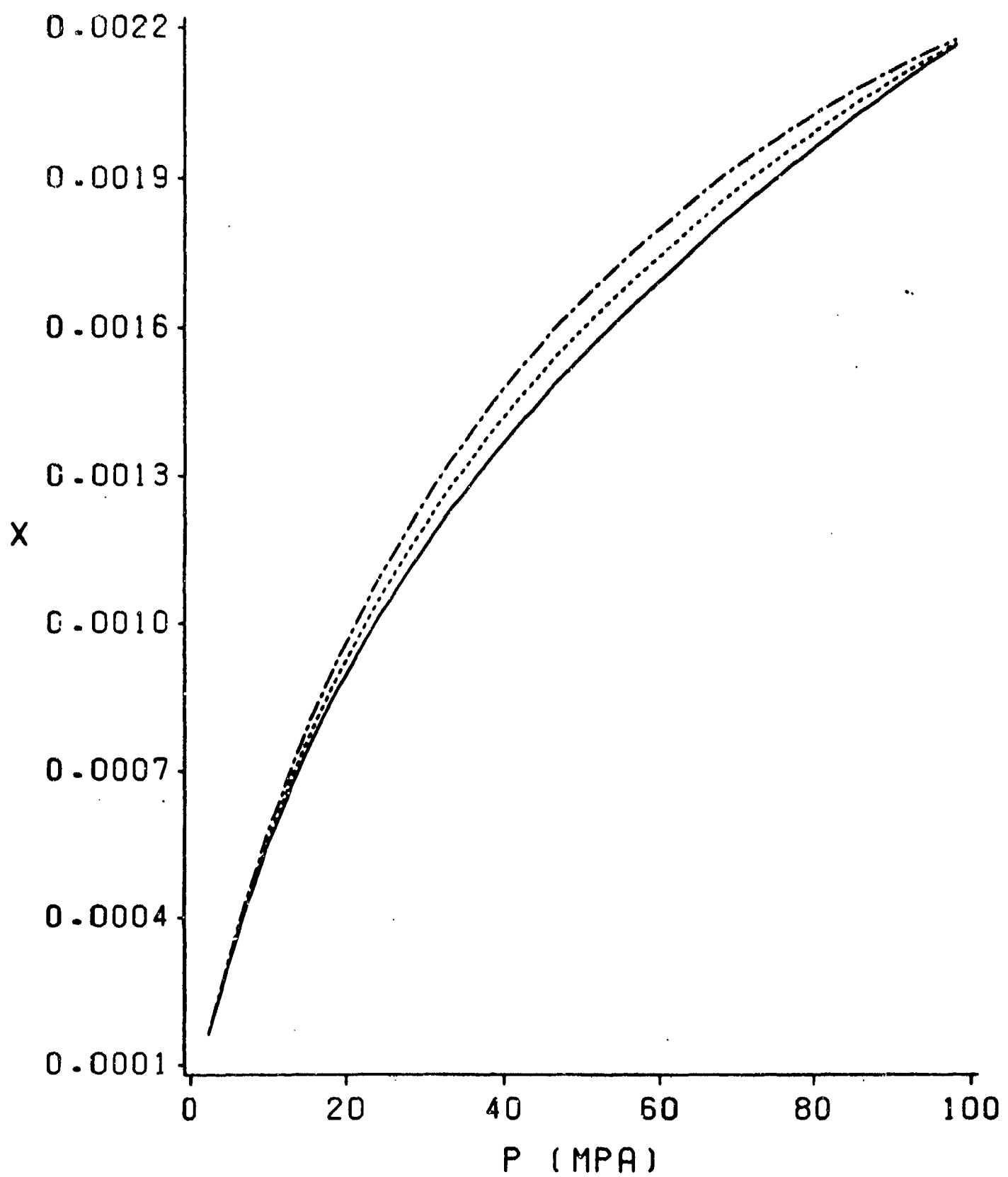


FIG. 3

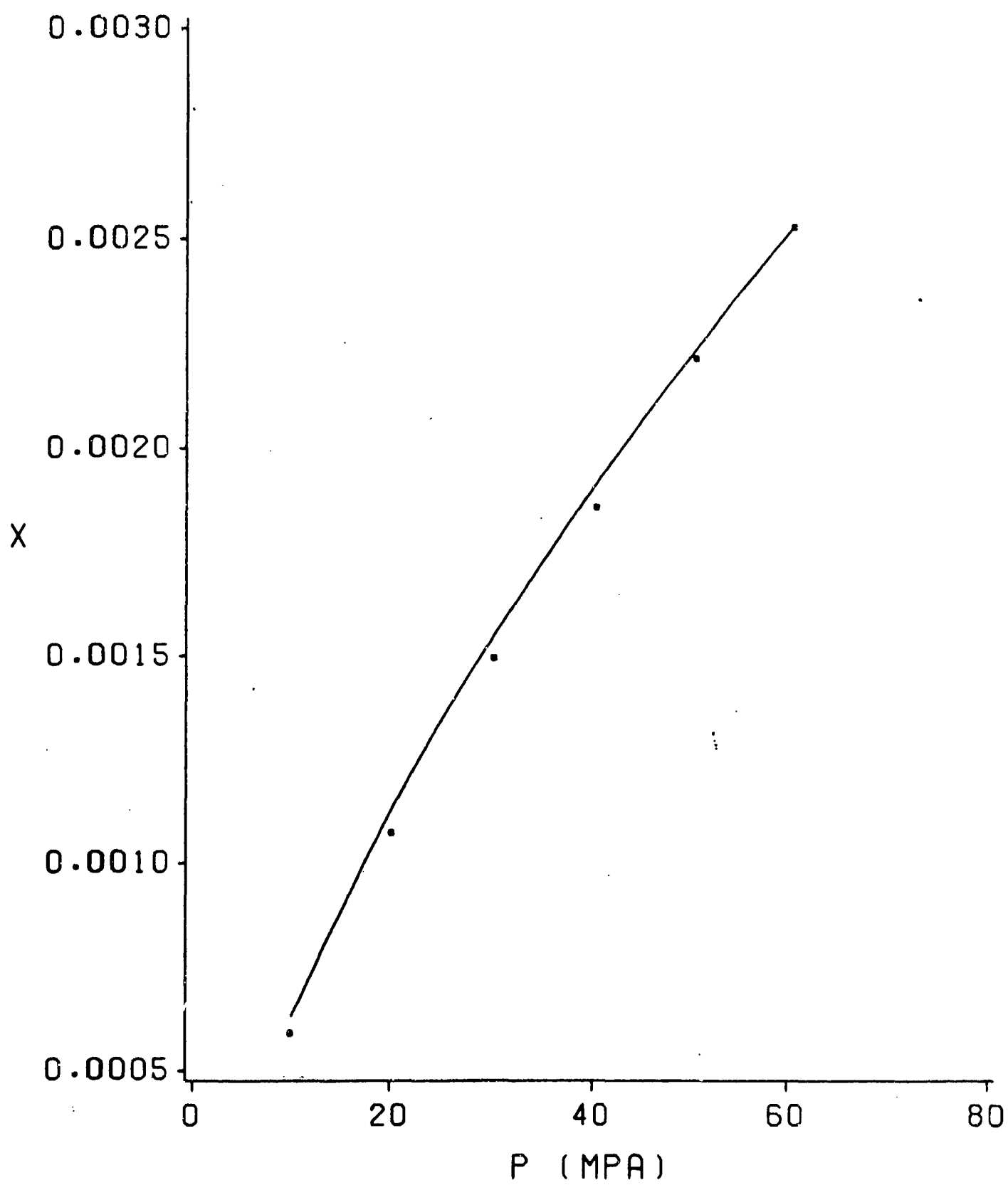


FIG 2A

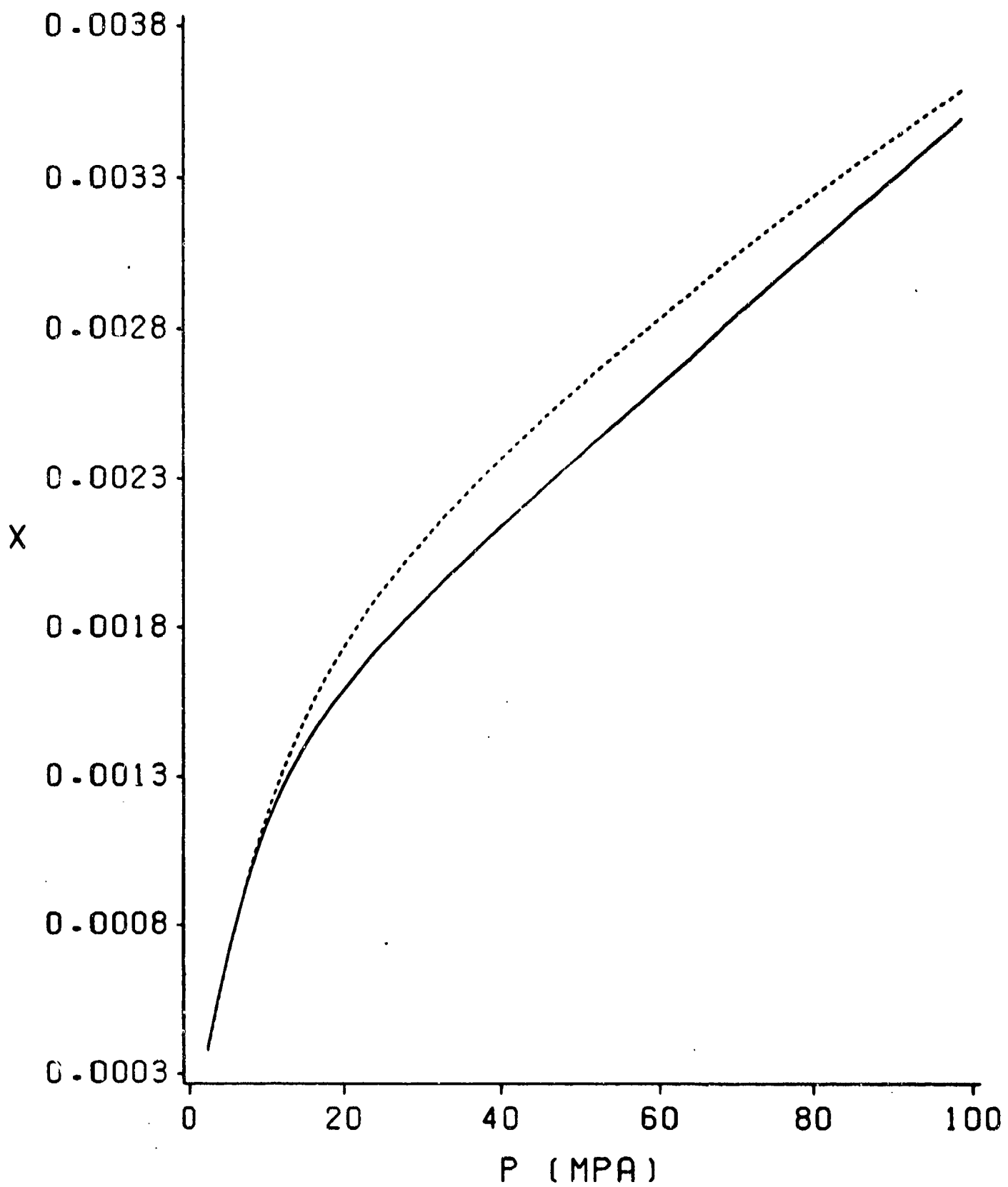


FIG. 4

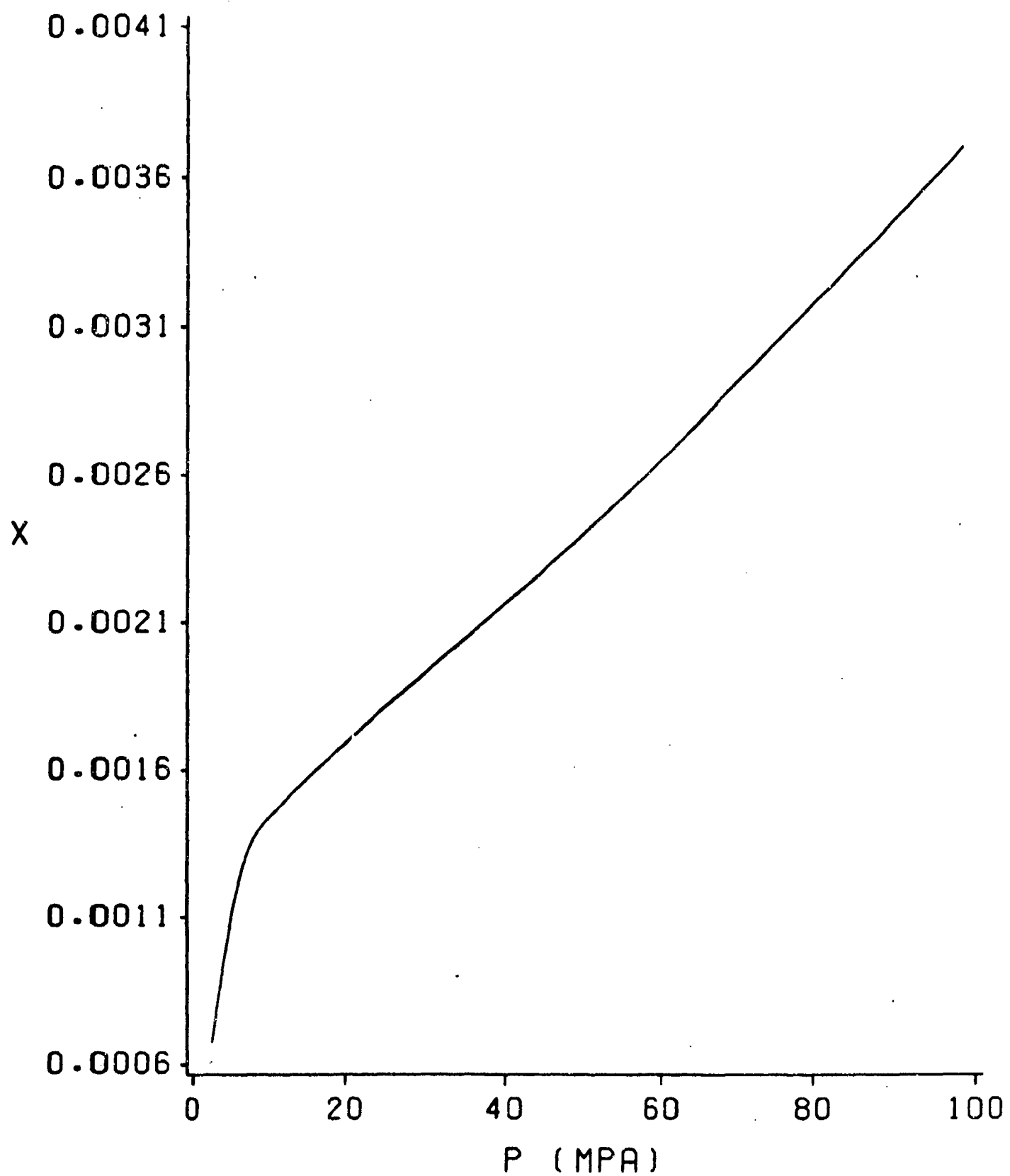


FIG. 5

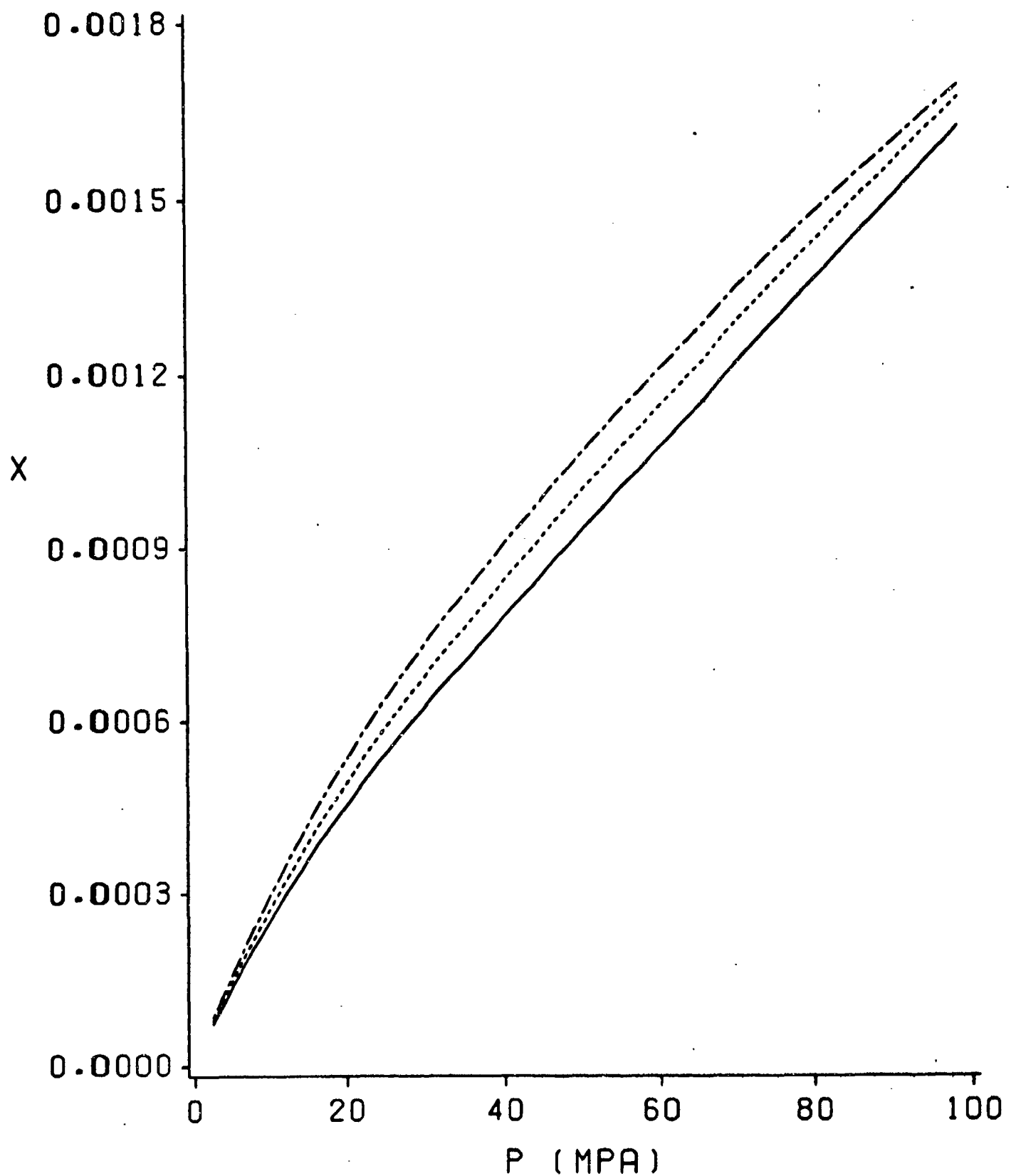


FIG. 6

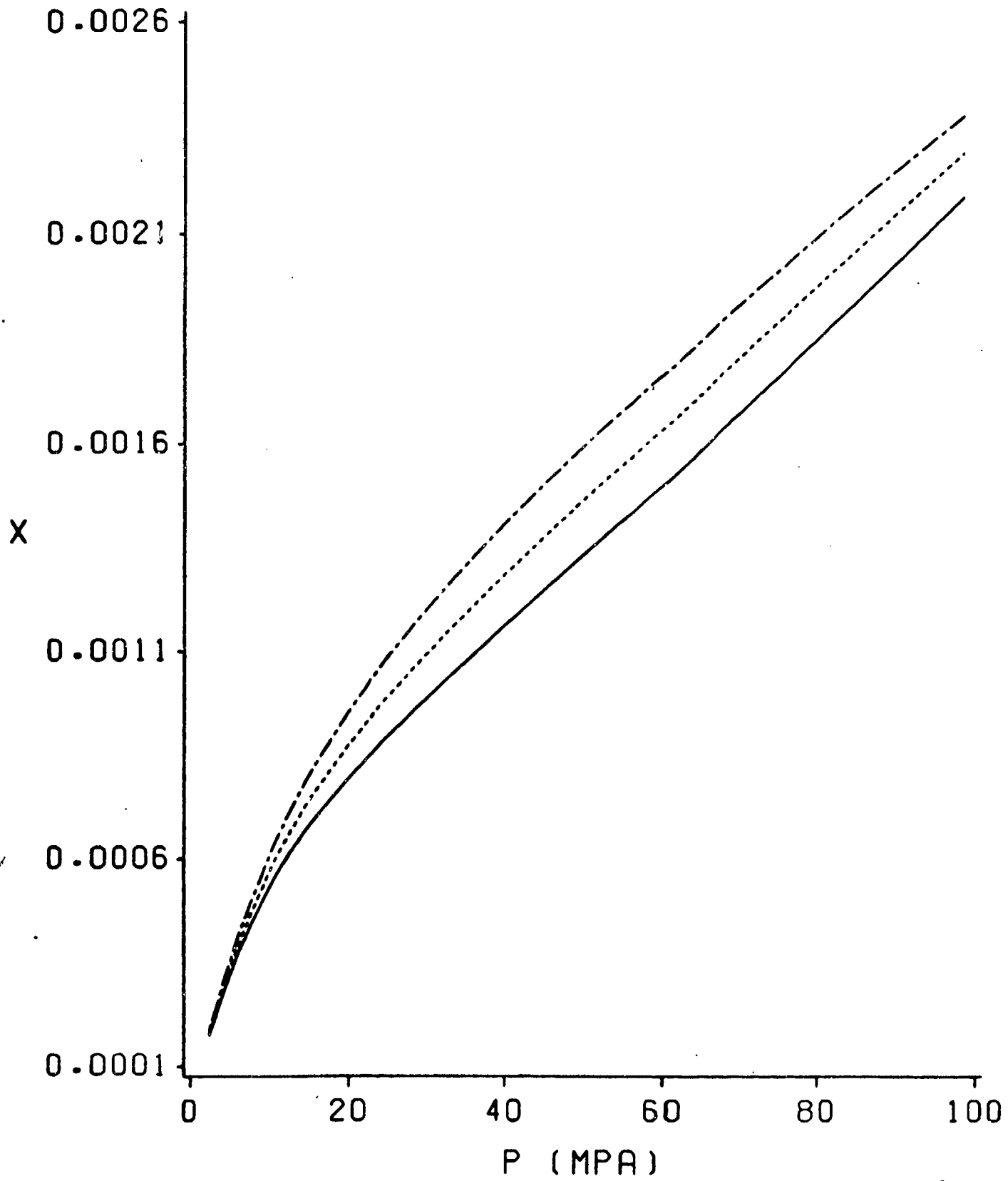


FIG. 7

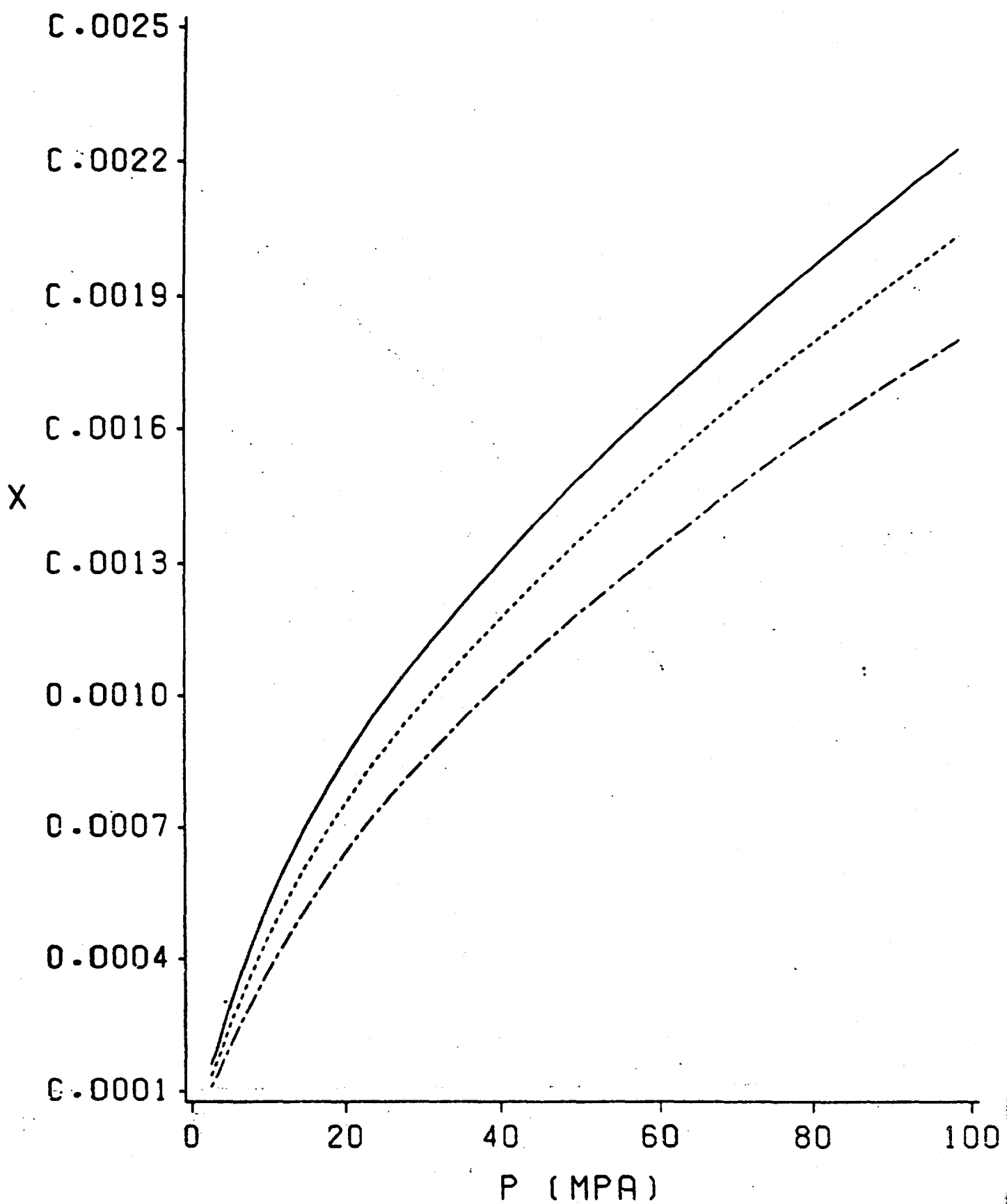


FIG. 8

Preceding Page Blank

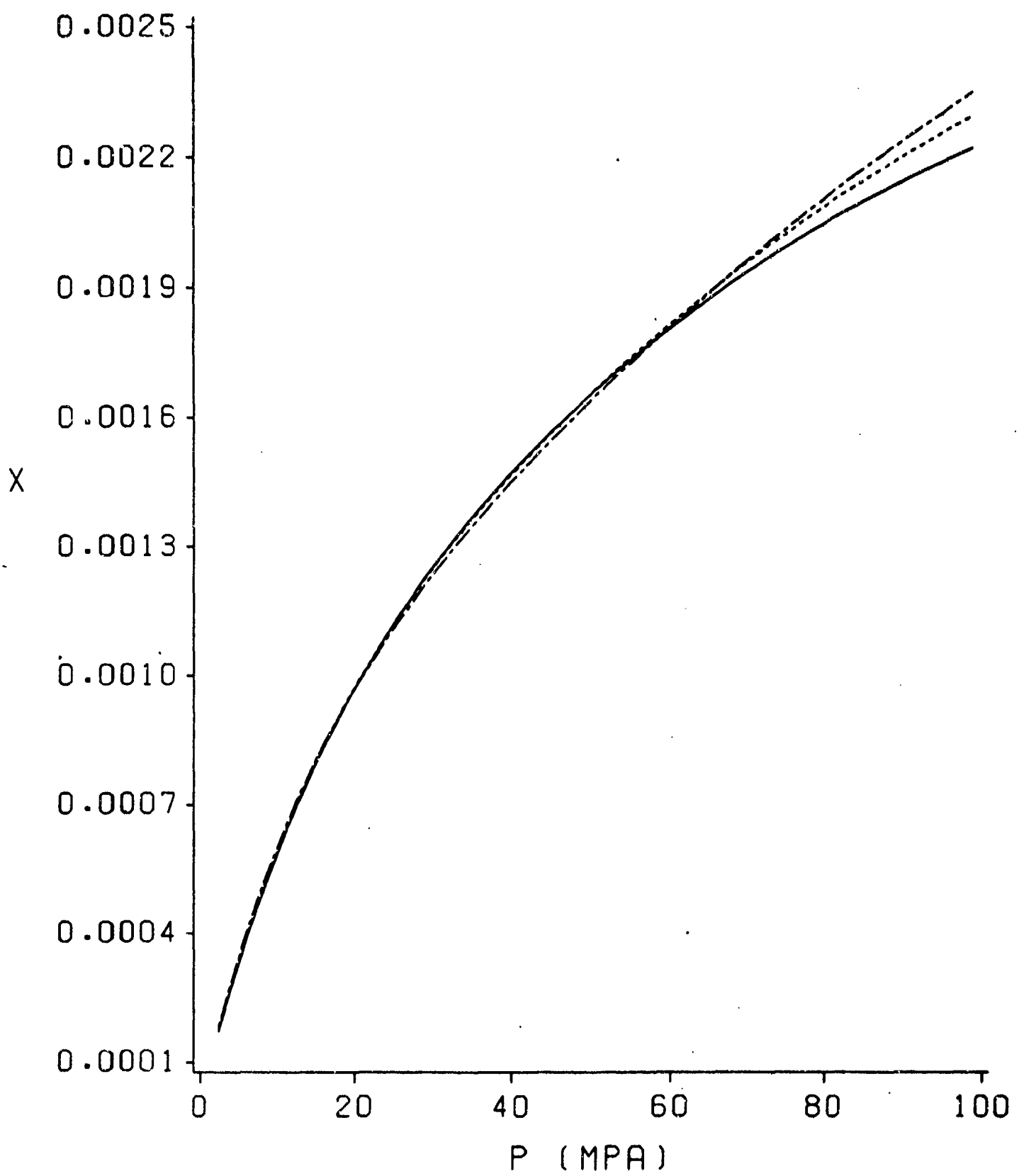


FIG. 9

COMPATIBILITY OF ELASTOMERIC MATERIALS WITH HAN-BASED LIQUID PROPELLANT 1846.

BY

GUMERSINDO RODRIGUEZ *
HENRY O. FEUER
ALAN R. TEETS

U.S. Army Belvoir RD & E Center
Fort Belvoir, VA 22060-5606

AUGUST 1988

**Presented at the 4th Annual Conference on HAN-Based Liquid
Propellant Structure and Properties, Ballistic Research
Laboratory, Aberdeen Proving Grounds, MD 21005-5066**

ELASTOMERS COMPATIBILITY WITH LIQUID PROPELLANT

G. Rodriguez, H.O. Feuer and A. R. Teets

Rubber and Coated Fabrics Research Group,
Materials, Fuels and Lubricants Directorate
U.S. Army Belvoir Research, Development and Engineering Center,
Fort Belvoir, VA 22060-5606

ABSTRACT

The Advanced Ballistic Concepts Branch of the Ballistic Research Laboratory, BRL, tasked the Rubber and Coated Fabrics Research Group of the Belvoir RD&E Center, BRDEC, to study the compatibility of various elastomers with liquid propellant 1846.

In order to generate a practical system for the handling and storage of liquid propellants a group of thirty seven elastomeric compositions were evaluated for compatibility with liquid propellant. All the materials tested were selected because they were either currently being considered for use in fuels or water handling equipment. In addition the materials were further selected on the basis of resistance to alkalies due to the composition of the liquid propellants currently in use. The measurements to assess elastomer compatibility with the liquid propellant included swelling of the elastomers, change in hardness, discoloration and retention of tensile strength, modulus and ultimate elongation.

Materials Used In The Liquid Propellant Compatibility Study.

1. CARBOXYLATED NITRILES RUBBER, XNBR
2. NITRILE RUBBER, NBR
3. HIGHLY SATURATED NITRILE RUBBER
4. POLYCHLOROPRENE
5. POLYURETHANES
6. THERMOPLASTIC ELASTOMERS
7. FLUOROCARBON ELASTOMERS
8. HALOGENATED BUTYL RUBBER
9. CHLOROSULFONATED ELASTOMERS
10. ETHYLENE PROPYLENE RUBBER

BRDEC/MFLL

TABLE 1

LIST OF MATERIALS FOR COMPATIBILITY WITH LIQUID PROPELLANT.

ELASTOMERS

A. HIGHLY SATURATED NITRILE RUBBER	TEST CODE
1. NBR-2	[LP-1]
B. NITRILE RUBBER	
1. NBR-8	[LP-2]
2. NBR-9	[LP-3]
3. 1203-F60-R2, RADIAN	[LP-4]
4. VT-380 (NBR/PVC), RADIAN	[LP-5]
5. BJLT M-40, UNIROYAL	[LP-6]
6. OZO-HA-0221, (70%NBR/30%PVC), UNIROYAL	[LP-7]
C. CARBOXYLATED NITRILE RUBBER	
1. XNBR-2	[LP-8]
2. XNBR-3	[LP-9]
3. XNBR-6	[LP-10]
D. POLYCHLOROPRENE RUBBER	
1. CR-1	[LP-11]
2. CR-2	[LP-12]
E. FLUOROELASTOMERS	
1. VITON-1	[LP-13]
2. VITON-2	[LP-14]
3. REEVES S/4616, (GUM)	[LP-15]
4. FLURAN F-5500-A NORTON IND. PLASTICS	[LP-16]
F. ETHYLENE-PROPYLENE RUBBER	
1. REEVES 4601, (GUM)	[LP-17]
2. REEVES 4594, (GUM)	[LP-18]
G. THERMOPLASTIC ELASTOMERS	
1. THP-1, ALCRYN R1201 B-70A	[LP-19]
2. THP-3, ALCRYN R1101 B70	[LP-20]
3. THP-4, MONSANTO GEOLAST	[LP-21]
4. THP-5, MOBAY TEXIN 355DR	[LP-22]
5. THP-6, MOBAY TEXIN 480 AR	[LP-23]
6. THP-7, GAFLEX	[LP-24]
7. THP-8, SANTOPRENE, 201-55	[LP-25]

8.	THP-9, SANTOPRENE, 101-64	[LP-26]
9.	THP-10, SANTOPRENE, 101-73	[LP-27]
10.	CD-9250, DISOGRIN	[LP-28]
11.	NORPRENE, NORTON IND. PLASTICS	[LP-29]

H. POLYURETHANES

1.	PU-1, UNIROYAL, Vibrathane 5004	[LP-30]
2.	PU-2, UNIROYAL, Adiprene CM	[LP-31]
3.	TSE-E-34-94, TSE INDUSTRIES, MILLATHANE	[LP-32]

I. SYNTHETIC RUBBER

1.	3130 TREAD	[LP-33]
2.	KRATON 1650, ILC DOVER	[LP-34]
3.	ATL-644-30, AERO TEC LABORATORIES, INC.	[LP-35]
4.	GOODYEAR COLLAPSIBLE TANKS GUM	[LP-36]

J. HALOGENATED BUTYL

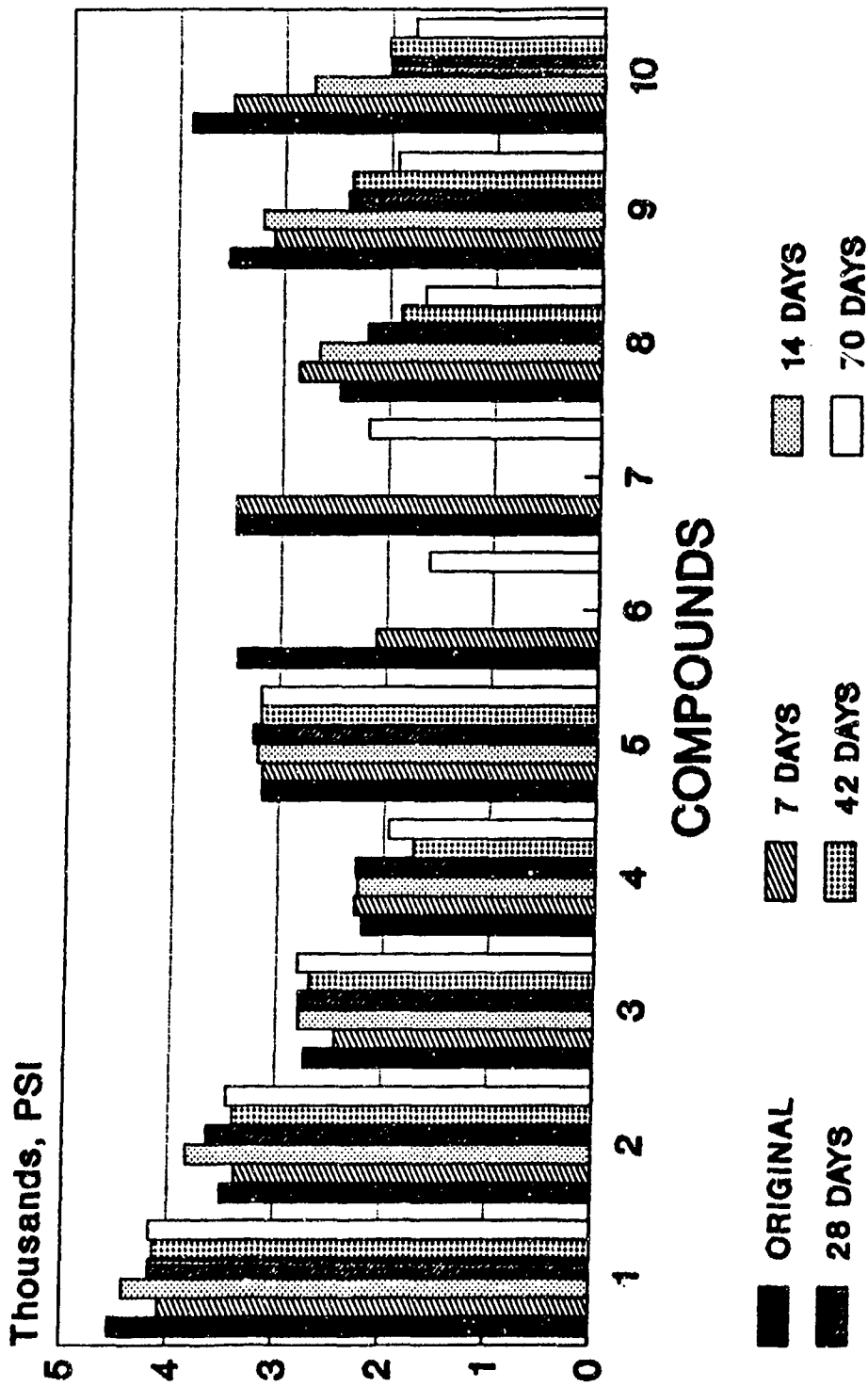
1.	PE 100A027, ILC DOVER Inc.	[LP-37]
----	----------------------------	---------

TEST METHODS TO DETERMINE COMPATIBILITY OF ELASTOMERS WITH LIQUID PROPELLANT

- TENSILE STRENGTH, ASTM D-412
- 200% MODULUS, ASTM D-412
- ULTIMATE ELONGATION, ASTM D-412
- VOLUME SWELL, ASTM D-471
- SPECIFIC GRAVITY
- HARDNESS, ASTM D-2240

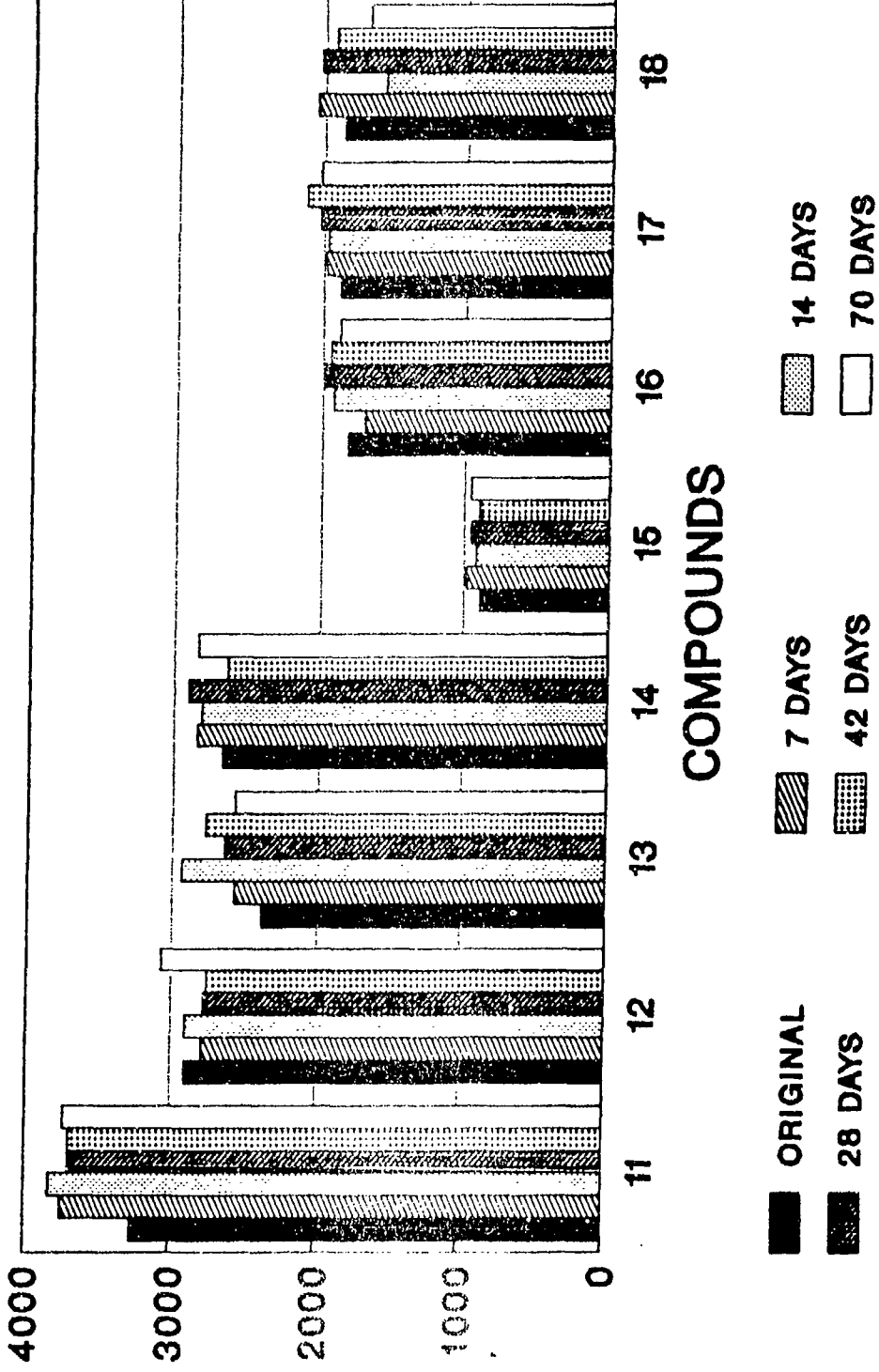
BRDEC/MFLL

NITRILE RUBBERS, {NBR, XNBR, HSN} TENSILE STRENGTH AFTER IMMERSION IN LP



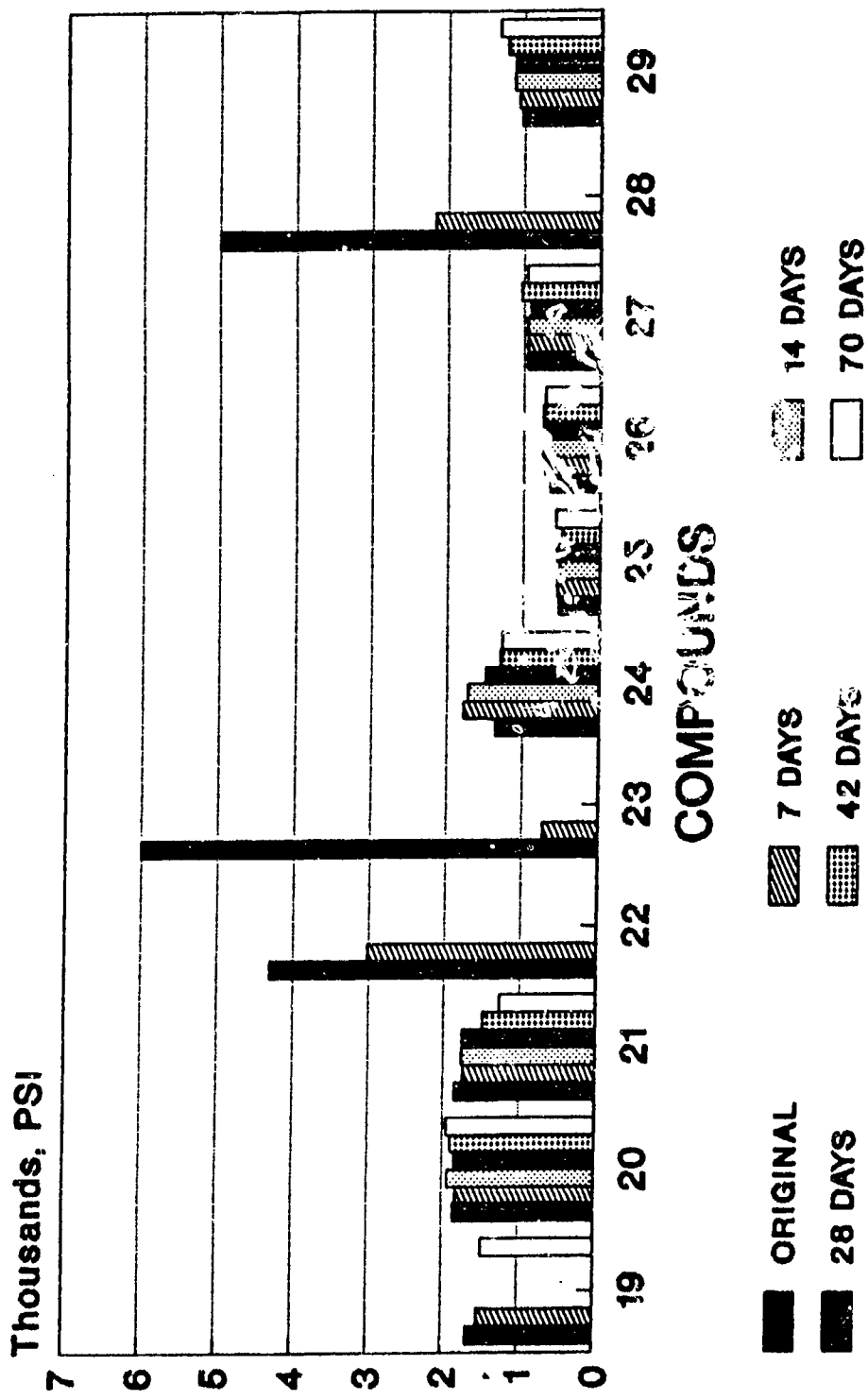
BRDEC/MFLL

FLUOROELASTOMERS, POLYCHLOROPRENES AND ETHYLENE-PROPYLENE RUBBER IN LP



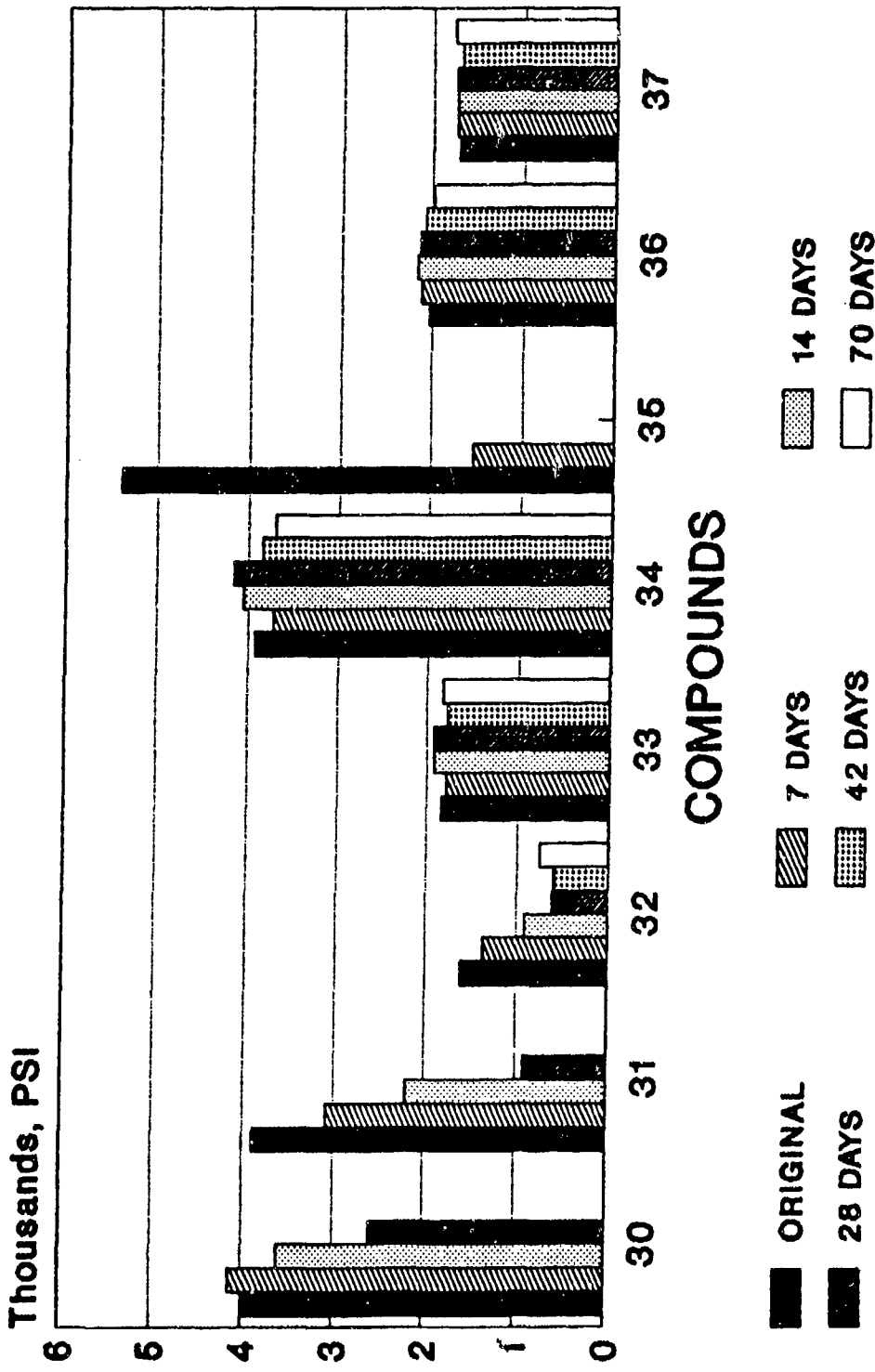
BRDEC/MFLL

THERMOPLASTIC ELASTOMERS IN LP TENSILE STRENGTH



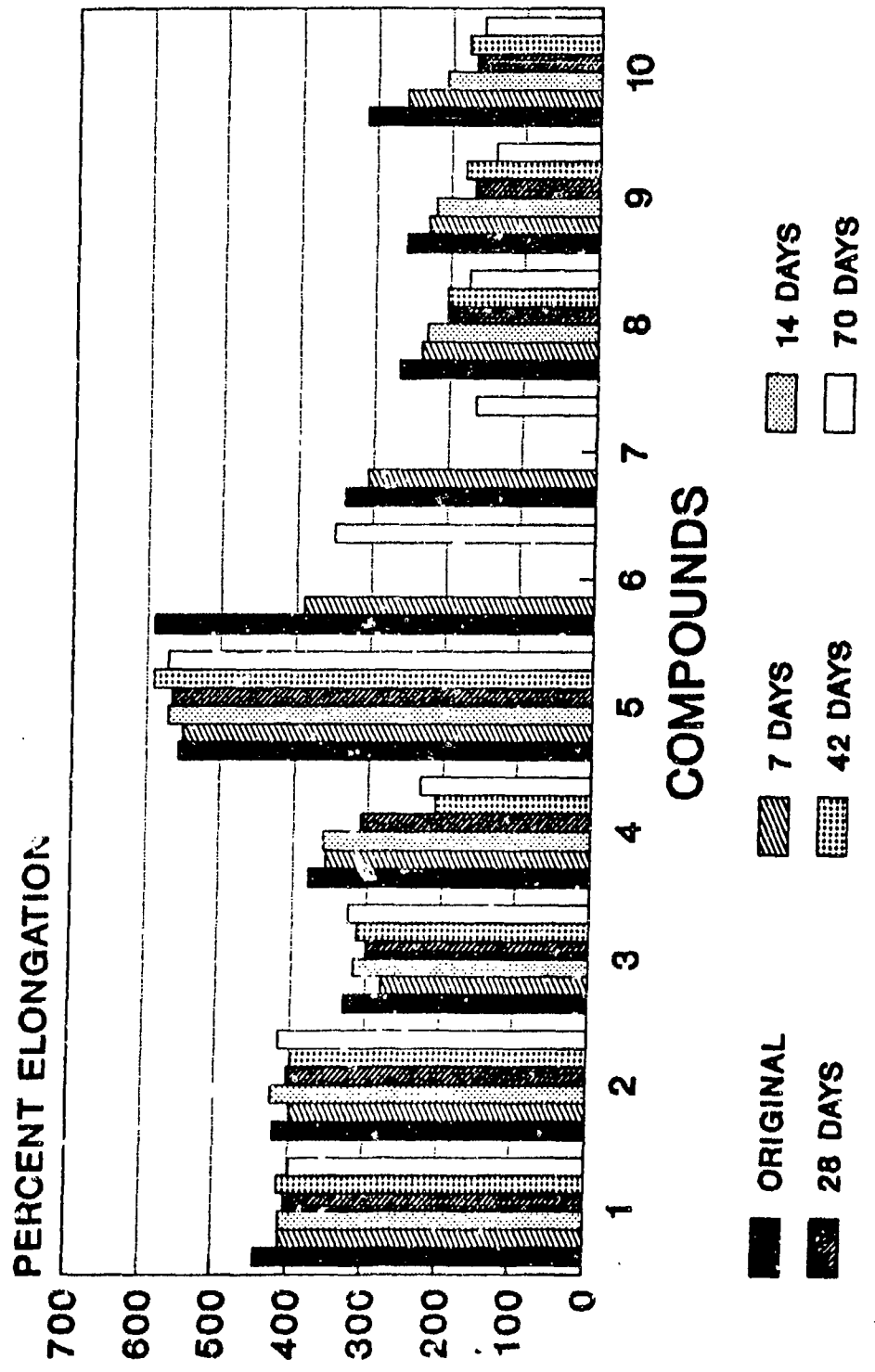
BRDEC/MFLL

POLYURETHANES, & OTHER SYNTHETIC RUBBERS IN LP. TENSILE STRENGTH



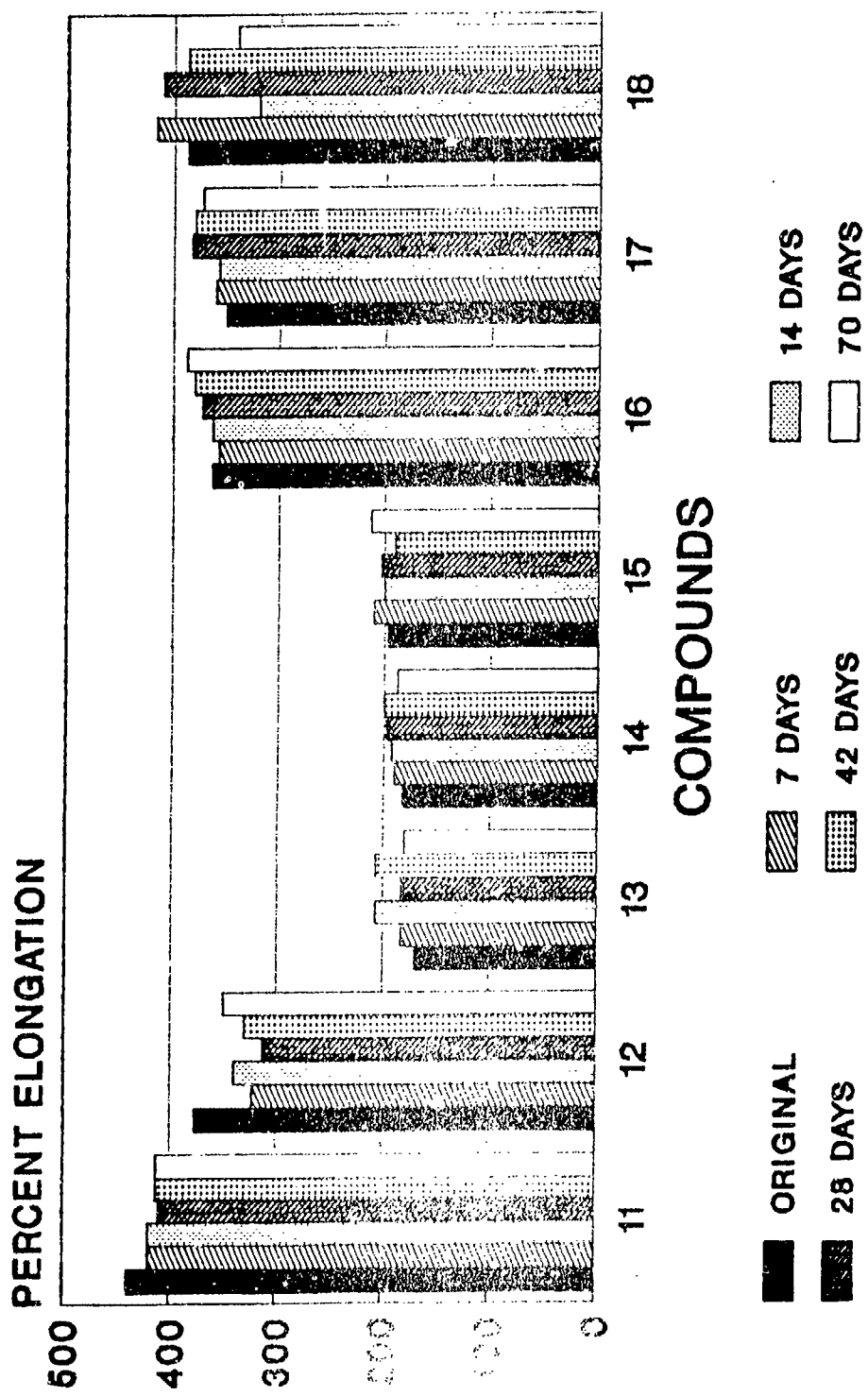
BRDEC/MFLL

ULTIMATE ELONGATION FOR MATERIALS IMMERSED IN LIQUID PROPELLANT 1846



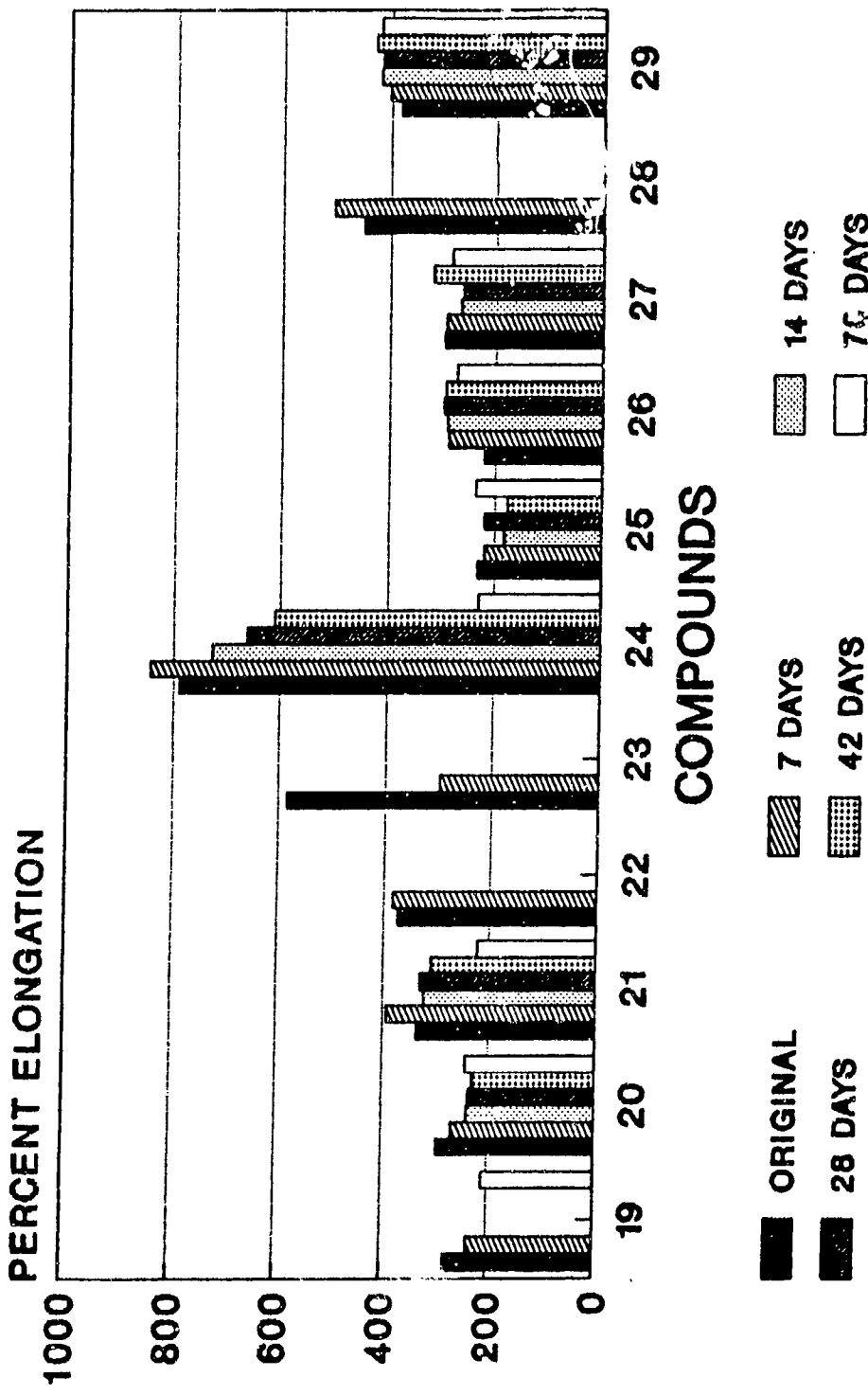
BRDEC/MFIL

ULTIMATE ELONGATION FOR MATERIALS IMMERSED IN LIQUID PROPELLANT 1846



BRDEC/MFLL

ULTIMATE ELONGATION FOR MATERIALS IMMERSED IN LIQUID PROPELLANT 1846



BRDEC/MFLL

ULTIMATE ELONGATION FOR MATERIALS IMMERSED IN LIQUID PROPELLANT 1846

PERCENT ELONGATION

800

600

400

200

0

30 31 32 33 34 35 36 37

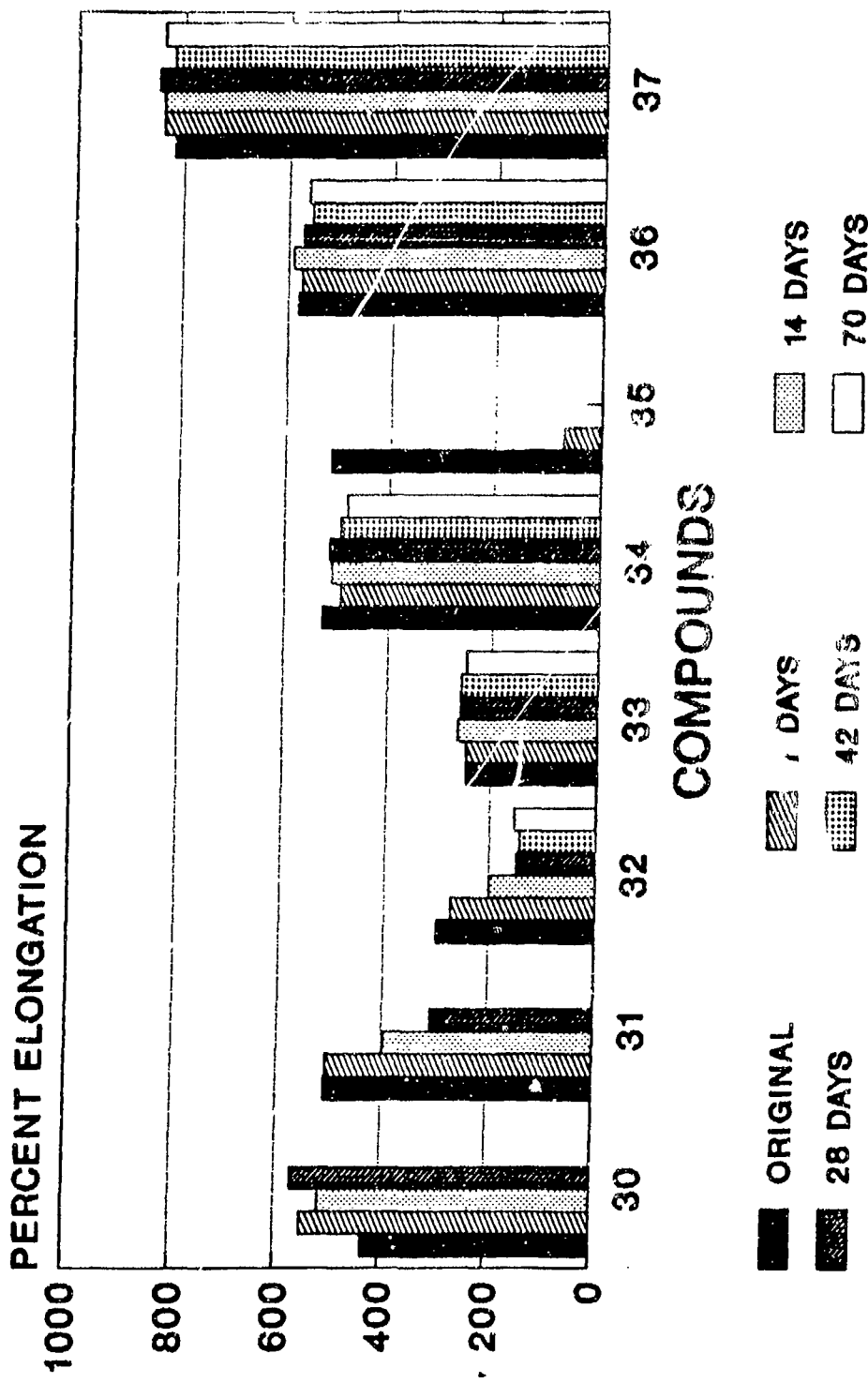
COMPOUNDS

- ORIGINAL
- 7 DAYS
- 14 DAYS
- 28 DAYS
- 42 DAYS
- 70 DAYS

BRDEC/MFLL

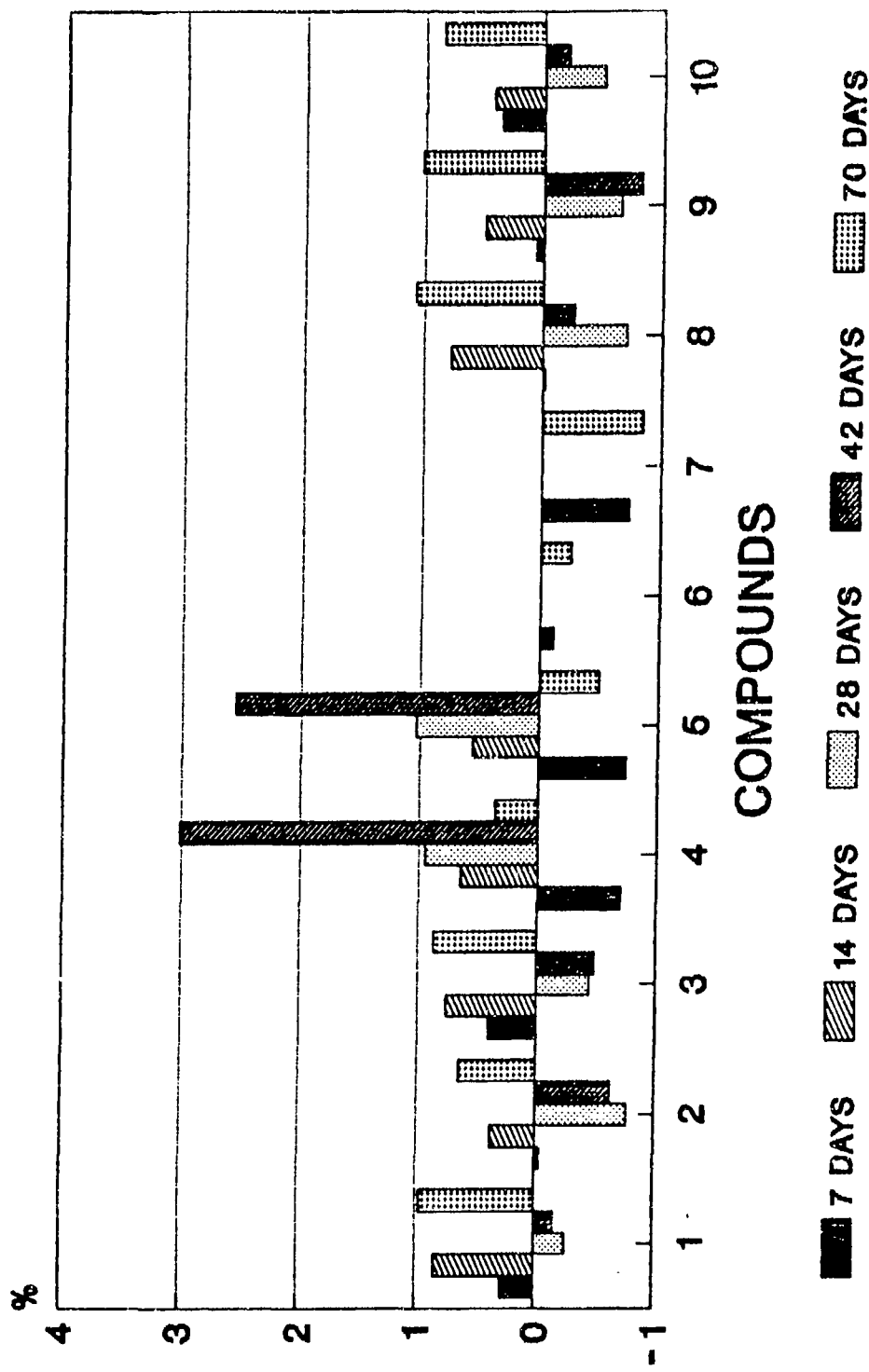
Reproduced From
Best Available Copy

ULTIMATE ELONGATION FOR MATERIALS IMMERSED IN LIQUID PROPELLANT 1846



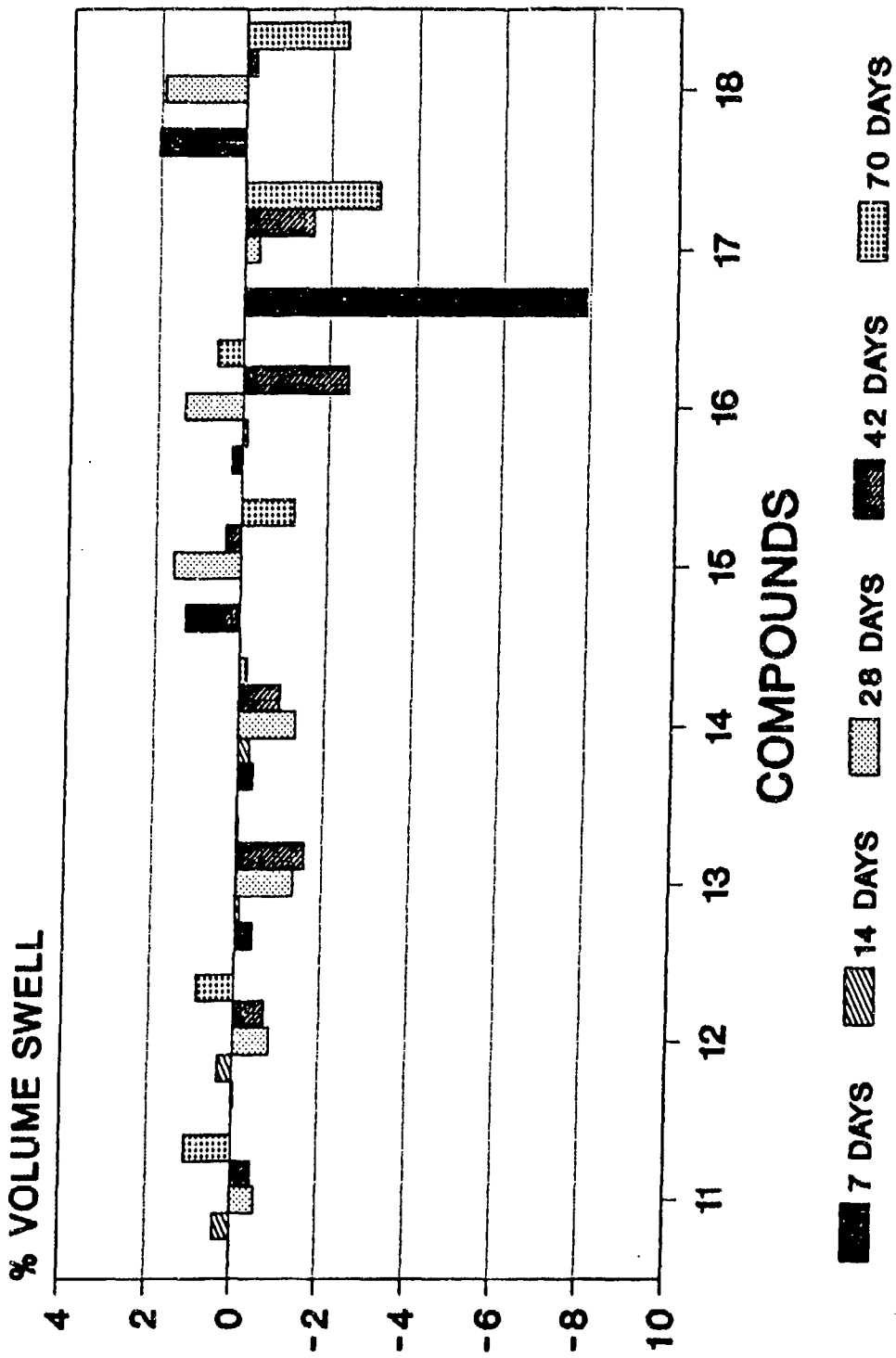
BRDEC/MFLL

NITRILE RUBBERS, {NBR, XNBR, HSN} VOLUME SWELL AFTER IMMERSION IN LP



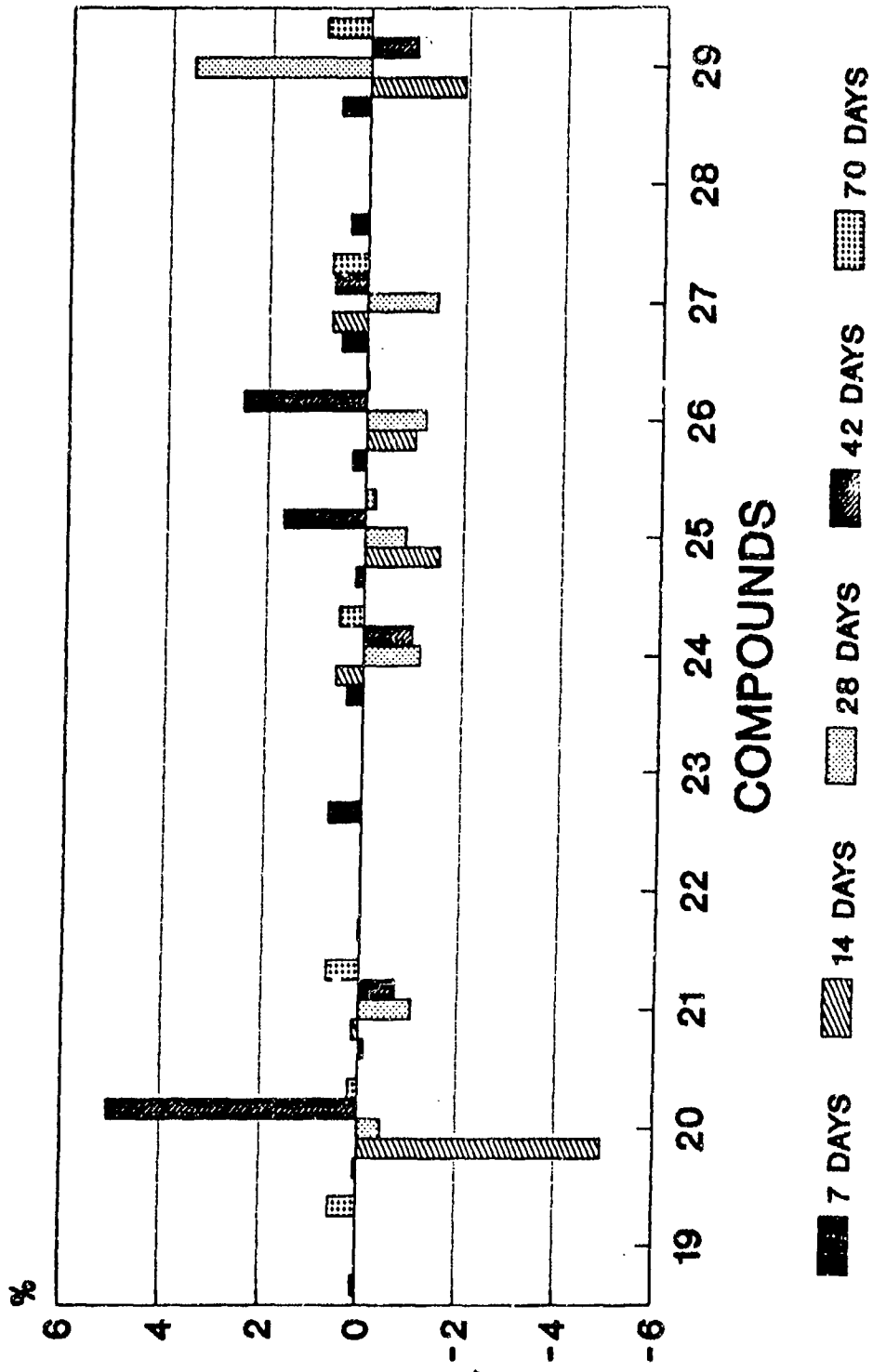
BRDEC/MFLL

FLUOROELASTOMERS, POLYCHLOROPRENES AND ETHYLENE-PROPYLENE RUBBER IN LP



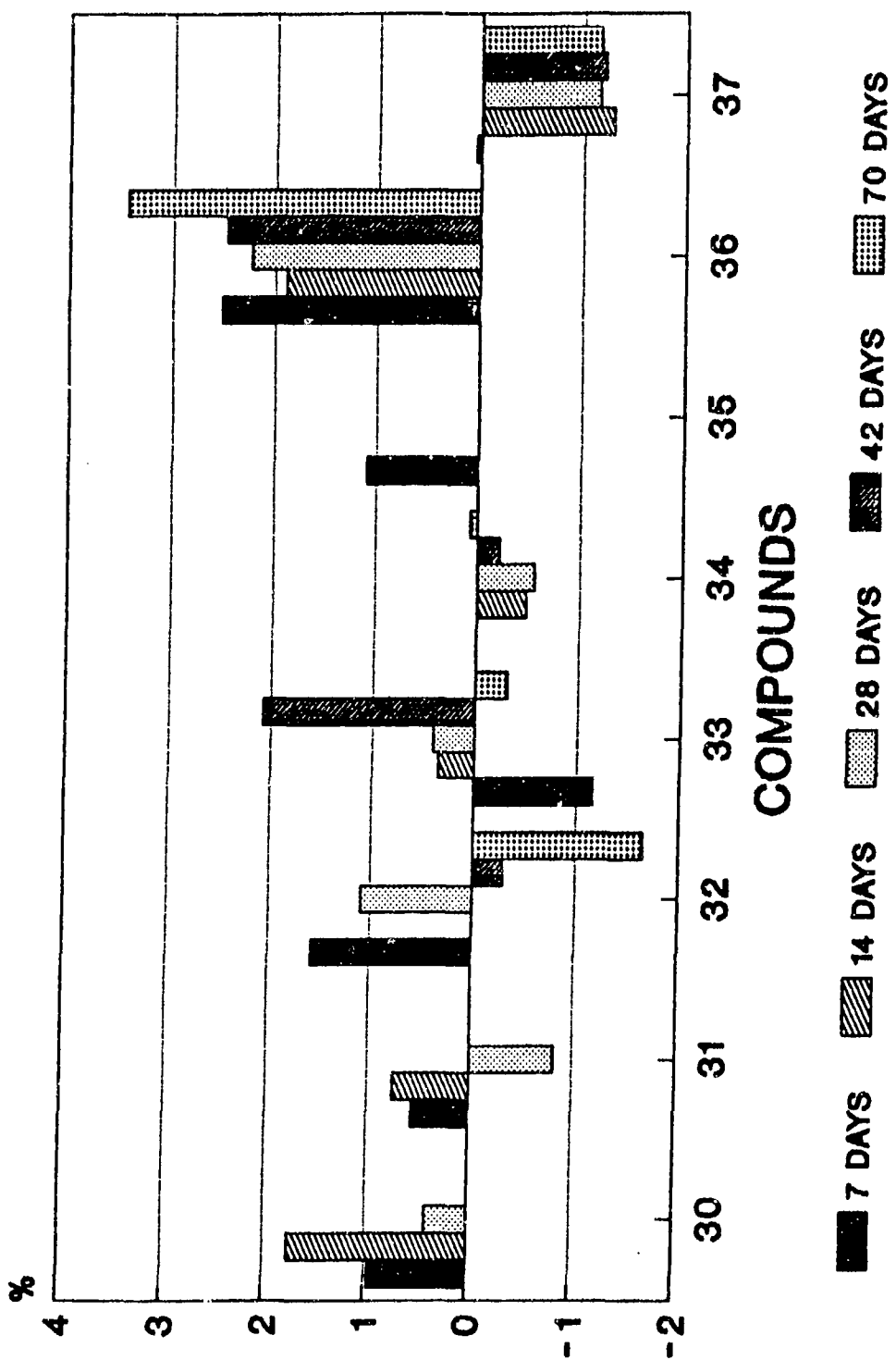
BRDEC/MFLL

THERMOPLASTIC ELASTOMERS IN LP VOLUME SWELL



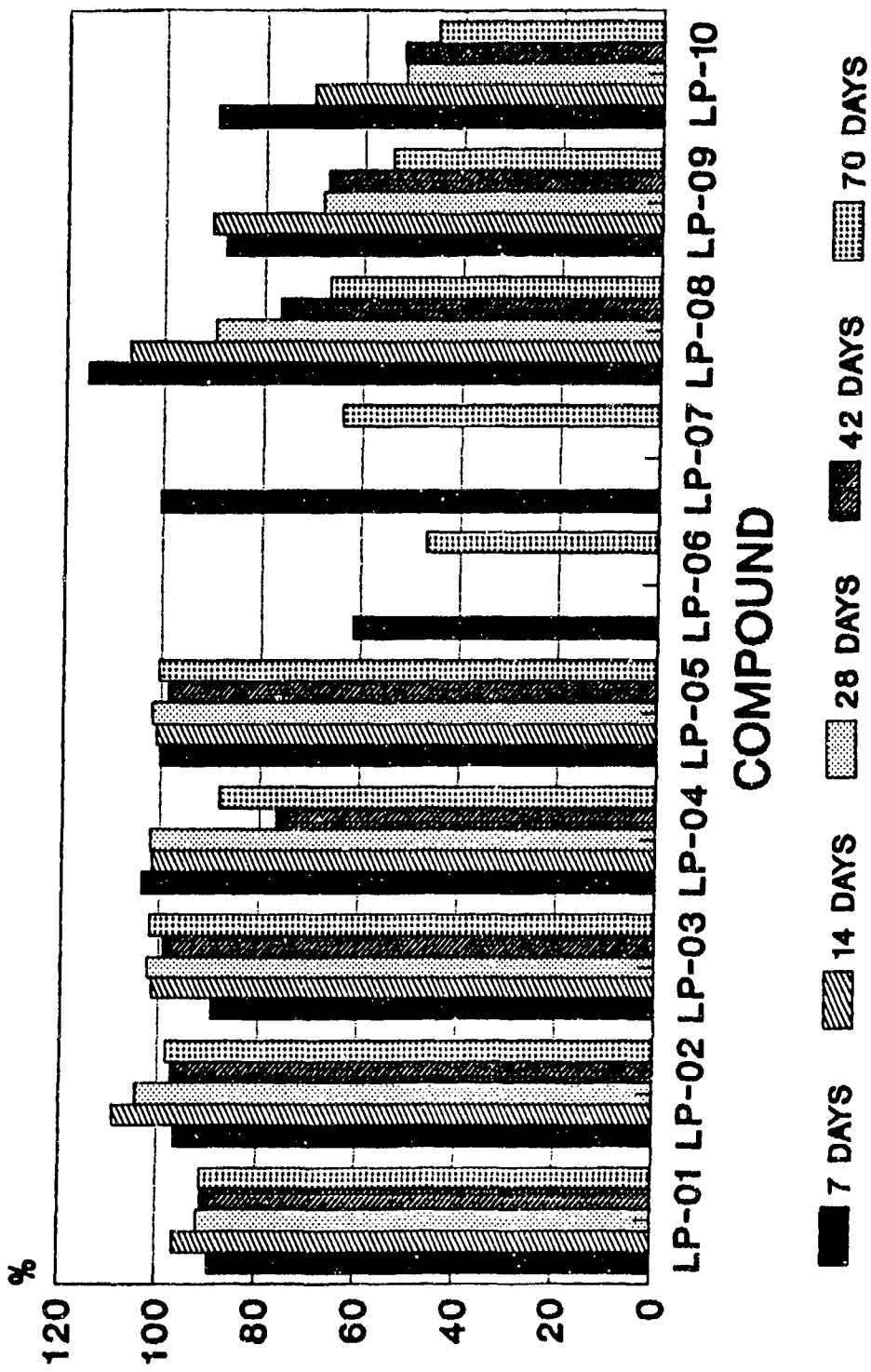
BRDEC/MFLL

POLYURETHANES, & OTHER SYNTHETIC RUBBERS
IN LP. VOLUME SWELL



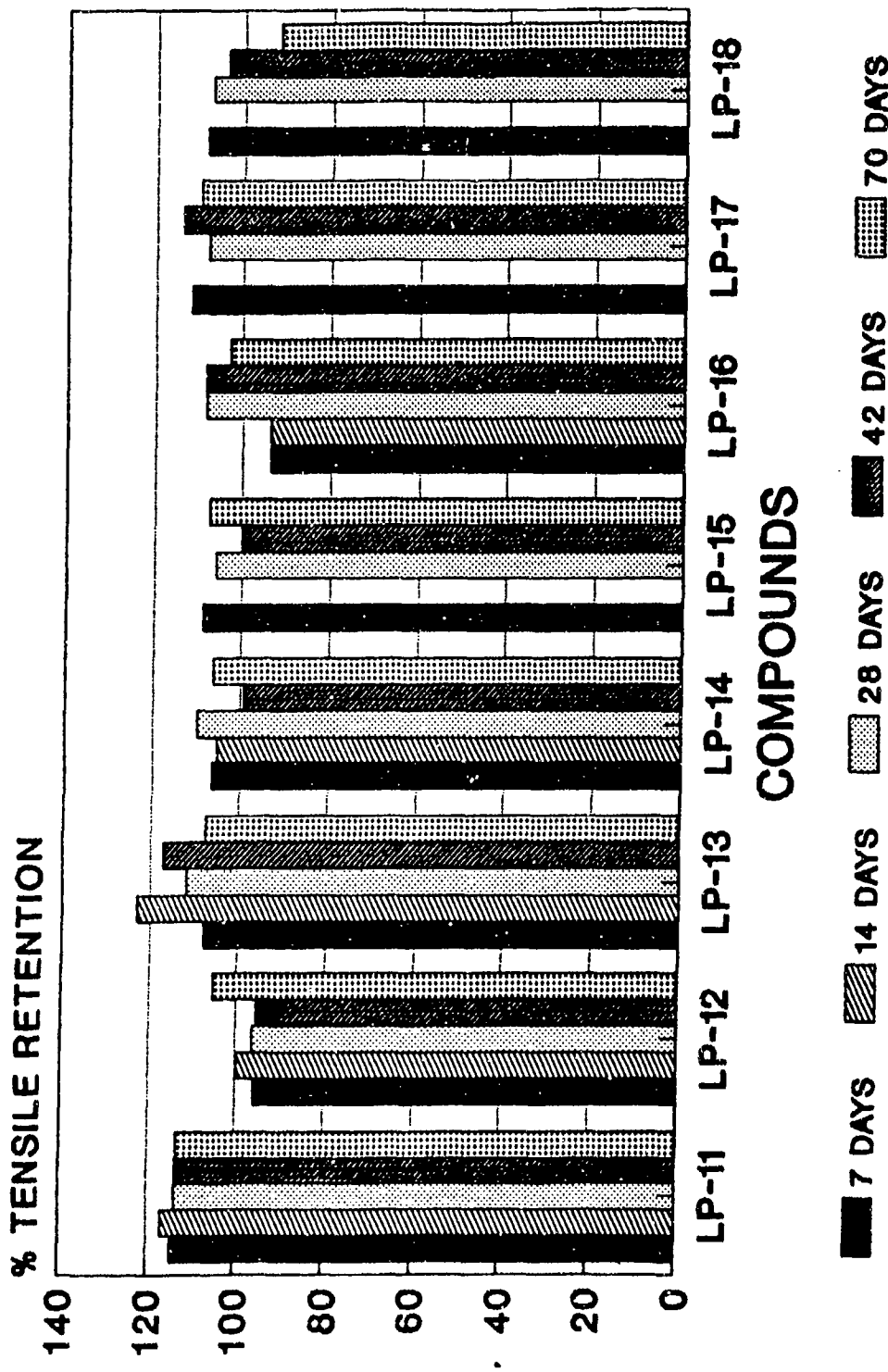
BRDEC/MFLL

NITRILE RUBBERS, {NBR, XNBR, HSN}
TENSILE RETENTION AFTER IMMERSION IN LP



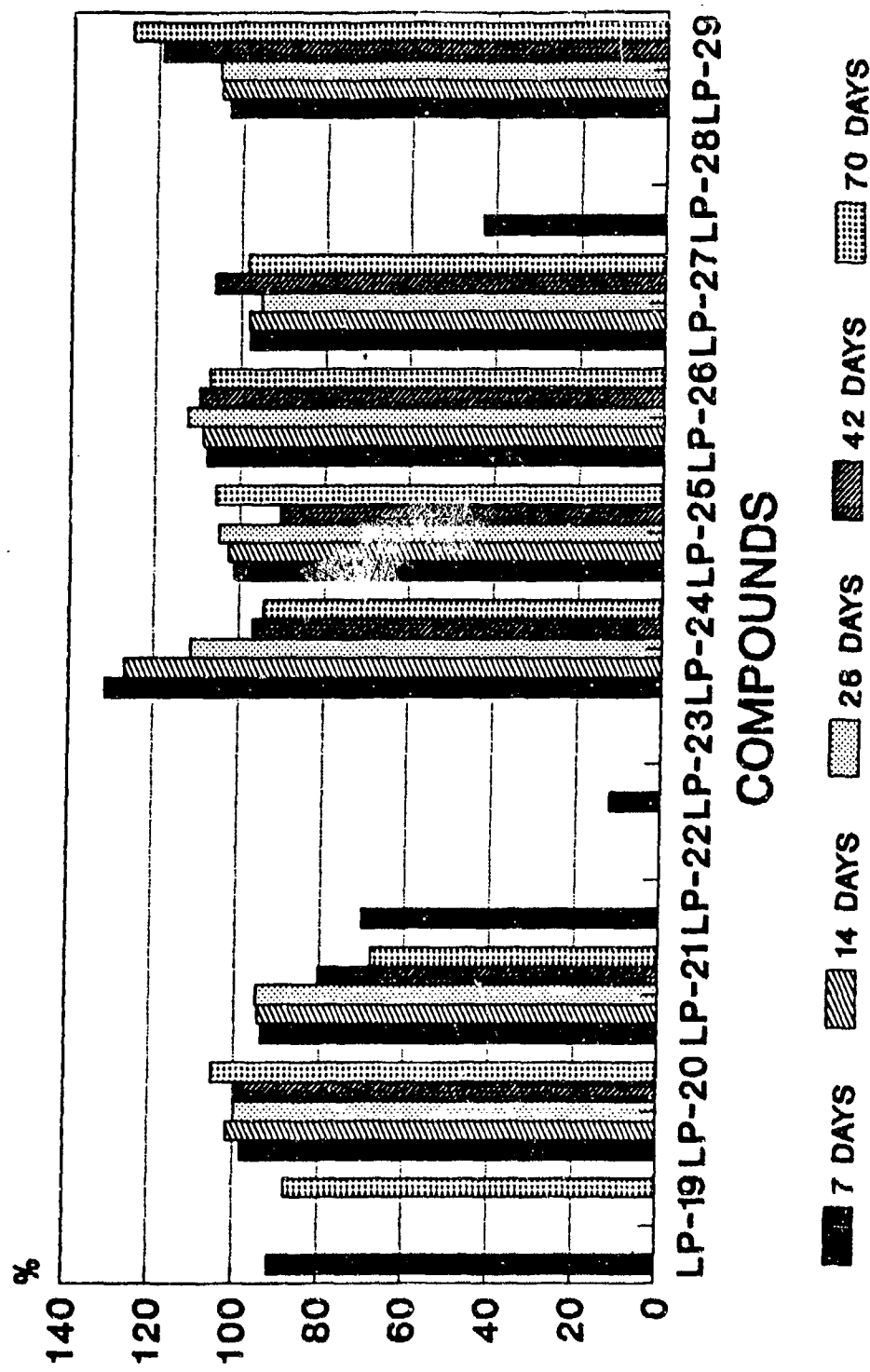
BRDEC/MFLL

FLUOROELASTOMERS, POLYCHLOROPRENES AND ETHYLENE-PROPYLENE RUBBER IN LP



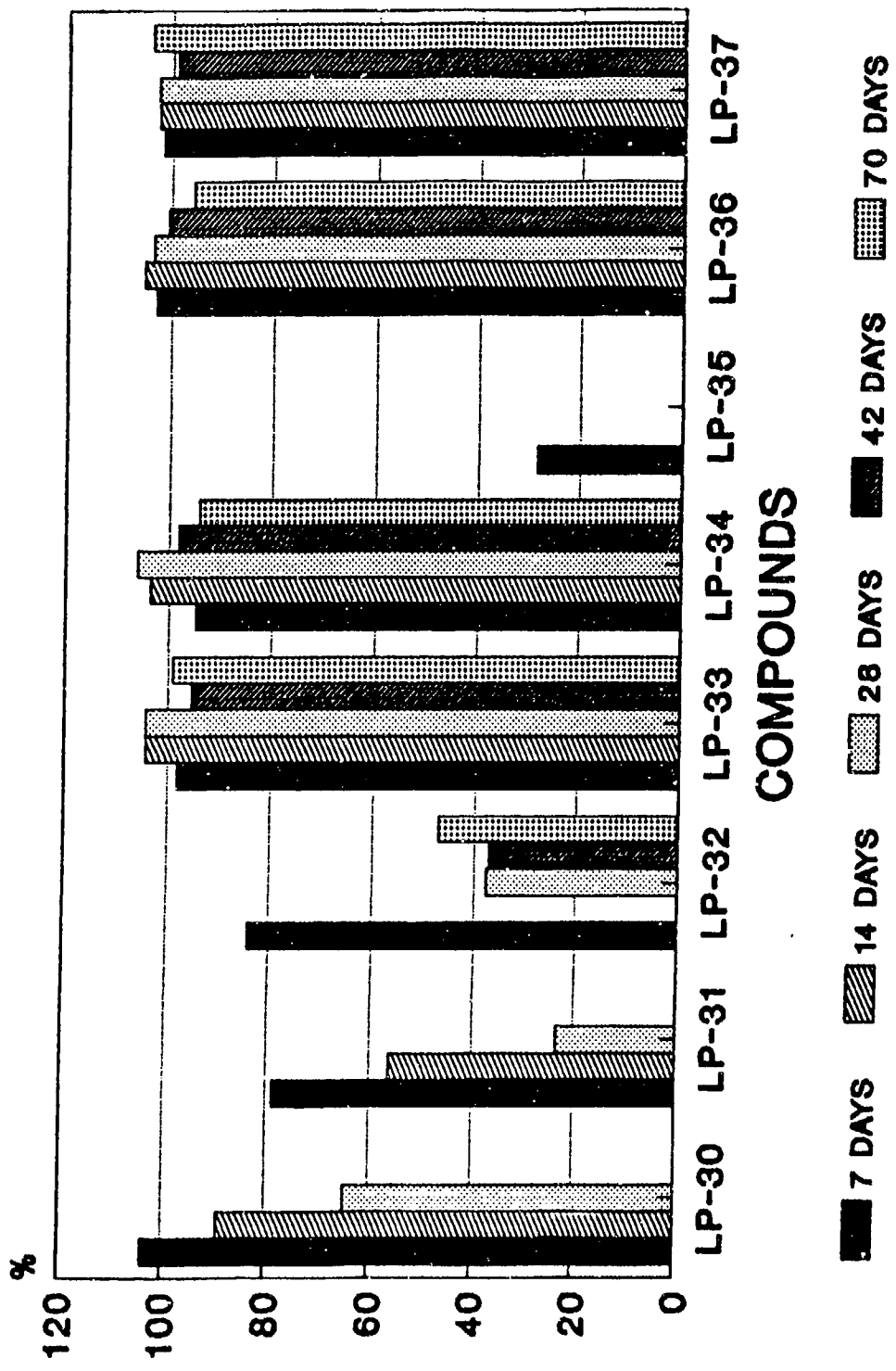
BRDEC/MFLL

THERMOPLASTIC ELASTOMERS IN LP TENSILE RETENTION



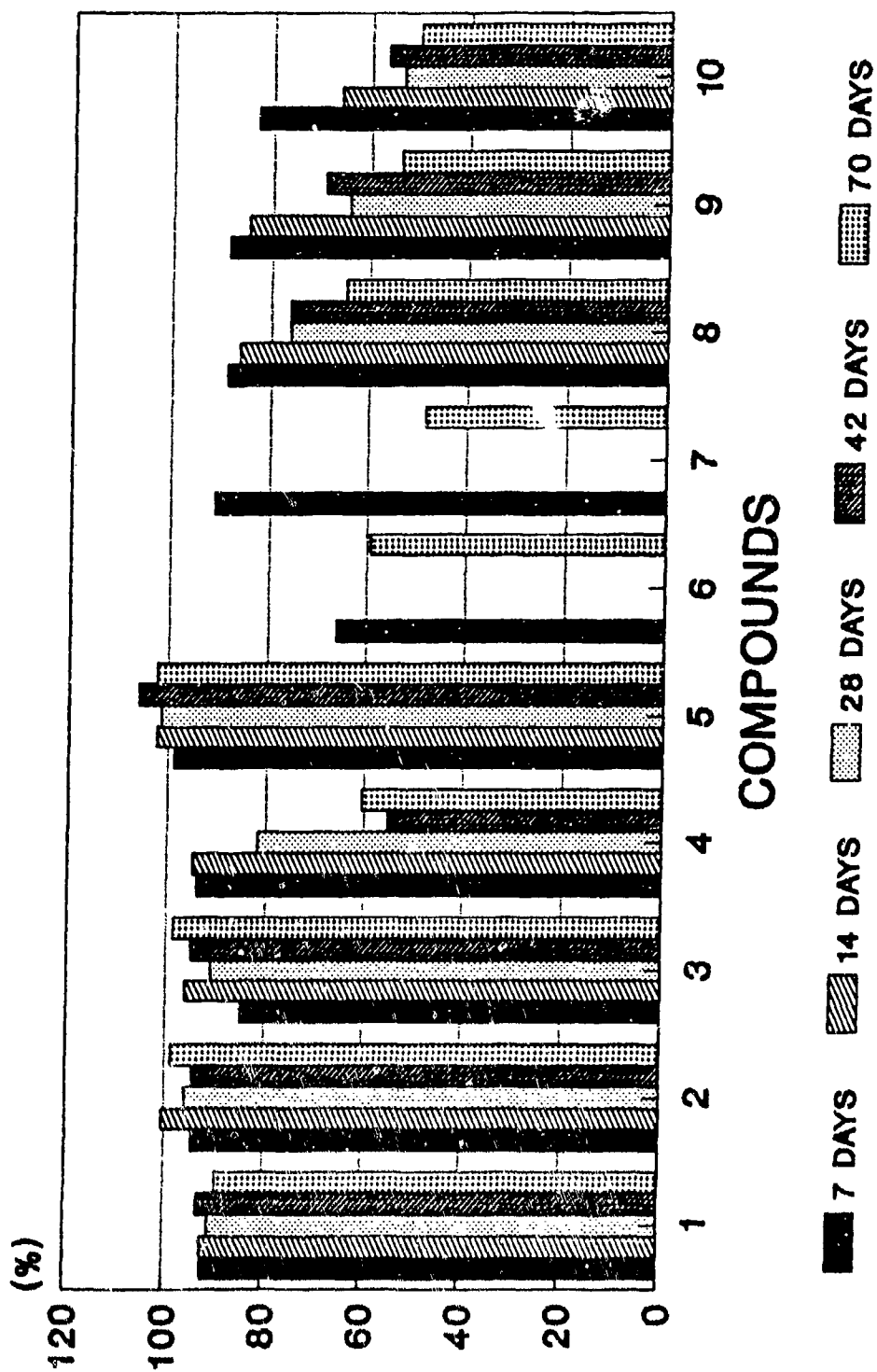
BRDEC/MFL

POLYURETHANES, & OTHER SYNTHETIC RUBBERS
IN LP. TENSILE RETENTION



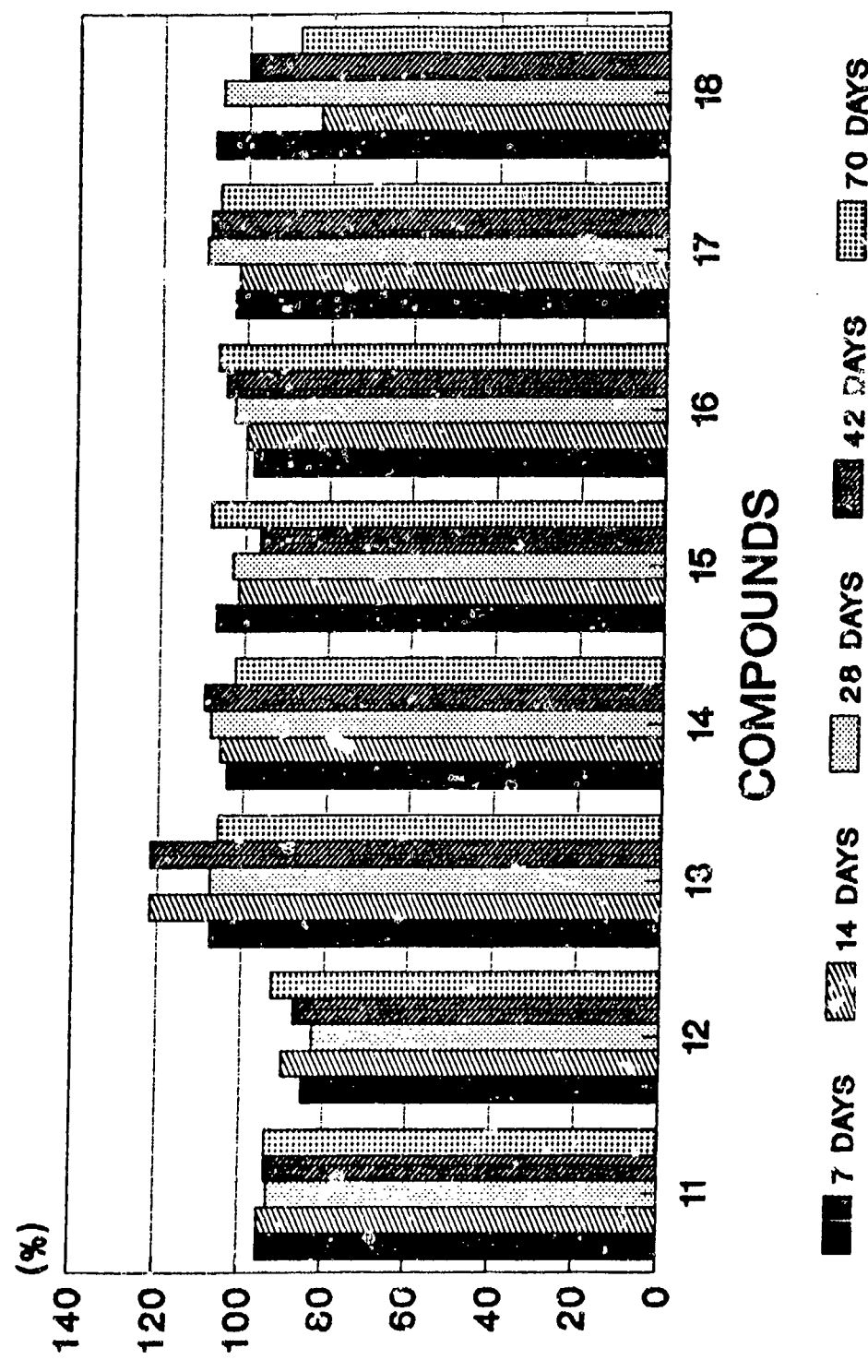
BRDEC/MFLL

ELONGATION RETENTION FOR MATERIALS IMMERSED IN LIQUID PROPELLANT 1846



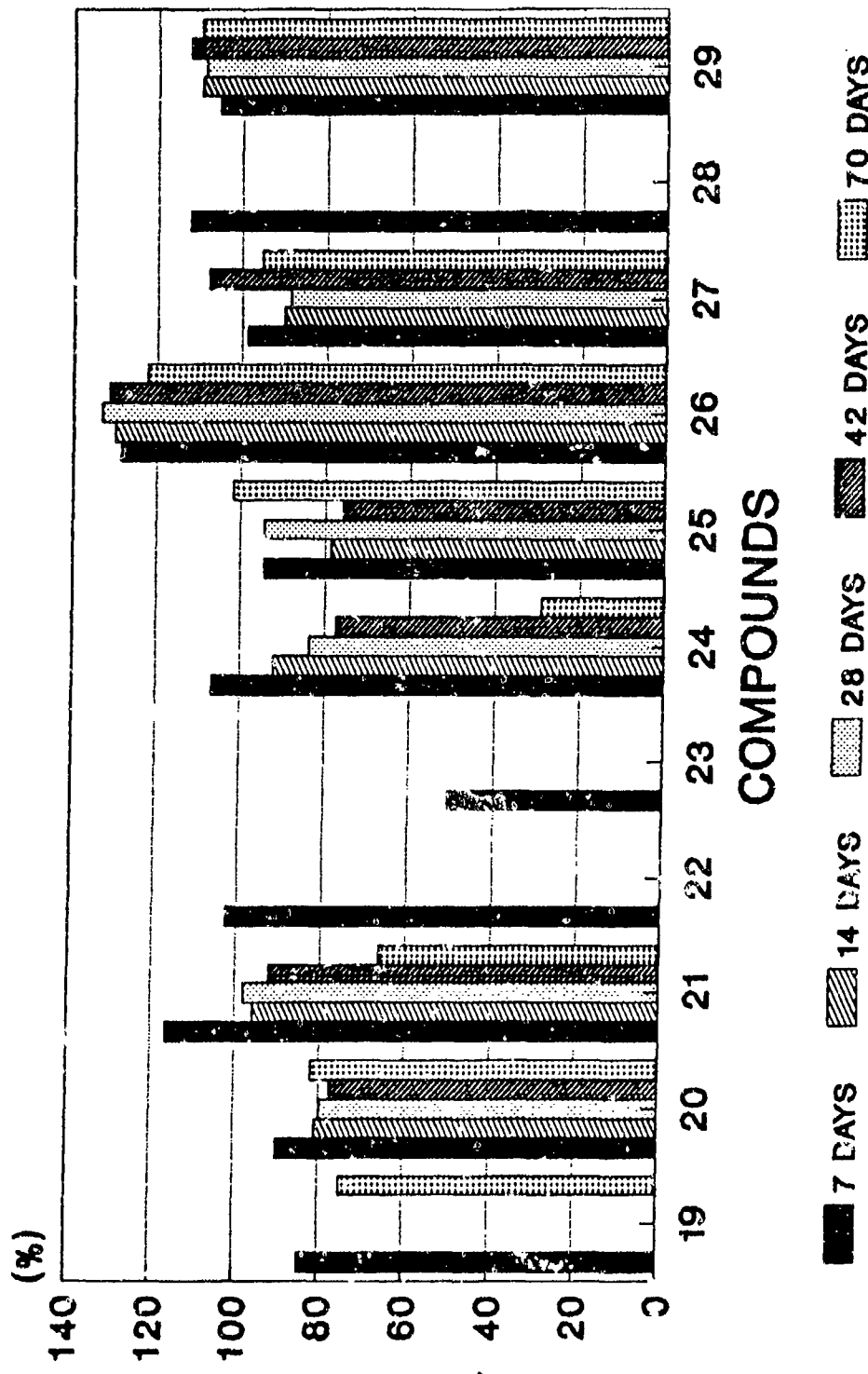
BRDEC/MFLL

ELONGATION RETENTION FOR MATERIALS IMMERSED IN LIQUID PROPELLANT 1846



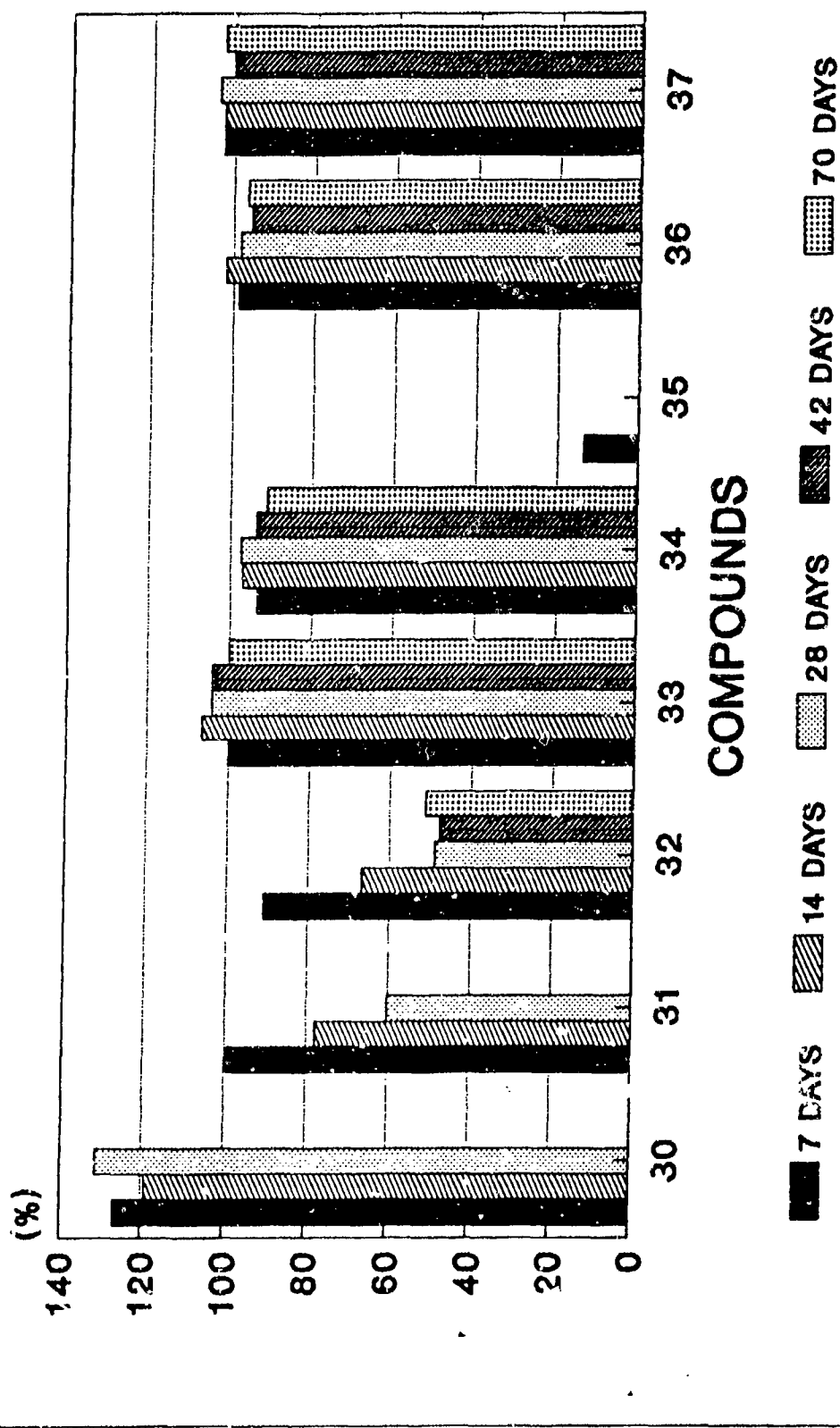
BRDEC/MFLL

ELONGATION RETENTION FOR MATERIALS IMMERSED IN LIQUID PROPELLANT 1846



BRDEC/MFLL

ELONGATION RETENTION FOR MATERIALS IMMERSED IN LIQUID PROPELLANT 1846



BRDEC/MFLL

PROJECT ACCOMPLISHMENTS

- LITERATURE SEARCH ON CHEMICAL RESISTANCE OF ELASTOMERS.
- CONTACTS WITH HOSE AND COLLAPSIBLE TANK INDUSTRY.
- IN-HOUSE MIXING AND MOLDING OF RUBBER COMPOUNDS.
- PROCUREMENT OF ADDITIONAL ELASTOMERS.
- DESIGN OF TEST JIG FOR COATED FABRICS.
- IMMERSION OF SAMPLES IN LP-1846.
- DETERIORATION ASSESSMENT FOR ELASTOMERS.

BRDEC/MFLL

The Influence of Metal Ions on the Stability
of Liquid Gun Propellants Containing HAN

Dr. R. Hansen

FRAUNHOFER-INSTITUT FUR
CHEMISCHE TECHNOLOGIE
(FR GERMANY)

ABSTRACT

In HAN-based liquid gun propellants (LP 1846), HAN (hydroxylammonium nitrate) is the chemically sensitive component. Traces of metal ions are capable of accelerating its decomposition rate. To assess the stability and storage life of the propellant and the effects of metallic impurities, the buildup of pressure was studied in relevant propellant samples.

The experiments to determine the lifetime of LP 1846 were carried out in sealed containers at a temperature of 90 °C (194 °F). The metal ions were added to the propellant at different concentrations. As a relative measure for assessing efficacy in each case, we used either the time up to the bursting of the containers or observation of the pressure through time, with a subsequent component analysis.

Table 1: The influence of 100 ppm metal ions on the storage life
of LP 1846 in ampoules at 90 °C (194 °F)

LP 1846 (Lot 49 - 1)		
Metal ions	Decomposition time in days	Relative decomposition time in %
Fe ³⁺	3,5	3,9
Ni ²⁺	80,7	88,9
Co ²⁺	73,0	80,4
Cu ²⁺	15,2	16,7
Hg ²⁺	64,1	70,6
W ⁶⁺	94,2	103,7
Mo ⁶⁺	62,6	68,9
Mn ²⁺	88,0	96,9
Al ³⁺	78,5	86,5
Ce ³⁺	82,6	91,0
Pb ²⁺	87,0	95,8
Ag ⁺	83,4	91,9
Mg ²⁺	87,3	96,1
Cr ³⁺	90,7	99,9
Fe ²⁺	3,5	3,9
Ti ⁴⁺	59,6	65,6
V ⁵⁺	11,9	13,1
Zn ²⁺	81,8	90,1
Cd ²⁺	78,1	86,0
B ³⁺	77,3	85,1
Pd ²⁺	31,4	34,6
Zr ⁴⁺	92,2	101,5
Sn ²⁺	83,6	92,1
Bi ³⁺	49,3	54,3

Table 2: Comparison of the relative decomposition times of LP 1846. Accelerated storage tests in glass ampoules at 90 °C. Metal ion concentrations in 2, 5, 10, 100 ppm

Metal ions	Relative decomposition time in %			
	2	5	10	100
W ⁺	115	120	103	104
Zr ⁺	-	98	100	102
Cr ⁺	-	-	92	100
Mn ²⁺	106	102	101	97
Mg ²⁺	-	98	95	96
Pb ²⁺	92	88	87	96
Sn ²⁺	103	98	100	92
Ag ⁺	101	99	93	92
Ce ⁺	103	98	80	91
Zn ²⁺	99	100	84	90
Ni ²⁺	105	97	(75)	89
Al ³⁺	101	88	80	87
Cd ²⁺	96	94	80	86
B ³⁺	102	97	96	85
Co ²⁺	100	99	(71)	80
Hg ²⁺	98	100	102	79
Mo ⁶⁺	-	-	98	69
Ti ⁴⁺	109	95	(69)	66
Bi ³⁺	93	100	93	54
Pd ²⁺	-	65	51	35
Cu ²⁺	73	59	48	17
V ⁵⁺	71	59	40	13
Fe ³⁺	55	36	24	4
Fe ²⁺	57	31	20	4

Table 3: The influence of iron and copper compounds on the storage life of LP 1846 in ampoules at 90 °C

Additive	Decomposition time in days
-	86,6
10 ppm Fe-ions	17,4
Ferrocene (10 ppm Fe ²⁺)	22,0
10 ppm Cu-ions	41,6
Copperphthalocyanine (10 ppm Cu ²⁺)	84,5

Table 4: Selection of complexing agents

Trade Name	Structural Formula	Chemical Name	Supplier
Turpinol SL	$\begin{array}{c} \text{HO} & \text{CH}_2 & \text{OH} \\ & & \\ \text{HO} - & \text{P} - & \text{C} - & \text{P} - & \text{OH} \\ & & & \\ \text{O} & \text{OH} & \text{O} & \text{OH} \end{array}$	1-Hydroxy-ethylidene-1,1-diphosphonic acid	Henkel KG Postfach 11 00 2000 Düsseldorf
Turpinol D 2	$\text{N} \left(\text{CH}_2 \text{P}(\text{OH})_2 \right)_3$	Amino-tris-(methylene phosphonic acid)	Henkel KG
Reonet		Benzotriazole	Ciba-Geigy CH-4002 Basel
-		N,N'-Disalicyloyl-hydrazone	Ciba-Geigy
Request 2000	Identical with Turpinol D 2	see above	Brenntag AG Postfach 10 03 52 4330 Mülheim-Ruhr 1
Request 2010	Identical with Turpinol SL	see above	Brenntag AG
Request 2041	$\left(\text{HO} \text{---} \text{P}(\text{CH}_2)_2 \text{---} \text{O} \right)_2$	Ethylenediamine-tetra-(methylene phosphonic acid)	Monsanto Europe N.V. Scheeldelaan B-2040 Antwerpen
Request 2060 S	$\text{HO} \text{---} \text{P}(\text{CH}_2 \text{CH}_2 \text{---} \text{N} \left[\text{---} \text{CH}_2 \text{CH}_2 \text{---} \text{N} \left(\text{---} \text{CH}_2 \text{---} \text{P}(\text{OH})_2 \text{---} \text{O} \right)_2 \right]_2$	Diethylenetriamine-penta-(methylene phosphonic acid)	Monsanto Europe N.V.

Table 5: The influence of stabilizers on the decomposition of LP 1846 containing 10 ppm iron ions. Decomposition times in days at 90 °C

stabilizer	iron : stab.	iron : stab.
	1 : 1 in moles	1 : 10 in moles
without stabilizer	17,4	17,4
Turpinal SL (Dequest 2010)	19,8	25,0
Turpinal D 2 (Dequest 2000)	34,2	42,5
Reomet	19,7	18,4
N,N'-Disalicyloyl-hydrazine	18,5	19,2
Dequest 2041	29,2	47,4
Dequest 2060 S	18,3	11,8
α,α'-Dipyridyl	-	19,2

Table 6: Analytical results of LP 1846 contaminated with metal ions after storage at 90 °C in a pressure-testing apparatus

Metal Ions (10 ppm)	storage time up to 4 bar (in days)	NH ₄ NO ₃ in g	HNO ₃ in g	HAN in g	TEAN in g
without metal ions	42,5	1,79	1,36	57,37	17,02
Fe ²⁺	8,2	2,41	2,07	55,23	18,76
Cu ²⁺	12,0	3,29	2,11	54,08	20,45
V ⁴⁺	7,3	1,71	1,60	56,58	18,60

Table 7: The influence of iron ions on the storage time of LP 1846.
 The propellant composition after storage tests at 90 °C.
 The final pressure was 4 bar

Iron concentration in ppm	storage time in days	NH ₄ NO ₃ in %	HNO ₃ in %	HAN in %	TAN in %
0	42.5	1.79	1.36	57.37	17.02
1	31.2	2.10	1.61	56.33	17.33
2	22.6	2.03	1.49	56.55	18.09
3	18.9	1.94	1.52	56.81	18.35
5	13.6	1.90	1.83	56.39	17.84
10	8.2	2.41	2.07	55.23	18.76

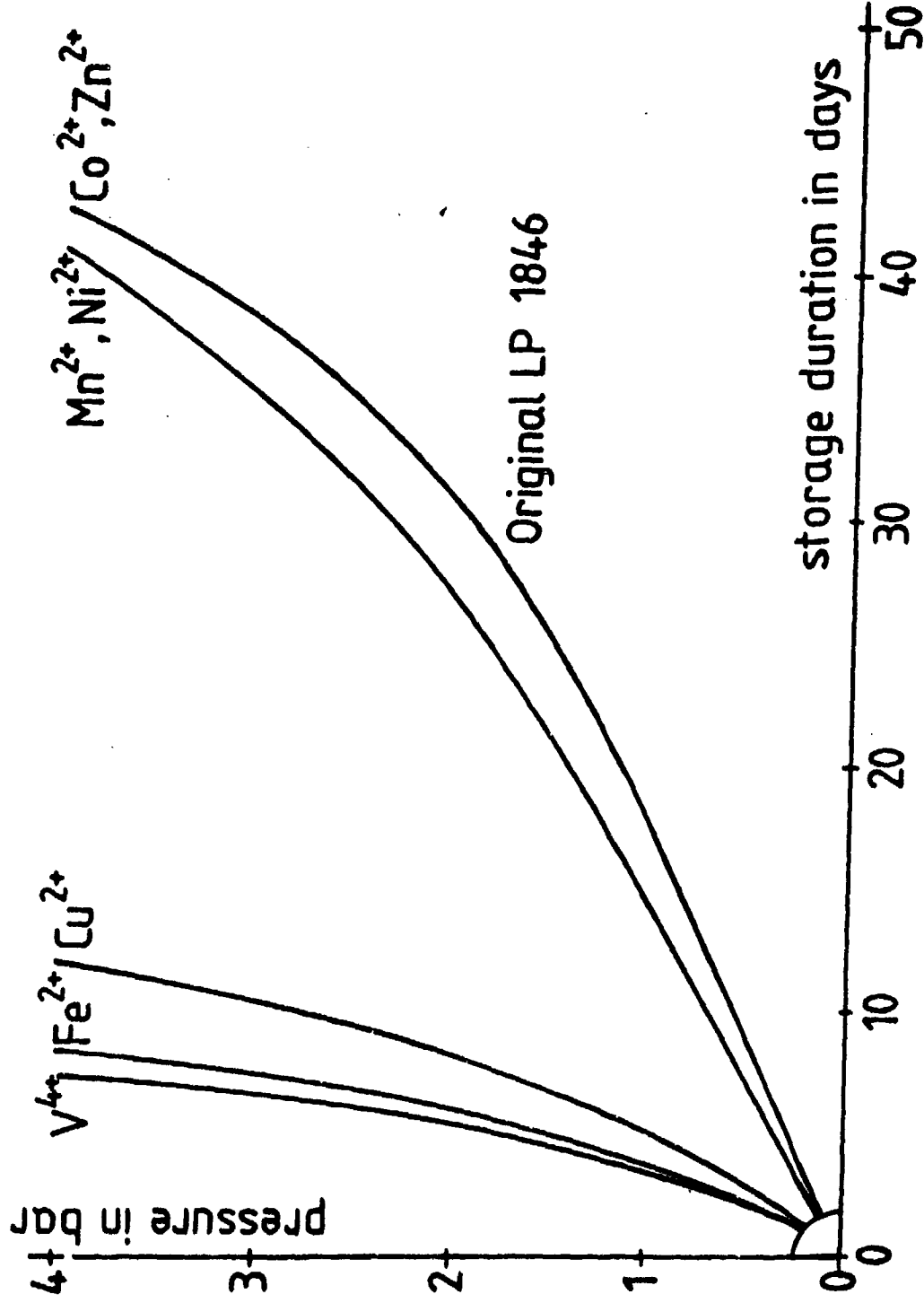


Fig. 1 : Pressure / time curves of contaminated LP 1846 at 90°C. Metal ion concentration 10 ppm.

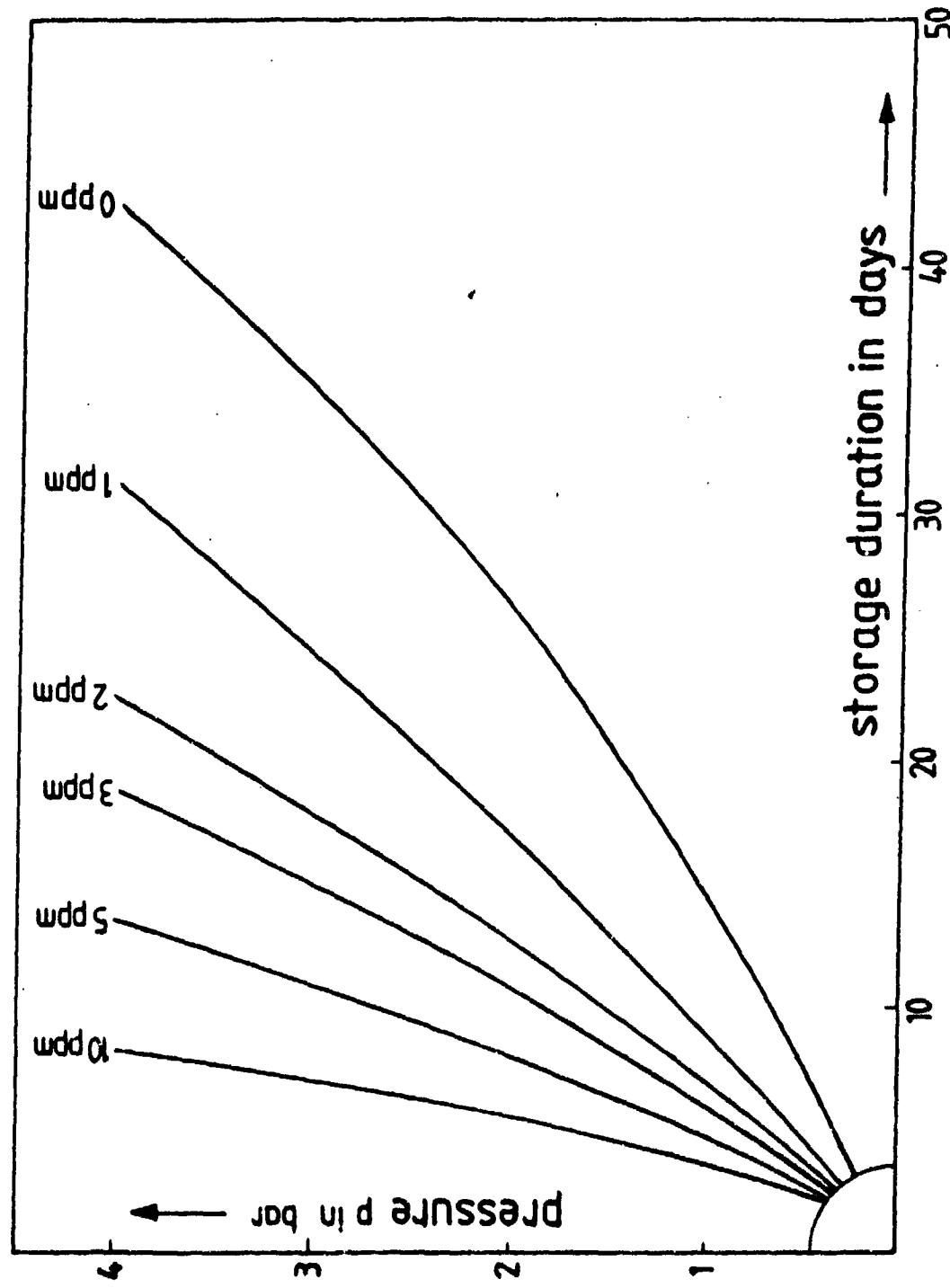


Fig. 2 : Pressure / time curves of LP 1046 at 90°C as depending on iron concentration.

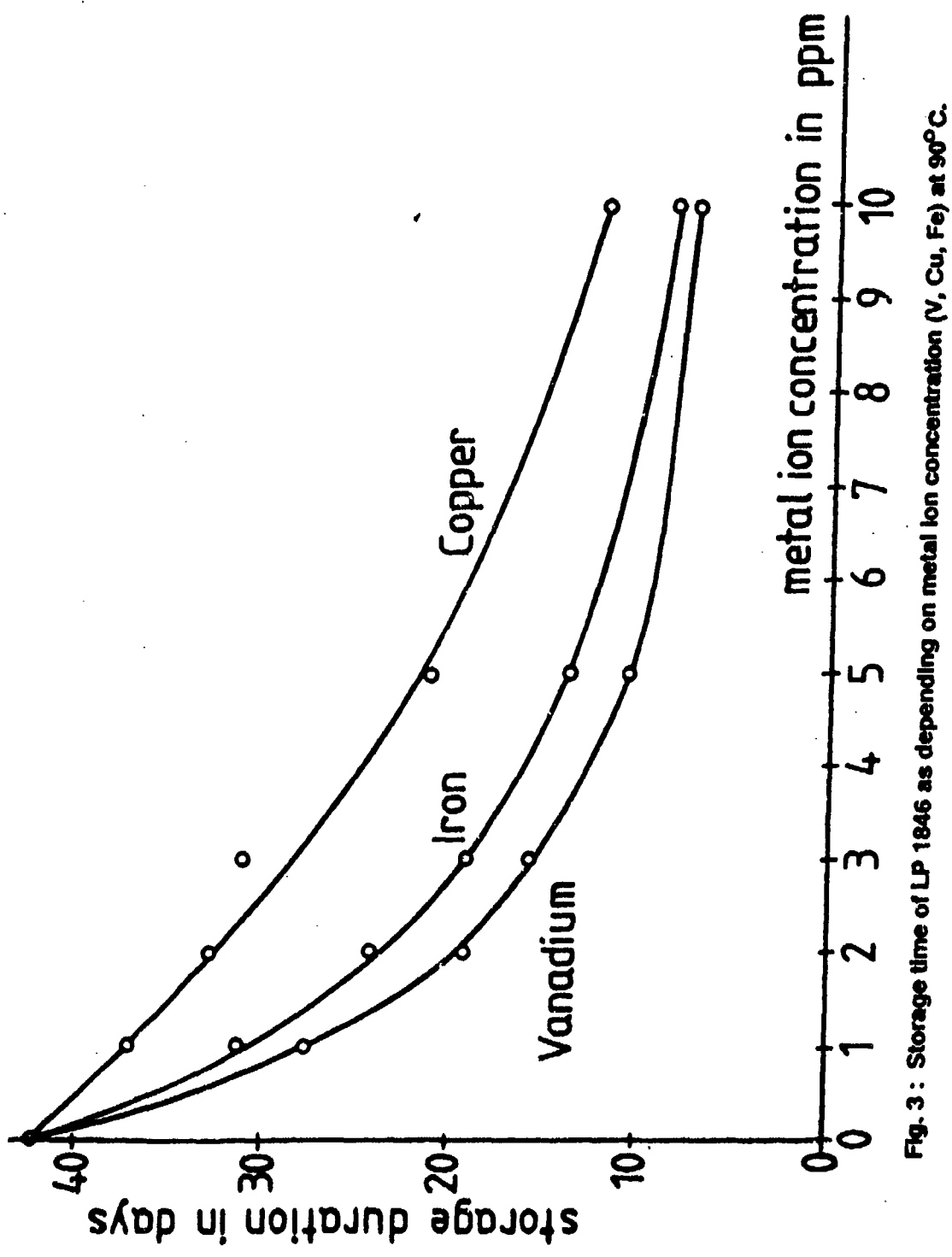


Fig. 3 : Storage time of LP 1846 as depending on metal ion concentration (V, Cu, Fe) at 90°C.

Selection Criteria for Metals and Plastics as
Construction Materials for Long Term Pressure-Testing
Apparatus on Liquid Propellants (LPs)

Dr. E. Backof

4th ANNUAL CONFERENCE ON HAN-BASED LIQUID PROPELLANT
STRUCTURE AND PROPERTIES
US ARMY BALLISTIC RESEARCH LABORATORY
ABERDEEN PROVING GROUND, MD
30 AUG - 1 SEP 88

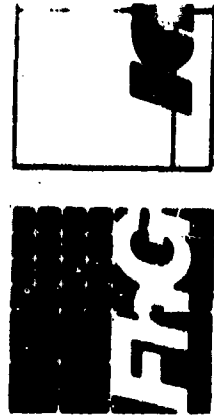
Abstract

The Paper describes the testing and selection of metallic and non-metallic materials for application in pressure-testing apparatus to determine the life term of HAN-based liquid propellants (LPs). Metallic materials are necessary for pressure sensors and non-metallic materials for sealing of the testing apparatus. Selection criteria for the metals are their corrosion-resisting quality and their capacity to influence or restrict the chemical stability of the LP. Selection criteria for the sealing materials are their impermeability to gases, deformation under strain and compatibility with the LP used. The testing apparatus is being used at the present time.

With effect from 1st July, 1988 we will carry the new name:

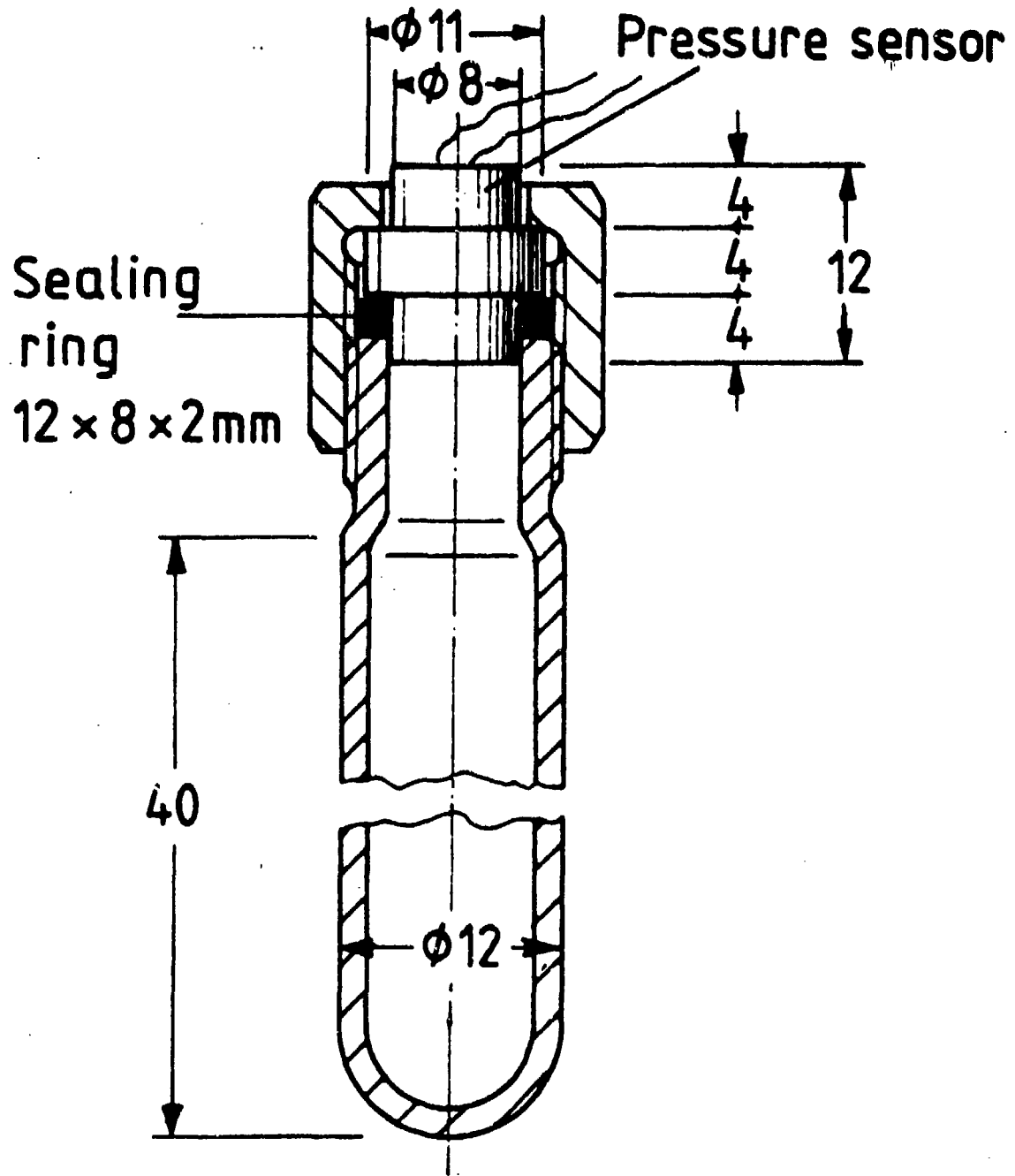
**FRAUNHOFER-INSTITUT FÜR
CHEMISCHE TECHNOLOGIE (ICT)**
Joseph-von-Fraunhofer-Straße
P.O. Box 12 40
D-7807 Pfinztal 1 (Berghausen)
Phone : (0721) 48 40 - 0
Telex : 7 828 800 lct d
Teletex: (0721) 48 40 - 111

FRAUNHOFER-INSTITUT
FÜR TREIB- UND EXPLOSIVSTOFFE



Selection Criteria for Metals and Plastics as
Construction Materials for Long Term Pressure-Testing
Apparatus on Liquid Propellants (LPS)

Dr. E. Backof



Test arrangement for pressure measurements on liquid propellants

1. The influence of metallic and non-metallic materials
on the chemical stability of LP 1846

In measuring the pressure rise in liquid HAN propellants at increased temperatures during long-term storage, it is first of all necessary to make sure that material components of the pressure sensors and the sealing elements exert no influence on the life term of propellant samples.

1.1 Metals and alloys

Accelerated storage tests were carried out on the effects of precious metals, metals, stainless steels and 2 gun steels on LP 1846 in glass ampoules.

The time measured up to bursting of a glass ampoule is a parameter for the compatibility of the propellant with the metal concerned. This is related to the storage life of the original (non-contaminated) propellant and given as the relative life term. This relative life term is given as a percentage of the original LP 1846, the life term of the original being fixed at 100 %.

Table 1: The influence of metals and alloys on the chemical stability of LP 1846. Accelerated storage test in ampoules at 90 °C (194 °F).

Metal/Alloy	Decomposition time in days	Relative decomposition time in %	Remarks
- (Original LP)	68,6	100	colourless
Gold	69,5	101,5	"
Silver	70,1	102,2	"
Mercury	68,2	99,0	"
Rhenium	1,5	2,2	"
Iridium	62,0	90,4	"
Platinum	56,7	82,7	"

Table 1 (continued-1):

The influence of metals and alloys on the chemical stability of LP 1846. Accelerated storage test in ampoules at 90 °C (194 °F).

Metal/Alloy	Decomposition time in days	Relative decomposition time in %
Copper	1,6	2,3
Zinc	69,2	100,9
Titanium	42,0	61,2
Tantalum *	47,5	61,2
Chromium	23,4	34,1
Molybdenum	47,8	69,7
Tungsten	34,4	49,7
Manganese	73,5	108,6
Iron	1,0	1,5
Cobalt	55,6	81,0
Nickel	56,8	82,8
Aluminium	73,0	106,0
Silicon	57,0	83,1
Tin	45,0	65,6
Lead	74,0	107,4
Antimony	4,0	5,8

* net, possibly polluted

Table 1 (continued - 2):

The influence of metals and alloys on the chemical stability
of LP 1846. Storage test in ampoules at 90 °C.

Metal / Alloy	Decomposition time in days	Relative decomposition time in %	Remarks
17/4 PH (1.4542)	15,7	22,9	colourless
V 2A (1.4541)	1,8	2,6	"
V 4A (1.4571)	50,4	73,5	"
30 CrNiMo8V (1.6580)	0,8	1,1	"
35 NiCrMoV125 (1.2760)	0,5	0,7	"

Of the precious metals tested, gold, silver and mercury showed no restriction in the life term of LP 1846.

The majority of added metals shorten the storage duration of LP 1846 considerably, some of them (such as iron, copper and antimony) by more than 90 % to < 6 % of the life term.

Long-term storage tests on LP 1846 when in contact with metallic materials (Table 1) have shown that gold causes no reduction at all in the storage life of the propellant. Consequently, the pressure sensors, made of construction material 17/4 PH were galvanically gold-plated.

1.2 Plastomers and elastomers

The demands made on the sealing materials are:

High chemical resistance to the liquid propellants (both in the liquid and gas spaces) as well as to the decomposition products of the LPS,

No influence on the sealing materials used to the chemical stability and storage life term of the liquid propellants.

Table 2: The selection of suitable sealing materials

Chemical name	Abbreviation	Colour
Ethylenepropylene-Diene Copolymers	EPDM	black
Vinylidenefluoride-Hexafluoropropylene Copolymers (Viton)	FPM	black-brown
Acrylonitrile-Butadiene Copolymers	NBR	black
Silicone Resin	VMQ	red
Ethylenepropylene Copolymers	EP	black

Table 2 (continued): The selection of suitable sealing materials

Chemical name	Abbreviation	Colour
Polytetrafluoroethylene	PTFE (PT 950)	white
Polytetrafluoroethylene	PTFE (TFM)	white
Tetrafluoroethylene-Perfluoroalkyl-vinyl Ether Copolymers	PFA, TFA	opalescent white
Polytrifluorochloroethylene	PCTFE	transparent-turbid
Perfluorelastomer	KALREZ 4079	black

Table 3: The influence of sealing materials on the chemical stability of LP 1846. Accelerated storage test in glass ampoules at 90 °C (194 °F)

Sealing material	Relative decomposition time in %	
	in contact with LP	in gas space
- (original LP)	100	100
EPDM	7,2	23,9
FPM (Viton)	21,6	21,9
NBR	23,8	22,1
VMQ	51,7	71,6
EP	7,5	25,5

Table 3 (continued): The influence of sealing materials on the
 chemical stability of LP 1846. Accelerated
 storage test in glass ampoules at 90 °C
 (194 °F)

Sealing material	Relative decomposition time in %	
	In contact with LP	In gas space
- (original LP)	100	100
PTFE (PT 950)	99,6	not determined
PTFE (TFM)	102,4	"
PFA, TFA	104,7	"
PCTFE	108,6	"
KALREZ 4079	48,4	"

The tests showed that only Teflon (PTFE - PT 950; PTFE TFM), PFA and polytrifluorochloroethylene (PCTFE) are here applicable. The decomposition time of these substances reaches that of the original LPS.

2. The physical properties of sealing materials

Apart from their chemical stability as well as their compatibility with the liquid propellant, selection criteria for materials used in sealing glass pressure containers also include their permeability to gases and their viscous flow behavior.

2.1 The permeation of gases through high-polymer substances

$$Q = P \frac{A}{d} \cdot \Delta p$$

$$P = P_0 \exp (-E/RT)$$

Table 4: The permeation coefficients *
 of sintered PTFE (Hostaflon,
 manufactured by Hoechst AG)
 at room temperature in
 accordance with DIN 53380

Gas	Material: PTFE (Hostaflon)	
	TF 1740	TFM 1700
air	100	80
O ₂	250	160
N ₂	80	60
CO ₂	700	450
He	2100	1700
Water vapor	0.03	0.03

$$* \quad P = Q \frac{d}{A \cdot \Delta p} \quad \left[\frac{\text{cm}^3 \cdot \text{mm}}{\text{day} \cdot \text{m}^2 \cdot \text{bar}} \right]$$

Table 5: The temperature dependency
of the permeation coefficients
of PTFE (Hostaflon) for Helium

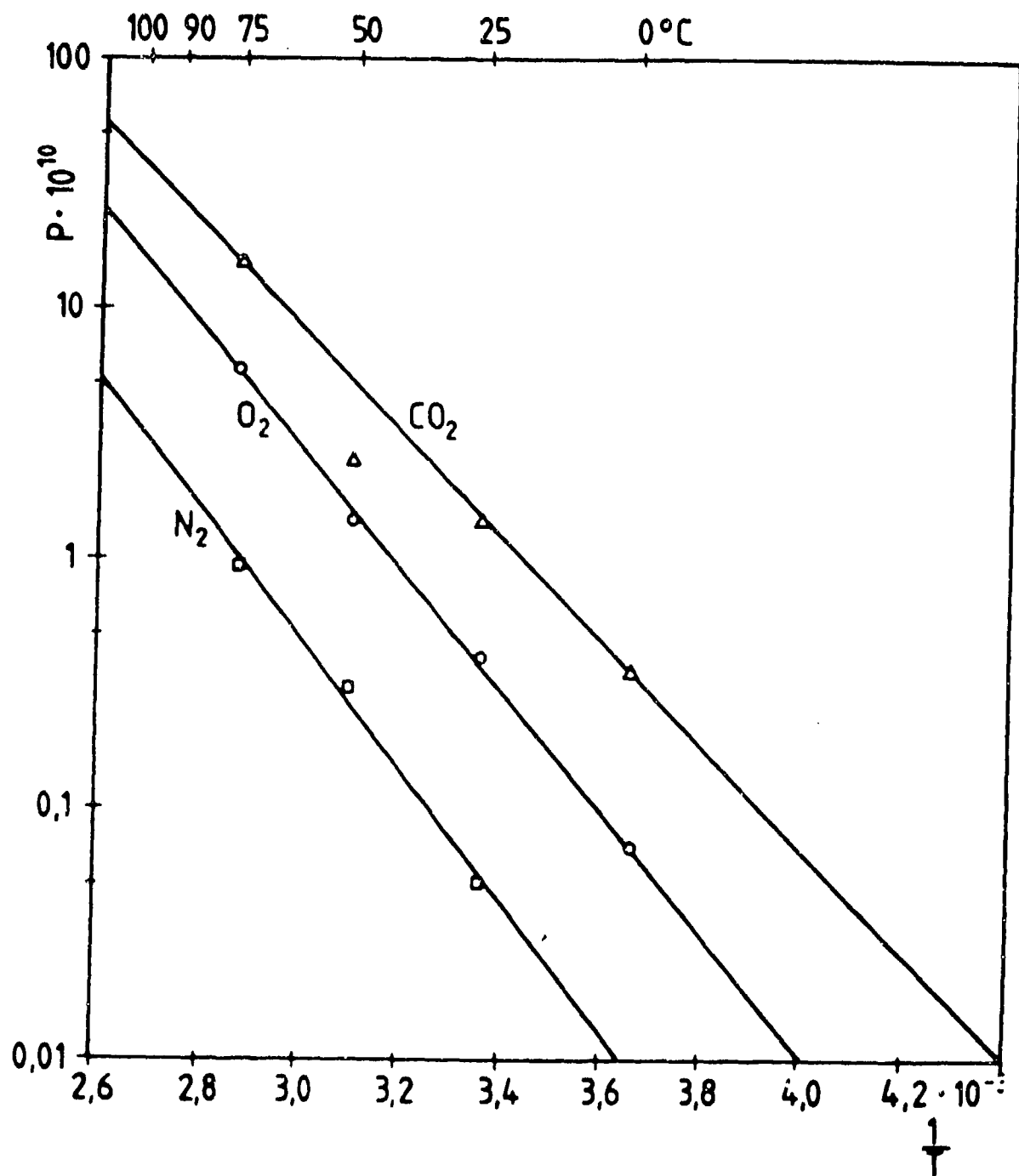
Temperature °C	Hostaflon TF 1632
23	2400
35	3000
50	4100

$$* \quad P = Q \frac{d}{A \cdot \Delta p} \left[\frac{\text{cm}^3 \cdot \text{mm}}{\text{day} \cdot \text{m}^2 \cdot \text{bar}} \right]$$

Table 6: The temperature dependency of the permeation
coefficients * of amorphous PCTFE (Voltalef 300)
for a number of gases. Permeation coefficient $\times 10^{10}$

Temperature in °C	Gas					H ₂ S	water vapor
	N ₂	O ₂	CO ₂	H ₂	H ₂ S		
0	-	0,07	0,35	3,20	-	-	-
25	0,05	0,40	1,40	9,80	-	1	-
50	0,30	1,40	2,40	24,0	0,35	10	-
75	0,91	5,70	15,0	-	2,0	28	-
100	-	-	-	-	-	100	-

$$P = Q \frac{d}{A \cdot \Delta p} \left[\frac{cm^3 \cdot mm}{s \cdot cm^2 \cdot (cm Hg)} \right]$$



Exponential temperature dependency of the permeation coefficients P of PCTFE (Voltalef 300)

P in $\text{cm} \cdot \text{mm} / \text{s} \cdot (\text{cm Hg})$

Table 7: Gas fluxes Q (in cm^3/day) through PTFE and PCTFE sealing materials at $\Delta p = 5$ bar, calculated for flat sealing elements ($r_o = 6$ mm; $r_i = 4$ mm; $d = 2$ mm; $A = 0.63 \text{ cm}^2$) of the testing apparatus

Gas	PTFE (Hostaflon)		PCTFE	
	TF 1740	TFM 1700	Voltalef 300	
	25 °C	25 °C	25 °C	90 °C
N ₂	$1.25 \cdot 10^{-2}$	$9.5 \cdot 10^{-3}$	$5.1 \cdot 10^{-3}$	$2.0 \cdot 10^{-3}$
O ₂	$3.92 \cdot 10^{-2}$	$2.52 \cdot 10^{-2}$	$4.1 \cdot 10^{-2}$	$1.1 \cdot 10^{-2}$
CO ₂	$1.1 \cdot 10^{-1}$	$7.1 \cdot 10^{-2}$	$1.4 \cdot 10^{-2}$	$2.7 \cdot 10^{-2}$
He				

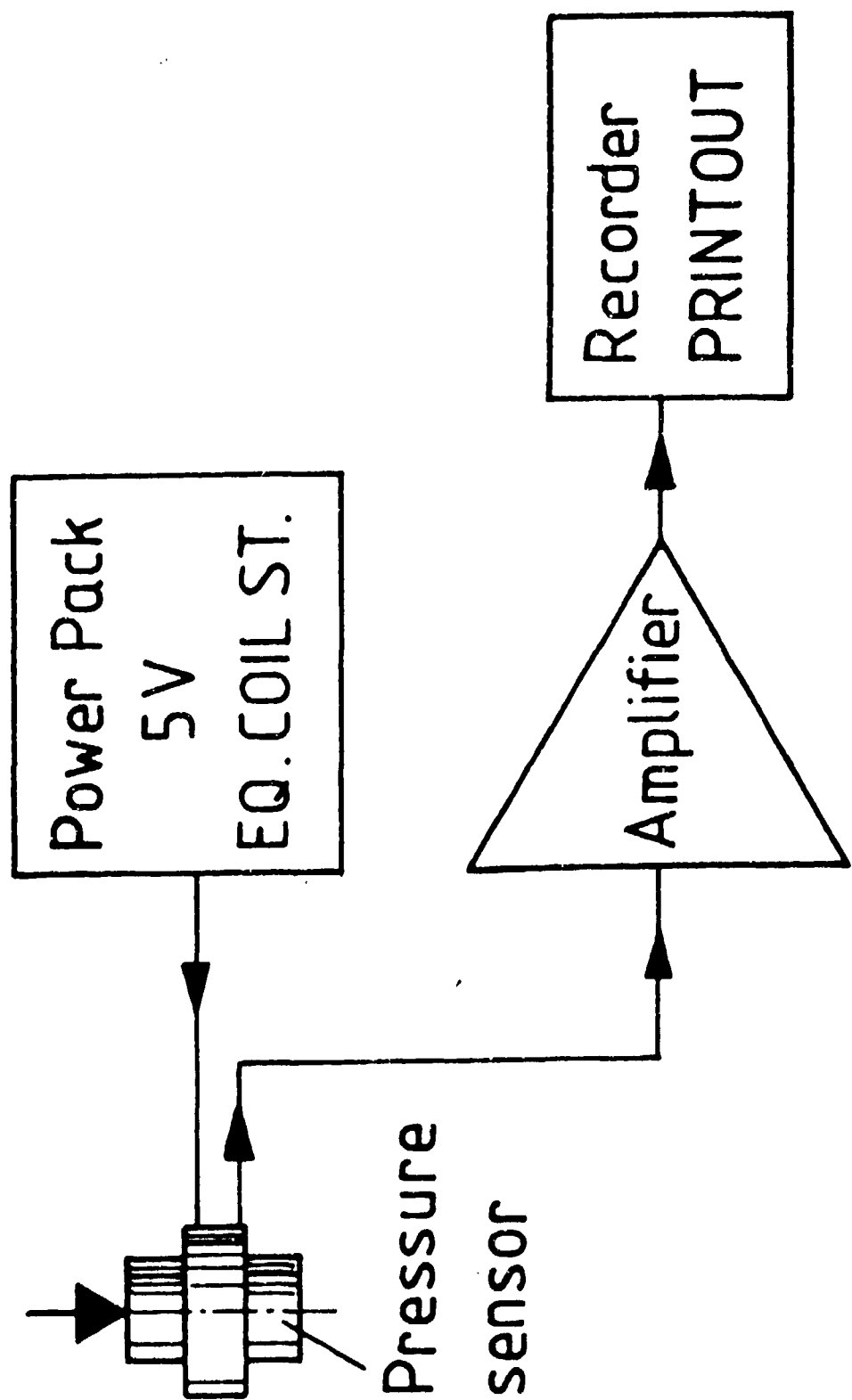
The mechanical properties of PTFE AND PCTFE:

Properties	PTFE TF 1740	PTFE TFM 1700	PFA	PCTFE Volutalef 300
Deformation under strain (7 MPa-24h/25°C)			1.5 %	-
Shore hardness	c. 55	60	64	77 - 79

On account of long-term stress of the sealing materials during storage of the LP samples at 90 °C (194 °F), PCTFE was thus selected as sealing material for storage of propellants in measuring the increase in pressure.

In comparison with TFM and PFA, PCTFE has the highest shore hardness, the lowest deformation under strain and the smallest permeation coefficient.

The measuring apparatus was thus fitted out with flat PCTFE sealing units (12 x 8 x 2 mm).



Compatibility Study With 60% HAN Solution

By

**Owen M. Briles
Leonard S. Joesten**

**Sundstrand Energy Systems
Rockford, Illinois 61125
Unit of Sundstrand Corporation**

**Work Performed for
Department of the Army
USA LABCOM/Ballistic Research Laboratory
Aberdeen Proving Ground, MD**

Contract No: DAA D05-86-C-0168

***Presented at 4th Annual Conference on HAN-Based Liquid Propellant
30 August - 1 September 1988
Ballistic Research Laboratory***

The materials tested and referenced throughout this report are not of Sundstrand manufacture and were supplied to Sundstrand by the United States Army or directly purchased by Sundstrand.

Abstract

A Hydroxylammonium Nitrate/Materials Compatibility Study was conducted for the Ballistic Research Laboratory in 1987. Fifty-one material specimens were exposed to 60 percent hydroxyl-ammonium nitrate solution for 30 days at 25°C, and 48 material specimens were exposed to 60 percent hydroxylammonium nitrate solution for 30 days at 65°C. Material specimens were examined at the end of the exposures, and gas evolution was monitored during the exposures. Gaseous species were identified and analyzed. The test procedures will be described and test results presented.

Introduction

PROBLEM:

There is limited information available on material resistance to HAN solutions and on the stability of HAN solutions when in contact with various materials.

OBJECTIVE:

Develop and demonstrate a test method whereby materials resistance to HAN and HAN stability can be simultaneously evaluated.

HAN Solution

- 2.8M solution procured from Southwest Analytical
- Concentrated to 60% (wt) by vacuum distillation

Analysis of HAN Solution

<u>Test</u>	<u>As Received</u>	<u>After Concentration</u>
Assay, % by wt.	23.7	61.7
Iron, ppm	<0.5	<0.5
Copper, ppm	<0.3	<0.5
Chromium, ppm	<0.5	<1.0
Nickel, ppm	0.4	1.4
Cobalt, ppm	<0.3	<0.5
Zinc, ppm	0.1	0.4

Test Specimens

- Purchased (5mm x 5mm x 1mm)

- Tantalum, 99.9%

- Iron, 99.99 + %

- Nickel, 99.98%

- Aluminum, 7075-T651

- Stainless Steel, 316

- Chromium, 99.99 + %

- Copper, 99.9%

- Supplied by the Army

- 58 Material specimens (including metal and plastic coupons, and metal coupons with metallic and nonmetallic coatings).

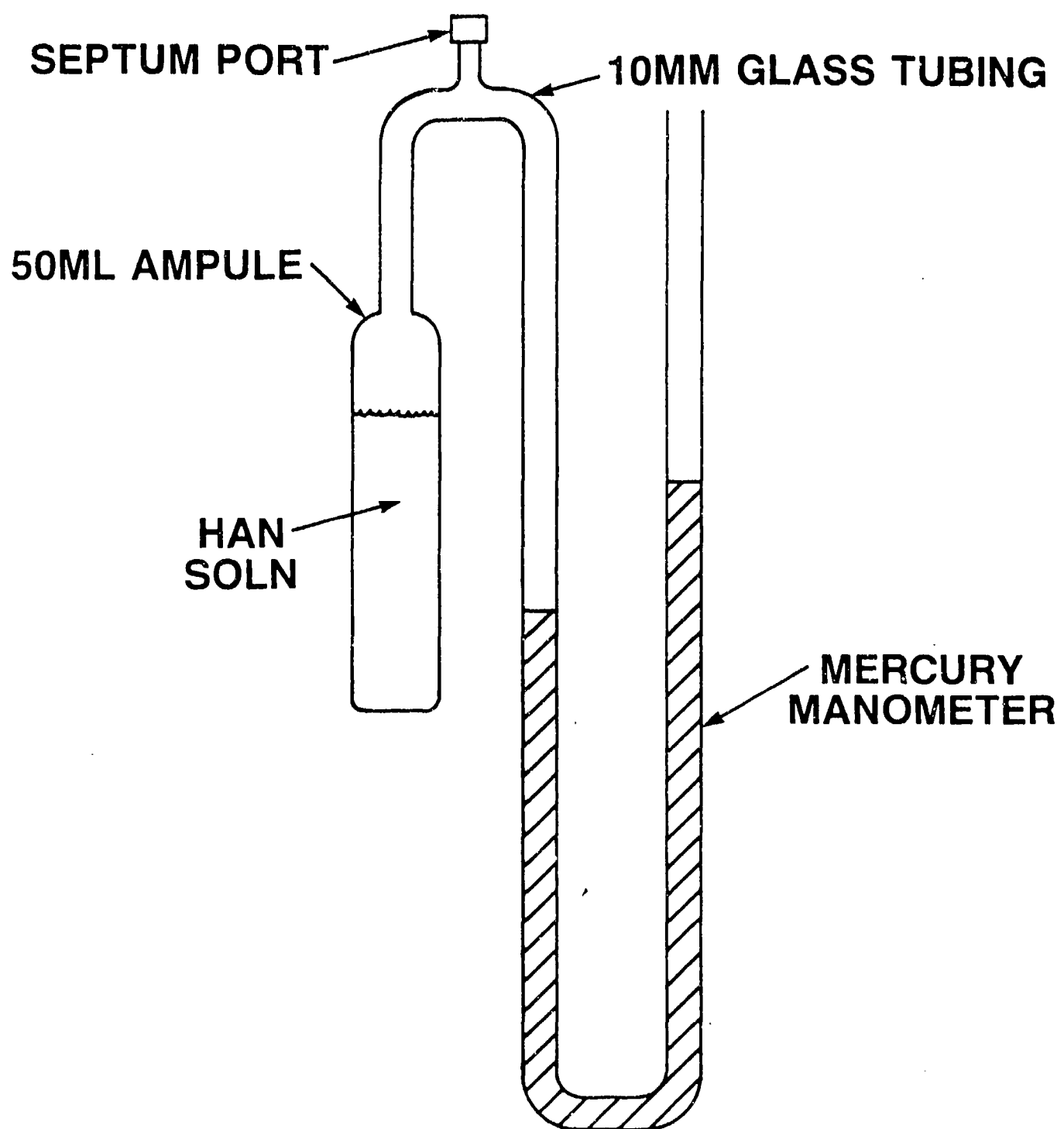
Specimens Tested

<u>Sample No.</u>	<u>G.E. No.</u>	<u>Description</u>
1 & 54	—	Tantalum
2	—	Iron
3 & 55	—	Nickel
4 & 56	—	7075 Aluminum
5 & 57	—	316SS
6 & 58	—	Chromium
7	—	Copper
8 & 59	4	Teflon 05-026®
9 & 60	5	Teflon 05-002®
10 & 61	6	Nylon 05-037
11 & 62	7	Polyamide 05-036
12 & 63	9	17-4PH
13 & 64	13	Poco Graphite ACF-10QE2®
14 & 65	21	Everlube 620C on 17-4®
15 & 66	22	Nibronze on 17-4
16	23	Metco 309N5-3 on 17-4®
17 & 67	24	Metco 505 on 17-4®
18 & 68	25	Nedox SF2 on 17-4®
19 & 69	26	Hi-T-Lube on 17-4
20 & 70	28	K-Ramic SCA1002 Coating on?
21 & 71	29	Vespel SP-210 (15% Graphite)®
22 & 72	30	Vespel SP-211D®
23 & 73	31	Torlon 7130®
24 & 74	33	Vespel SP-21®
25	—	Blank-A
26 & 75	41	Vespel SP-211®
27 & 76	42	Vespel SP-22®
28 & 77	43	Vespel SP-1®
78	—	Blank-C
29 & 79	44	UDEL Polysulfone P-1700
30 & 80	46	Nylasint MA®
31 & 81	47	Zytel 101L®
32 & 82	48	Zytel 70G43L®
33 & 83	49	Rynite 530®
34 & 84	50	Hytrex 7245®
35 & 85	51	Torlon 4275®
36 & 86	53	Jessop Alloy 20
37 & 87	54	Jessop Alloy 276
38 & 88	55	303SS
39 & 89	72	Teflon 55450-3®
40 & 90	77	Fluorocarbon 33
41 & 91	78	Fluorocarbon PEEK
42 & 92	79	Stellite 21 Weld Rod®
43 & 93	83	CrB ₂ on 17-4
44 & 94	84	Hard Chrome on 17-4
45 & 95	86	Kennametal K602®
46 & 96	89	Kennametal K801®
47 & 97	91	Tiolube 1175 on 17-4
48 & 98	100	Rynite SST-35®
48 & 99	102	Hostalen 102®
50	—	Blank-B
51 & 100	105	K-Barb
52 & 101	110	Nitronic 50
53 & 102	111	Haynes 718®
103	—	Blank-D

Test Vessels

- Glass ampule with attached manometer
- Specimens placed in ampule before assembly
- HAN solution added, mercury added, and vessels sealed in Argon atmosphere

Reaction Test Vessel



Phase I Testing

- 25 ± 0.2°C constant temperature bath
- 48 Vessels with specimens/2 blanks
- Record pressure daily
- Terminate after 30 days, or if pressure increase exceeds 3cm-Hg/day

Phase II Testing

- 65 ± 0.2°C constant temperature bath
- 48 Vessels with specimens/2 blanks
- Record pressure daily
- Terminate after 30 days, or if pressure increase exceeds 3cm-Hg/day

Gas Evolution Rates

- Daily manometer readings
- Pressure readings converted to standard cc's of gas produced:

$$V_C = (T_0/P_0) [V_2 (P_0/T_2) - V_1 (P_0/T_1)]$$

where: V_C = Corrected Volume (gas)

V_2 = Uncorrected Volume (gas)

V_1 = Initial Volume (gas)

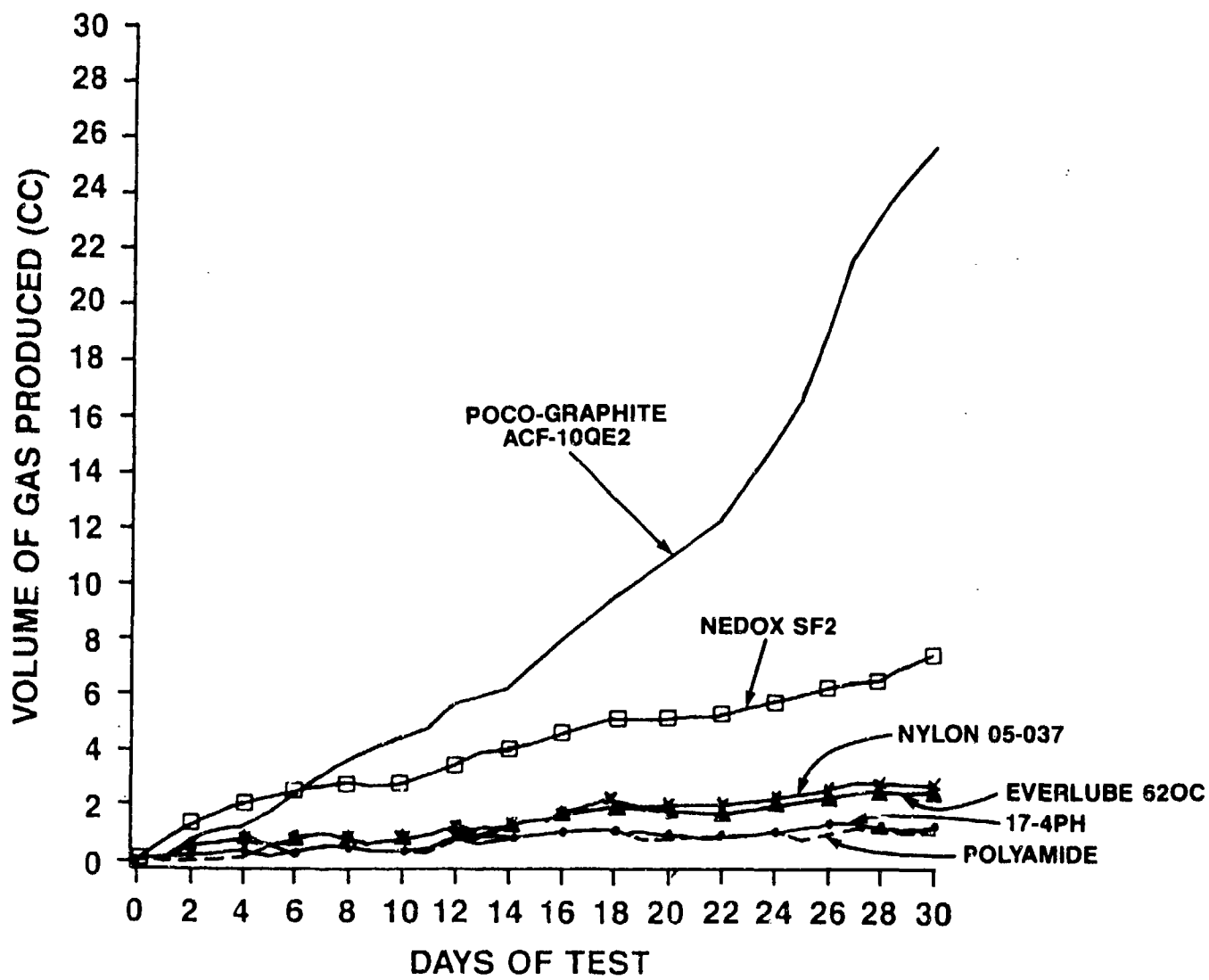
T_2, P_2 = Temperature and Pressure Measurements

T_1, P_1 = Initial Temperature and Pressure

T_0/P_0 = Standard Temperature and Pressure

- A statistical analysis system (SAS) program was used to calculate and graph results.

HAN Outgassing 65°C



Gas Analysis

- Gas samples taken via syringe through rubber septa if >0.3 cc gas produced
- Analysis performed by gas chromatography

Gas Evolution Rates and Gases Produced at 25°C

Sample No.	Sample Material	Days in Test	Volume of Gas Produced cc			Average Rate, cc/Day
			N ₂	N ₂ O	Total	
1	Tantalum	30	—	—	<0.30	<0.010
2	Iron	9	4.09	11.53	15.62	1.736
3	Nickel	30	0.39	0.46	0.85	0.028
4	7075 Aluminum	30	0.54	0.54	1.08	0.036
5	316SS	30	—	—	<0.30	<0.010
6	Chromium	30	—	—	<0.30	<0.010
7	Copper	9	4.98	14.52	19.50	2.167
8	Teflon 05-026®	30	—	—	<0.30	<0.010
9	Teflon 05-002®	30	—	—	<0.30	<0.010
10	Nylon 05-037	30	—	—	<0.30	<0.010
11	Polyamide 05-036	30	—	—	<0.30	<0.010
12	17-4PH	30	—	—	<0.30	<0.010
13	Poco Graphite®	30	0.63	0.40	1.03	0.034
14	Everlube 620C®	30	—	—	<0.30	<0.010
15	Nibronze	30	2.8	2.31	5.11	0.170
16	Metco 309N5-3®	2	—	—	4.13	2.065
17	Metco 505®	30	7.25	17.62	24.87	0.829
18	Nedox SF2®	30	0.24	0.16	0.40	0.013
19	HI-T-Lube	30	—	—	<0.30	<0.010
20	K-Ramic	30	—	—	<0.30	<0.010
21	Vespel SP-210®	30	—	—	<0.30	<0.010
22	Vespel SP-211D®	30	—	—	<0.30	<0.010
23	Torlon 7130®	30	—	—	<0.30	<0.010
24	Vespel SP-21®	30	—	—	<0.30	<0.010
51	K-Barb	30	—	—	<0.30	<0.010
52	Nitronic 50	30	—	—	<0.30	<0.010
53	Haynes 718®	30	—	—	<0.30	<0.010
25	Blank-A	30	—	—	<0.30	<0.010
26	Vespel SP-211®	30	—	—	<0.30	<0.010
27	Vespel SP-22®	30	—	—	<0.30	<0.010
28	Vespel SP-1®	30	—	—	<0.30	<0.010
29	UDEL Polysulfone	30	—	—	<0.30	<0.010
30	Nylasint MA®	30	—	—	<0.30	<0.010
31	Zytel 101L®	30	—	—	<0.30	<0.010
32	Zytel 70G43L®	30	—	—	<0.30	<0.010
33	Rynite 530®	30	—	—	<0.30	<0.010
34	Hytrel 7245®	30	—	—	<0.30	<0.010
35	Torlon 4275®	30	—	—	<0.30	<0.010
36	Jessop 20	30	—	—	<0.30	<0.010
37	Jessop 276	30	—	—	<0.30	<0.010
38	303SS	30	2.47	0.80	3.27	0.109
39	Teflon 55450-3®	30	—	—	<0.30	<0.010
40	Fluorocarbon 33	30	—	—	<0.30	<0.010
41	Fluorocarbon PEEK	30	—	—	<0.30	<0.010
42	Stellite 21®	30	—	—	<0.30	<0.010
43	CrB ₂	30	—	—	<0.30	<0.010
44	Hard Chrome	30	—	—	<0.30	<0.010
45	Kennametal K602®	30	—	—	<0.30	<0.010
46	Kennametal K801®	30	0.21	0.38	0.59	0.197
47	Triolube 1175	30	—	—	<0.30	<0.010
48	Rynite SST-35®	30	—	—	<0.30	<0.010
49	Hostalen 102®	30	—	—	<0.30	<0.010
50	Blank-B	30	—	—	<0.30	<0.010

Gas Evolution Rates and Gases Produced at 65°C

Sample No.	Sample Material	Days Volume of Gas Produced			Average Rate, cc/Day	
		Test	N ₂	cc N ₂ O		
54	Tantalum	30	5.77	4.17	9.94	0.331
55	Nickel	30	1.01	0.36	1.37	0.046
56	Aluminum	6	2.20	5.50	7.70	1.283
57	316SS	12	2.91	2.83	5.74	0.478
58	Chromium	30	1.46	0.57	2.03	0.068
59	Teflon 05-026®	30	3.96	2.65	6.61	0.220
60	Teflon 05-002®	30	5.80	8.23	14.03	.468
61	Nylon 05-037	30	2.05	0.63	2.68	0.089
62	Polyamide 05-036	30	0.73	0.23	0.96	0.032
63	17-4PH	30	0.84	0.25	1.09	0.036
64	Poco Graphite®	30	6.89	18.57	25.46	0.849
65	Everlube 620C®	30	1.71	0.71	2.42	0.081
66	Nibronze	1	0.74	1.31	2.05	2.05
67	Metco 505®	1	6.07	14.73	20.80	20.80
68	Nedox SF-2®	30	4.37	2.96	7.33	0.244
69	HI-T-Lube	30	2.99	1.72	4.70	0.157
70	K-Ramic	4	1.78	8.36	10.14	2.535
71	Vespel SP-210®	30	1.05	0.30	1.35	0.045
72	Vespel Sp-211D®	30	1.15	0.33	1.48	0.049
73	Torlon 7130®	30	0.94	0.28	1.22	0.041
74	Vespel SP-21®	30	0.88	0.21	1.09	0.036
75	Vespel SP-211®	30	.077	0.25	1.02	0.034
76	Vespel SP-22®	30	1.64	0.82	2.46	0.082
77	Vespel SP-1®	30	0.81	0.22	1.03	0.034
78	Blank-C	30	0.61	0.16	0.77	0.026
79	UDEL Polysulfone	30	0.72	0.19	0.91	0.030
80	Nylasint MA®	6	2.37	6.33	8.70	1.450
81	Zytel 101L®	30	0.97	0.27	1.24	0.041
82	Zytel 70G43L®	30	0.89	0.15	1.04	0.035
83	Rynite 530®	30	0.52	0.13	0.65	0.022
84	Hytrel 7245®	30	2.51	0.72	3.23	0.108
85	Torlon 4275®	30	0.63	0.15	0.78	0.026
86	Jessop 20	30	0.60	0.18	0.78	0.026
87	Jessop 276	30	2.70	1.41	4.11	0.137
88	303SS	30	2.59	1.37	3.96	0.132
89	Teflon 55450-3®	30	0.24	0.15	0.39	0.013
90	Fluorocarbon 33	12	4.30	5.87	10.17	0.848
91	Fluorocarbon PEEK	30	0.65	0.13	0.78	0.026
92	Stellite 21®	30	0.52	0.13	0.65	0.022
93	CrB ₂	14	2.24	6.97	9.21	0.658
94	Hard Chrome	30	1.00	0.27	1.27	0.042
95	Kennametal K602®	30	0.96	0.44	1.40	0.047
96	Kennametal K801®	15	3.75	9.80	13.56	0.904
97	Tiolube 1175	30	2.53	1.34	3.87	0.129
98	Rynite SST-35®	17	4.49	12.48	16.79	0.988
99	Hostalen 102®	30	0.72	0.19	0.91	0.030
100	K-Karb	30	2.90	1.96	4.86	0.162
101	Nitronic 50	30	0.95	0.22	1.17	0.039
102	Haynes 718®	30	0.78	0.20	0.98	0.033
103	Blank-D	30	0.56	0.16	0.72	0.024

Specimen Examination

- Test vessels opened, specimens washed and dried
- Specimens weighed (wt. changes recorded), and visually examined

Specimen Examinations, 25°C

Sample No.	Description	Wt. Before, gms	Wt. After, gms
1	Tantalum	0.4251	0.4245
2	Iron	0.2040	Disintegrated
3	Nickel	0.2188	Dissolved
4	7075 Aluminum	0.0725	0.0443
5	316SS	0.2035	0.2028
6	Chromium	0.1852	0.1851
7	Copper	0.2190	Dissolved
8	Teflon 05-026®	0.4428	0.4428
9	Teflon 05-002®	0.5297	0.5308
10	Nylon 05-037	0.3310	0.3393
11	Polyamide 05-036	0.3693	0.3703
12	17-4PH	2.0022	2.0026
13	Poco Graphite®	0.4219	0.4099
14	Everlube 620C®	1.7668	1.7667
15	Nibronze	1.9124	1.7577
16	Metco 309N5-3®	2.2978	1.999 (Coating Gone)
17	Metco 505®	2.6021	2.4130
18	Nedox SF2®	1.9302	1.8638
19	HI-T-Lube	1.9192	1.9038
20	K-Ramic	1.7657	1.7655
21	Vespel SP-210®	0.3258	0.3276
22	Vespel SP-211D®	0.3369	0.3387
23	Torlon 7130®	0.2386	0.2396
24	Vespel SP-21®	0.3363	0.3381
51	K-Barb	0.2973	0.3036
52	Nitronic 50	1.9106	1.9106
53	Haynes 718®	2.3438	2.3437
25	Blank-A	—	—
26	Vespel SP-211®	0.3318	0.3329
27	Vespel SP-22®	0.3580	0.3591
28	Vespel SP-1®	0.3128	0.3141
29	UDEL Polysulfone	0.2955	0.2961
30	Nylasint MA®	0.2112	0.2357
31	Zytel 101L®	0.2491	0.2631
32	Zytel 70G43L®	0.3246	0.3322
33	Rynite 530®	0.3733	0.3734
34	Hytrel 7245®	0.1962	0.1968
35	Torlon 4275®	0.2387	0.2401
36	Jessop 20	1.8598	1.8602
37	Jessop 276	3.4406	3.4404
38	303SS	2.0420	2.0285
39	Teflon 55450-3®	0.5183	0.5187
40	Fluorocarbon 33	0.5557	0.5558
41	Fluorocarbon PEEK	0.2471	0.2478
42	Stellite 21™	1.4531	1.4531
43	CrB ₂	1.8120	1.8110
44	Hard Chrome	1.8400	1.8397
45	Kennametal K602®	3.8297	3.8294
46	Kennametal K801®	6.0968	6.0609
47	Tiolube 1175	1.9458	1.9447
48	Rynite SST-35®	0.2721	0.2742
49	Hostalen 102®	0.2655	0.2654
50	Blank-B	—	—

Specimen Examinations, 65°C

Sample No.	Description	Wt. Before, gms	Wt. After, gms
54	Tantalum	0.4254	0.4249
55	Nickel	0.1859	0.1857
56	7075 Aluminum	0.0697	0.0358
57	316SS	0.2015	0.2004
58	Chromium	0.1873	0.1872
59	Teflon 05-026®	0.4350	0.4352
60	Teflon 05-002®	0.5316	0.5331
61	Nylon 05-037	0.4087	0.4264
62	Polyamide 05-036	0.3237	0.3247
63	17-4PH	1.8115	1.8122
64	Poco Graphite®	0.4669	0.4492
65	Everlube 620C®	1.9498	1.9479
66	Nibronze	2.3115	2.1489
			(Corroded)
67	Metco 505®	2.7061	2.5614
68	Nedox SF-2®	1.9855	1.9243
69	HI-T-Lube	1.9385	1.9240
70	K-Ramic	1.9501	1.9500
71	Vespel SP-210®	0.3354	0.3372
72	Vespel SP-211D®	0.3958	0.3972
73	Torlon 7130®	0.3018	0.3028
74	Vespel SP-21®	0.3899	0.3918
75	Vespel SP-211®	0.4028	0.4040
76	Vespel SP-22®	0.4182	0.4192
77	Vespel SP-1®	0.3718	0.3732
78	Blank-C	—	—
79	UDEL Polysulfone	0.2606	0.2610
80	Nylasint MA®	0.2072	0.1997
81	Zytel 101L®	0.2799	0.2221
			(Cracked)
82	Zytel 70G43L®	0.3585	0.3586
83	Rynite 530®	0.3466	0.3466
84	Hytrex 7245®	0.2183	0.2154
85	Torlon 4275®	0.2988	0.3003
86	Jessop 20	1.8773	1.8778
87	Jessop 276	3.7662	3.5857
88	303SS	2.1353	2.1312
			(Dark)
89	Teflon 55450-3®	0.5652	0.5657
90	Fluorocarbon 33	0.5299	0.5298
91	Fluorocarbon PEEK	0.2382	0.2908
92	Stellite 21®	1.5565	1.5564
93	CrB ₂	2.0173	2.0083
			(Flaking)
94	Hard Chrome	2.0114	2.0111
95	Kennametal K602®	4.2569	4.2564
96	Kennametal K801®	6.8260	6.7622
97	Tiolube 1175	1.7228	1.7208
98	Rynite SST-35®	0.3011	0.2988
99	Hostalen 102®	0.2943	0.2943
100	K-Karb	0.2874	0.2976
101	Nitronic 50	2.1129	2.1130
102	Haynes 718®	2.5248	2.5246
103	Blank-D	—	—

Discussion and Conclusions

1. The test method provides a very sensitive method to measure propellant stability at the same time material compatibility is being determined.
2. Iron, copper and Metco 309N5-3® were the most reactive. These plus 11 other materials exceeded the 3-cm/day limit. None of the reactions were considered vigorous.
3. Temperature had a definite effect on reaction rate. Only 11 of 51 materials tested at 25°C produced measurable quantities of gas. All tests (including blanks) produced measurable amounts of gas at 65°C.
4. N₂ and N₂O were the only gaseous species produced. The N₂/N₂O ratio was < 1.0 for reactive materials and above 3.0 for nonreactive materials.

METALS

5. Chromium, 17-4PH, Jessop 20, Stellite 21®, Kennametal K606®, Nitronic 50, Haynes 718®, and hard chrome plating performed well.

NON METALS

6. Polyamide, Vespel®, Torlon®, Udel, Rynite®, Hytrel®, Hostalen® and some Teflons/Zytels® performed well.

COATINGS

7. Everlube 620C® and Tiolube 1175 dry film lubricants performed well.

DISTRIBUTION LIST

<u>No. of Copies</u>	<u>Organization</u>	<u>No. of Copies</u>	<u>Organization</u>
12	Administrator Defense Technical Info Center ATTN: DTIC-DDA Cameron Station Alexandria, VA 22304-6145	2	Cmdr, US Army Armament, Rsch, Development & Engr Center ATTN: SMCAR-AEB, Paul Marinkas SMCAR-AE, Jean Paul Picard Picatinny Arsenal, NJ 07806-5000
2	Director Defense Advanced Research Projects Agency ATTN: J. Lupo J. Richardson 1400 Wilson Boulevard Arlington, VA 22209	4	Commander US Army Armament, Rsch, Development & Engr Center ATTN: SMCAR-FSS-DA, Bl : 94 C. Daly R. Kopmann J. Irizarry N. Kendl Picatinny Arsenal, NJ 07806-5000
2	HQDA (SARD-TR/B. Zimmerman, I. Szkrybalo) Washington, DC 20310-0001		
1	Commander US Army Materiel Command ATTN: AMCDRA-ST 5001 Eisenhower Avenue Alexandria, VA 22333-0001	5	Director Benet Weapons Laboratory US Army Armament, Rsch, Development & Engr Center ATTN: SMCAR-CCB-DS, A. Graham SMCAR-CCB, L. Johnson SMCAR-CCB-S, F. Heiser SMCAR-LCB-TL SMCAR-LCB, J. Frankel Watervliet, NY 12189-4050
1	HQ, US Army Materiel Command ATTN: AMCICP-AD, B. Dunetz 5001 Eisenhower Avenue Alexandria, VA 22333-0001		
15	Cmdr, US Army Armament, Rsch, Development & Engr Center ATTN: SMCAR-TSS SMCAR-TDC (2 COPIES) SMCAR-MSI (2 COPIES) SMCAR-AEE-BR, B. Brodman SMCAR-AEE-B, D. Downs SMCAR-AEE-BR, W. Seals A. Beardell, D. Chin SMCAR-AEE-W, Dr. Pai Lu SMCAR-AEE, A. Bracuti J. Lannon SMCAR-FSS-D, L. Frauen SMCAR-FSA-S, H. Liberman Picatinny Arsenal, NJ07806-5000	1	Commander US Army Armament, Munitions and Chemical Command ATTN: SMCAR-ESP-L Rock Island, IL 61299-5000
		1	Commander US Army Aviation Systems Cmd ATTN: AMSAV-DACL 4300 Goodfellow Blvd St. Louis, MO 63120-1798

DISTRIBUTION LIST

<u>No. of Copies</u>	<u>Organization</u>	<u>No. of Copies</u>	<u>Organization</u>
1	Director US Army Aviation Rsch and Technology Activity Ames Research Center Moffett Field, CA 94035-1099	1	Commander US Army Tank Automotive Cmd ATTN: AMSTA-TSL Warren, MI 48397-5000
1	Commander ERADCOM Technical Library ATTN: STET-L Ft. Monmouth, NJ 07703-5301	1	Director US Army Laboratory Cmd Army Research Office ATTN: Tech Library PO Box 12211 Research Triangle Park, NC 27709-2211
2	Commander US Army Laboratory Cmd ATTN: SLCHD-TA-L AMSLC-DL 2800 Powder Mill Rd Adelphi, MD 20783-1145	1	Director TRADOC Analysis Command ATTN: ATAA-SL White Sands Missile Range NM 88002-5502
1	Commandant US Army Infantry School ATTN: ATSH-CD-CSO-OR Fort Benning, GA 31905-5660		
1	Commander US Army Missile Command ATTN: AMSMI-RD-CS-R (DOC) Redstone Arsenal, AL 35898-5241	1	Commander US Army Armament, Rsch, Development and Engr Center ATTN: SMCAR-CCS-C, T Hung Picatinny Arsenal, NJ 07806-5000
3	Commander US Army Belvoir RD&E Ctr ATTN: STRBE-WC Tech Library (Vault) B-315 STRBE-VU, G. Rodriguez STRBE-VL, G. Farmer Fort Belvoir, VA 22060-5606	2	Commandant US Army Field Artillery School ATTN: ATSF-CMW ATSF-TSM-CN, J. Spicer Fort Sill, OK 73503
3	Commander US Army Environ. Hygiene Agency ATTN: HSHB-MO-T, M. Weeks H. Snodgrass HSHB-MO-A, MAJ P. Joe Aberdeen Proving Ground, MD 21010	1	Commandant US Army Armor Center ATTN: ATSB-CD-MLD Fort Knox, KY 40121

DISTRIBUTION LIST

<u>No. of Copies</u>	<u>Organization</u>	<u>No. of Copies</u>	<u>Organization</u>
3	<p>Commander US Army Biomedical Research and Development Lab ATTN: SCRD-UBG-O, MAJ Farmer MAJ Smart Dr. R. Finch Fort Detrick Frederick, MD 21701-5010</p>	1	<p>Superintendent Naval Postgraduate School Dept of Mechanical Engr ATTN: Code 1424, Library Monterey, CA 93943</p>
1	<p>Commander Letterman Army Institute of Research ATTN: SGRD-UL-T0, MAJ Korte, Jr. Presidio of San Francisco, CA 94129-6800</p>	1	<p>AFWL/SUL Kirtland AFB, NM 87117-5800</p>
1	<p>Commander Naval Surface Warfare Center ATTN: D.A. Wilson, Code G31 Dahlgren, VA 22448-5000</p>	1	<p>Air Force Armament Lab ATTN: AFATL/DLOPL Eglin AFB, FL 32542-5000</p>
1	<p>Commander Naval Surface Warfare Center ATTN: J. East, Code G33 Dahlgren, VA 22448-5000</p>	1	<p>AFOSR/NA (L. Caveny) Bldg 410 Bolling AFB, DC 20332</p>
1	<p>Commander US Naval Surface Warfare Ctr ATTN: O. Dengel K. Thorsted Silver Spring, MD 20902-5000</p>	2	<p>AFAL/RKPA ATTN: CPT M. Husband John Rusek Edwards AFB, CA 93523-5000</p>
1	<p>Commander Naval Weapons Center China Lake, CA 93555-6001</p>	1	<p>Commandant USAFAS ATTN: ATSF-TSM-CN Fort Sill, OK 73503-5600</p>
1	<p>Commander Naval Ordnance Station ATTN: P. Skahan, Code 2810G Indian Head, MD 20640</p>	2	<p>Director Jet Propulsion Lab ATTN: Tech Library Dr. Emil Lawton 4800 Oak Grove Drive Pasadena, CA 91109</p>
	<p>Commander Naval Ordnance Station Indian Head ATTN: Tech Library Indian Head, MD 20640-5000</p>	1	<p>Director National Aeronautics and Space Administration ATTN: MS-603, Tech Lib 21000 Brookpark Road Lewis Research Center Cleveland, OH 44135</p>

DISTRIBUTION LIST

<u>No. of Copies</u>	<u>Organization</u>	<u>No. of Copies</u>	<u>Organization</u>
1	Director National Aeronautics and Space Administration Manned Spacecraft Center Houston, TX 77058	7	General Electric Ord Sys Div ATTN: J. Mandzy, OP43-220 H. West W. Pasko R. Pate J. Scudiere T. Giovanetti J.B. Haberl 100 Plastics Avenue Pittsfield, MA 01201-3698
10	Central Intelligence Agency Office of Central Reference Dissemination Branch Room GE-47 HQS Washington, DC 20502	1	General Electric Company Armament Systems Department ATTN: D. Maher Burlington, VT 05401
1	Central Intelligence Agency ATTN: Joseph E. Backofen HQ Room 5F22 Washington, DC 20505	1	IITRI ATTN: Library 10 W. 35th St Chicago, IL 60616
5	Sandia National Laboratory ATTN: Dr. R.W. Carling Dr. Steve Vosen R.C. Armstrong R.E. Rychowsky David Dandy Combustion Research Facility Livermore, CA 94550	1	Olin Chemicals Research ATTN: David Gavin PO Box 586 Cheshire, CT 06410-0586
1	National Bureau of Standards ATTN: Jennifer C. Colbert Bldg 222, Room B-348 Gaithersburg, MD 20899	2	Olin Corporation ATTN: Dr. J. Leistra Dr. Ronald L. Dotson PO Box 30-9644 New Haven, CT 06536
2	Bell Aerospace Textron ATTN: Roger Nelson Glenn Johnston PO Box One Buffalo, NY 14240	3	Olin Corporation ATTN: Ken Woodard Dave Cawfield Sanders Moore PO Box 248 Charleston, TN 37310
1	Calspan Corporation ATTN: Tech Library PO Box 400 Buffalo, NY 14225	1	Safety Consulting Engr ATTN: Mr. C. James Dahn 5240 Pearl St Rosemont, IL 60018

DISTRIBUTION LIST

<u>No. of Copies</u>	<u>Organization</u>	<u>No. of Copies</u>	<u>Organization</u>
1	Science Applications, Inc. ATTN: R. Edelman 23146 Cumorah Crest Woodland Hills, CA 91364	2	Aerojet Corporation ATTN: Bob J. Agow Dr. A.M. Helmy P.O. Box 15699C Sacramento, CA 95852-1699
2	Science Applications Int'l Corporation ATTN: Dr. F. T. Phillips Dr. Fred Su 10210 Campus Point Drive San Diego, CA 92121	2	GeoCenters, Inc ATTN: Gerry Doyle Stanley Griff 315 Richard Mine Road Wharton, NJ 07805
1	Science Applications Int'l Corporation ATTN: Norman Banks 4900 Waters Edge Drive Suite 255 Raleigh, NC 27606	1	Freedman Associates ATTN: Dr. Eli Freedman, Pres. 2411 Diana Road Baltimore, MD 21209
2	Sundstrand Aviation Operations ATTN: Mr. Owen Briles Leonard S. Joesten PO Box 7202 Rockford, IL 61125	1	Hercules, Inc. ATTN: Billy Riggleman Wilmington, DE 19894
1	Veritay Technology, Inc. ATTN: E.B. Fisher 4845 Millersport Highway PO Box 305 East Amherst, NY 14051-0305	1	Hercules, Inc. ATTN: Dale Mellow 111 Howard Blvd, Suite 200 Mt Arlington, NJ 07856
2	Morton-Thiokol, Inc. ATTN: R. Biddle R. Brasfield P.O. Box 241 Elkton, MD 21921-0241	2	Martin Marietta Laboratories ATTN: Dr. V. Pai Verneker E. Fernandez 1450 South Rollings Rd Baltimore, MD 21227
2	Southwest Research Institute ATTN: Bill Herrera Nollie Swynerton 6220 Culebra Road San Antonio, TX 78284	1	Director Applied Physics Laboratory The Johns Hopkins Univ. Johns Hopkins Road Laurel, MD 20707
		2	Director CPIA The Johns Hopkins Univ. ATTN: T. Christian Tech Library Johns Hopkins Road Laurel, MD 20707

DISTRIBUTION LIST

<u>No. of Copies</u>	<u>Organization</u>	<u>No. of Copies</u>	<u>Organization</u>
1	The Johns Hopkins University ATTN: Prof. W.S. Koski Dept of Chemistry Charles and 34th Streets Baltimore, MD 21218	2	Princeton Combustion Rsch Laboratories, Inc. ATTN: N.A. Messina M. Summerfield 4275 US Highway One North Monmouth Junction, NJ 08852
1	U. of Illinois at Chicago ATTN: Professor Sohail Murad Dept of Chemical Engr Box 4348 Chicago, IL 60680	1	University of Arkansas Dept of Chemical Engr ATTN: J. Havens 227 Engineering Building Fayetteville, AR 72701
1	U. of MD at College Park ATTN: Professor Franz Kasler Department of Chemistry College Park, MD 20742	3	University of Delaware Department of Chemistry ATTN: Mr. James Cronin Professor Thomas Brill Mr. Peter Spohn Newark, DE 19711
1	U. of Missouri at Columbia ATTN: Professor R. Thompson Department of Chemistry Columbia, MO 65211	1	U. of Texas at Austin Bureau of Engineering Rsch ATTN: BRC EME133, Room 1.100 H. Fair 10100 Burnet Road Austin, TX 78758
1	U. of Michigan ATTN: Prof. Gerard M. Faeth Dept of Aerospace Engr Ann Arbor, MI 48109-3796	1	Brigham Young University ATTN: Dr. Bevan Ott Dept. of Chemistry Provo, UT 84602
1	U. of Missouri at Columbia ATTN: Professor F.K. Ross Research Reactor Columbia, MO 65211	2	Yale University ATTN: Prof. R. Chang David Leach Applied Physics P.O. Box 2157 Yale Station New Haven, CT 06520
1	U. of Missouri at Kansas City Department of Physics ATTN: Prof. R.D. Murphy 1110 East 48th Street Kansas City, MO 64110-2499	1	Purdue University ATTN: Prof. C. Austin Angell Dept. of Chemistry West Lafeyette, IN 47907
1	Pennsylvania State University Dept of Mechanical Engr ATTN: Prof. K. Kuo University Park, PA 16802		

DISTRIBUTION LIST

<u>No. of Copies</u>	<u>Organization</u>	<u>No. of Copies</u>	<u>Organization</u>
2	University of California ATTN: Prof. C.K. Law S.C. Deevi Dept. of Mechanical Eng. Davis, CA 95616		<u>Aberdeen Proving Ground</u> Dir. USAMSA ATTN: AMXSY-D AMXSY-MP, H. Cohen
1	Lehigh University ATTN: A. Macpherson Dept. of Mechanics Bldg. 19 Bethlehem, PA 18017		Cdr, USATECOM ATTN: AMSTE-TO-F
2	Rensselaer Polytechnic Inst. ATTN: J.W. Haus J. Schroeder Dept of Physics Troy, NY 12181		Cdr, CRDEC, AMCCOM ATTN: SMCCR-RSP-A SMCCR-MU SMCCR-SPS-IL
1	University of Akron ATTN: Paul Garn Dept of Chemistry Akron, OH 44325		

DISTRIBUTION LIST

<u>No. of Copies</u>	<u>Organization</u>	<u>No. of Copies</u>	<u>Organization</u>
2	George Cook Peter Henning RARDE Ft. Halstead Sevenoaks, Kent TN14 7BT England	1	LBDir H. Schwalber Amt fuer Studien und Uebungen der Bundeswehr Friedrich-Ebert-Strasse 72 5060 Bergisch Gladbach 1 FRG
2	Paul Bunyan Sally Westlake RARDE Powder Mill Lane Waltham Abbey Essex, England 1 AX	1	Dr. Hans-Juergen Frieske Dynamit Nobel Waltherstrasse 80 5000 Cologne 80 FRG
3	Fraunhofer-Institut fuer Treib-und Explosivstoffe ATTN: Dr. R. Hansen Dr. E. Backof Dr. F. Volk D-7507 Pfinztal-Berghausen FRG		
1	Dr. H. Schmidt Bundesministerium der Verteidigung Rue V11-4 Postfach 1328 5300 Bonn 1 FRG		
2	G. Klingenberg H. Rockstroh Fraunhofer-Institut fuer Kurzzeitdynamik Ernst- Mach-Institut Abteilung fuer Ballistik Hauptstrasse 18 D-7858 Weil am Rhein FRG		

USER EVALUATION SHEET/CHANGE OF ADDRESS

This laboratory undertakes a continuing effort to improve the quality of the reports it publishes. Your comments/answers below will aid us in our efforts.

1. Does this report satisfy a need? (Comment on purpose, related project, or other area of interest for which the report will be used.)

2. How, specifically, is the report being used? (Information source, design data, procedure, source of ideas, etc.)

3. Has the information in this report led to any quantitative savings as far as man-hours or dollars saved, operating costs avoided, or efficiencies achieved, etc? If so, please elaborate.

4. General Comments. What do you think should be changed to improve future reports? (Indicate changes to organization, technical content, format, etc.)

BRL Report Number _____ Division Symbol _____

Check here if desire to be removed from distribution list.

Check here for address change.

Current address: Organization _____
Address _____

-----FOLD AND TAPE CLOSED-----

Director
U.S. Army Ballistic Research Laboratory
ATTN: SLCBR-DD-T(NEI)
Aberdeen Proving Ground, MD 21005-5066

OFFICIAL BUSINESS
PENALTY FOR PRIVATE USE \$300



NO POSTAGE
NECESSARY
IF MAILED
IN THE
UNITED STATES



Director
U.S. Army Ballistic Research Laboratory
ATTN: SLCBR-DD-T(NEI)
Aberdeen Proving Ground, MD 21005-9989